Towards a Functional Analysis of Human Carcinoma Disseminating Tumor Cells

PhD thesis in Cancer Biology
Presented to the Faculty of Natural Sciences,
Ruprecht-Karl University of Heidelberg, by
Irène Baccelli

Jury
Prof. Dr. Andreas Trumpp, thesis director, first advisor
Prof. Dr. Klaus Pantel, second advisor
Prof. Dr. Herbert Steinbeisser, chairman
Prof. Dr. Ingrid Grummt

HEIDELBERG 2011

TABLE OF CONTENTS

TABLE OF CONTENTS

1. ABSTRACT

Metastasis is the first cause of cancer-related deaths. Current metastasis models propose that metastases arise from a sub-fraction of Disseminating Tumor Cells (DgTCs), which can act as Metastasis Initiating Cells (MetICs). DgTCs are found in several mesenchymal compartments of the body: in the blood vasculature (Circulating Tumor Cells, CTCs), in the lymphatics or in the bone marrow (Disseminated Tumor Cells, DTCs). Moreover, the presence of DgTCs in carcinoma patients correlates with metastasis occurrence and metastatic relapse. However, the tumorigenicity of DgTCs has never been assessed due to the lack of suitable *in vivo* models. The bone marrow is a dynamic microenvironment with a high concentration of growth factors and cytokines, making it a permissive zone for cancer cell homing, survival and possibly self-renewal. Furthermore, it has been shown to shelter DTCs in a high frequency of carcinoma patients, suggesting that the bone marrow functions as a reservoir for potential MetICs.

A novel functional xenograft model was set up and optimized in order to analyze the metastatic potential of DgTCs. Briefly, human tumor cells were transduced with a high titer lentivirus to introduce a high expression of the luciferase reporter gene and transplanted into the bone marrow of NOD/SCID/$\gamma_c^{-/-}$ immuno-compromised mice. The engraftment and the expansion of the tumor cells were then quantified in a non-invasive manner using the Xenogen imaging system and a CT-scan. A first line of experiments was carried out using the MDA-MB-231 breast cancer metastatic cell line. The bone marrow metastatic niche was then further characterized using this model. Additionally, primary DgTC samples from breast and prostate cancer patients were analyzed.

DgTCs were found to be able to usurp the haematopoietic stem cell niche in the bone marrow, and their engraftment in the niche was CXCR4-dependent. Also, it could be demonstrated that cell line CTCs are in general less tumorigenic than tumor cells from the parental cell line, due to an arrest in cell cycle. Quiescence was associated with CD26 expression while activated states were associated with C-MET expression. CTCs were found to be highly heterogeneous; among others, an activated phenotypic circulating cancer stem cell subpopulation was detected in a breast cancer patient, specifically within C-MET positive CTCs.

Metastasierung ist die Hauptursache für krebsbedingte Todesfälle. Aktuelle Metastasierungsmodelle schlagen vor, dass Metastasen von einer Subpopulation der "disseminierenden Tumorzellen" (DgTCs) abstammen, welche auch als "Metastasen-initiierende Zellen" (MetICs) agieren können. DgTCs sind in mehreren mesenchymalen Kompartimenten des Körpers zu finden: in den Blutgefäßen (zirkulierende Tumorzellen, CTCs), in den Lymphgefäßen (Lymphknoten Tumorzellen LNTCs) oder im Knochenmark (disseminierte Tumorzellen, DTC). Außerdem korreliert das Auftreten von DgTCs in Karzinompatienten mit dem Auftreten von Metastasen und dem Auftreten von Rezidiven. Allerdings konnte die Tumorigenität von DgTCs nie gezeigt werden, da keine geeigneten in vivo Modelle existieren. Das Knochenmark ist eine dynamische Umgebung mit hoher Konzentration von Wachstumsfaktoren und Zytokinen, die es zu einer idealen Nische für das Einnisten und Überleben von Krebszellen macht. Zudem verdichten sich die Hinweise, dass das Knochenmark als ein vorübergehendes Reservoir für DgTCs dienen kann.

Ein neuartiges funktionelles Xenograftmodell wurde etabliert, um das metastatische Potential von DgTCs zu analysieren. Menschliche Tumorzellen wurden mit einem lentiviralen Vektor Konstrukt, welches Luciferase als Reportergen exprimiert (LUC), transduziert und in das Knochenmark von NOD/SCID/γc-/- immundefizienten Mäusen transplantiert. Das Anwachsen und die Expansion dieser Tumorzellen wurde nicht-invasiv mit Hilfe des Xenogen Imaging-System und des CT-scan analysiert. Die ersten Versuche wurden mit der metastasierenden MDA-MB-231 Brustkrebs-Zelllinie durchgeführt. Dabei wurde das etablierte in vivo Model zur Charakterisierung des Knochenmarks als potentielle metastatische Nische herangezogen. Zusätzlich wurden Proben von primären DgTC Brust- und Prostatakrebs-Patienten analysiert.

Die DgTCs waren in der Lage, die hämatopoetische Stammzellnische im Knochenmark zu nutzen, wobei das Anwachsen der Tumorzellen CXCR4-abhängig war. Außerdem konnte gezeigt werden, dass CTCs aufgrund eines Zellzyklusarrests weniger tumorigen sind als die Tumorzellen der parentalen Zelllinie. Quiescence war mit der Expression von CD26 assoziiert, wohingegen die Expression von C-MET mit einem aktivierten Zellstatus in Verbindung gebracht werden konnte. CTCs scheinen aus einer heterogenen Population von Zellen zu bestehen. Eine aktivierte zirkulierende Krebsstammzell Subpopulation wurde in Brustkrebspatientinnen detektiert, vor allem unter den C-MET positiven CTCs.

2. INTRODUCTION

Metastasis is the first cause of cancer-related morbidity and mortality (Jemal et al., 2010). The understanding of its ontology is therefore crucial for improving cancer patients' chance of surviving this disease. Metastasis is more and more studied, thanks to the development of *in vivo* models using immuno-compromised mice. In the next chapter, known facts and theories currently proposed by the field are presented.

2.1 Carcinoma metastasis

Carcinomas are cancers originating from epithelial tissues as opposed to connective, muscle, hematopoietic or nervous tissues. The epithelium is composed of differentiated cells that line the cavities and surfaces of structures throughout the body (for instance the skin, the mammary gland, the prostate, or the gastrointestinal tract…). It is a well-organized structure, lying on top of connective tissues, separated by a basement membrane. Epithelial cells are generally apical-basal polarized and attached to each other through tight cell-cell junctions: let alone during developmental stages, they are unable to migrate as single cells throughout the body (Fuchs, 2007).

Tumors developing from such well-organized structures are conserving some of the characteristics of epithelial tissues: well-differentiated carcinomas, such as *in situ* carcinomas, are generally consisting of phenotypic epithelial tumor cells that grow into tight structures. They generally continue to express proteins that are characteristic of epithelial cells such as the CYTOKERATINS (CK). They form solid structures that are still delimitated by the basement membrane and contained within the healthy epithelial tissue. To be able to develop metastases, carcinoma cells must as a consequence undergo major physical changes: they need to acquire invasiveness and motility in order to be able to evade from the basement membrane of the primary tumor and to disseminate throughout the body (Steeg, 2006) (Eccles and Welch, 2007). In the next chapters, the different steps that cancer cells undergo during the metastatic process will be presented, as well as the physical and molecular changes that are required both for the cancer cells as well as for the surrounding microenvironment.

2.1.1 Metastasis: a multistep cascade

Metastasis consists of a series of subsequent steps during which, Disseminating Tumor Cells (DgTCs) move from the primary neoplasm to a distant site (Figure 1) (Steeg, 2006), (Pantel and Brakenhoff, 2004).

First, some cells from the primary tumor succeed to evade from the solid delimitated structure, most likely at the edge of the tumor mass (invasive front) that starts to break through the basement membrane. In a second step, invasive DgTCs become motile and either enter a lymphatic vessel (passive mechanism) or penetrate the blood vasculature by intravasation. During a third step, DgTCs follow the natural routes of the body until they reach a secondary organ where they can engraft: a lymph node in the first case, or, for instance, in the lungs (in the case of a haematogenous spread). Consequently, DgTCs extravasate from the vasculature and seed into the target tissue. Eventually, seeded DgTCs start to colonize the new environment, forming a secondary neoplasm, after an optional step of dormancy: DgTCs might exit the cell cycle for a variable time length, until they are re-activated, causing a delayed metastatic relapse (Hedley and Chambers, 2009). In other cases, DgTCs might enter an ”angiogenic dormancy” phase: the balance between proliferation and apoptosis forbids any macro-metastatic development due to the lack of sufficient angiogenesis (Aguirre-Ghiso, 2007).

Overall, each step of the metastatic cascade is very limiting. In particular, colonization is a very inefficient process (MacDonald et al., 2002), (Fidler, 1970). In an experimental melanoma metastasis model, the majority (>80%) of injected tumor cells survived the circulation and successfully extravasated into the liver. However, only 1 in 40 cells formed micro-metastases by day 3, and only 1 in 100 micro-metastases progressed into macroscopic metastases 10 days later (Luzzi et al., 1998). Indeed, successful colonization crucially depends on the interaction between DgTCs and the microenvironment or “soil” of the distant tissue: this aspect will be further developed in section 2.1.3.

Importantly, metastasis might not always occur in a unidirectional manner. A recent paper (Kim et al., 2009) shows that tumors, as well as secondary or tertiary metastases might be sustained or initiated by re-seeding of DgTCs. Using two differentially labeled tumor cell lines, the authors could demonstrate that both cell lines contributed to the growth of syngenic or xenograft tumors, even when implanted each in different locations.

Dissemination might occur constantly and stem from all tumor masses, being primary tumors or metastases: the metastatic cascade might be more complex and dynamic than a single-sourced waterfall.

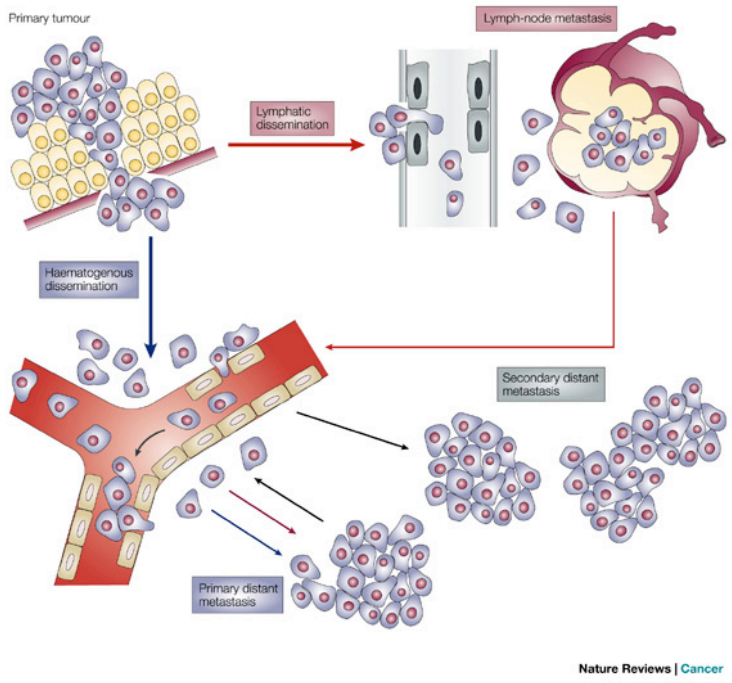

Figure 1. Scheme of the metastatic cascade. Disseminating Tumor Cells (DgTCs) can spread either through haematogenous dissemination or through a lymphatic dissemination. In both cases, DgTCs have to break free from the primary tumor and evade through the basement membrane. In the case of a haematogenous spread, DgTCs additionally intravasate into the vasculature, survive in the blood stream and extravasate from the vasculature endothelium. All routes can lead to the other and secondary metastases might result from re-seeding of primary metastases. Figure taken from Pantel and Brakenhoff, 2004.

2.1.2 Epithelial to Mesenchymal Transition

In order to perform the different steps of the metastatic cascade (see chapter 2.1.1), carcinoma cells need to acquire invasiveness, motility and an increased resistance to apoptosis. However, carcinoma cells are of epithelial origin, displaying tight cell-cell interactions, basal-apical polarization and an inability to migrate. Metastasizing DgTCs therefore undergo major phenotypic changes, known as the Epithelial to Mesenchymal Transition (EMT).

The EMT was first described as a cell culture phenomenon. Its relevance for *in vivo* physiological processes was long debated. However it is now well accepted that this trans-differentiation program takes place in embryonic development as well as in carcinogenesis (Yang and Weinberg, 2008), (Polyak and Weinberg, 2009).

Tumor cells that evade from the primary tumor (Disseminating Tumor Cells or DgTCs) start loosing their rigid cytoskeleton and cuboidal structure to adopt a more malleable spindle shape (Figure 2). On the molecular level, cell-cell adhesions are repressed by a decrease in E-CADHERIN expression and cell-basement membrane adhesions are repressed by a decrease in some INTEGRINS; instead, DgTCs start to express N-CADHERIN (cell binding to the stroma during invasion), OSTEOPONTIN (OPN), TYPE 1 COLLAGEN and other types of INTEGRINS that provide more transient adhesive properties to the Extra Cellular Matrix (ECM). Additionally, cytoskeletal elements are reorganized: the peripheral ACTIN cytoskeleton is replaced by stress fibers, whereas CYTOKERATIN intermediate filaments are replaced by VIMENTIN. The expression of epithelial markers such as EPITHELIAL CELL ADHESION MOLECULE (EPCAM) can also be down-regulated (Muller et al., 2010).

A lot of oncogenic molecular pathways like TRANSFORMING GROWTH FACTOR BETA (TGFβ) (Mani et al., 2008), WNT (Vincan and Barker, 2008), NOTCH, SONIC HEDGEHOG (SHH) and BONE MORPHOGENETIC PROTEIN (BMP) signaling (Bailey et al., 2007), as well as numerous RECEPTOR TYROSINE KINASES (RTKs), such as C-MET can induce EMT (Gentile et al., 2008). In addition, physiological processes such as hypoxia (Gort et al., 2008) as well as heterotypical interactions between tumor cells and activated stromal cells surrounding them (Sheehan et al., 2008) have also been reported as inducers of the EMT trans-differentiation. Last but not least, a lot of transcriptional factors such as TWIST1, TWIST2, FOXC2, SNAI1, ZEB2 (or SIP1) (Moreno-Bueno et al., 2008) as well as non-coding RNAs such as the *miR-200* family (*miR-200a, miR-200b, miR-200c, miR-141* and *miR-429*) and the *miR-205* family (Gregory et al., 2008) have been ascribed a role in activating the EMT program.

After going through EMT, DgTCs acquire the ability to invade and move into the extracellular matrix. They also acquire resistance to apoptosis and anoikis (produced by the loss of attachment to neighboring cells) and begin to respond to extracellular cues, directing them along specific routes to their destination. Interestingly, upon arriving to their destination, these mesenchymal-looking cells may undergo the reverse process of Mesenchymal to Epithelial Transition (MET): due to the absence of heterotypical interactions with the activated primary tumor stroma, DgTCs regain their epithelial phenotype and form solid epithelial-looking metastases (Chaffer et al., 2007) (Figure 2). As a conclusion, DgTCs might often drastically modify their phenotype throughout the metastatic process, which renders their study all the more complex.

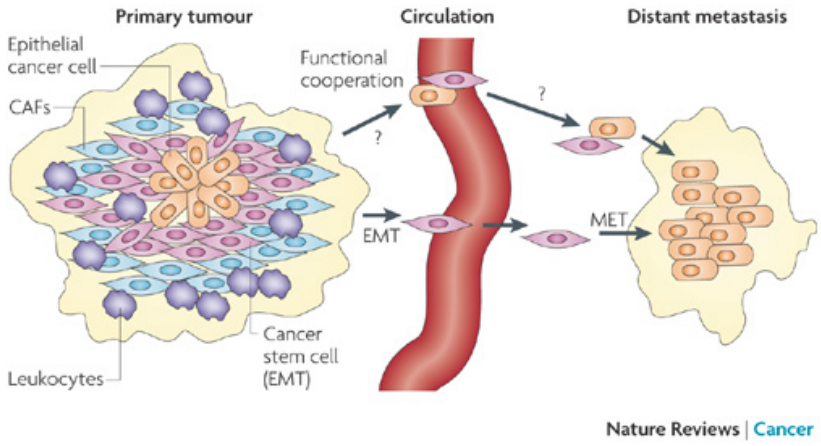

Figure 2. Schematic view of the Epithelial to Mesenchymal Transtition (EMT) and Mesenchymal to Epithelial Transition (MET) mechanisms during metastasis. Epithelial cells form the bulk of the tumor. Some cells, possibly induced by interactions with the surrounding activated stroma such as Carcinoma Associated Fibroblasts (CAFs), undergo EMT. They acquire a cancer stem cell phenotype and they are able to disseminate from the primary tumor to a distant site. After regaining epithelial traits (MET), the Disseminating Tumor Cells (DgTCs) develop into solid metastases. Figure taken from Polyak and Weinberg, 2009.

2.1.3 Microenvironment of metastases: towards a metastatic niche

One of the big challenges of disseminating carcinoma cells is to be able to appropriate different microenvironments at each step of the metastatic cascade: at the site of the primary tumor, during the systemic spread and at the metastatic site.

The primary tumor niche and its role in metastasis:

Some constituents of the primary tumor niche such as Tumor Associated Macrophages (TAMs), Myeloid Derived Suppressor Cells (MDSCs) and Mesenchymal Stem Cells (MSCs) play important roles in the metastatic cascade (Joyce and Pollard, 2009) (Figure 3).

First of all, TAMs are enhancing cancer cell invasion through a paracrine loop: in the case of breast cancer, TAMs are secreting the EPIDERMAL GROWTH FACTOR (EGF), while its receptor, EGFR is expressed by tumor cells; the tumor cells then secrete COLONY STIMULATING FACTOR 1 (CSF1) which attracts CSF1-R positive macrophages. TAMs are thought to induce the tethering of collagen fibers from the tumor to the neighboring blood vessels. TAMs as well as the tumor cells then use these collagen fibers as guidelines towards the vasculature (Condeelis and Segall, 2003). Moreover, it was shown that TAMs enhance the capability of DgTCs to intravasate in the blood vessels (Wyckoff et al., 2007).

Second, MDSCs are described as $CD11b^+/GR1^+$ cells in the mice or $MHCI/^+MHCII^{low}/CD11c^+/CD33^+/CD34^+/CD86^-$ in humans (Ostrand-Rosenberg and Sinha, 2009). They act as suppressors of the adaptive and innate immune responses against tumor cells. For instance, MDSCs are blocking the action of $CD4^+$ and $CD8^+$ T cells through the production of ARGINASE and NITRIC OXIDE. MDSC accumulation in the blood circulation but also in the lymph nodes, the bone marrow and the spleen of patients is associated with metastasis occurrence (Ostrand-Rosenberg, 2008). The mechanisms leading to MDSC accumulation are still poorly understood but have been linked to inflammation signaling. For instance, mice lacking the pro-inflammatory S100A9 protein develop efficient anti-tumor immune responses and reject implanted cancer cells; by injecting wild-type MDSCs in the tumor-implanted mice, the effect can be reversed (Cheng et al., 2008).

Third, MSCs seem to play a role in priming tumor cells on the site of the primary neoplasm, before dissemination. This priming occurs through a paracrine loop where breast cancer cells stimulate *de novo* secretion of the chemokine CCL5 (or RANTES) from MSCs. CCL5 secreting MSCs then enhance invasion and motility of the cancer cells *via* signaling through the chemokine receptor CCR5 (Karnoub et al., 2007).

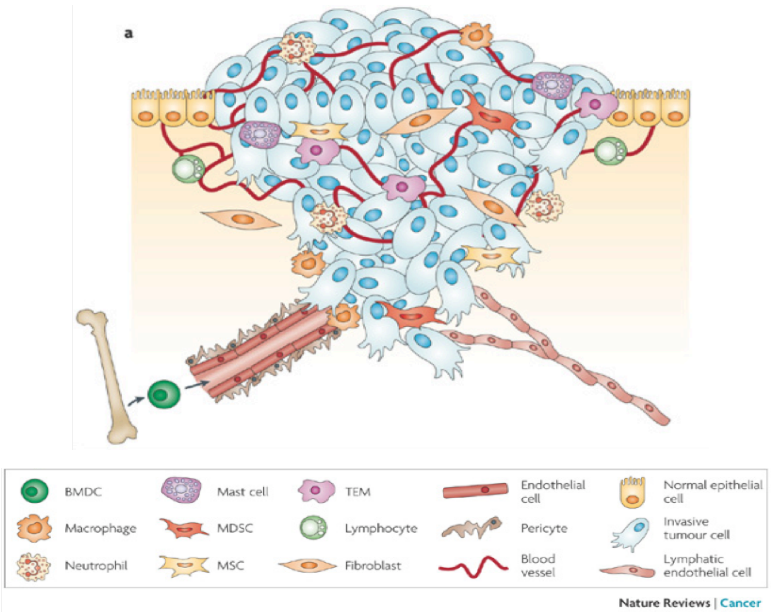

Figure 3. The different players of the primary tumor niche. Some constituents such as Tumor Associated Macrophages (TAMs), Myeloid Derived Suppressor Cells (MDSCs) and Mesenchymal Stem Cells (MSCs) are particularly involved in enhancing tumor cell dissemination. Figure adapted from Joyce and Pollard, 2009.

Role of the environment during the systemic spread of DgTCs:

The vast majority of the cells entering the blood vasculature (more than 99%) does not give rise to metastasis (Fidler, 1970). The extremely stressful shear force of the blood circulation, as well as in the active immuno-surveillance performed by NK cells are some of the reasons for such poor success rates. In order to circumvent these challenges, Circulating Tumor Cells (CTCs) develop protective strategies, involving the surrounding environment.

For instance, a very controversial theory states that some CTCs fuse with macrophages in the blood circulation, increasing their chances of survival and acquiring mesenchymal traits, as observed in the EMT field (Pawelek and Chakraborty, 2008). A better-accepted theory claims that some (CTCs) secrete TISSUE FACTOR (TF), which enables platelet aggregates to form a shield around them. Such CTC-associated microthrombi reduce shear forces, provide protection against NK-mediated lysis and facilitate the slowing, arrest and adhesion of CTCs before they extravasate through the tight inter-endothelial junctions of the blood vessels (Palumbo, 2008).

Contrary to blood vessels, lymph vessels and lymph nodes are easy to penetrate since they do not display any tight cell-cell junctions. The mechanism by which cancer cells are drained from the primary tumor through lymphatic vessels to the lymph nodes is therefore considered quite passive. Some data show that tumor cells might migrate towards the lymph nodes depending on the interstitial flow but also according to an autocrine CCR7 signaling (Shields et al., 2007). Lymph nodes may represent an intermediary environment where cancer cells accumulate, survive (thanks to the close interactions with other tumor cells) and acquire additional mutations and metastatic capacities through time. They become truly metastatic only after some maturation period.

Role of the environment in DgTC recruitment, seeding and colonization:

Organ selectivity is observed for metastatic seeding and colonization. For instance, breast cancer cells preferentially metastasize to the bones, the lungs, and the brain, whereas colorectal cancer cells usually colonize the liver. Two main theories propose mechanisms for metastasis recruiment, seeding and colonization after a haematogenous spread.

In the first one, it is suggested that the microenvironment plays only a passive role. This first theory states that the localization of metastases in the body simply reflects the physical entrapment of tumor cells by the blood capillaries along the route they take (Chambers et

al., 2002). The repartition of secondary tumors then of course varies according to the site of origin of the primary tumor, which determines the route the DgTCs can take. For instance it is physiologically understandable that breast cancer cells spread predominantly to the lungs, the lymph nodes and the bones, whereas liver tumor cells first travel through the liver *via* the hepatic-portal vein. This theory thus favors the idea of a selection of good "seeds", meaning cells that would survive and develop metastasis in the site where they are physically shed, rather than the selection of a good soil. Some data from the group of Joan Massagué corroborates this idea: by selecting sub-clones of a breast metastatic cell line, the expression of distinct gene signatures by the different sub-clones was shown to determine their ability to form metastasis in a specific organ (Nguyen et al., 2009), (Nguyen and Massague, 2007).

A second theory, which does not exclude the first one, suggests that if the cells, or "seeds" are selected to become Metastasis Initiating Cells (MetICs), the environment of the target organ, or "soil" is also playing a pivotal role. This theory was historically first proposed by Stephen Paget and then further developed by Isaiah Fidler (Paget, 1889), (Fidler, 1970). The interaction between DgTCs and the microenvironment determines the repartition of metastases throughout the body: "When a plant goes to seed, its seeds are carried in all directions; but they can only live and grow if they fall on congenial soil" (Paget, 1889). Indeed, there is now growing evidence that the environment plays a crucial role in DgTC recruitment (pre-metastatic niche) and in DgTC seeding and colonization (metastatic niche).

<u>* The pre-metastatic niche</u>

First of all, tropism for specific organs is mediated by local expression of chemoattractants: chemokine receptor-expressing DgTCs are guided towards the site of future metastasis formation as a result of chemokine gradients. For instance, poor prognosis breast cancer patients show expression of a chemokine receptor, CXCR4 (Zlotnik, 2008). CXCR4+ DgTCs have been shown to be attracted to organs naturally expressing its ligand, SDF1, like the lung and the bone. CXCR4 mediated signaling induces ACTIN polymerization and pseudopod formation, leading to invasion (Muller et al., 2001). In addition, a mouse xenograft model showed that the neutralization of either SDF1 or CXCR4 leads to breast cancer metastasis impairment (Muller et al., 2001).

Very interestingly, DgTC recruitment might also be controlled by the primary tumor, through the recruitment of distant myeloid cells, or Bone Marrow Derived Cells (BMDCs), which prepare the metastatic site before the arrival of the DgTCs. Together with residing endothelial and stromal cells, they secrete chemokines, growth factors, matrix degrading enzymes as well as adhesion molecules, thus gathering all the ingredients for the establishment of a metastatic lesion and creating a "pre-metastatic niche" (Figure 4) (Psaila and Lyden, 2009), (Psaila et al., 2006).

Several types of cells contribute to the pool of BMDCs. First of all, Haematopoietic Progenitor Cells (HPCs) are implicated in the initiation of the pre-metastatic niche. They secrete a variety of growth factors (TGFβ), cytokines (TUMOR NECROSIS FACTOR ALPHA (TNFα)) and enzymes (MATRIX METALLOPROTEINASE 9 (MMP9)), which prepare the site for the arrival of DgTCs. They are also involved in angiogenesis promotion and express the receptor 1 for VASCULAR ENDOTHELIAL GROWTH FACTOR (VEGFR1) (Kaplan et al., 2005). Second, Endothelial Progenitor Cells (EPCs) are mobilized from the bone marrow during angiogenesis. Their recruitment contributes to the "angiogenic switch" pushing dormant micrometastases out of their quiescence (Gao et al., 2009) (Gao et al., 2008). Platelets releasing SDF1 granules might play a role in guiding CXCR4 expressing cells but also $CXCR4^+$ HPCs (Jin et al., 2006). Last but not least, Mesenchymal Stem Cells (MSCs) give rise to activated fibroblasts. These activated fibroblasts secrete an adhesion molecule, FIBRONECTIN, in the pre-metastasic niche, thereby enhancing $INTEGRIN^+$ DgTC's homing to the metastatic site (Kaplan et al., 2005).

BMDCs are recruited to the future site of metastasis in response to growth factors secreted by the primary tumor. For instance, BMDCs are mobilized following secretion of VASCULAR ENDOTHELIAL GROWTH FACTOR A (VEGFA), PLACENTAL GROWTH FACTOR (PlGF), TGFβ and inflammatory S100 chemokines (Hiratsuka et al., 2006), (Hiratsuka et al., 2008). Hypoxia also mediates BMDC recruitment *via* LYSYL OXIDASE (LOX) induction. LOX is an enzyme secreted by human hypoxic tumors that crosslinks COLLAGEN and ELASTINS in the Extra Cellular Matrix (ECM). It accumulates at the pre-metastatic niche where it modifies the ECM and makes it more hospitable for BMDC infiltration. Furthermore, inhibition of LOX synthesis in a breast cancer model prevented metastasis (Erler et al., 2009).

Very briefly, pre-metastatic lymphangiogenesis was also observed before the infiltration of the first breast tumor cells within the sentinel lymph node (Hirakawa et al., 2007).

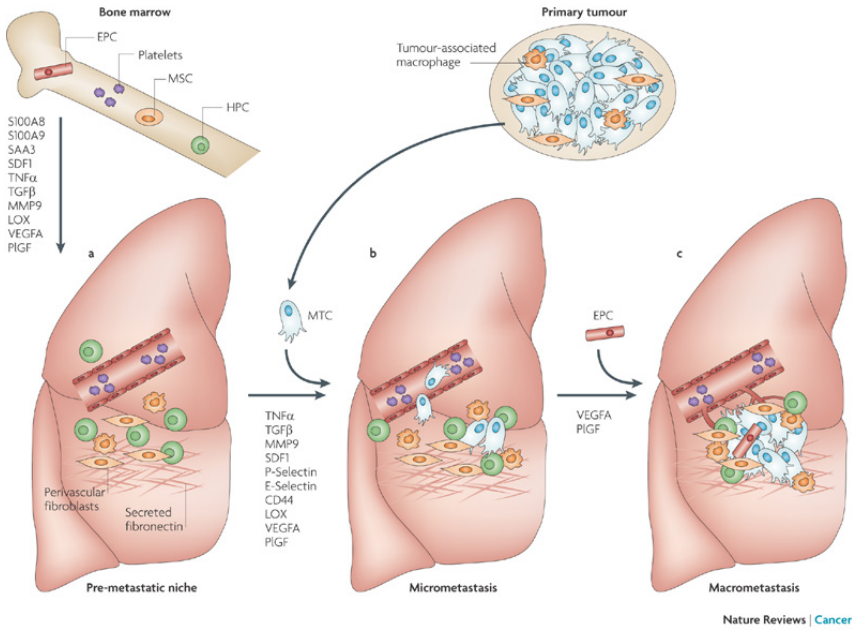

Figure 4. The pre-metastatic, micrometastastatic and macrometastasic niches. The pre-metastatic niche is created through the recruitment of Bone Marrow Derived Cells (BMDCs). Among them, Haematopoietic Progenitor Cells (HPCs), Mesenchymal Stem Cells (MSCs), which give rise to perivascular fibroblasts, as well as platelets, are early recruits. The activation of the residing endothelial cells and the secretion of FIBRONECTIN by the perivascular fibroblasts attract Migrating Tumor Cells (MTCs), traveling in the circulation shielded with SDF1-expressing platelets. MTCs engraft in the target organ and create a micrometastasis. Upon recruitment of Endothelial Progenitor Cells (EPCs), the micrometastasis undergoes an angiogenic switch, which allows the outgrowth of macrometastasis. Figure taken from Psaila and Lyden, 2009.

* The Metastatic niche

Residing activated endothelial cells start to express P-SELECTIN and E-SELECTIN, which enhance DgTC adhesion to the endothelium and subsequent extravasation (Biancone et al., 1996). Subsequently, apoptosis-resistant DgTCs engraft in the niche and develop into micrometastases: we will further refer to these "successful" DgTCs as Metastasis Initiating Cells or MetICs. The receptor for HYALURONATE (but also for FIBRONECTIN, COLLAGEN I, OPN and LAMININ), CD44, is a prominent factor enabling tumor cells to evade cell death signals. It was shown that the inhibition of the interaction between CD44-bearing breast tumor cells and the lung matrix did not interfere with the initial adherance and invasion of the lung parenchyma but lead to massive apoptosis and prevented micrometastasis formation (Yu et al., 1997). After the recruitment of EPCs from the bone marrow *via* VEGFA and PlGF, the metastatic niche undergoes an angiogenic switch, allowing progression into macrometastasis. The transcription factor INIHIBITOR OF DIFFERENTIATION 1 (ID1) is crucial for the recruitment of EPCs at the site of the micrometastasis; short hairpin RNA inhibition of ID1 did not affect lung colonization by tumor cells but prevented progression to macrometastasis due to the absence of EPC recruitment (Gao et al., 2009) (Gao et al.,

2008). Signals initiating EPC recruitment to micrometastases and signals controlling macrometastatic progression are still unclear.

This rather new concept of a pre-existing niche or pre-metastatic niche was mostly obtained from mouse model studies and largely focused on the lungs as a target organ. It still requires further investigation. Nevertheless, the pre-metastatic niche discovery underlines the complexity of carcinogenesis: metastasis might be a global-regulated process, prepared in advance by the recruitment and the activation of the surrounding healthy environment.

2.1.4 Metastasis regulatory elements

Once the first oncogenic events have taken place (through activation of oncogenes such as *HER2, KRAS, MYC*…), other events are necessary for transformed cells to acquire metastatic abilities (Minna et al., 2003). Either transformed cells acquire metastatic traits through loss of expression/loss of function of metastasis suppressor genes or by gain of expression/gain of function of metastasis inducing genes (Figure 5). In addition, MicroRNAs form a new class of metastasis regulators (suppressors and inducers). MicroRNAs (or miRNAs) are 19 to 24 nucleotide-long RNAs that are processed from longer transcripts and arise from hairpin loop structures after successive enzymatic maturation steps. MicroRNAs regulate gene expression in a sequence specific manner: they bind mRNAs through partial complementarity of their "seed" sequence. Subsequently, the target mRNA translation is impaired, leading to reduced protein expression levels. MiRNAs that are generally lost in tumors (or metastases) usually participate in oncogene over-expression, whereas MiRNAs that are over-expressed in tumors (or metastases) contribute to oncogenesis by down-regulating tumor or metastasis suppressor genes.

<u>Metastasis suppressor elements</u>:

Metastasis suppressor elements are defined by their ability to impair metastasis but not primary tumor growth. A growing number of suppressor proteins have been identified, especially since the development of metastatic *in vivo* models *via* the use of immuno-compromised mice. Among others, let's mention NM23, the first identified metastasis suppressor protein by Steeg and colleagues (Steeg et al., 1988), KAI1 (CD82), KISS1 (encoding KISSEPTINS), BREAST METASTASIS SUPPRESSOR 1 (BRMS1) … Most of these proteins rule over the last but most limiting step of metastasis: distant organ colonization.

For instance, expression of BRMS1 in human cancer cell lines has no effect on primary tumor growth or haematogenous seeding, but selectively attenuates colonization (Vaidya et al., 2008). During dissemination, KAI1 anchors tumor cells to the endothelium through its interaction with DUFFY ANTIGEN CHEMOKINE RECEPTOR (DARC) and induces senescence of bound epithelial cells (Bandyopadhyay et al., 2006).

Some metastasis suppressor genes have been used for therapeutic exploitation but none of them is used in clinical routine. Three strategies have been followed: reconstitution of metastasis suppressor function by induction of the endogenous locus (for instance for *NM23 via* the administration of medroxy-progestorone acetate, (Palmieri et al., 2005)) or gene therapy (for instance for *KAI1*, by administration of liposomes containing *KAI1* plasmid expression vector, (Xu et al., 2008)), direct administration of the suppressor protein itself (for instance for KISS1, by administration of KISS1-derived peptide through an osmotic pump, (Ohtaki et al., 2001)), or targeting essential downstream pathways that are activated by loss of suppressor function (for instance for *NM23*, by administration of the inhibitor Ki6425 for LYSOPHOSPHATIC ACID RECEPTOR 1, LPAR1, (Boucharaba et al., 2006)).

Additionally, a new class of miRNAs has recently been shown to inhibit metastasis. For instance, metastasis growth requires the suppression of *miR-126* and *miR-335* in lung and breast carcinomas. *MiR-126* notably represses CRK (adaptor signaling protein that participates in cell migration and ACTIN remodeling), thus inhibiting motility of lung cancer cells. *MiR-335*, on the other hand, represses the expression of the glycoprotein TENASCIN C (TNC), involved in reducing cell-ECM interactions and invasion of breast tumor cells (Tavazoie et al., 2008). Another example is the *miR-146* family: in the MDA-MB-231 breast cancer metastatic cell line, *miR-146* was shown to repress INTERLEUKIN 1 RECEPTOR–ASSOCIATED KINASE 1 (IRAK1) and TNF RECEPTOR-ASSOCIATED FACTOR 6 (TRAF6) as well as the activity of NUCLEAR FACTOR KAPPA B (NFκB); such repressions lead to a deduced metastatic potential (Bhaumik et al., 2008). Eventually, the repression of the *miR-200* family members during breast cancer EMT sustains the process by releasing ZEB1, ZEB2 and TGFβ2. ZEB1 and ZEB2 transcriptionally repress the *miR-200* members (Gregory et al., 2008).

Metastasis inducing elements:

Metastasis inducing elements can be subdivided in 3 different groups, following the metastatic cascade steps: metastasis initiating elements (involved in invasion and systemic spread), metastasis progression elements (involved in the seeding and latency of metastasis) and metastasis virulence elements (involved in metastasis colonization) (Figure 5), (Nguyen et al., 2009).

First of all, metastasis-initiating elements allow transformed cells to invade the surrounding environment, to travel *via* systemic routes and to recruit BMDCs to the pre-metastatic niche. For instance genes that promote EMT such as *TWIST1*, *SNAI1* and *SLUG* (or *SNAI2*) can be considered as metastasis initiating genes. Also, modulators of C-MET, the HEPATOCYTE GROWTH FACTOR (HGF) RECEPTOR, such as METHADERIN in breast cancer are involved in invasion: in a mouse model, it was shown that METHADERIN specifically binds to the pulmonary vasculature and enhances lung metastasis (Brown and Ruoslahti, 2004). Very recently it was also shown that INSULIN GROWTH FACTOR 1 RECEPTOR (IGF1R) supports survival of Circulating Tumor Cells (CTCs): its inhibition might render CTCs more susceptible to anoikis while the primary tumor remains unaffected (Sachdev et al., 2009). Several miRNAs have also been shown to activate metastasis initiation by acting on multiple signaling pathways and targeting major metastasis players. For instance, *miR-10b* is over-expressed in 50% of metastatic breast cancers in comparison to non-metastatic tumors or normal breast tissue (Ma et al., 2007). *MiR-10b* is activated by the transcription factor TWIST1, involved in EMT. In turn, *mir-10b* indirectly increases RHOC levels by direct down-regulation of its transcriptional repressor HOXD10. The RHO GTPase RHOC induces invasion and migration, thus participating to metastasis initiation (Myers et al., 2002).

Secondly, metastasis progression elements enhance DgTCs' capacity to seed in the pre-metastatic niche. These elements might vary according to the metastatic site since capillary structures vary enormously from one organ to the other: for instance, cells metastasizing to the brain have to penetrate the blood-brain barrier, while cells engrafting in the bone marrow can infiltrate much more easily through the fenestrations of the marrow sinusoids. MATRIX METALLOPROTEINASE 1 (MMP1), MMP2, EPIREGULIN and PROSTAGLANDIN G/H SYNTHASE 2 (PTGS2, also known as COX2) mediate breast cancer cell intravasation in the pulmonary parenchyma (Gupta et al., 2007a). Also, the cytokine ANGIOPOIETIN LIKE 4 (ANGPTL4) induces the infiltration of tumor cells into the lungs by promoting the dissociation of endothelial cell-cell junctions (Padua et al., 2008). Finally, *miR-21*

participates to metastasis progression by repressing RECK and TIMP3 (TISSUE INHIBITOR OF METALLOPROTEINASE 3), two MMP inhibitors *via* the loss of the tumor suppressor protein PTEN (Meng et al., 2007).

Last but not least, metastasis virulence elements enable MetICs to colonize the metastatic niche. These elements are of course niche-dependent. For example, osteoclast mobilizing factors such as PARATHYROID HORMONE-RELATED PROTEIN (PTHRP) and INTERLEUKINE 11 (IL-11) do not provide selective advantages to breast cancer cells in the primary tumor but enable them to establish osteolytic lesions in the bone (Kang et al., 2003). Also, the expression of INIHIBTOR OF DIFFERENTIATION 1 (ID1) and ID3 supports the ability of human breast cancer cells to bypass senescence and reinitiate growth after extravasation in the lungs of mice (Gupta et al., 2007b) thanks to the recruitment of EPCs (Gao et al., 2009) (see chapter 2.1.3). More recently, the tyrosine kinase SRC has been shown to be dispensable for homing to the bones or to the lungs in breast cancer but critical for the survival and outgrowth of the tumor cells in the bone marrow (Zhang et al., 2009). In addition, multiple sets of genes have been described as organ specific metastasis signatures (Massague, 2007).

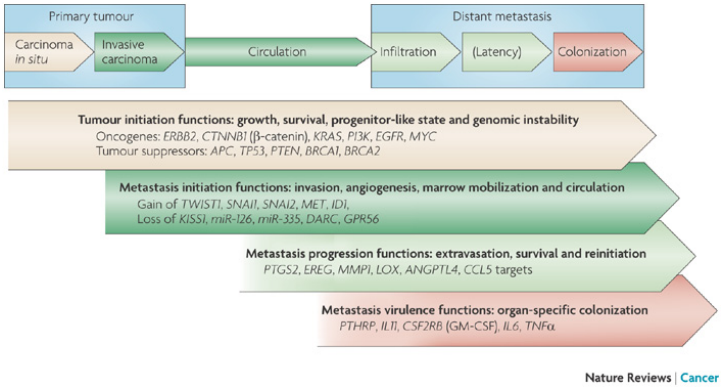

Figure 5. Metastasis suppressor genes and metastasis inducing genes. These genes can be subdivided in different categories. After the initial oncogenic transformation occurring in the primary tumor cells, DgTCs have to acquire metastasis initiation, metastasis progression as well as metastasis virulence functions through activation or repression of different sets of genes. Abbreviations: *ANGPTL4, ANGIOPOIETIN-LIKE 4; APC, ADENOMATOUS POLYPOSIS COLI; CCL5, C-C CHEMOKINE LIGAND 5; DARC, DHFFY ANTIGEN CHEMOKINE RECEPTOR; EGFR, EPIDERMAL GROWTH FACTOR RECEPTOR; EREG, EPIREGULIN; GM-CSF, GRANULOCYTE-MACROPHAGE COLONY STIMULATING FACTOR; GPR56, G PROTEIN-COUPLED RECEPTOR 56; HGF, HEPATOCYTE GROWTH FACOTR; ID1, INHIBITOR OF DIFFERENTIATION 1; IL, INTERLEUKIN; KISS1, KISSEPTIN 1; LOX, LYSYL OXIDASE; MMP1, MATRIX METALLOPROTEINASE 1; PTGS2, PROSTAGLANDIN G/H SYNTHASE 2; PTHRP, PARATHYROID HORMONE-RELATED PROTEIN; TNFα, TUMOR NECROSIS FACTOR ALPHA*. Figure taken from Nguyen et al., 2009.

As a conclusion from this first chapter, it is reasonable to think that macrometastasis results from the outgrowth of very few DgTCs that successfully evaded from the primary tumor, entered systemic routes to travel throughout the body, and achieved seeding and colonization of a secondary target organ. This can happen only after a series of very complex molecular and cellular modifications that allow the primary tumor cells to acquire phenotypical traits of motile cells during the journey (EMT), and to re-acquire epithelial characteristics once arrived in the target organ (MET). The mobilization and the activation of the healthy niche cells coming from the primary tumor but also from the bone marrow seem to play an important role for metastasis initiation, in the pre-metastatic niche. Last but not least, many genes and miRNAs are regulating each step of the metastatic cascade *via* complex molecular networks. Only rare DgTCs, under specific conditions, eventually succeed to colonize a new metastatic niche and to develop into overt macro-metastasis, thus behaving as Metastasis Initiating Cells (MetICs).

2.2 The Metastasis Initiating Cell Hypothesis

In order to narrow down the search for Metastasis Initiating Cells (MetICs), it is crucial to delimitate their kinetics of dissemination. It is still under active discussion whether MetICs are to be found among early or late DgTCs. The two main theories are exposed in this chapter.

2.2.1 Metastasis progression models

The linear progression model proposes that tumor cells go through multiple selective rounds of mutations and are progressively selected for their aggressiveness before becoming metastatic (Figure 6). Individual tumor clones expand in the primary tumor and then disseminate throughout the body. Therefore, the bigger the primary tumor is, the higher the chance is for developing metastatic clones and subsequent metastasis. This model fits with the routinely used Tumor, Node, Metastasis (TNM) international classification system: tumor size is associated with higher metastatic frequency. A corollary to this model is that metastatic founder cells or MetICs disseminate at rather late stages of the disease. Indeed, late stage invasive primary tumors show a close genetic resemblance with matched overt metastases (Ramaswamy et al., 2003). Fully metastatic cells can also disseminate from a first metastatic tumor to another organ, thus leading to the development of multiple metastases developing one after the other (Kim et al., 2009).

For instance, colorectal carcinoma seems to fit particularly well to this model: the transition from colorectal hyperplasia to adenoma, to invasive carcinoma is characterized by the acquisition of specific genetic alterations over a period of time up to 30 years. Once a colon tumor invades the underlying colonic wall, metastatic progression can proceed without any delay: colorectal tumors usually spread through the mesenteric circulation up to the liver, where 80% of the patients developing metastasis, acquire secondary tumors (Hess et al., 2006). It is estimated that most genetic alterations for metastasis are acquired during progression to the invasive carcinoma stage: only few, if any, additional events are required for the formation of distant liver metastases (Jones et al., 2008).

The same might be true for other types of cancers following swifter courses with rapid expansion to multiple organs, like pancreatic adenocarcinomas. In two recent and groundbreaking studies, genomic sequencing was carried out to examine the phylogenetic relationship between pancreatic primary tumors and their respective metastases (Yachida

et al., 2010) (Campbell et al., 2010). The authors could evaluate the time between the appearance of the parental clone and the appearance of the metastatic clone within the primary tumor. Yachida and colleagues could conclude that in pancreatic cancer, metastatic clones arise rather late during cancer progression (more than 10 years after tumor initiation) and disseminate 5 to 6 years later from the primary tumor.

As a third example, in breast cancer, metastasis usually occurs in an orderly fashion, affecting one organ after the other: this observation also favors a linear progression model: indeed if DgTCs would evolve in an independent and parallel manner in each target organ, we would not observe any pattern of metastatic development.

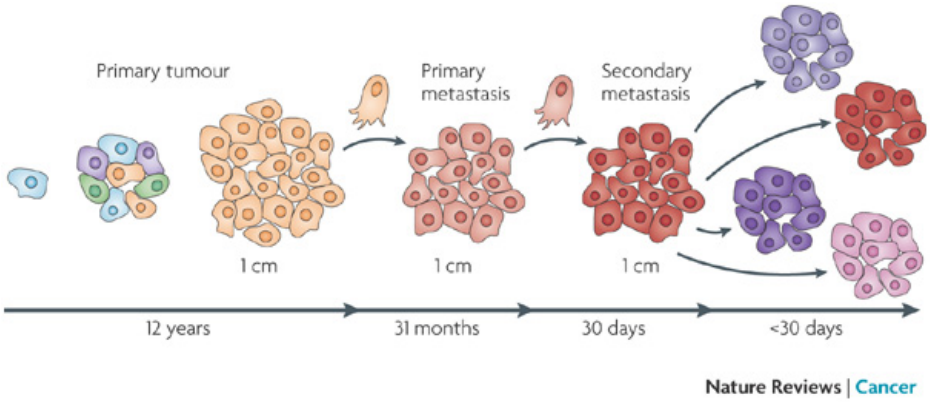

Figure 6. The linear progression model. Primary tumors accumulate genetic alterations and start to develop metastatic clones. Only at the stage of late invasive primary tumors do MetICs disseminate and develop into overt macrometastases. Metastases might even seed other organs, creating multiple and successive metastatic colonization. Figure taken from Klein, 2009.

The parallel progression model:

On the other hand, the parallel progression model proposes that there is an independent and parallel accumulation of genetic and epigenetic alterations in the primary tumor and in the metastatic lesions (Figure 7). The seeding of the DgTCs is occurring in different sites in parallel and independent niche-related adaptations occur in each site. The metastatic founder cells or MetICs can disseminate very early in the disease, long before the primary tumor is clinically detectable (< 1mm). Each MetIC develops and accumulates mutations in an independent and parallel fashion.

For instance, breast cancer and prostate cancer metastasis might become manifest only decades after the removal of even a small primary malignancy (Lee, 1985), (Johansson et al., 2004). The absence of immediate clinical relapse implies that early DgTCs are not fully

competent to overtake organs immediately after infiltration. A period of dormancy might be occurring, during which, microenvironmental cues or further malignant evolution of the cells, or both, might be necessary for overt metastases to develop. These arguments suggest a parallel progression model for these cancers.

Also, already at early stages, DgTCs are very different from the primary tumor cells taken at the same time point (Klein et al., 2002) and they show much less genetic aberrations. This divergence again corroborates the fact that early DgTCs might not be yet fully metastatic and might enter dormancy phases before being capable of colonizing secondary organs.

However, the presence of early dissemination might also be a simple indication of a primary tumor's propensity to invade and spread "pre-metastatic" cells, which might correlate with the primary tumor's propensity to produce fully metastatic MetICs at later stages. Another important argument against the parallel progression model is the fact that late stage primary tumors and their corresponding metastases have similar genetic aberrations (Ramaswamy et al., 2003): if MetICs would evolve in an independent manner, they might not at all develop the same traits as the primary tumor cells. Last but not least, for pancreatic cancer, two recent papers refute the parallel progression model, showing that metastatic clones disseminate late (Yachida et al., 2010) (Campbell et al., 2010).

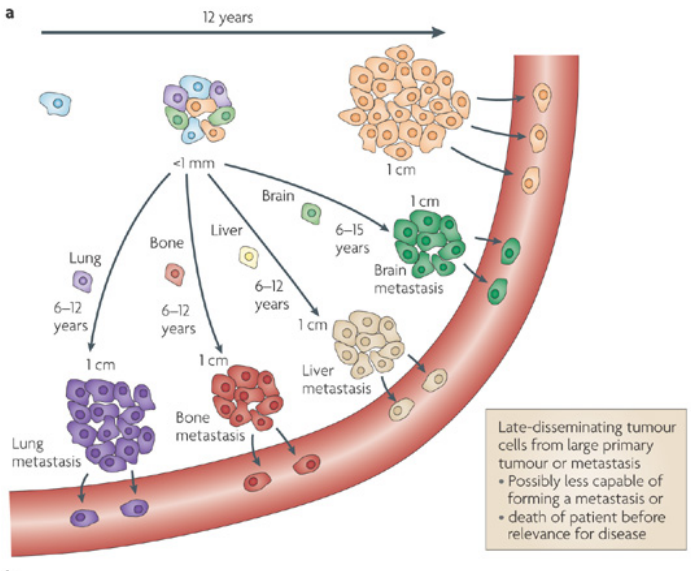

Figure 7. The parallel progression model. Metastasis Initiating Cells or MetICs disseminate early form the primary tumor. They evolve independently form each other and from the primary tumor; they are specific for their target organ microenvironment. They might enter dormancy phases in case of long metastatic delay, before developing into overt macrometastases. Figure taken from Klein, 2009.

As a conclusion, both the parallel and the linear progression models might be applicable, according to the type of cancer. Each cancer might indeed have its specific dissemination kinetics. Stronger pieces of evidence seem to argue as a whole for the linear progression model rather than for the parallel progression model; but additional data should be accumulated before making a clear statement.

2.2.2 Stem cells and Cancer Stem Cells

Metastases are of clonal origin: one single MetIC initiates one secondary neoplasm (Talmadge, 2007). Primary neoplasms are also clonal, as they derive from so-called Cancer Stem Cells (CSCs). It is still unclear whether MetICs derive from these same CSCs or from other types of invasive tumor cells. In order to discuss this particular point, short introductions on physiological stem cells and CSCs as well as on the techniques that are currently being used to define "stem cells" are presented in the next paragraphs.

Physiological Stem cells:

* Theoretical definition:

Adult stem cells form specific compartments in the body, which are responsible for the maintenance of our tissues. One single stem cell is theoretically capable of replenishing a whole tissue while all other components of the tissue are unable to do so. Stem cells can self-renew *via* mitotic divisions, differentiate into specialized lineages or stay quiescent.

For instance, one of the best-characterized physiological stem cells are the Haematopoietic Stem Cells (HSCs) (Wilson et al., 2009). They reside in a specialized niche, located in the bone marrow (see chapter 2.4). They can enter different levels of dormancy: Long Term HSCs (LT-HSCs), Short Term HSCs (ST-HSCs) and activated cycling HSCs. Activated HSCs differentiate into progenitors, which then give rise to all the differentiated cells of the haematopoietic system, including the myeloid lineage and the lymphoid lineage. Quiescent HSCs form a protected reservoir for hematopoietic replenishment in case of myelo-ablation (for instance after irradiation). Dormant HSCs can be activated by specific signals such as stress response to infections (for instance, after administration of INTERFERON ALPHA, IFNα, (Essers et al., 2009)). Impairing interactions between HSCs and their niche, which controls their quiescence, can lead to stem cell exhaustion and subsequent death (Wilson and Trumpp, 2006), (Wilson et al., 2007). Also, the oncogene *MYC* is an important regulator of HSC maintenance (Wilson et al., 2004), (Laurenti et al., 2008).

* Experimental definition:

For all tissues, the only way to prove the stemness of a cell is *via* the use of functional assays: for murine HSCs, the capacity of a cell to replenish the haematopoietic system of a lethally irradiated mouse is the only criteria recognized as a non-equivocal proof for stemness. However, great work has now been achieved in the identification of cell surface markers for HSCs (Spangrude et al., 1988), (Kim et al., 2006), (Mazurier et al., 2003). The identification of cell surface markers is pivotal for the stem cell field, since it provides an indirect but lighter tool (than functional assays) for the everyday study of stem cells: for instance, *via* the use of Fluorescence Activated Cells Sorting (FACS), HSCs can be phenotypically recognized and characterized in different genetically modified mice. Also, Label Retaining Cell (LRC) assays enable the detection of long-term quiescent cells in the bone marrow, a signature for stemness (Wilson et al., 2008). In the end, proof still has to be shown that the phenotype observed corresponds to a stemness capacity, but all the preliminary experiments can be carried out with much lighter and quicker protocols than bone marrow reconstitutions.

The cancer stem cell hypothesis:

* Theoretical definition:

Following a parallel trend of thought to the one of the physiological stem cell field, Cancer Stem Cells (CSCs) have been proposed as a hypothesis to describe and explain cancer initiation and progression: CSCs are defined as a subset of cells of the primary tumor that is responsible for the initiation and the maintenance of the disease. A single CSC is thought to have the capacity to form a whole new tumor when transplanted into a healthy and compatible recipient, while the other subsets of the tumor are non-tumorigenic (Figure 8 A.). CSCs are described as self-renewing cells that can stay quiescent. They have now been reported in many cancers such as breast, colon and prostate carcinomas (Al-Hajj et al., 2003), (Ricci-Vitiani et al., 2007), (Collins et al., 2005), brain tumors (Singh et al., 2004) and leukemia (Lapidot et al., 1994). Some cases still remain to be unequivocally confirmed, particularly in solid tumors. Others, like acute myeloid leukemia are now unanimously acknowledged (Lapidot et al., 1994).

CSCs sometimes derive from physiological stem cells or progenitors, like in Acute Myeloid Leukemia (AML), deriving from myeloblasts (Bonnet and Dick, 1997) or in intestinal cancer, deriving from crypt stem cells (Barker et al., 2009). CSCs can also originate from

differentiated cells, which re-acquired stemness traits like in multiple myeloma, derived from B lymphocytes (Kyle and Rajkumar, 2008). The re-acquisition of stem cell characteristics is carried out *via* chromosomal re-arrangements, epigenetic deregulations or mutations that lead to the upregulation of "stemness genes" such as *NANOG* or *OCT4*, as recently shown for lung cancer (Chen et al., 2008).

* Experimental definition:

The only unequivocal proof for stemness of human CSCs remains the ability for a cancer cell to seed tumors *in vivo* as a xenograft in immuno-deficient mice. A wide variety of such mice now exist on the market; also, numerous ways of implanting human cancer cells in mice have been described. A recent paper demonstrated that such variability in functional assays could be misleading: depending on the mouse strain and on the xenograft model, different results can be obtained using the same starting material (Quintana et al., 2008). This paper points out the difficulty to study human cells in general: scientists are bound to use xenograft models for any *in vivo* functional assay and xenograft models are always, by definition, artificial. However, to date, there is no other ethically acceptable way to functionally study human cancers. It is hence crucial to keep in mind that the results obtained by such models are to be thoroughly questioned and confronted to patient data in order to be proven valid.

After discovering that neural stem cells, but not differentiated neurons can grow *in vitro* as spheres (Bez et al., 2003), several groups transposed this "sphere assay" to stem cells and CSCs. It is currently proposed that CSCs can also be distinguished from the other tumor cells by their ability to grow *in vitro* as spheres: for instance, mammospheres (Dontu et al., 2003) and intestinal spheres are described as tools to detect breast and intestinal CSCs (Sato et al., 2009), (Fang et al., 2010). However, the validity of such assays for the discrimination of CSCs from other tumor cells often remains to be formally shown. For the study of CSCs, *in vitro* spheroid assays are therefore most of the time accompanied by *in vivo* experiments

CSCs are thought to be resistant to classical systemic chemotherapy and are therefore held responsible for tumor relapse (Reya et al., 2001), (Trumpp and Wiestler, 2008): their specific eradication within the tumor mass is mandatory for providing patients with relapse-free treatments. Therefore a search for CSC markers is carried out in many laboratories (Trumpp and Wiestler, 2008). Some markers have putative functions in carcinogenesis while others remain solely descriptive. For instance, it was proposed that

breast cancer stem cells display a lineage^{low}/CD44^{high}/CD24^{low} cells surface phenotype (Al-Hajj et al., 2003). The receptor for hyaluronate CD44 was reported as enhancing motility, invasion and survival, while CD24's role remains unclear (Keysar and Jimeno, 2010). Some cell surface markers are involved in several cancers: CD44 is a positive marker for both breast and prostate CSCs while Prominin-1 or CD133 describes brain and pancreatic CSCs (Singh et al., 2004). Lgr5 was recently shown to be a marker for both physiological and cancer stem cells in intestinal cancer (Barker et al., 2009). CD47 allowed the elegant identification of bladder CSCs (Chan et al., 2009), (Chan et al., 2010). Enzymatic activity can also allow the detection of CSCs: for instance, ALDH1 activity depicts breast CSCs (Ginestier et al., 2007). The capacity to evacuate cytotoxic drugs like Hoechst by ABC transporters (side populations) is also commonly used as a CSC detection tool, like recently shown in small-cell lung carcinoma (Salcido et al., 2010). Eventually, as in physiological stem cells, Label Retaining Cell (LRC) assays allow the detection of CSCs, taking advantage of their capacity for quiescence, as shown very elegantly for breast cancer (Pece et al., 2010).

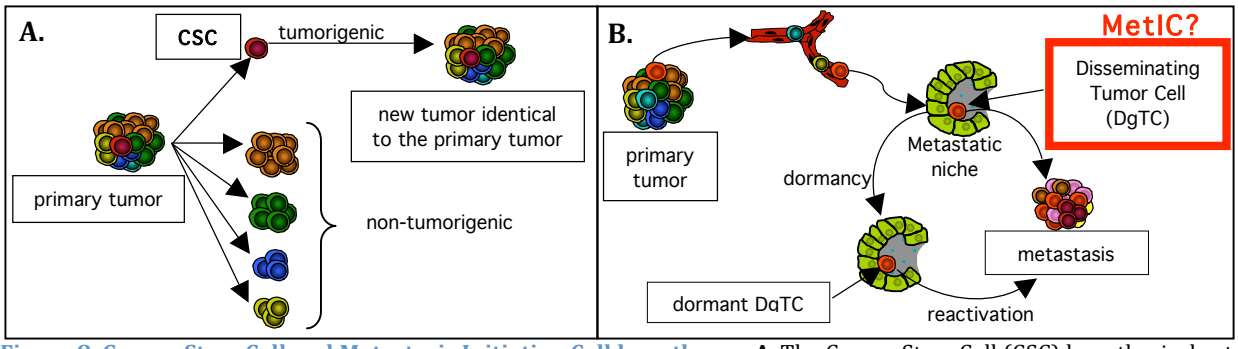

Figure 8. Cancer Stem Cell and Metastasis Initiating Cell hypotheses. **A**. The Cancer Stem Cell (CSC) hypothesis: best examples were uncovered in leukemia. **B**. The Metastasis Initiating Cell (MetIC) hypothesis: some Disseminating Tumor Cells (DgTCs) can act as MetICs. However, no MetIC has been identified to date. Adapted from Trumpp and Wiestler,

2.2.3 Metastasis Initiating Cells

As a parallel to the Cancer Stem Cell hypothesis, Metastasis Initiating Cells or MetICs are believed to be able to initiate and maintain metastases. They are thought to either directly proliferate into overt metastases upon arrival to the target organ in the metastatic niche, or to be able to stay dormant until reactivation, causing a delayed metastatic relapse (Figure 8 B.), (Pantel and Brakenhoff, 2004). One single MetIC might be able to initiate metastasis, as shown by the clonal origin of secondary tumors (Talmadge, 2007). However, no MetIC was identified so far.

A series of functional traits are mandatory for MetICs: they must be able to survive in the primary tumor, to go through all the different metastatic cascade steps: invasion, intravasation, survival in the circulation, extravasation, seeding, and colonization (see chapter 2.1). Such requirements are probably to be found in very rare cells that succeeded to accumulate all the necessary genetic alterations. The rareness of MetICs is also suggested by metastatic simulations with human cancer cell lines in mice, where only 1% of cells directly injected in the circulation can seed and grow into xenografted metastases (Luzzi et al., 1998).

CSCs are known to be resistant cells, capable of self-renewal; both characteristics are also required for metastasis initiation. Moreover, the link between invasiveness and CSCs was uncovered in a 2008 study, which shows that breast tumor cells undergoing EMT acquire a cancer stem cell phenotype (Mani et al., 2008). CSCs thus seem to have a predisposition for metastatic capabilities. This suggests that MetICs could be derived from CSCs. However, it cannot be ruled out that some other types of invasive tumor cells, accumulating numerous alterations through time, might be responsible for metastasis initiation and not CSCs. To conclude, it is still unclear whether MetICs derive from CSCs or from other invasive tumor cells.

Most cancer patients die from their metastases and not from their primary tumor: therapeutic targeting of MetICs should therefore be the priority. Unfortunately, to date, almost nothing is known about these still hypothetical cells. Many research groups are starting to screen for markers that could discriminate between metastatic and non-metastatic cells. For instance, it was shown that pancreatic cancer cells displaying CD133 and the chemokine receptor CXCR4 are able to form liver metastases in mice while other tumor cells cannot (Hermann et al., 2007). In liver cancer, $CD90^+/CD44^+$ tumor cells demonstrate an aggressive phenotype leading to metastatic lesions in the lung. Blockade of CD44 prevents the formation of local but also metastatic lesions by $CD90^+$ cells (Yang et al., 2008). In inflammatory breast cancer, $ALDH1^+$ cancer cells are proposed as mediators for metastasis and are associated with early metastasis and decreased survival (Charafe-Jauffret et al., 2010). Recently, CD26 expression has been shown to correlate with metastasis occurrence in colorectal cancer. Furthermore, the authors claim that $CD133^+/CD26^+$ tumor cells are capable of initiating metastases when injected into the caecum wall of xenografted mice, while $CD133^+/CD26^-$ cells are not (Pang et al., 2010).

As a conclusion to this chapter, the Metastasis Initiating Cell hypothesis is a very exciting theory since it proposes to take the stem cell and CSC concepts a step further to try to understand the initiation of metastases in cancer patients. However, no MetIC has ever been identified so far, and if some protein expressions are starting to be associated with metastasis occurrence, very little is known about the few cells that are able to initiate metastasis.

However, the metastatic cascade model for metastasis proposes that MetICs must be found, at least at some time point during disease development, among the pool of Disseminating Tumor Cells (DgTCs) (see chapter 2.1). The next chapter is giving an overview on what is currently known about DgTCs.

2.3 Disseminating tumor cells

Carcinoma Disseminating Tumor Cells (DgTCs) are tumor cells that evaded from the primary neoplasm and disseminated throughout the body. They are detectable in non-epithelial compartments (blood, lymph nodes or bone marrow) using epithelial specific markers such as CYTOKERATINS (CK) or carcinoma associated markers such as EPITHELIAL CELL ADHESION MOLECULE (EPCAM) (Braun and Pantel, 1999), (Pantel et al., 2009). DgTCs can be divided in three different groups according to their location in the body: Circulating Tumor Cells (CTCs) are found in the blood, Lymph Node Tumor Cells (LNTCs) are located in the lymph nodes, and Disseminated Tumor Cells (DTCs) are detected in the Bone Marrow (BM) of carcinoma patients. Various clinical studies tend to show that the presence of DgTCs in carcinoma patients correlates with the probability for these patients to undergo metastasis or metastatic relapse. Different approaches were conducted for the analysis of each type of DgTCs; the most prominent results are depicted in the next paragraphs.

2.3.1 Circulating Tumor Cells

Contrary to LNTCs or DTCs, CTCs are painlessly and non-invasively collectable from carcinoma patients *via* simple phlebotomies. They are therefore much more studied than the other DgTCs. It is estimated that, per gram of primary tumor, 1 million tumor cells are released daily in the blood circulation (Chang et al., 2000). Nevertheless, CTCs are very rare cells: they usually represent not more than 1 out of 100 million of normal blood cells in patients with metastatic disease. The study of CTCs is therefore very challenging.

Methods for CTC isolation:

CTCs are very rare cells. Their study is therefore closely dependent on the development of appropriate technologies. Encouraging results associating CTCs with metastatic progression in patients with advanced disease have lead to the Food and Drug Administration (FDA) approval of the CellSearch™ system. The **CellSearch™ system** is a semi-automated system, which uses EPCAM-antibody coupled ferrofluids to enrich for CTCs. The cells are subsequently stained for CK (positive marker), the common leukocyte antigen CD45 (negative marker) and a nuclear dye such as DAPI. It allows the analysis of 7.5 mL of blood per patient. Typically, CTCs are detected in half of M1 stage patients with an average yield of

approximatively 1 CTC/mL of blood and a purity of 0.1%. Its use has been FDA approved for metastatic breast, colon and prostate cancers.

Various non-FDA approved techniques for the isolation of CTCs have also been established in parallel, for various applications. Most methods use similar systems as the CellSearch™ system. For instance, the **CTC-chip microchip** is a recently established microfluidic platform, which consists of an array of anti-EPCAM antibody –coated microposts (Nagrath et al., 2007). Tumor cells are identified by subsequent CK/CD45/DAPI staining, as in the CellSearch™ system. However, the high detection rate (up to 100% positive M-1 patients), the high yield (50 CTCs/mL of blood) and the sometimes-low purity (between 1% and 80%) warrant further investigations for its use in the clinic. Along the lines of the CellSearch™ system, a new automated immunomagnetic separation technology, the **MagSweeper,** also allows to positively enrich for $EPCAM^+$ CTCs (Talasaz et al., 2009). Also, the **Laser scanning cytometry Maintrac®**, a specialized laser scanning cytometer, sorting $EPCAM^+$ cells, combines microfluidic technologies to microscopy, allowing morphological analysis of single positive cells (Pachmann et al., 2008). However, the abnormally high detection rates of the system warrant further investigations for its use in the clinic. Similarly, the **Ikonoscope®** and the **Ariol® systems** are slide-based automated scanning microscopes using EPCAM as a positive marker. They allow subsequent immunocytochemical analyses (Ntouroupi et al., 2008). Some other technologies are based on size, like **ISET**, which utilizes membrane filters to isolate CTCs from smaller haematopoietic cells (Wong et al., 2006). However, the size-range of different tumor cells is highly variable and sometimes overlap with that of normal blood cells. It was also recently proposed that based on the supposed invasive properties of CTCs, the tumor cells can be isolated using a **Collagen Adhesion Matrix (CAM)** assay: the ingestion of fluorescent CAM *in vitro* by CTCs and subsequent EPCAM/CD45 immunostaining could help to isolate CTCs from other blood cells (Lu et al., 2010). Eventually, some CTC isolation or analysis methods are more indirect. For instance, the **Adnatest** is a method, which utilizes RT-PCR to identify cells expressing the putative transcripts of tumor-specific genes following immunomagnetic separation of MUC1/HER2/EPCAM triple positive cells (Fehm et al., 2009). However, this test does not quantify the number of CTCs since transcripts could be coming from 1 or hundreds of tumor cells. Also, the **EPithelial Immuno-SPOT (EPISPOT) assay** detects the presence of CTCs based on released or secreted proteins during 48 hours of short-term culture, after the depletion of CD45-positive cells (Alix-Panabieres et al., 2009). Finally, two studies propose

that CTCs express the Folate Receptor and might be successfully detected using **fluorescent Folate molecules** (He et al., 2008), (Galanzha et al., 2009).

Most of these techniques are relying on the expression of EPCAM by circulating cancer cells. However, recent papers indicate that CTCs frequently undergo EMT (Aktas et al., 2009) and might loose the expression of EPCAM or of other epithelial specific markers, at least partially (Muller et al., 2010). This could explain why some metastatic cancer patients are detected negative with the CellSearch™ system. More unbiased strategies, such as depletion of the haematopoietic cells surrounding the tumor cells might be considered. Also, very few existing techniques allow the isolation of viable CTCs, which is crucial for the development of functional studies.

Clinical significance of CTCs:

Most CTC studies focus on metastatic (stage M1) carcinoma patients, since more CTCs are observed than at earlier stages. CTCs found in metastatic carcinomas usually range between 0 up to 10000 cells per 7.5 mL of blood using the FDA approved CellSearch™ system (Allard et al., 2004). Not all metastatic patients show CTCs: still using the CellSearch™ system, only 57% of prostate, 37% of breast, 30% of colorectal and 20% of lung M-1 cancer patients were diagnosed with more than 2 CTCs per 7.5 mL in a cohort of 1000 patients (Allard et al., 2004). The presence of tumor cells in the blood of M1 carcinoma patients was found to correlate with decreased relapse free survival and decreased overall survival in many cancers such as breast (Cristofanilli et al., 2007), prostate (de Bono et al., 2008) and colon (Cohen et al., 2009), (Figure 9). The number of CTCs in M1 breast cancer patients was even found to be a better indicator of disease progression than traditional imaging techniques such as computed tomography and magnetic resonance imaging (Budd et al., 2006).

Detection of CTCs in earlier tumor stages (non-metastatic or M0) is also possible but it remains a challenge because these patients have very low CTC counts: between 0 and 5 cells in 10 mL of blood (Pantel et al., 2009). These very low numbers might explain the variability of the results obtained, ranging from 10% to 100% positive findings in comparable groups of patients (Nagrath et al., 2007), (Stott et al., 2010). Nevertheless, recent results indicate that the detection of CTCs before neoadjuvant chemotherapy is an independent prognostic factor predicting overall survival in M0 breast cancer patients; it was found that the presence of even a single CTC in 7.5 mL of blood correlates with an increased risk for

metastasis development (Bidard et al., 2010). Overall, the clinical relevance of CTCs in non-metastatic patients still needs to be evaluated in larger multicenter trials.

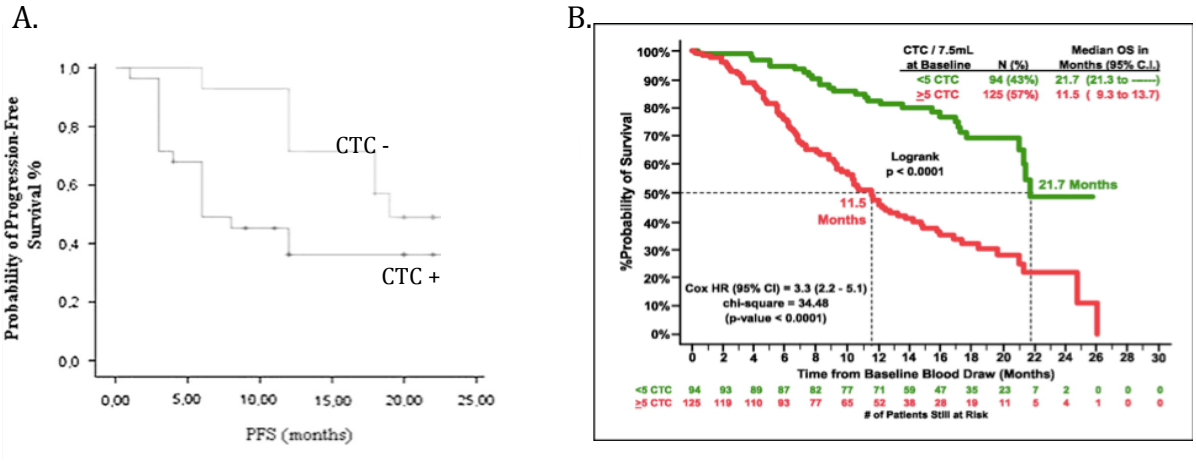

Figure 9. CTC Kaplan-Meyer curves of **A.** breast metastatic patients (Gradilone et al., 2011) and **B.** prostate metastatic patients (de Bono et al., 2008) according to their CTC status. CTC- patients have less than 5 CTCs per 7.5 mL of blood, while CTC+ patients have 5 or more than 5 CTCs per 7.5 mL of blood. CTC+ patients have drastically reduced survival probabilities.

2.3.2 Lymph Node Tumor Cells

LN resection is invasive and can only be performed by surgery. However, with the advent of the Sentinel Lymph Node (SLN) biopsy technique, lymphatic spread is systematically assessed during the staging of carcinoma patients (see the international Tumor Node Metastasis, or TNM classification). Lymph node metastasis is one of the most decisive prognostic observations and often guides the surgeon to the appropriate therapy. LNTCs are disseminated cells found in the LN, before the development of overt LN metastasis: in the literature, they are often referred to as LN micrometastases or LN isolated tumor cells (ITCs) (Cserni, 2008).

Methods for LNTC isolation:

Most LN resections are kept for pathologists in order to evaluate the lymphatic spread of the disease. A frozen section procedure is commonly employed (which takes less than 20 minutes), so that if cancer cells are detected in the lymph node, a further LN dissection can be performed. Frozen section procedures unfortunately kill any DgTCs present in the LN biopsy. Therefore, functional studies of LNTCs, requiring live intact tumor cells, remain out of reach for research laboratories.

Clinical significance of LNTCs:

The 2003 edition of the Tumor-Node-Metastasis (TNM) classification uses 2.0 mm as the cutoff between micro- and macrometastases and 0.2 mm as the cutoff for ITCs. In daily practice, 12% patients with operable breast cancer have micrometastases or ITCs in their SLN (van Rijk et al., 2006). However, the identification rate of ITC or micrometastases depends on the employed protocol (CK immunostaining, Reverse-Transcriptase Polymerase Chain Reaction or RT-PCR, etc…) and may vary substantially. More importantly, the prognostic significance of micrometastases and ITCs is uncertain. For instance, in colorectal cancer, it was recently concluded that the presence of LNTCs does not correlate with a decreased survival of T1-T4, N0, M0 stage patients (Uribarrena-Amezaga et al., 2010). In gastrointestinal cancer, a few groups found a prognostic relevance for ITCs (Matsuda et al., 2004) but this was denied in a more recent paper (Fukagawa et al., 2009). For breast and prostate carcinomas, no decisive paper suggests a prognostic role for LN micrometastasis and clinicians stay doubtful (Rutgers, 2008).

2.3.3 Bone marrow Disseminated Tumor Cells

Bone marrow (BM) biopsies can be performed during or independently of surgery, using an aspiration trocar. BM sampling is an invasive and painful procedure and, even though it is routinely performed on patients with haematologic malignancies, it is very rarely included in carcinoma patients' medical care.

Methods for DTC isolation:

Disseminated Tumor Cells (DTCs) are usually isolated from BM aspirates by Ficoll density gradient and subsequent immunostaining of the mononucleated BM cells on cytospins. Tumor cells are defined by their negativity for the common leukocyte antigen CD45, and positivity for a pan-CK antibody. Because of the use of various pan-CK antibodies and the manual Ficoll + cytospin technique for the isolation of DTCs, no standardized method is currently applied for the detection of DTCs (Braun et al., 2005), even though a European consensus was reached, defining technical standards to use for the determination of DTCs in the bone marrow (Fehm et al., 2006). It is also possible to use the EPISPOT assay as well as the MAINTRAC® cytometer to quantify DTCs, but this is seldom the case.

Clinical significance of DTCs:

The presence of BM Disseminated Tumor Cells (DTCs) in stage M0 carcinoma patients was found to strongly correlate with a decreased relapse free survival and a decreased overall survival (Figure 10). This was shown for many cancers, including breast (Pantel and Woelfle, 2005), prostate (Morgan et al., 2009) and colorectal (Leinung et al., 2000) cancers. The largest database on the association between DTCs in the BM and clinical outcome was carried out for breast cancer: in a pooled analysis of 4703 patients, the presence of DTCs was found to be predictive for skeletal metastases and metastases in other organs (Braun et al., 2005). DTCs can persist in the BM many years after the surgery; the persistence of DTCs is also associated with an increased risk for late metastatic relapse (Wiedswang et al., 2004), (Janni et al., 2005). As for CTCs, DTCs are very rare cells: they are found in 20-40% of N0-M0 carcinoma patients. They are usually present at a very low frequency: between 1 and 10 cells per million BM mononucleated cells (Alix-Panabieres et al., 2007). BM aspirates positivity does not correlate with CTC positivity in the blood, as shown in an M0 breast cancer study (Fehm et al., 2009): the two types of DgTCs might have different dissemination kinetics, and represent different subpopulations of disseminating cells. Indeed, the bone marrow might be a homing organ for DTCs, while blood analyses only allow a "snapshot" of tumor cell dissemination. This would explain why more M0 patients are DTC positive than CTC positive (Benoy et al., 2006). Also, in M0 breast cancers, DTCs but not CTCs provide prognostic information (Wiedswang et al., 2006). Noticeably, DTCs in M1 patients are very rarely studied.

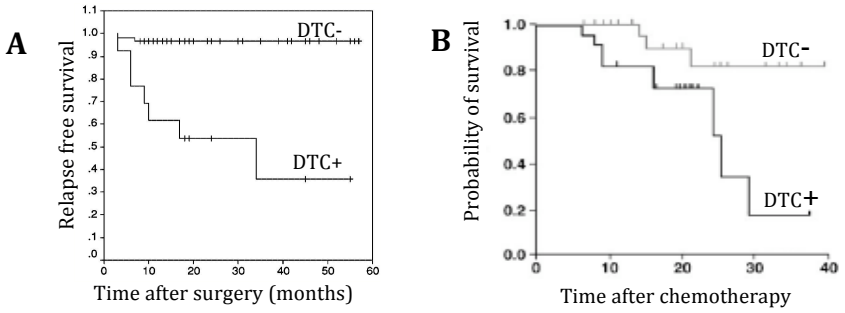

Figure 10. DTC Kaplan-Meyer curves. Examples of clinical studies showing the correlation between the presence of Disseminated Tumor Cells (DTCs) and the probability for patients to undergo metastasis. **A**. Colorectal carcinoma (Leinung et al., 2000) **B**. Breast carcinoma (Pantel and Woelfle, 2005).

2.3.4 Molecular characterization of Disseminating Tumor Cells

Most studies focus on breast cancer CTCs and DTCs. Both phenotypic (see Figure 11) and genomic characterizations have started to be carried out.

Phenotypic characterization of DgTCs:

* CSC characteristics:

Despite a considerable phenotypic heterogeneity in DgTCs, some groups tried to identify the expression of some antigens *via* immunocytochemical double or triple stainings. Importantly, DTCs were found to display phenotypic CSC characteristics. For instance, 90% of stage M0 DTCs appear to be quiescent (Figure 11) (Pantel et al., 1993). This finding is further corroborated by the fact that half of DTC-positive patients remain tumor free over a 10-year follow-up period (Braun et al., 2005). Furthermore, DTCs show resistance to systemic chemotherapy (Naumov et al., 2003), (Wimberger et al., 2007). In addition, in breast cancer, 72% of the DTCs display a putative CSC ($CD44^+/CD24^-$) cell surface phenotype (Balic et al., 2006).

As for CTCs, it is not settled whether the cells found in M1 patients are proliferative or quiescent cells. Studies show between 1% and 80% of Ki67 positive CTCs depending on the type of cancer and the progression of the disease (Muller et al., 2005), (Stott et al., 2010). However, some subpopulations of CTCs seem to display CSC markers: in metastatic breast cancer, it was recently shown by immunofluorescence microscopy that on average, 35% of CTCs have a $CD44^+/CD24^{-/low}$ cell surface phenotype and that 17% of CTCs have a $CD24^{-/low}/ALDH1^+$ cell surface phenotype (Theodoropoulos et al., 2010): CD44, CD24 and ALDH1 are markers that were linked to putative breast CSCs (see chapter 2.2.2, (Al-Hajj et al., 2003), (Ginestier et al., 2007)).

* Additional characteristics:

HER2, UROKINASE PLASMINOGEN ACTIVATOR RECEPTOR (UPAR) and EXTRACELLULAR MATRIX METALLOPROTEINASE INDUCER (EMMPRIN) were also identified on CTCs (Figure 11) (Meng et al., 2006), (Hemsen et al., 2003), (Reimers et al., 2004). In particular, the *HER2* oncogene amplification has become the most prominent target for biological therapies in breast cancer and a humanized anti-HER2 monoclonal antibody (trastuzumab), was approved by the FDA. Some studies show that the HER2, but also the ESTROGEN RECEPTOR (ER) and the PROGESTERONE RECEPTOR (PR) molecular statuses are not conserved

between the primary tumor and DgTCs, or between different types of DgTCs, suggesting different origins and/or clinical relevance of each (Riethdorf et al., 2010), (Fehm et al., 2009). Moreover, the detection of *HER2*-amplified CTCs correlates significantly with disease-free and overall survival (Wulfing et al., 2006). In a multicenter trial (GUEPARQuattro), HER2 overexpression in CTCs was found exclusively in ductal carcinomas and was associated with high tumor grade (Riethdorf et al., 2010).

Furthermore, EMMPRIN expression enhances ECM degradation *via* the induced expression of MMP1, 2 and 3. Its expression by 90% of DTCs in the BM (Reimers et al., 2004) confirms that these DgTCs already acquired invasive properties. Another characteristic of DTCs is the deficient expression of MAJOR HISTOCOMPATIBILITY COMPLEX (MHC) CLASS I molecules (Pantel and Brakenhoff, 2004), which participates in T-lymphocyte-mediated tumor cell recognition. This might explain how DTCs can avoid recognition by the immune system for decades.

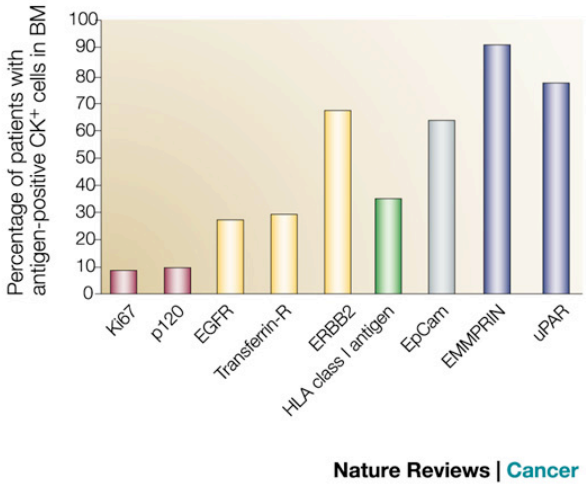

Figure 11. Phenotypic characterization of DTCs in the BM of breast cancer patients. Proliferation-associated proteins are in red (Ki67, p120), growth factor receptors are in yellow (EPIDERMAL GROWTH FACTOR RECEPTOR EGFR, and TRANSFERRIN-R), immune response antigens are in green (HUMAN LEUKOCYTE ANTIGEN HLA class I antigen), adhesion molecules are in grey (EPITHELIAL CELL ADHESION MOLECULE or EPCAM) and proteases or proteases-associated proteins are in blue (EXTRACELLULAR MATRIX METALLOPROTEINASE INDUCER or EMMPRIN and UROKINASE PLASMINOGEN ACTIVATOR RECEPTOR or UPAR). Figure taken from Pantel and Brakenhoff, 2004.

More recently, TWIST1, an important transcription factor of the EMT, was identified on DTCs; its expression by M0 breast-DTCs seems to correlate with the occurrence of distant metastasis and local progression, even in pre-treatment BM samples (Watson et al., 2007).

This finding hints that DTCs might have undergone EMT. Also, the full-length CK19 is surprisingly secreted by DTCs of breast cancer patients, as found with the EPISPOT assay (Alix-Panabieres et al., 2009).

Genomic characterization of DgTCs:

Thanks to the development of single cell amplification methods, genetic analyses of DTCs have become feasible. Most data are based on metaphase comparative genomic hybridization (CGH), which enables to screen the whole genome for chromosomal copy number gains and losses. It was shown by the group of Christoph Klein, that in breast, prostate and oesophageal cancers, DTCs generally display fewer genetic abnormalities than matched primary tumours: while primary tumours often accumulate chromosomal gains and losses typical for the respective type of tumour, DTCs displaying these typical changes are mostly undetectable at the time of primary surgery (Schardt et al., 2005), (Stoecklein et al., 2008), (Weckermann et al., 2009) . Later, when manifest metastasis is diagnosed, such changes are found in almost all DTCs isolated at this stage. Comparative analysis with the primary tumour has revealed that these changes were not transmitted from the primary tumour to the manifest metastasis but must have been acquired independently, supporting the idea of a parallel progression model for metastasis (see chapter 2.2.1) (Stoecklein and Klein, 2009).

However, these first phenotypic and genomic results still need to be confirmed by other groups.

2.3.5 Functional analysis of Disseminating Tumor Cells

Only 2 studies on DgTCs' function have been published. In the first one, Christoph Klein's group attempted to characterize the tumorigenicity of DTCs. Using a murine transgenic model of breast cancer, the authors transplanted disseminated tumor cells collected from the BM of diseased mice into wild type recipients. They report the growth of carcinosis in the injected bones, suggesting that dormant DTCs could be released from dormancy when transplanted into a fresh host. However, no other group has confirmed these results since then (Husemann et al., 2008).

A second study attempted to study CTCs *in vivo* by using a metastatic cell line-based xenograft model (Ameri et al., 2010). The authors showed the presence of CTCs in their

metastatic xenografted mice and demonstrated that cell line CTCs display greater *in vitro* colony formation during chronic hypoxia than the parental cell line. They also claim that cell line xenografted CTCs grow faster and metastasize faster than parental xenografts. However these last results are based on a very low number of mice and the data on metastasis are not shown (Ameri et al., 2010).

As a conclusion for this chapter, DgTCs are studied for some years in the clinic, but the scientific knowledge about them is still scarce. The idea that the presence of detectable DgTCs in the body (mostly CTCs and DTCs) correlates with metastasis occurrence, or with overall survival, fits very well with the metastatic cascade theory (see chapter 2.1.1): metastasis has to occur *via* dissemination, so detectable dissemination in patients must correlate with an increased probability for metastasis to successfully develop. However, it should be noted that there is only a correlation between the presence of DgTCs and metastasis occurrence. Some carcinoma patients have DgTCs but do not develop metastases; therefore, not all DgTCs might be able to initiate metastasis. Along these lines, a recent report showed that all CTC fragments found in the blood (large tumor particles, as well as small tumor fragments) have the same prognostic value for patient survival as live, nucleated CTCs (Coumans et al., 2010). It is very unlikely that tumor cell fragments can themselves initiate metastasis, hence the highest cautiousness to observe when confronted with seducing correlations… Last, but not least, the metastatic potential of DgTCs has not been assessed yet, mostly due to the lack of suitable xenograft *in vivo* models.

2.4 The bone marrow niche

Out of the three DgTC compartments, the bone marrow (BM) has raised considerable interest in the last decades. It is a dynamic microenvironment with a high concentration of growth factors and cytokines necessary for haematopoiesis, making it a permissive zone for cancer cell homing, survival an possibly self-renewal. Indeed, the BM withholds one of the best-characterized stem cell microenvironment: the Haematopoietic Stem Cell (HSC) niche. Two such HSC niches are described in the literature: the endosteal niche and the vascular niche.

On the one hand, the endosteal niche serves as a stem cell reserve, which controls HSC maintenance and activation. It is located at the endosteum of the trabecular zone of long bones (Wilson and Trumpp, 2006). BM stromal cells (fibroblasts, adipocytes, endothelial cells and osteoblasts) are the major source of growth factors and cytokines in the BM niches. N-CADHERIN$^+$ osteoblasts seem to be necessary and rate limiting for the niche function; they are in direct contact with HSCs *via* homotypic N-CADHERIN interactions (Zhang et al., 2003), (Calvi et al., 2003). CXC CHEMOKINE LIGAND 12 (CXCL12) ABUNDANT RETICULAR (CAR) cells surround sinusoidal endothelial cells close to the endosteum, and are in direct contact with HSCs, which express its receptor, CXCR4 (Raaijmakers and Scadden, 2008). Very recently, it was shown that Nestin$^+$ Mesenchymal Stem Cells (MSCs) are also important components of the HSC niche (Mendez-Ferrer et al., 2010).

On the other hand, the vascular niche maintains a boundary between immature cells and the peripheral blood circulation. It is responsible for regulating the release of mature erythrocytes, platelets and granulocytes. Deregulation of the vascular niche can lead to the development of intra-sinusoidal haematopoiesis and the circulation of leukemic blasts, leading to the development of diseases such as primary myelofibrosis (Lataillade et al., 2008).

The BM is a dynamic environment (Figure 12, (Wilson and Trumpp, 2006)). There is a striking resemblance between the mechanisms of HSC migration and carcinoma dissemination. In particular, mobilized HSCs home back to the BM through the blood circulation in response to VERY LATE ANTIGEN 4 (VLA4), VLA5, CD26 or SELECTINS. E-SELECTIN and P-SELECTIN are similarly involved in the seeding of DgTCs in the pre-metastatic niche, enhancing tumor cell arrest and extravasation to the metastatic site (see

chapter 2.1.3). CD26 was also recently incriminated in colorectal metastasis (see chapter 2.2.2). After entering the bone marrow, HSCs specifically lodge in the HSC niche, a process requiring membrane-bound STEM CELL FACTOR (SCF), CXCL12, OSTEOPONTIN (OPN), HYALURONIC ACID, and their corresponding receptors (Wilson and Trumpp, 2006). The CXCL12-CXCR4 axis, CD44, and OPN are also involved in the lodging of metastatic cells in the metastatic niche (see chapter 2.1.3).

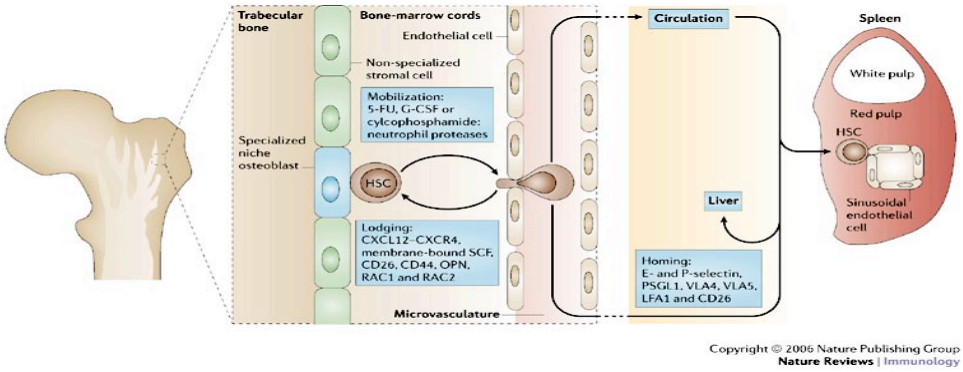

Figure 12. Mobilization and homing of Haematopoietic stem cells (HSCs). There is a striking resemblance between the mechanisms of HSC migration and carcinoma dissemination. Abbreviations: GRANULOCYTE COLONY-STIMULATING FACTOR (G-CSF), 5-fluorouracil (5-FU), VERY LATE ANTIGEN 4 (VLA4), VLA5, LYMPHOCYTE FUNCTION-ASSOCIATED ANTIGEN 1 (LFA1) STEM-CELL FACTOR (SCF), CXC-CHEMOKINE LIGAND 12 (CXCL12), OSTEOPONTIN (OPN), CXCR4, CXC-CHEMOKINE RECEPTOR 4; E-SELECTIN, ENDOTHELIAL CELL SELECTIN; P-SELECTIN, PLATELET SELECTIN; PSGL1, P-SELECTIN GLYCOPROTEIN LIGAND 1. Figure taken from Wilson and Trumpp, 2006.

Moreover, the bone marrow sinusoids form low-pressure vascular channels surrounded by a single layer of fenestrated endothelium and represent a very permissive barrier for circulating cells, such as carcinoma CTCs. DgTCs can thus easily penetrate the BM compartment. In addition, important findings show that, in haematological malignancies, leukemic cells engraft in the BM, and that a close relationship between leukemic cells and the HSC niches is established: an elegant *in vivo* confocal imaging study reported that circulating leukemic cells engraft in the BM *via* specialized vascular structures, also sheltering HSCs. These specific vascular micro-domains express CXCL12 and the engraftment of the tumor cells in the vascular niche can be prevented by the inhibition of the interaction of CXCL12 with its receptor CXCR4 (Sipkins et al., 2005). More recently, it was shown that leukemic cells usurp HSC BM niches, disrupting the behavior of normal HSCs (Colmone et al., 2008).

Last but not least, BM derived progenitors (BMDCs) have been implicated in the establishment of the pre-metastatic niche in distant organs (see chapter 2.1.3) (Psaila et al.,

2006). Their physiological presence might attract CTCs to the BM, as it is the case when they are mobilized to distant organs such as the lungs (Kaplan et al., 2005).

To conclude, the BM is a very permissive and attractive environment containing specialized stem cell niches. Mechanisms regulating the dynamics of HSC mobilization and homing resemble closely the ones ruling over metastasis. Haematological malignancies have been shown to usurp the HSC niche. Moreover, some of the cells involved in the establishment of the carcinoma pre-metastatic niche reside in the BM, and could attract tumor cells. Based on this knowledge, but also on clinical observations showing that DgTCs often reside in the BM (see chapter 2.3.3 on DTCs), current papers propose that the BM might play a pivotal role in carcinoma metastasis, creating a reservoir for disseminating tumor cells. DgTCs might stay in the BM in a quiescent state or, alternatively, mature and acquire additional metastatic traits, before being mobilized to pre-metastatic niches in other organs (Pantel and Alix-Panabieres, 2010). Only a few of the DTCs might evolve enough to become Metastasis Initiating Cells (MetICs).

3. AIM OF THE THESIS

The goal of this PhD work is to detect and characterize human carcinoma MetICs within DgTCs of carcinoma patients. Very few existing techniques allow the isolation of viable DgTCs (see chapter 2.3). Therefore, an unbiased and live DgTC isolation procedure has to be established. Since only *in vivo* assays allow unequivocal proof of stemness (see chapter 2.2), the second aim of this PhD work is to set up a functional mouse xenograft model adapted for the detection and growth of rare metastatic cells, as a read-out for metastasis initiation capacity. Eventually, since the BM might function as a reservoir for DgTCs (see chapter 2.4), a third aim is the characterization of a potential BM metastatic niche for carcinoma DgTCs.

4. RESULTS

4.1 Establishment of a novel metastatic xenograft model

In order to study the metastatic potential of Disseminating Tumor Cells (DgTCs), it is first of all necessary to have in hand an appropriate metastatic *in vivo* model: in particular, the choice of the injection site in the recipient mice (or "soil") as well as the detectability of the injected cells (or "seeds") have to be optimal.

4.1.1 Choice of a good "soil" and detectability of the "seeds"

Most metastatic *in vivo* models use intra-venous or intra-cardiac injections of tumor cells in order to mimic the dissemination of cells through a haematogenous spread (Kang and Massague, 2004). These models do not recapitulate the first steps of the metastatic cascade (invasion and intravasation, see chapter 2.1). But they are appropriate for studying cells that are already known to be able to disseminate from the primary tumor into the circulation, as it is the case for DgTCs, by definition (see chapter 2.3). However, DgTCs are very rare cells and intravenous or intra-cardiac injections might confront the tumor cells with such a strong shear stress that they might be lost shortly after being injected. Therefore, a novel metastatic xenograft model was established, more suitable for the study of rare DgTCs.

The bone marrow (BM) is a dynamic microenvironment with high concentration of growth factors and cytokines necessary for haematopoiesis, making it a permissive zone for cancer cell homing, survival and possibly self-renewal (see chapter 2.4). Also, current papers propose that the BM might constitute a reservoir for disseminating tumor cells; DgTCs are thought to mature and to acquire additional metastatic traits in the BM, before being mobilized to pre-metastatic niches in other organs (Pantel and Alix-Panabieres, 2010). Therefore, the BM niche seems to be an excellent "soil" for the screening of Metastasis Initiating Cells (MetICs) among DgTCs. In the Haematopoietic Stem Cell (HSC) field, injection of human stem cells in the BM of immuno-compromised mice is a common transplantation method (Mazurier et al., 2003). This method was therefore adapted for the xeno-transplantation of human carcinoma DgTCs in mice.

In addition, the detection of rare cells *in vivo* requires the use of very sensitive tools. In the last decades, in parallel to the fluorescence-based techniques, bioluminescence technologies developed enormously, establishing new *in vivo* detection instruments. The most sensitive one, the Xenogen device (IVIS® 200 series, Caliper) allows the detection of only a few thousand cells expressing the *FIREFLY LUCIFERASE* (*LUC*) reporter gene, in anesthetized mice (Sweeney et al., 1999), (Lim et al., 2009). On the other hand, bioluminescence is not detectable by Fluoresence Activated Cell Sorting (FACS): fluorescent reporter genes such as *ENHANCED GREEN FLUORESCENT PROTEIN* (*EGFP*) remain the main tools for *ex vivo* cell analysis (Patterson et al., 1997). Therefore, both *LUC* and *EGFP* reporter genes were used in the xenograft assay.

4.1.2 A novel intra-bone metastatic xenograft model

For the functional analysis of DgTCs, a metastatic xenograft assay was established, in which DgTCs were directly injected into the BM of host mice (Figure 13): LUC-EGFP-expressing human tumor cells were transplanted into the BM of immuno-compromised mice *via* intra-femoral injections. The engraftment and the expansion of the tumor cells was quantified in a non-invasive manner using the Xenogen imaging system ((IVIS® 200 series, Caliper) and Computed Tomography (CT-scan). The human origin of the tumors was assessed by human specific DNA detection methods. After tumor cell isolation, molecular analysis was further carried out using FACS.

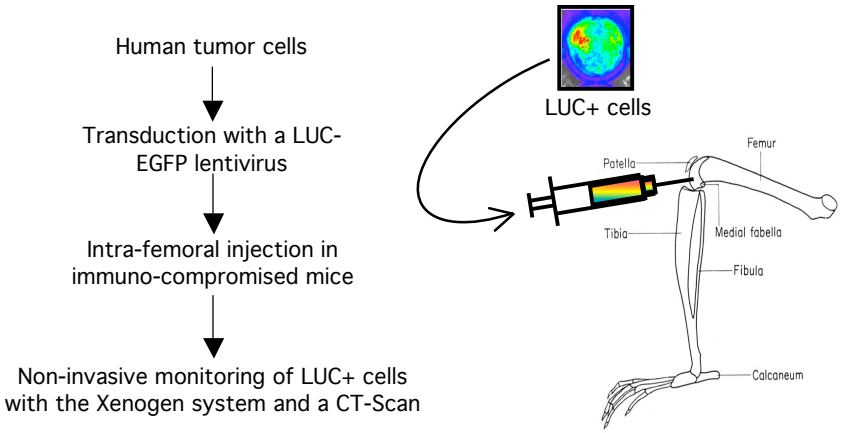

Figure 13. Scheme of the functional intra-bone xenograft assay: the LUC-EGFP+ human tumor cells are introduced into the BM of immuno-compromised mice. The engraftment and expansion of the tumor cells is monitored in a non-invasive way using the Xenogen imaging system (Caliper) and *via* the use of Computed Tomography (CT-scan). The human origin of the tumors is evaluated by human specific DNA detection methods. After tumor cell isolation, molecular analysis is further carried out using FACS.

4.1.3 Characterization of the metastatic xenograft model using MDA-MB-231 cells

This new metastatic xenograft model was first tested using the MDA-MB-231 breast cancer metastatic cell line. This cell line is derived from the ESTROGEN RECEPTOR negative (ER^-) pleural effusion of a breast adeno-carcinoma patient (Cailleau et al., 1974) and is frequently used to study breast cancer metastasis (Minn et al., 2005), (Kang et al., 2003).

Non-invasive monitoring and quantification of metastasis

MDA-MB-231 cells were infected with a high titre lentivirus in order to introduce high expressions of the *LUC* reporter gene 5.10^4 MDA-MB-231 LUC^+ cells were injected in each femur of nonobese diabetic severe combined immunodeficiency disease (NOD/SCID) mice. The detection of bioluminescent signals using the Xenogen system indicated that the tumor cells engrafted and expanded very rapidly in the host animals (Figure 14). All the injected animals developed tumors both in the lungs and in the hind limb bones, which are the two main sites of metastasis in breast cancer patients (Paget, 1889). In addition, at late stages (5 to 7 weeks after the xenograft), other sites of metastasis were detected such as the liver, the adrenal gland and the lymph nodes, which are also frequent sites of metastasis in breast cancer patients (Paget, 1889).

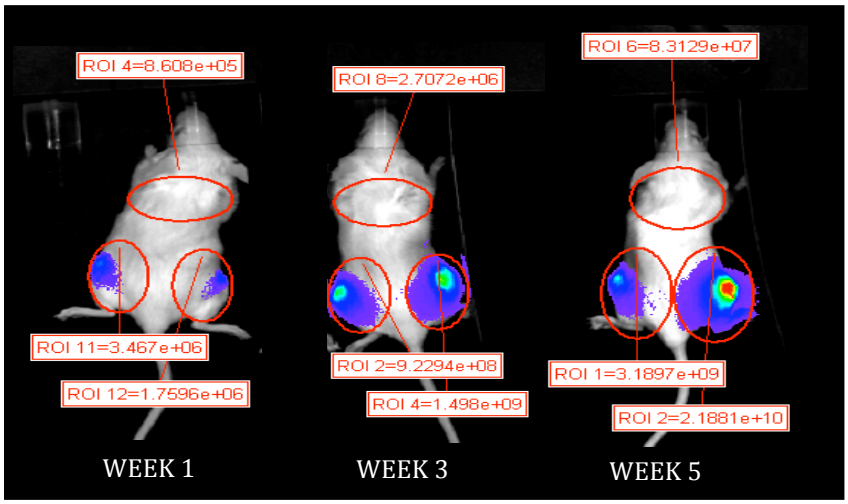

Figure 14. Detection of metastasis using the Xenogen system. NOD/SCID mice were injected intra-bone with 5.10^4 MDA-MB-231 LUC+ cells per femur and monitored weekly with the Xenogen system. The absence of colored signal in the lungs is due to the low exposure of the photographs. R.O.I. = Region Of Interest in photons per second and per cm^2.

The bioluminescent signals were quantified weekly in order to follow the expansion of MDA-MB-231 LUC+ cells in the target organs. Examples of bioluminescent signals quantified in the hind limbs (site of injection) and in the lung metastases are shown in Figure 15.

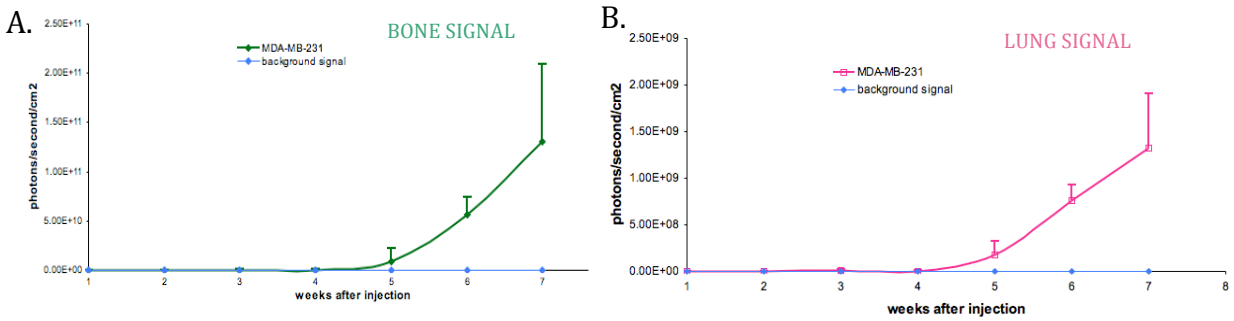

Figure 15. Quantification of metastasis using the Xenogen system. The bioluminescent signals are quantified in photons per second and per cm^2 using the Xenogen system. The mean metastatic growth of MDA-MB-231 LUC+ cells was measured weekly in **A.** hind limb bones and **B.** in the lungs of 5 NOD/SCID mice, injected each intra-bone with 5.10^4 cells/femur.

In order to monitor bone tumor growth, CT-scans were performed in a non-invasive manner, by simple radiographies (Figure 16) or by building 3 dimensional reconstructions of the hind limb bones (Figure 17). The intra-bone injection itself did not perturb the structure of the bone, since mice injected with PBS (Phosphate Buffer Saline) showed no bone lesion nor other sign of discomfort even several months after the injection (Figure 17 A.). However, the introduction of 5.10^4 MDA-MB-231 cells in the BM of NOD/SCID mice induced massive osteolytic lesions (Figure 16 B. and C., Figure 17 B.) typical of breast cancer bone metastasis (Guise and Mundy, 1998). The lesions were only observed in the hind limbs that were injected. No tumor was found in any other part of the skeleton (not shown), suggesting that bone seeking tumor cells did not disseminate away from the primary site of injection. The lesions started to be visible 3 to 4 weeks after the xenograft. Most tumors were observed at the metaphysis (extremities of the bone/trabecular zone) and rarely at the diaphysis (intermediate zone/cortical zone) of the femurs, in agreement with published data (Phadke et al., 2006). This point will be further discussed in chapter 4.2.

Similarly, lung metastatic growth was monitored by CT-scan (Figure 18). Transversal sections of the mice chests were reconstituted in order to visualize the lungs surrounded by the heart, the backbone and the ribs. Lung metastases (appearing as white cloudy dots on the sections) started to be visible 5 weeks after the injection of the human tumor cells.

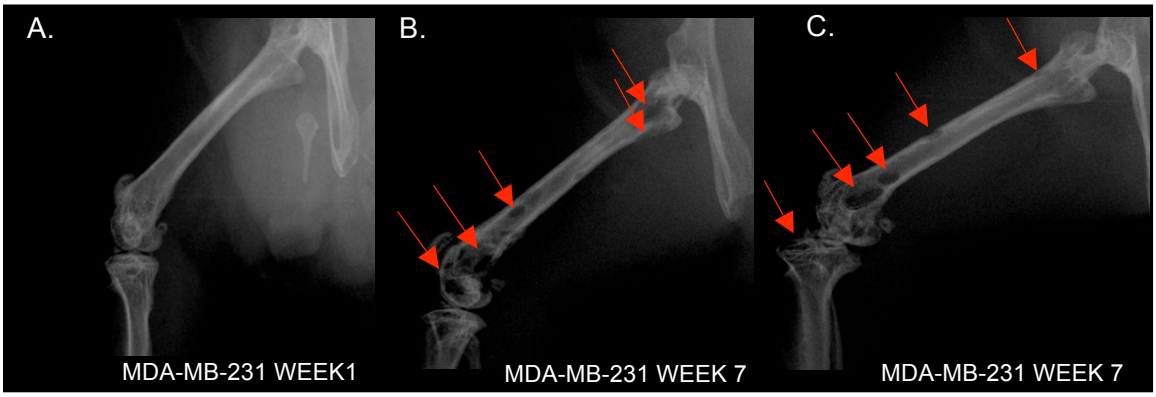

Figure 16. CT-scan radiographies of the right femurs of NOD/SCID mice **A.** 1 week and **B. C.** 7 weeks (2 experimental mice shown) after the intra-bone injection of 5.10^4 MDA-MB-231 cells per leg. The red arrows point the osteolytic lesions, typical of breast cancer bone metastasis.

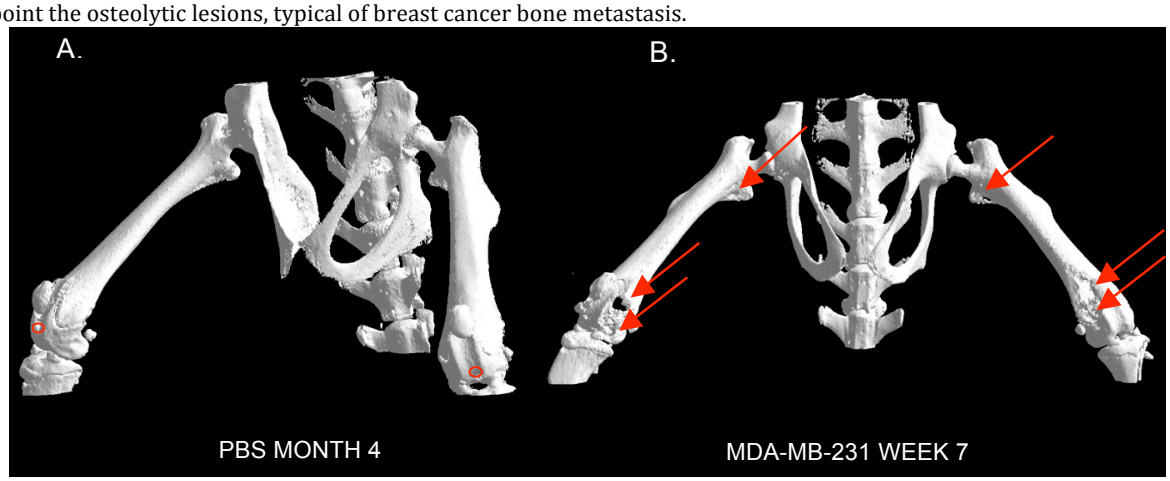

Figure 17. 3 dimensional reconstitution of CT-scans of femurs of NOD/SCID mice, **A.** 4 months after injecting PBS or **B**. 7 weeks after injecting 5.10^4 MDA-MB-231 cells per leg**. A.** The red circles show the wholes created by the needle during the surgery. No other anomaly was detected after injecting PBS intra-bone. **B.** The red arrows show the osteolytic lesions induced by the MDA-MB-231 cells.

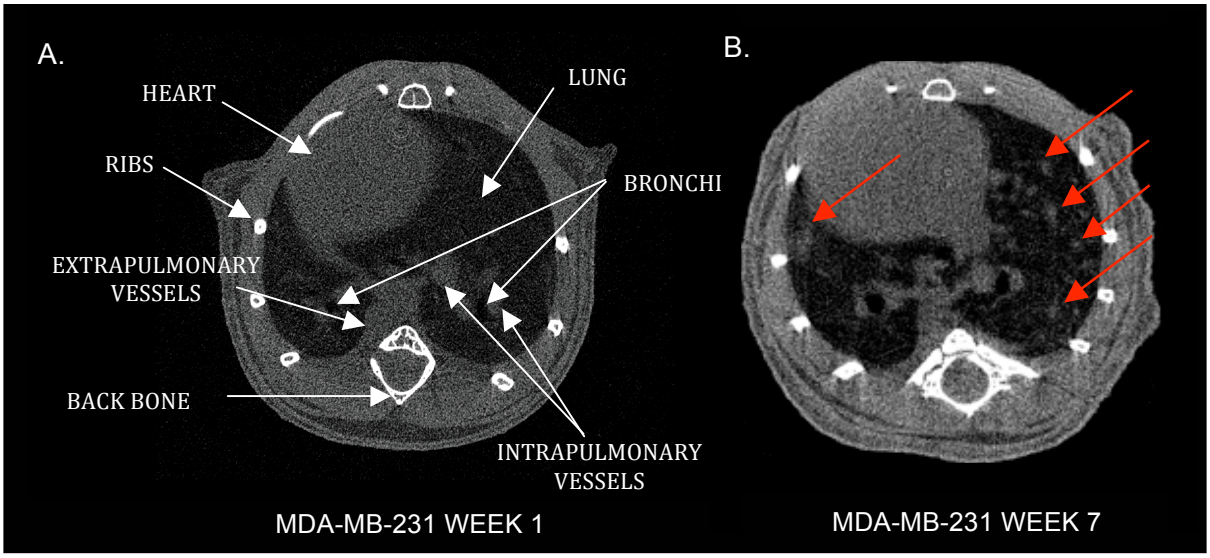

Figure 18. CT-scans of lung metastases. NOD/SCID mice were injected intra-bone with 5.10^4 MDA-MB-231 cells per femur. **A.** 1 week after the injection, the lungs appeared clean (uniformly black). **B.** 7 weeks after the injection, the lungs were invaded by lung metastases (white cloudy dots), shown by the red arrows.

Presence of DgTCs:

To test whether Disseminating Tumor Cells (DgTCs) were also present in the novel metastatic xenograft model, a screen for Circulating Tumor Cells (CTCs) was carried out.

Blood was drawn from the heart of host mice, from week 0 (time of the xenograft) until week 7 (fully metastasized state). MDA-MB-231 LUC-EGFP CTCs were detected using fluorescence microscopy or FACS. Some tumor cells were observed 1 hour after the xenograft, probably due to the injection in the BM: the introduction of a needle inside the bone marrow, might lead to partial disruption of the vasculature and to subsequent leakage into the circulation. Alternatively, the very permissive marrow sinusoids might themselves enable tumor cell dissemination at the time of the injection. Cell line CTCs were however not detected after this time-point until week 4, suggesting that the physical shedding is happening only during the first hours after the injection. Variable but growing numbers of CTCs were detectable after week 4 (Figure 19 A.).

The number of detected CTCs did not correlate with the tumor load, as reflected by the total bioluminescence quantified in the host mice (Figure 19 B.). This is in agreement with what has been reported in cancer patients (Muller et al., 2005).

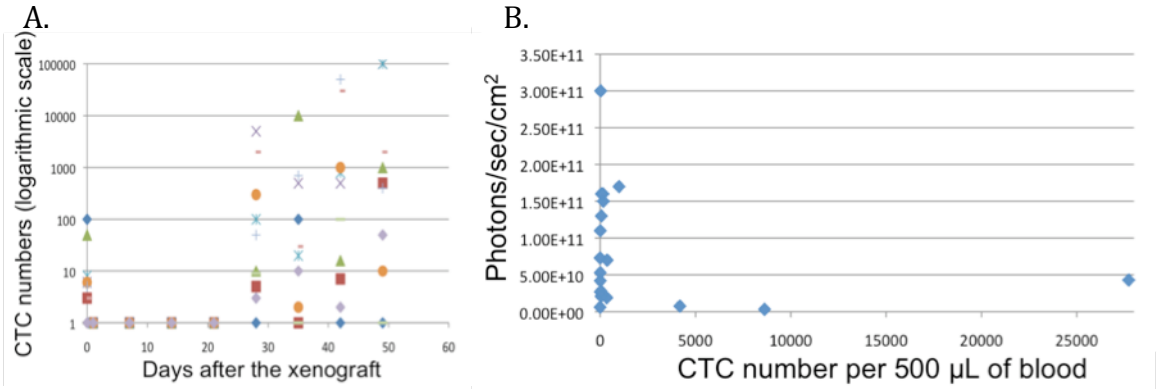

Figure 19. CTC numbers detected in recipient mice. **A.** CTC numbers detected in 500 µL of blood, according to time. Some CTCs were present 1 hour after the xenograft. However, after this time-point, no CTCs were detected until week 4. **B.** CTC numbers (per 500 µL of blood according to tumor load, evaluated by quantification of total bioluminescence (in Photons/seconds/cm²). There is no correlation between tumor load and CTC numbers.

4.1.4 Validation of the novel metastatic xenograft model using primary samples

Human tumor cell lines are derived from primary samples but may have genetically drifted, due to excessive *in vitro* and/or *in vivo* passaging. Therefore, a crucial verification needs to be done before validating the intra-bone metastatic xenograft model: can fresh primary samples, known to be tumorigenic, also grow in this system?

The group of Michael Clarke demonstrated that pleural effusions are a good source for breast cancer stem cells, as they are tumorigenic when implanted into the mammary fat pads of immuno-compromised mice (Al-Hajj et al., 2003). Using pleural effusions from breast cancer patients, the intra-bone xenograft model also allowed tumorigenesis, as shown by CT-scan and by immuno-histochemistry (Figure 20). The human origin of the tumors growing in the bone marrow was further validated by human specific quantitative PCR (see chapter 6, Materials § Methods).

However, the xeno-transplanted mice did not develop tumors at other sites than the BM. This last point might be explained by the fact that tumor cells in pleural effusions are not fully metastatic: pleural effusion cells are passively exuded by small blood and/or lymph vessels in the pleural lining and have therefore not been confronted with the last steps of the metastatic cascade (extravasatiom, seeding and colonization of a new environment).

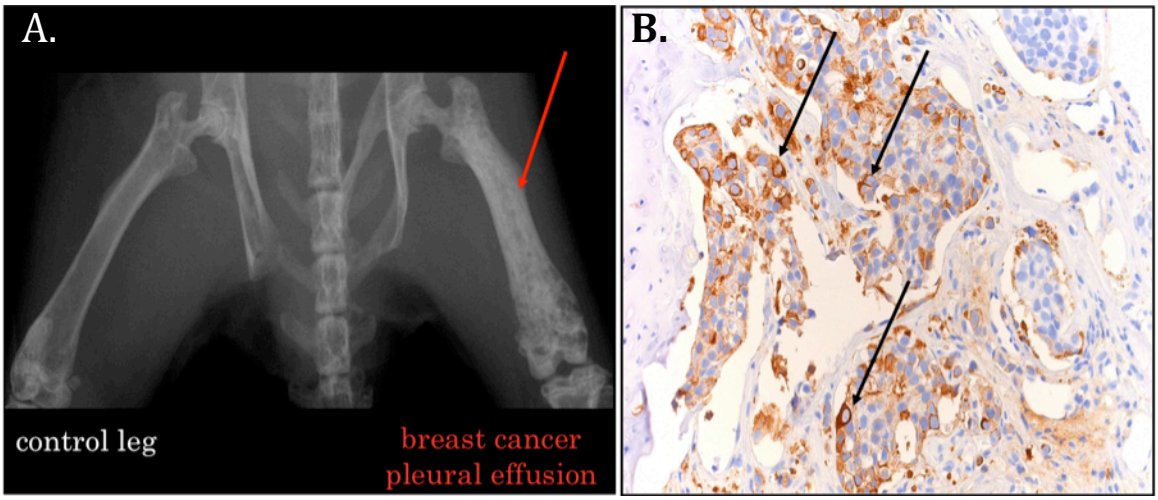

Figure 20. Pleural effeusion induced tumors. **A.** CT-Scan of a mouse injected intra-femoral with a primary sample of breast cancer pleural effusion. On the right, experimental leg injected with tumor cells, on the left, control leg, injected with PBS. **B.** Paraffin section of a mouse femur, 9 months after the xenograft of a breast cancer pleural effusion. The bone marrow section was stained with a human pan-CK antibody. The human origin of the tumor cells was further confirmed by human specific qPCR (not shown).

As a conclusion for this first chapter, the BM of immuno-compromised mice seems to act as a good "soil" for the seeding of metastatic cells. After the intra-bone injection of a breast cancer metastatic cell line (MDA-MB-231 cells), the growth of tumors was observed in many organs, usually described as metastatic sites in breast cancer. Moreover, the neoplasms could be tracked in non-invasive ways, using bioluminescence or CT-scans, allowing a long-term observation of the host animals and quantitative measurements of metastasis development. Eventually, this novel metastatic xenograft model seems not only to enable tumor cell line growth but also the development of tumor cells coming from known tumorigenic primary samples, such as breast cancer patient pleural effusions.

The BM thus seems to be a particularly favorable microenvironment for the sheltering of breast cancer metastatic cells. In order to further characterize the BM niche in the context of breast cancer metastasis, additional experiments were carried out using the novel xenograft model.

4.2 Characterization of the bone marrow metastatic niche

Recent studies from the group of David Lyden uncovered the existence of metastatic and pre-metastatic niches (see chapter 2.1.3). Notably, bone marrow-derived precursor cells play a pivotal role in the establishment of the pre-metastatic niche, preparing the foreign "soil" to shelter and feed metastatic cells (Psaila and Lyden, 2009). The bone marrow (BM) thus gathers precursor cells that are known to be involved in early metastasis initiation and could therefore constitute a good niche for carcinoma MetICs.

4.2.1 Localization of the bone marrow metastatic niche

In order to investigate the localization of a potential BM metastatic niche for human breast cancer cells, 5.10^4 MDA-MB-231 EGFP+ cells/femur were injected intra-bone into NOD/SCID mice. EGFP+ cancer cells were then visualized on cryo-sections of femurs, at different time points after the injection, by fluorescence microscopy (Figure 21).

The sections revealed single disseminated tumor cells 1 day after the xenograft, micro-metastases one week later and whole tumor masses 2 weeks after the injection (Figure 21). Long bones can be divided into two distinct zones (Figure 21): the cortical zone (intermediate area) and the trabecular zone (the extremities of the bone). The cavities in the trabecular bone are known to shelter hematopoietic stem cells (HSCs), in the endosteal niche (Wilson and Trumpp, 2006) (see chapter 2.4). Very interestingly, most tumor cells were also found to engraft in the trabecular zone, which is in agreement with published data (Phadke et al., 2006). This was also observed on CT-scans (Figures 16 and 17).

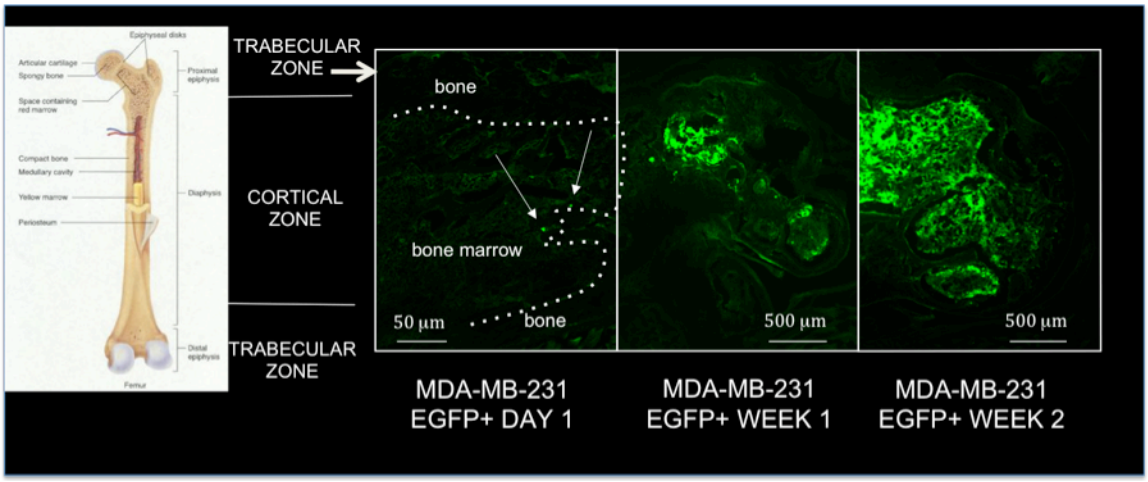

Figure 21. Bone MetICs localization on cryo-sections of xenografted murine femurs at different time-points after the xenograft. NOD/SCID mice were injected intra-bone with 5.10^4 MDA-MB-231 EGFP+ cells per femur (magnification: 10X and 5X objective. White arrows indicate single disseminated tumor cells.

This last observation raises the possibility that bone metastatic cells and HSCs use the same niche in the BM. Further studies were carried out to test this hypothesis.

4.2.2 Bone marrow MetICs are usurping the Haematopoietic Stem Cell niche

In order to test whether BM MetICs are using the same niche as HSCs in the BM, competitive BM reconstitutions were carried out (Figure 22 A.). Metastatic MDA-MB-231 and non-metastatic MCF7 breast cancer cell lines as well as MCF10A normal breast cells were used to compete with CD45.2 HSCs for the engraftment in the BM niche of irradiated CD45.1 immuno-compromised mice. Metastatic cells only were able to significantly affect HSC numbers in the BM (Figure 22 B.).

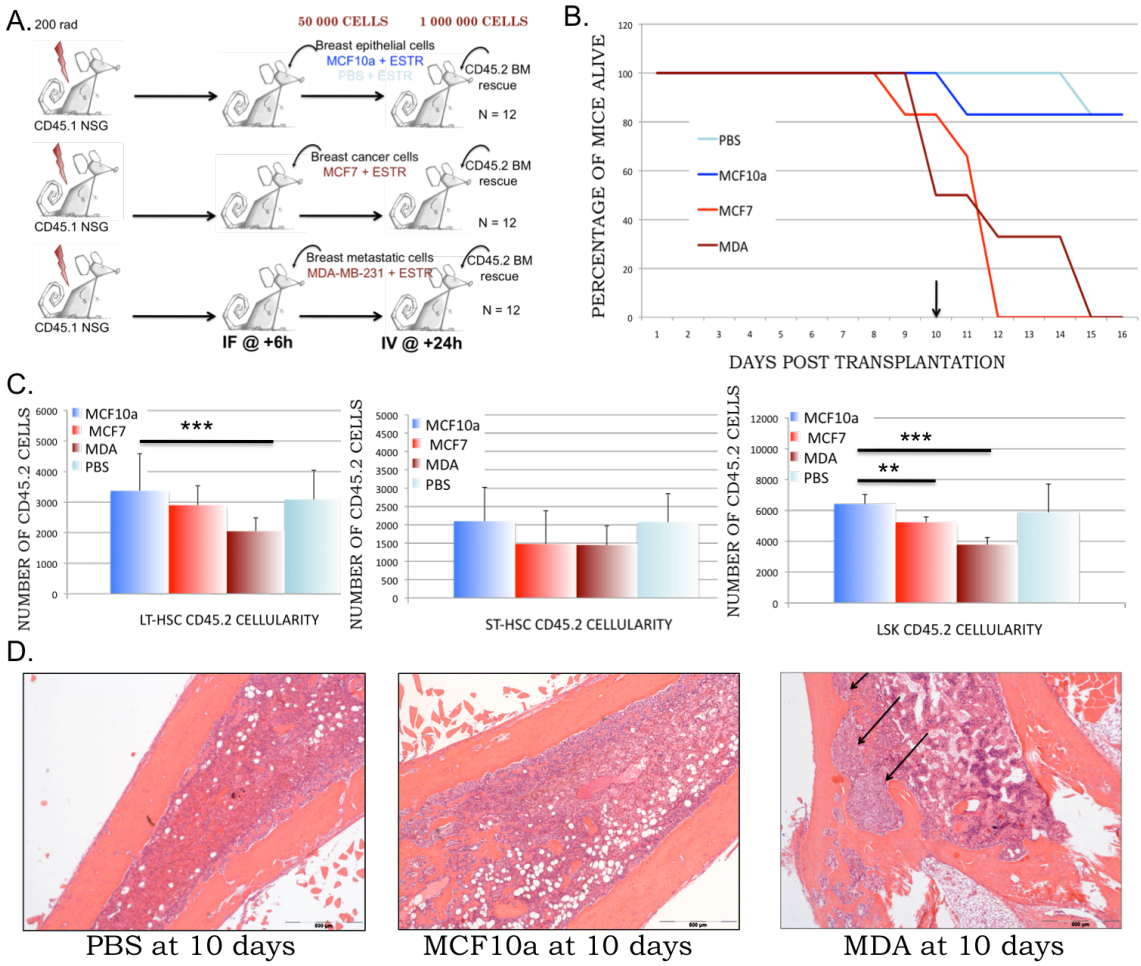

Figure 22. Tumor cells impair early LT-HSC engraftment in the BM and further repopulation of the haematopoietic system. **A.** Scheme of the competitive chimeras assay. **B.** Survival curves of PBS, MCF10a, MCF7 and MDA recipient chimera mice. **C.** Number of foreign long-term (LT-) HSC, short-term (ST-) HSC and lineage-SCA1+ C-KIT+ (LSK) cells (CD45.2) 10 days after putting in competition HSCs with normal breast cells (MCF10A), or breast tumor cells (MCF7 and MDA-MB-231). Both LT-HSCs and LSK engraftments are significantly impaired in presence of metastatic tumor cells **D.** H&E (Hematoxylin and Eosin) sections of PBS, MCF10a and MDA-injected femurs. Small tumor islets are detected at the trabecular endosteum at 10 days (right). Abbreviations: ESTR = estrogen, IV = intra-venous, IF = intra-femoral, NSG = NOD/SCID/γc-/- mice.

The normal breast cells (MCF10a) did not impair foreign HSC engraftment since similar CD45.2 HSC numbers were observed in PBS and MCF10a injected mice in long-term (LT-) HSCs, in short-term (ST-) HSCs, as well as in progenitors (lineage-/SCA1+/C-KIT+ cells, or LSK cells).

The decrease in CD45.2 HSC numbers concomitant to MDA metastatic cell injection was stronger in LT-HSCs and LSK cells than in ST-HSCs. It is currently unknown whether the endosteal niche is occupied by all HSCs, LT-HSCs or only dormant LT-HSCs. If only LT-HSCs have the capacity to occupy the niche, this could explain why ST-HSC numbers are less affected than LT-HSC numbers. The total BM cellularity was not significantly changed at day 10, (graph not shown) suggesting that the competition effect is at first mainly observed on HSCs and progenitors.

The negative effect of MDA tumor cells was much stronger than the one created by the injection of MCF7 tumor cells; this might be explained by the fact that MDA cells are metastatic cells, while MCF7 are not: the MCF7 cell line derives from a pleural effusion of an invasive breast ductal carcinoma but is not able to metastasize in mice injected into the mammary fat pad or intra-venous (Levenson and Jordan, 1997). MCF7 might be less efficient at usurping the BM niche than MDA cells, although at least a subpopulation is able to engraft and grow in the BM microenvironment.

Interestingly, a reduction of resident CD45.1 stem and progenitor cells was also observed (Figure 23). However, these reductions occurred only in injected bones and not in control contra-lateral bones, suggesting that the tumor cells locally mediate their negative impact on HSCs and progenitors. The local negative effect of tumor cells on HSC presence in the BM was also further supported by the fact that foreign CD45.2 HSC numbers were not affected in control contra-lateral bones.

Breast tumor cells engrafted at the endosteum of the trabecular area (Figure 22 D.) and expanded from there until they invaded of the whole BM cavity. The exact cause of death for tumor cell-receiving mice (between 12 and 15 days after the xenograft) requires further investigation.

Thus, similarly to leukemic cells (Colmone et al., 2008), breast cancer cells seem to be able to usurp the HSC niche in the BM and to compete with HSCs for its occupancy. This is mediated by a local signal that seems to be able to affect both foreign and resident HSCs and progenitors.

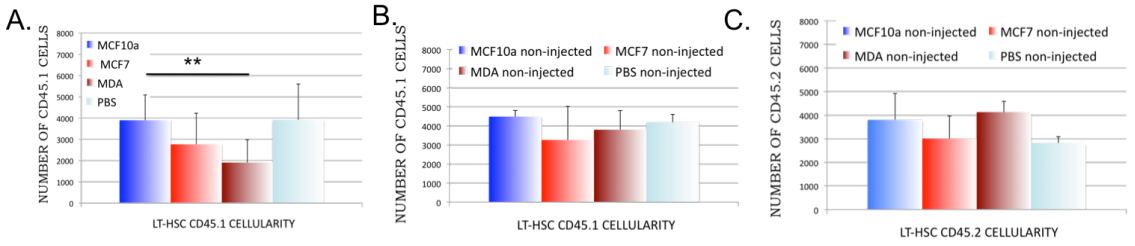

Figure 23. Tumor cells have a local negative effect on HSCs. **A.** The numbers of resident LT-HSCs (CD45.1) as well as foreign LT-HSCs (CD45.2, see Figure 22 C.) are reduced in metastatic tumor cell-injected bones. **B** and **C.** The numbers of LT-HSCs in contra-lateral control bones that were not injected with tumor cells are not affected at all.

4.2.3 HSC in the bone marrow are impaired by high-dose estrogen treatment

About 80% of breast cancers are estrogen dependent. Estrogen treatments have been shown to increase the risk for breast cancer development and breast cancer invasiveness, as shown by studies on hormonal replacement therapy in menopausal women (Chlebowski et al., 2010), (Liang et al., 2010). Since metastatic breast cancer cells are able to usurp the BM stem cell niche, the effect of estrogen treatment on the BM stem cell niche and HSCs was investigated.

In order to test whether estrogen affects HSC engraftment in the BM niche, BM reconstitutions were carried out (Figure 24 A.). Foreign CD45.2 HSCs were injected intra-venous in irradiated CD45.1 recipient mice, 24 hours after irradiation. Two groups of 12 mice were treated with estrogen *via* the implantation of estrogen pellets (high (0.72 mg/pellet) and low (0.18 mg/pellet) concentrations), 6 hours after irradiation. 12 other mice were subjected to sham operations and did not receive any treatment.

Mice receiving estrogen died within 30 days. The mice treated with higher concentrations of estrogen died faster (within 22 days) than mice treated with lower concentrations of estrogen (Figure 24 B.). Remarkably, CD34 expression in progenitors (lineage$^-$, C-KIT$^+$ SCA1$^+$ or LSK) was significantly upregulated in mice receiving estrogen (Figure 24 C.). The number of CD45.2 foreign stem and progenitor cells was dramatically reduced in treated mice compared to untreated mice (Figure 24 D.). Interestingly, resident stem and progenitor cells also significantly dropped, suggesting that estrogen not only inhibits the engraftment of foreign HSCs but also negatively affects resident HSCs and progenitor cells (Figure 24 F.). Estrogen treated mice also showed a massive decrease in BM cellularity

(Figure 24 E.). When looking at BM sections (Figure 24 G.) of non-irradiated control, sham control and estrogen-treated mice, an increased presence of fat droplets in the BM shaft of estrogen-treated mice was observed. The bones themselves did not appear to be macroscopically affected by the treatment.

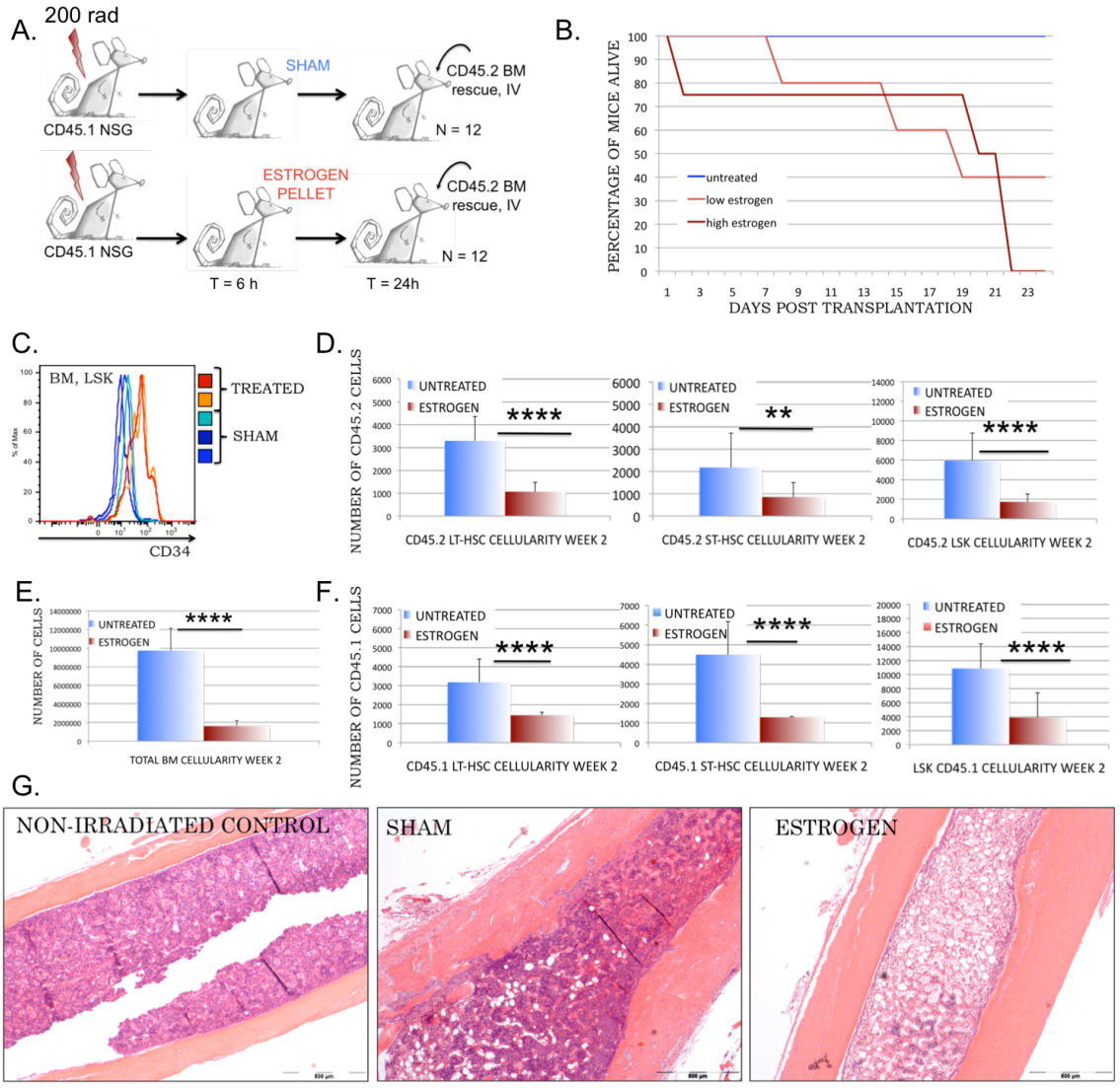

Figure 24. High dose estrogen impairs HSC engraftment in the BM and further repopulation of the haematopoietic system. **A.** Scheme of the BM reconstitution assay. **B.** Survival curves of SHAM, estrogen "high" (0.72 mg/pellet) and estrogen "low" (0.18 mg/pellet) treated mice. Estrogen low-concentration treated mice died between week 4 and week 5. Results obtained after estrogen "high" treatment are shown in **C.** to **G. C.** Increase in CD34 expression after estrogen treatment in lineage- SCA1+ C-KIT+ (LSK) progenitor cells. **D.** Number of long-term (LT-) HSC, short-term (ST-) HSC and lineage- SCA1+ C-KIT+ (LSK) cells (CD45.2) 2 weeks after irradiation. All populations are significantly impaired in presence of estrogen **E.** The total BM cellularity dropped dramatically. **F.** Number of LT-HSC, ST-HSC and LSK resident cells (CD45.1) 2 weeks after irradiation: all populations are significantly impaired in presence of estrogen. **G.** Paraffin sections of femurs, stained with H&E (Hematoxylin and Eosin). The non-irradiated control and SHAM operated control bones contain BM cells while the estrogen treated mice show almost empty bone shafts. Fat droplets seemed to be more present in the bones of treated mice than in control mice. Abbreviations: ESTR = estrogen, IV = intra-venous, NSG = NOD/SCID/γc-/- mice.

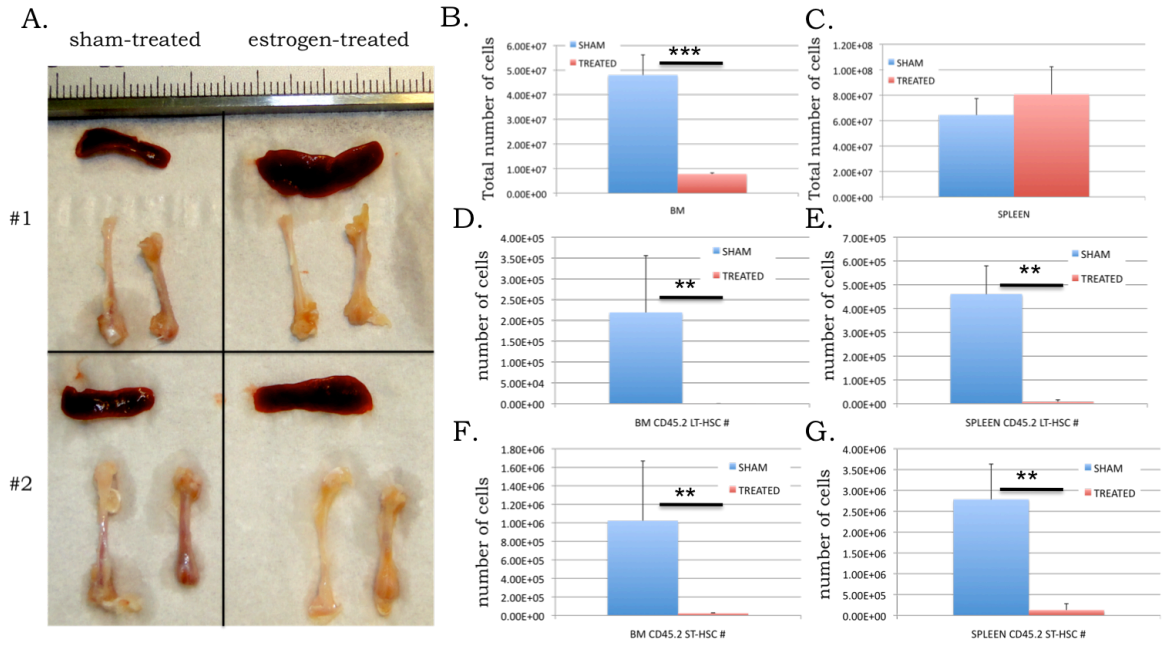

Figure 25. High dose estrogen does not mobilize HSCs out of the BM. Estrogen-treated mice (0.18mg/pellet) were analyzed 4 weeks after the BM reconstitution. **A.** The spleens were enlarged while the bones were anemic (white aspect) in treated mice compared to control sham treated mice. **B.** Total BM cellularity dropped dramatically, as already seen in Figure 24 E., while **C.** total spleen cellularity slightly increased in a non-significant manner. **D.** and **E.** BM and splenic exogenous (CD45.2) LT-SHCs as well as **F.** and **G.** BM and splenic ST-HSCs decreased significantly in treated mice compared to sham treated control mice.

Estrogen-treated mice were analyzed 4 weeks after BM reconstitution (Figure 25). Bones were anemic and spleens were enlarged (see Figure 25 A.). The total number of cells in the BM dropped dramatically (Figure 25 B.), as seen before (Figure 24 E.) while the number of splenic cells slightly increased, in a non-significant manner (Figure 25 C.). Exogenous (Figure 25 D.-G.) and resident (not shown) LT-HSCs, ST-HSCs and LSK cells in the BM and in the spleen dramatically dropped, suggesting that the whole haematopoietic system was failing and that no extra-medullary haematopoiesis was occurring in the spleen.

Hematology profilings were also done on peripheral blood using the Hemavet 950S system (DREW): while control mice showed only mild anemia and leukopenia, due to the BM reconstitution process, estrogen treated mice showed severe neutropenia, lymphocytopenia and anemia (see Chapter 7.7), confirming the occurrence of a total BM failure.

Further studies are needed to understand the molecular mechanism underlying the observed BM failure.

Since HSCs and metastatic breast tumor cells might use the same niches in the BM, similar molecular cues might regulate the engraftment of both types of cells into these niches. Circulating leukemic cells and HSCs are known to engraft in the BM *via* the interaction of CXCL12 (or SDF1) with its receptor CXCR4 (Sipkins et al., 2005). It was therefore ivestigated whether the CXCR4-SDF1 axis also plays a role in breast cancer cell engraftment in the BM.

4.2.4 Engraftment in the bone marrow metastatic niche is CXCR4-dependent

CXCR4, (a CXC chemokine Receptor), also called fusin, is an alpha-chemokine receptor specific for STROMAL-DERIVED-FACTOR-1 (SDF1, also called CXCL12), a molecule endowed with potent chemotactic activity for lymphocytes. CXCR4's ligand SDF1 is known to be important in hematopoietic stem cells (HSCs) homing to their niche in the BM and in HSC quiescence (Lapidot and Kollet, 2002). Drugs that block CXCR4 are capable of mobilizing HSCs into the bloodstream. Plerixafor (or AMD3100) is a drug, not yet in routine clinical use, which directly blocks the CXCR4 receptor. It is a very efficient inducer of hematopoietic stem cell mobilization in animal and human studies (Broxmeyer et al., 2005).
MDA-MB-231 cells, as well as many breast cancer metastatic cells express CXCR4 (chapter 7.10). Massague's group demonstrated that CXCR4 might play an important role in bone metastasis, since it appears in the list of genes identified as the "bone metastatic signature" (Kang et al., 2003). In addition, some publications show that the inhibition of CXCR4 impairs breast cancer primary tumor as well as metastasis growth (Epstein, 2004) (Liang et al., 2004). However, little is known about the implication of CXCR4 in the bone metastastic niche.

In order to investigate the role of CXCR4 in the BM metastatic niche, a 28-day AMD3100 treatment was started 13 days before the xenograft of recipient mice. Tumor growth was quantified by bioluminescence measurement. After intra-femoral injections of MDA-MB-231 LUC+ cells, the tumor growth in the bones was significantly decreased in response to AMD3100 pre-treatment; on the other hand, lung metastases were not significantly affected (Figure 26).

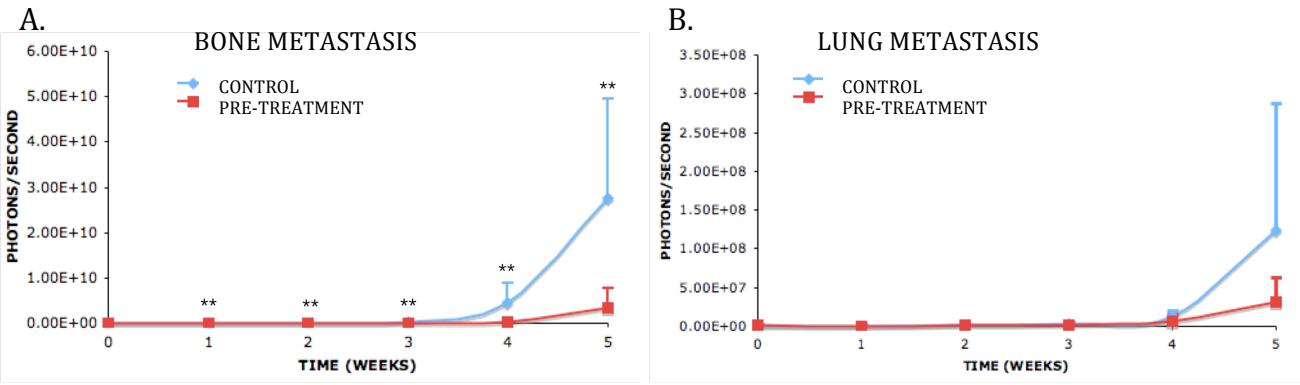

Figure 26. Bone tumor growth is inhibited by AMD3100 pre-treatment. Pre-treatment with AMD3100 (PRE-TREATMENT) significantly inhibits bone tumor growth, but not lung metastasis growth compared to PBS treated mice (CONTROL). Tumor growth curves in **A.** the hind limb bones and **B.** the lungs of NOD/SCID mice injected intra-bone with 5.10^4 MDA-MB-231 LUC+ cells per femur.

While in PBS-treated control mice, tumors always arose in the trabecular area, tumors were smaller and less frequent in pre-treated mice. Also and surprisingly, some rare AMD3100 pre-treated tumors grew from outside the bones. This observation was made on cryosections of MDA-MB-231 EGFP+ femurs, 10 days after the xenograft (Figure 27).

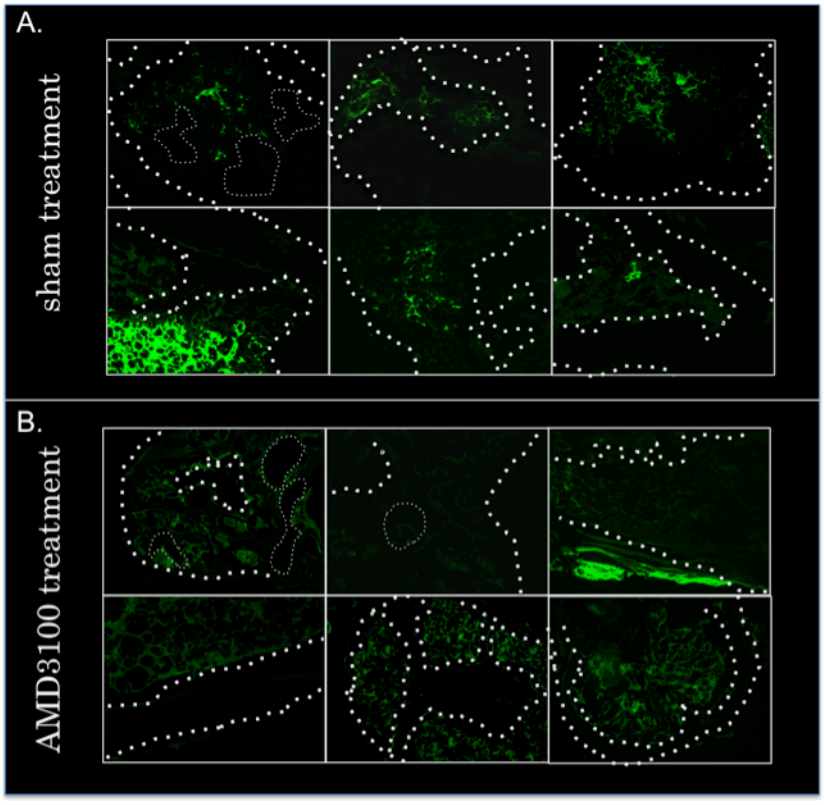

Figure 27. Localization of tumor cells after AMD3100 pre-treatment. Cryo-sections of femurs from NOD/SCID mice injected with EGFP+ MDA-MB-231 cells 10 days earlier. The mice underwent either a sham treatment (**A.**) or an AMD3100 pre-treatment (**B.**). While tumor cells engraft at the endosteum of the trabecular zone of the bones in the sham treated animals, tumors rarely engraft there in the AMD3100 treated animals.

Since preliminary results were obtained suggesting that BM MetICs might use the same niche as HSCs, CXCR4 inhibition might have a similar mobilizing effect on bone MetICs as it has on HSCs. While HSCs are mobilized only temporarily and are then able to home back to the BM niche (Broxmeyer et al., 2005), AMD3100 continuous treatment might help to durably prevent the engraftment of tumor cells in the bone metastatic niche. Importantly, it seems that AMD3100 treatment did not enhance the growth of metastases at other locations, for instance in the lungs (Figure 23 B.).

4.2.5 Bone marrow Metastasis Initiating Cells and Cancer Stem Cells

Putative breast cancer stem cells (CSCs) have been described as displaying high CD44 and low CD24 cell surface markers (Al-Hajj et al., 2003). Very interestingly, it has recently been published that 80% of DTCs and 35% of CTCs display this same putative CSC phenotype (Balic et al., 2006), (Theodoropoulos et al., 2010). Yet, whether the CD44+ CD24- cell surface phenotype is also a good marker for putative BM Metastasis Initiating Cells (MetICs) is not known.

To test this hypothesis, the frequency of MDA-MB-231 cells capable of engrafting in the bone marrow ("bone MetICs") was calculated thanks to a limiting dilution assay, and compared to the known frequency of CD44+ CD24- cells in this cell line (80-100%, (Sheridan et al., 2006) and confirmed by FACS). 1 into 20 000 MDA-MB-231 cells, that is 0.05% of MDA-MB-231 cells were found to be able to initiate bone tumors in the intra-femoral xenograft assay (Figure 28). Thus, the CD44+ CD24- cell surface phenotype alone does not seem to be sufficient to describe bone MetICs. Further characterization of MetIC surface markers should be carried out in the future.

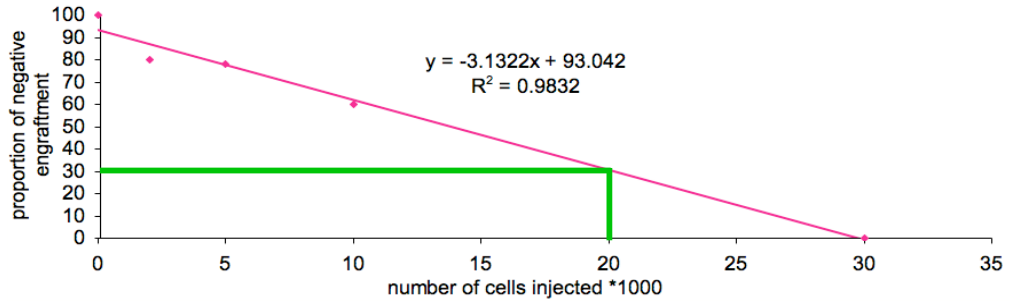

Figure 28. Limiting Dilution Assay to calculate the frequency of Metastasis Initiating Cells (MetICs). Different dilutions of MDA-MB-231 cells were injected intra-bone into NOD/SCID mice to measure the corresponding engraftment of the human tumor cells in the recipient mice. The Poisson law indicates that the number of "stem cells" corresponds to the number of cells injected that induced a 37% negative engraftment in the mice.

To conclude this chapter, the BM displays considerable advantages for the seeding of metastatic cells and might even shelter DgTCs in its physiological endosteal niche. Indeed, metastatic cells were shown to be able to locally empty some of the HSC BM niches and to colonize them. The exact mechanisms by which tumor cells usurp the HSC niches remain to be identified. In addition, estrogen, a key hormone in the vast majority of breast cancers, was observed to greatly impair HSC occupation of the BM niche. Also, preliminary data suggest that the seeding of metastatic cells in the BM might be dependent on the SDF1-CXCR4 axis, since its inhibition impairs tumor cell growth in the BM. Last, a limiting dilution assay using MDA-MB-231 cells indicates that BM MetICs are less frequent than putative phenotypic breast CSCs (if such cells really exist in cell lines). As discussed in chapter 2.2.3, MetICs might derive from CSCs but not all CSCs might be able to initiate metastasis.

In order to further optimize a method for the detection of rare MetICs within DgTCs in carcinoma patients, additional experiments were carried out, as presented in the next chapter.

4.3 Model suitability for the study of rare Disseminating Tumor Cells

In order to test the metastatic potential of DgTCs, a novel intra-bone xenograft metastatic model was set up (see chapter 4.1). In addition, the enrichment, the recovery and the detection levels of DgTCs were optimized in order to improve the handling of such rare cells.

4.3.1 Optimization of the enrichment procedure of live Disseminating Tumor Cells

The enrichment step of DgTCs from the mesenchymal compartment they originate from, is one of the most limiting steps since DgTCs are extremely rare cells (see chapter 2.3) and no specific cell surface markers has been identified yet (Pantel and Brakenhoff, 2004).

DgTCs are by definition surrounded by haematopoietic cells; because our aim is to inject and grow DgTCs in immuno-deficient mice, these haematopoietic cells must be depleted in order to avoid graft versus host disease (GvHD), mediated by T lymphocytes (van Rijn et al., 2003). EPCAM is the most popular positive marker used for DgTC isolation (see chapter 2.3). However, its expression might be down-regulated when cells undergo EMT, and indeed some studies found that a substantial amount of DTCs in the BM do not express EPCAM (Pantel and Brakenhoff, 2004). We therefore decided to test only depletion methods, in which blood cells are negatively targeted.

As explained earlier (see chapter 2.3), peripheral blood samples are much easier to collect than bone marrow (BM) or lymph node (LN) samples: phlebotomies are almost painless for the patients and can be done at frequent intervals, while BM or LN collections are invasive and painful procedures. Therefore, most experiments were achieved using peripheral blood and CTCs.

Several depletion methods for the enrichment of CTCs exist on the market. A study by He and colleagues from 2008 ((He et al., 2008), Figure 29) points out that out of 9 different depletion methods, RosetteSep® (StemCell Technologies) is providing the best recovery rate (around 63%). Briefly, RosetteSep® uses Tetrameric Antibody Complexes (TAC) to deplete specific cells from whole blood: the RosetteSep® cocktail links unwanted cells to multiple red blood cells already present in the sample, forming immunorosettes. When centrifuged

over a density medium such as Ficoll-Paque™, the unwanted cells pellet along with the red blood cells, leaving the desired cells untouched. The RosetteSep® protocol includes an antibody cocktail composed of anti-CD2, CD16, CD19, CD36, CD38, CD45, CD66b and glycophorin A antibodies, thus targeting all differenciated blood cells, including platelets.

TABLE II – SUMMARY OF RECOVERY EFFICIENCIES OF 9 ENRICHMENT METHODS

Method no.	Method name	The efficiency of recovery (%)			
		Exp. 1	Exp. 2	Exp. 3	Mean ± SD
1	Ficoll	45.1	39.5	42.2	42.3 ± 2.8
2	A23187 treatment plus Ficoll	33.9	31.5	30.2	31.9 ± 1.9
3	RosetteSep-Ficoll	61.3	64.2	62.0	62.5 ± 1.5
4	Ammonium chloride lysis	5.0	5.2	5.6	5.3 ± 0.3
5	Histopaque 1077	24.3	25.1	27.2	25.5 ± 1.5
6	Histopaque 1083	27.5	26.9	28.1	27.5 ± 0.6
7	Histopaque 1199	17.2	18.1	16.3	17.2 ± 0.9
8	OncoQuick	20.0	22.4	21.9	21.4 ± 1.3
9	LeucoSep with Ficoll	30.0	33.2	32.1	31.8 ± 1.6

Figure 29. Enrichment methods for CTCs. Table published by He and colleagues in 2008 in the International Journal of Cancer (He et al., 2008) comparing different depletion methods for the recovery of human carcinoma cells in blood.

Spike-in experiments were carried out in order to evaluate the recovery rate of three different enrichment methods: the RosetteSep® protocol and two new protocols proposed by Myltenyi using the MACS® (Magnetic microbeads Associated Cell Sorting) technology. Briefly, the MACS® technology labels unwanted cells with specific atibodies coupled to magnetic micro-beads. After passage of the labeled sample in a magnetic column, wanted and unwanted fractions can be retrieved separately. Two different protocols were tested: a first protocol where whole blood is directly labeled and run through magnetic separation columns ("autoMACS whole blood") and a second protocol where mononucleated cells are isolated from whole blood using a Ficoll-Paque™ density gradient prior to cell separation on columns ("AutoMACS + Ficoll"). Both MACS® protocols were tested with anti-CD45 (or "leukocyte common antigen") micro-beads in order to deplete all differentiated haematopoietic cells, except platelets (which do not express CD45).

Different amounts of MDA-MB-231 EGFP+ cells were spiked in human blood samples and EGFP+ cells were counted after enrichment using either the RosetteSep® protocol (StemCell Technologies), the "autoMACS whole blood" protocol or the "autoMACS + Ficoll" protocol (Miltenyi) (Figure 30). The RosetteSep® protocol provided the best recovery rate (around 70%), according to our study, especially when low numbers of tumor cells were introduced, which corresponds to real ranges of patient DgTC numbers (see chapter 2.3). A similar recovery rate (70%) was also observed when spiking MDA-MB-231 EGFP+ cells in human BM, using the RosetteSep® protocol (not shown).

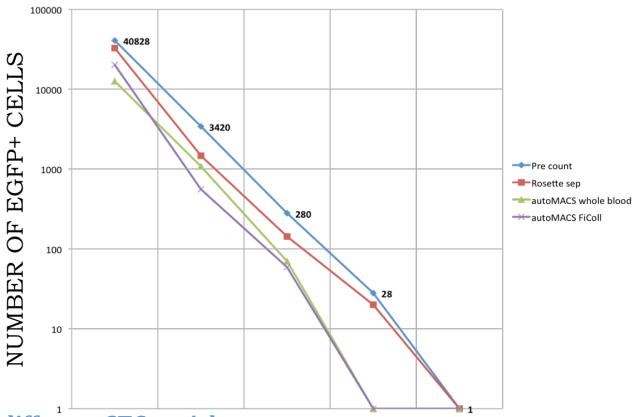

Figure 30. Comparison of different CTC enrichment recovery rates. Number of recovered spiked-in EGFP+ tumor cells in human blood, using different depletion methods. In red squares: RosetteSep®, in green triangles: "autoMACS whole blood" protocol, in purple crosses: "autoMACS+Ficoll" protocol. The three methods are compared to the number of spiked-in cells initially added to the blood (in blue rounds, "pre-count"). The RosetteSep® method enables very good recovery of the spiked-in tumor cells, especially when low numbers of tumor cells are introduced, which corresponds to real ranges of patient DgTCs.

The recovery rate of primary human CTCs from a breast cancer patient sample was also evaluated, using the RosetteSep® protocol. The number of Propidium Iodide $PI^-/CD45^-/EPCAM^+$ defined live CTCs detected by FACS after RosetteSep® was compared to the numbers of intact looking CTCs counted with the FDA-approved CellSearch™ device (see chapter 2.3): the numbers were identical, indicating that both protocols have similar recovery rates. It is estimated that the CellSearch™ device enables a 70-80% recovery rate (Riethdorf et al., 2007). This rate also corresponds to the one evaluated by my spike-in experiments (see above).

In addition, it was evaluated that the RosetteSep® protocol leads to a 130-fold enrichment (from 0.032% to 4.26%) of CTCs as measured by FACS counts of the PI$^-$/CD45$^-$/EPCAM$^+$ cell population (Figure 31).

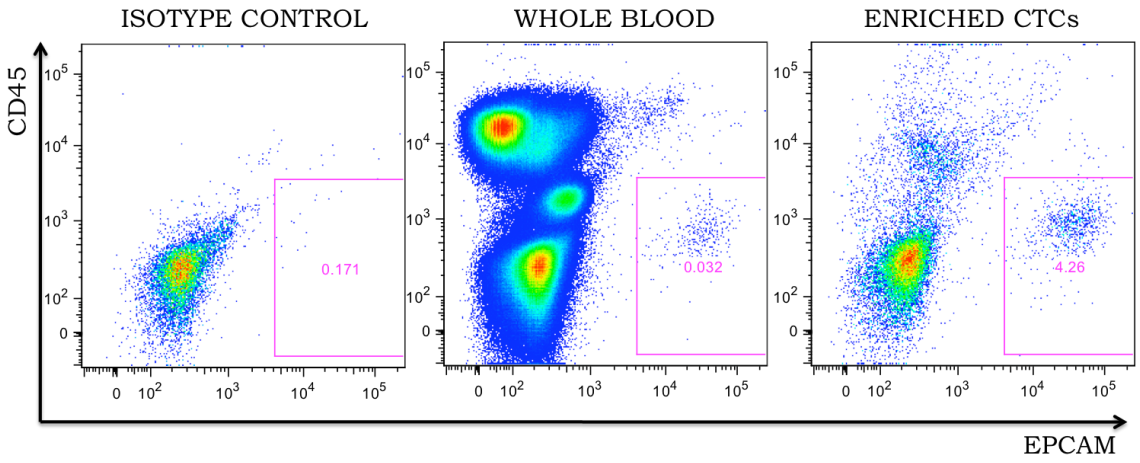

Figure 31. Enrichment of CTCs from a patient sample. FACS plots corresponding to patient number 86 from CLINICAL STUDY #3 (see chapter 5.4). The CellSearch™ technology evaluated that this patient carries 15000 CTCs/7.5 mL of blood. A simple Ficoll gradient (no depletion) or the RosetteSep® protocol were applied to equal volumes of blood. The samples were analyzed by FACS. The RosetteSep™ method enabled an enrichment of tumor cells of more than a 130-fold. Also, since similar numbers of live CD45$^-$/EPCAM$^+$ defined CTCs were counted on the FACs and after CellSearch™ processing, we evaluated the recovery rate of our method as of 70%.

It was also observed that the use of glass syringes was much more efficient than the use of plastic syringes for the injection of the enriched tumor cells in the mice. Indeed, around 50% of tumor cells were lost in plastic syringes while only 30 to 20% were lost in a glass syringe. However, due to needle size restrictions linked to the small size of murine femurs, plastic syringes were mostly used during the studies depicted in chapters 4.4 and 4.5.

As a conclusion, the RosetteSep® protocol was selected to enrich live DgTCs from patient samples, since it provides the best recovery rate compared to the other exiting methods. The enrichment is evaluated around 130%. The total recovery rate (without the lentiviral infection step) is evaluated around 35% (50% of 70%) from the moment the sample is taken from the patient until the cells are injected in the recipient mice.

4.3.2 Xenograft recipient: NOD/SCID mice versus NOD/SCID/$\gamma_c^{-/-}$ mice

A second decisive choice is the one of the recipient mouse strain. Several immuno-compromised strains have been developed during the past years. The two most immuno-compromised strains (NOD/SCID and NOD/SCID/$\gamma_c^{-/-}$ mice) were studied and compared for their suitability for the DgTC functional xenograft assay.

Nonobese diabetic severe combined immunodeficiency disease (NOD/SCID) mice are homozygous for the severe combined immunodeficiency (SCID) mutation. They are characterized by an absence of functional T cells and B cells, a general lymphopenia, but a normal hematopoietic microenvironment. On the other hand, NOD/SCID/$\gamma_c^{-/-}$ are double homozygous for the severe combined immunodeficiency (SCID) mutation and the allelic mutation of the common gamma chain ($\gamma_c^{-/-}$) of the interleukin-2 receptor (IL-2R) (Yahata et al., 2002). These mice are functionally incompetent for B, T and NK cells, and are deficient in cytokine signaling. They are therefore devoid of adaptive immune response, while NOD/SCID mice still have some functional NK cells.

In order to determine which of the NOD/SCID or NOD/SCID/$\gamma_c^{-/-}$ mice would be better recipients for the xenograft assay, tumor growth rates of 5.10^4 MDA-MB-231 LUC+ cells injected intra-bone were compared between the 2 mouse strains. Tumor cells grew much faster in NOD/SCID/$\gamma_c^{-/-}$ than in standard NOD/SCID mice (Figure 32), suggesting that NOD/SCID/$\gamma_c^{-/-}$ mice are more permissive recipients for human tumor cells than NOD/SCID mice. This result also suggests that NOD/SCID resident NK cells have a worse impact on tumor cells engraftment than the cytokine signaling deficiency observed in NOD/SCID/$\gamma_c^{-/-}$ mice.

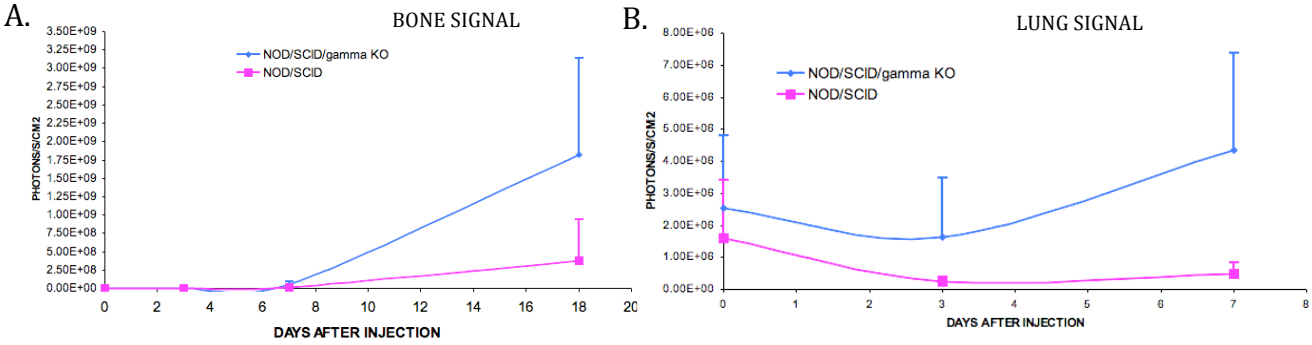

Figure 32. Comparison of tumor growth speed in **A.** hind limb bones and **B.** lungs of NOD/SCID/$\gamma_c^{-/-}$ (NOD/SCID/gamma KO) versus NOD/SCID mice injected intra-bone with 5.10^4 MDA-MB-231 LUC+ cells per femur.

In addition, NOD/SCID mice have a very limited lifespan since they often die of lymphomas at around 6 to 8 months of age (http://jaxmice.jax.org/strain/001303.html). On the contrary, NOD/SCID/$\gamma_c^{-/-}$ mice can live for more than a year without detectable disease (http://jaxmice.jax.org/strain/005557.html). It is suspected that DgTCs have the ability to stay quiescent for very long periods of time. In case such dormant cells are transplanted, the length of the assay should be extended as much as possible, in order to have a chance to detect them when they develop into metastases.

Showing an increased permissivity for human cancer cell growth and a superior lifespan, NOD/SCID/$\gamma_c^{-/-}$ mice were therefore selected over NOD/SCID mice as the recipient strain for the DgTC functional xenograft assay.

4.3.3 Optimizing luciferase expression in tumor cells

In order to enable an optimal detection of luciferase (LUC) expressing tumor cells *in vivo*, the best LUC expression-providing method was selected.

Retroviruses have the ability to stably integrate into the host genome. However they are in general unable to transduce cells that are not in cycle. Lentiviruses (like HIV) are a subclass of Retroviruses. They represent the most efficient method of a gene delivery vector, thanks to their ability to integrate into non-dividing cells. Since MetICs might be dormant cells, it is clear that Lentiviruses are a better choice than Retroviruses for the transduction of DgTCs.

For the expression of luciferase, a CAG promoter was used. The CAG promoter is a combination of the cytomegalovirus (CMV) early enhancer element and chicken beta-actin promoter. It provides high levels of gene expression in mammalian expression vectors, even in stem cells (Alexopoulou et al., 2008). Also, for mRNA stabilization, a Woodchuck post-transcriptional response element was included (WPRE) (see Chapter 7.6).

4.3.4 Detection limit of the xenograft assay using the Xenogen system

In the scheme of the novel xenograft assay, the potential growth of DgTCs in the mice is assessed using the Xenogen system (IVIS® 200 series, Caliper), which detects LUC+ tumor cells (see figure 13). It is therefore important to measure the detection limit of the system. Since it is impossible to predict the level of LUC expression obtainable in DgTCs, the detection limit of the system was evaluated using the MDA-MB-231 LUC+ cells.

The global bioluminescent signal of NOD/SCID/$\gamma_c^{-/-}$ mice was measured 10 minutes after intra-bone injections of 5.10^4 MDA-MB-231 LUC+ cells per femur (experimental mice) or PBS (negative control mice). The mean global background bioluminescence was evaluated by measuring the signal produced by negative control mice. Provided that the 1.10^5 LUC+ tumor cells injected are all still alive 10 minutes after the injection, the global bioluminescence corresponding to 1.10^5 MDA-MB-231 LUC+ cells can be calculated. In these experimental conditions, the detection limit of the xenograft assay was estimated around 8000 cells (Table 1).

Number of cells injected	Whole body signal	Whole body background level	Detection limit
2 x 50 000 cells	$4{,}6.10^{07}$p/sec/cm^2	$3{,}88.10^{05}$ p/sec/cm^2	~8000 cells

Table 1. Detection limit of the xenograft assay. Calculation of the detection limit of the xenograft assay when injecting intra-bone 5.10^4 MDA-MB-231 LUC+ cells into each femur of NOD/SCID/γ^{-}/- mice. The intensities of the bioluminescent signals were measured 10 minutes after injection.

As observed in CLINICAL STUDY #1 (see chapter 4.4.2) CTCs usually range between 1 to 600 cells with a median of only 6.5 cells per 7.5 mL of blood. It means that most probably the Xenogen detection system will initially not allow the detection of the injected DgTCs. Provided that DgTCs might be transduced as efficiently as MDA-MB-231 cells, they will become visible by bioluminescence only if they develop into tumors bigger than 8000 cells. Unfortunately, more sensitive devices for the detection of disseminated cells *in vivo* do not exist yet.

As a conclusion to this chapter, the assay was optimized at different levels: the viable DgTC isolation method was carefully selected and tested, the best available host mouse strain was chosen, a lentiviral approach was selected to introduce LUC expression in the tumor cells, and, to finish with, the sensitivity of the Xenogen system (IVIS® 200 series, Caliper), applied to this setting was assessed.

Unfortunately, the overall recovery rate of the assay (35%) and its sensitivity of detection (8000 cells) are still not optimal for the detection of rare cells like DgTCs. Also, the optimization was carried out on a cell line, which might provide better results than when handling primary DgTCs. However, one can speculate that the xenograft assay can still allow the detection of early metastasis onset (tumors bigger than 10^4 cells) in recipient mice.

In order to functionally characterize human carcinoma DgTCs, the newly developed and optimized assay was applied to the MDA-MB-231 breast cancer metastatic cell line, as presented in the next chapter.

4.4 Functional study of cell line Disseminating Tumor Cells

The MDA-MB-231 cell line-based metastasis model was first used to analyze DgTCs, as it provides a more controllable tool than the direct study of primary samples from patients.

4.4.1 Circulating Tumor Cells have poor clonogenic and sphere forming abilities

Upon intra-femoral injection of MDA-MB-231 breast tumor cells, immuno-compromised host mice developed bone tumors as well as multiple metastases (see chapter 4.1). They also started to bear Circulating Tumor Cells (CTCs) in their blood, 4 weeks after the xenotransplant (see Figure 19-A). It was chosen to isolate cell line-CTCs from week #7 time-points because more cells could be retrieved on average (see Figure 19 A.); the tumorigenicity and the molecular characteristics of MDA-CTCs was then assessed.

MDA-CTCs were isolated from intra-cardiac punctures of xenografted mice, 7 weeks after the injection of 5.10^4 MDA-MB-231 EGFP+ cells per femur. After a Ficoll-Paque™ density gradient, the tumor cells were separated from the remaining mono-nucleated blood cells by differential adherence: after four hours, thanks to their adherence capacities, most EGFP+ MDA CTCs attached to the bottom of culture dishes, while blood cells remained in suspension. Pure populations of MDA-CTCs could thus be retrieved without any sorting or magnetic bead-based separation assays and be grown *in vitro* under standard culture conditions (see Material § Methods, chapter 7), (Figure 33). Single CTCs displayed heterogeneous phenotypes, as seen by fluorescence microscopy (Figure 32). This is in agreement with the careful cytomorphologic analyses reported for colon cancer CTCs (Marrinucci et al., 2010)

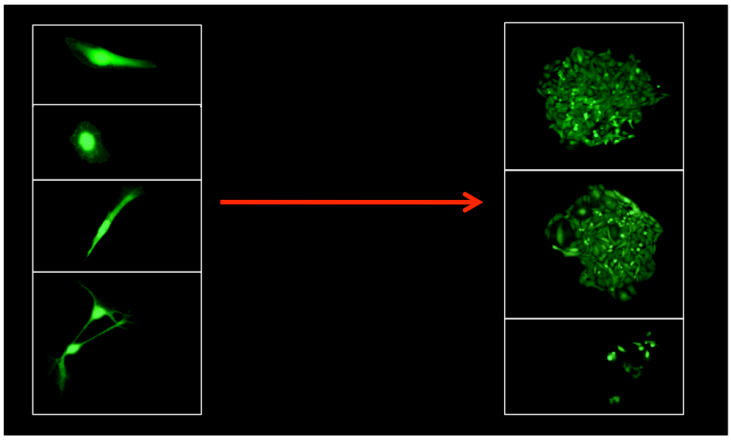

Figure 33. *In vitro* growth of MDA-CTCs. MDA-MB-231 CTCs could be purified from the peripheral blood of metastatic xenografted mice and grown in standard culture medium. Single CTCs were retrieved by differential adherence; they grew into clones of heterogeneous phenotypes.

In order to test the clonogenic capacity of cell line CTCs, MDA-MB-231 LUC+ CTCs (MDA-CTCs) and parental MDA-MB-231 LUC+ cells were sorted as single cells in 96 well plates, by flow cytometry (Figure 34 A.). Fewer clones grew out of single MDA-CTCs than from single parental MDA cells. Furthermore, the size of the clones was in general smaller than in those observed in the parental plate (Figure 34 A.). Overall, MDA-CTCs had a 3-fold lower clonogenic capacity than their parents, as quantified by bioluminescence (Figure 34 B.).

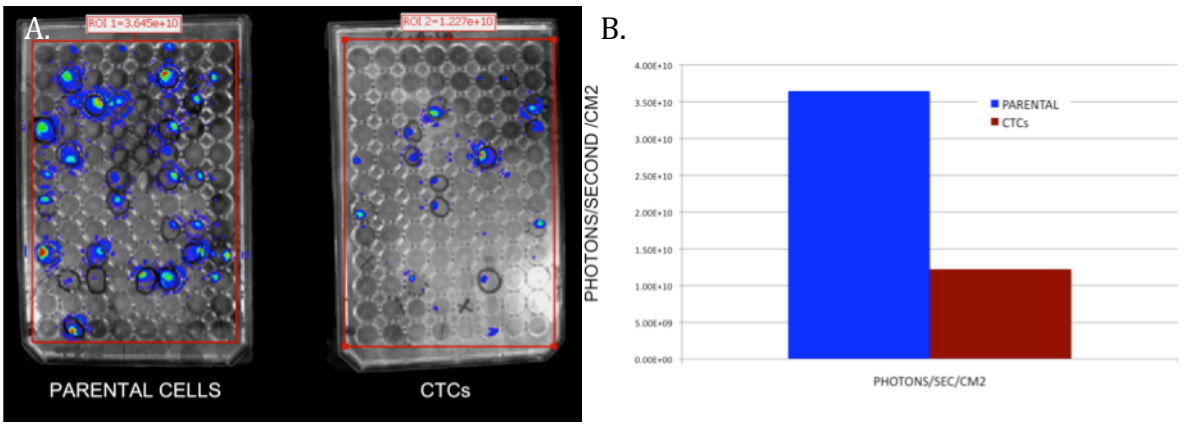

Figure 34. Clonogenicity of MDA-CTCs. CTCs were less clonogenic than the corresponding parental cells. **A.** Xenogen photographs of 96 well plates containing clones grown out of sorted MDA-MB-231 LUC+ parental cells or CTCs. **B.** Quantification of the total bioluminescence of clones growing from parental versus CTC MDA-MB-231 LUC+ cells.

Mammosphere (or spheroid) forming capacities of MDA-CTCs and MDA parental cells were also compared (Dontu et al., 2003). 10^5 MDA-CTCs and 10^5 MDA parental cells were sorted in parallel into mammosphere medium (see chapter 7, Material § Methods), (Figure 35). The sphere forming capacity of CTCs was found to be around 3-fold lower than those of the parental cells, 4 weeks after seeding. This result fits with the 3-fold reduced clonogenic capacity of CTCs depicted above.

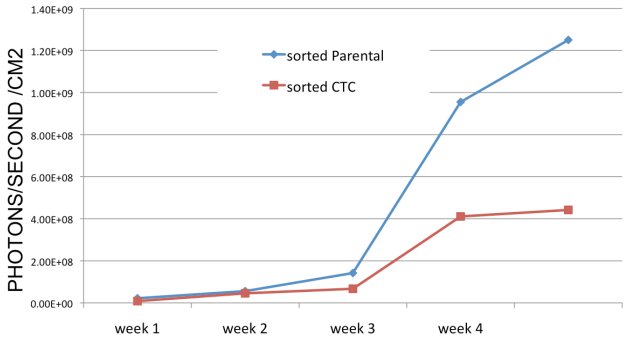

Figure 35. Sphere forming capacity of MDA-CTCs. Sphere forming capacity of 10^5 CTCs versus 10^5 parental MDA-MB-231 cells when directly sorted into mammosphere medium. The overall growth of spheres was measured by global bioluminescence in Photons/seconds/cm^2 during 4 weeks. Overall, parental cells were 3-fold more efficient than CTCs.

4.4.2 Circulating Tumor Cells are poorly tumorigenic and metastatic *in vivo*

Sorted MDA-CTCs and sorted parental CTCs were injected either into the mammary fat pads or in the BM of host mice. Their respective growths were monitored using the Xenogen system (IVIS® 200 series, Caliper).

Compared to parental MDA cells, MDA-CTCs demonstrated reduced growth in the mammary fat pads (Figure 36 A.) and in the BM (Figure 36 B.) of recipient mice. They formed tumors that were on average 10-fold smaller (Figure 36 D.). Also, they tended to induce fewer metastases (Figure 36 C.). Interestingly, MDA-CTCs were found to induce an increased release of CTCs in recipient mice compared to parental cells (Figure 36 C.).

Overall, MDA-CTCs were found to be less tumorigenic and less capable of inducing metastases than MDA parental cells.

A.

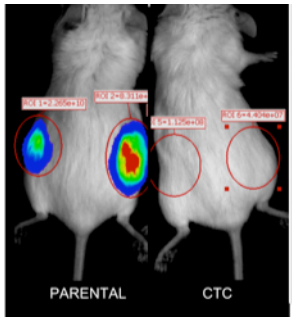

C.

LUNG METASTASIS	ADRENAL METASTASIS	LYMPH NODE METASTASIS	NUMBER OF CTCs	MOUSE INJECTED WITH
Yes	Yes	Yes	238	PARENTAL 1 (50 000 cells IF)
Yes	Yes	Yes	4 374	PARENTAL 2 (50 000 cells IF)
Yes	Yes	Yes	1 948	PARENTAL 3 (50 000 cells IF)
No	No	No	39	CTC 1 (50 000 cells IF)
No	Yes	Yes	11 334	CTC 2 (50 000 cells IF)
No	No	No	18 629	CTC 3 (50 000 cells IF)

B.

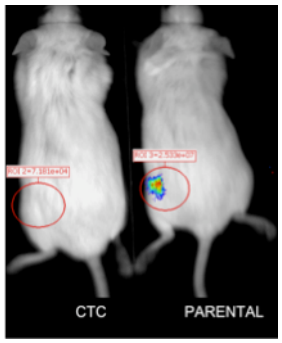

D.

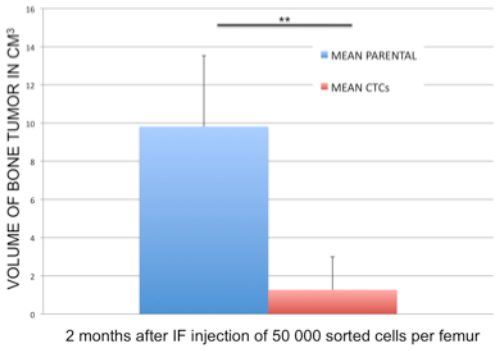

Figure 36. Tumorigenicity of MDA-CTCs. **A.** Parental or CTC MDA-MB-231 cells were injected in the mammary fat pad of NOD/SCID mice. **B.** Parental or CTC MDA-MB-231 cells were injected in the femurs of NOD/SCID mice. **C.** List of metastases and number of CTCs observed in mice injected intrafemoral with parental versus CTC MDA-MB-231 cells. **D.** Mean volume of bone tumors grown from parental versus CTC MDA-MB-231 cells. Overall, it seems that CTCs are less tumorigenic in mice than the parental cells and that they produce less metastases. However, they tend to induce increased numbers of CTCs.

4.4.3 A high proportion of Circulating Tumor Cells is quiescent

The cell cycle status of MDA-CTCs was subsequently analyzed by FACS. A variable but important proportion of quiescent cells ($Ki67^-$) was observed (Figure 37 A.). This is in agreement with the data published on patient CTCs, where a variable but consistent proportion of CTCs has been described as $Ki67^-$, by immunocytochemistry (Muller et al., 2005), (Stott et al., 2010).

Overall, CTCs were found to be much less in cycle than parental cells and than cells isolated from metastases growing in the host mice (Figure 37 B.).

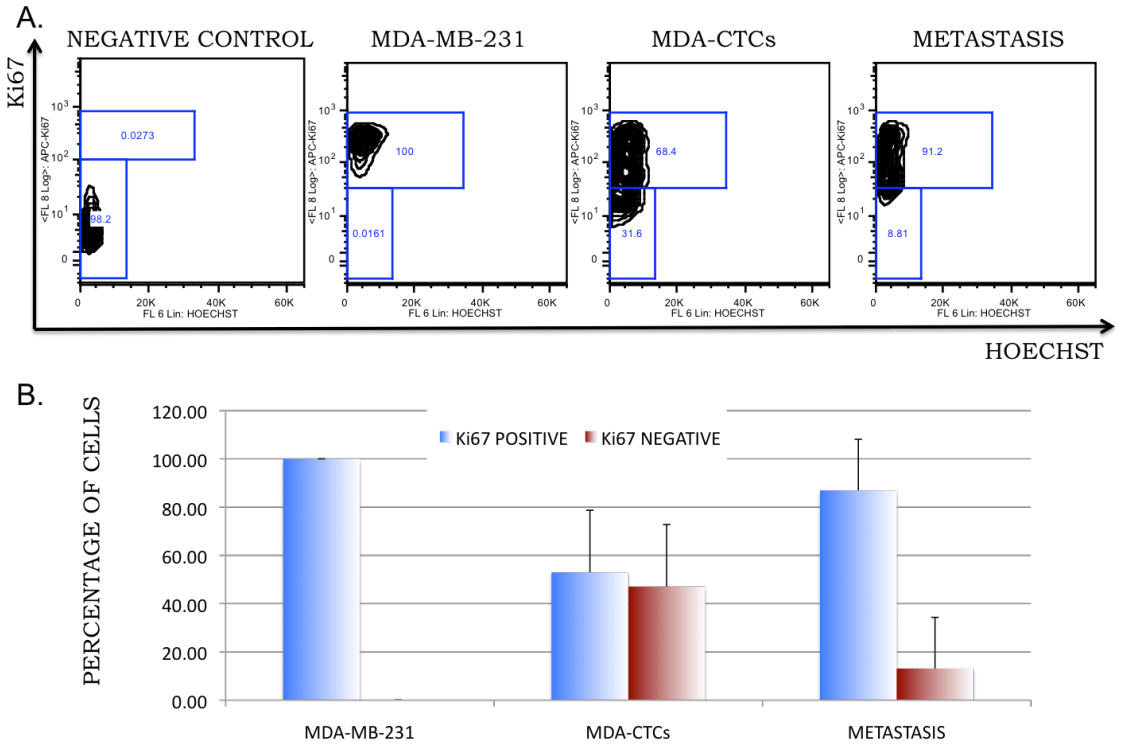

Figure 37. Cell cycle analysis of MDA-CTCs. **A.** Ki67-Hoechst FACS plots of negative control cells, parental cells as well as MDA-CTCs and LN metastases found in the recipient mice, 7 weeks after the xenograft. **B.** Quantification of the percentage of tumor cells in G0 (Ki67-) or in cycle (Ki67+) in parental cells, in the MDA-CTCs and in metastases found in the host mice. Overall, CTCs were found to be significantly more quiescent than the other tumor populations.

4.4.4 Circulating Tumor Cells are very heterogeneous

In order to screen for differentially expressed markers in CTCs versus other tumor populations, a FACS gating strategy was set up to study live CTCs within the blood of recipient mice. The FACS plots shown later in the manuscript are all gated on single cells, HLA-ABC positive (Human Leukocye Antigen corresponding to MHC (Major Histocompatibility Complex) class I, which is expressed by all human cells) or EGFP positive (in case of MDA-MB-231 EGFP+) cells, as well as Propidium Iodide (PI) negative cells, to look at live human CTCs only (Figure 38). On average, 98% of MDA-CTCs were non-apoptatoic (PI negative). So the difference in clonogenicity between CTCs and parental cells should not arise from a difference in cell survival.

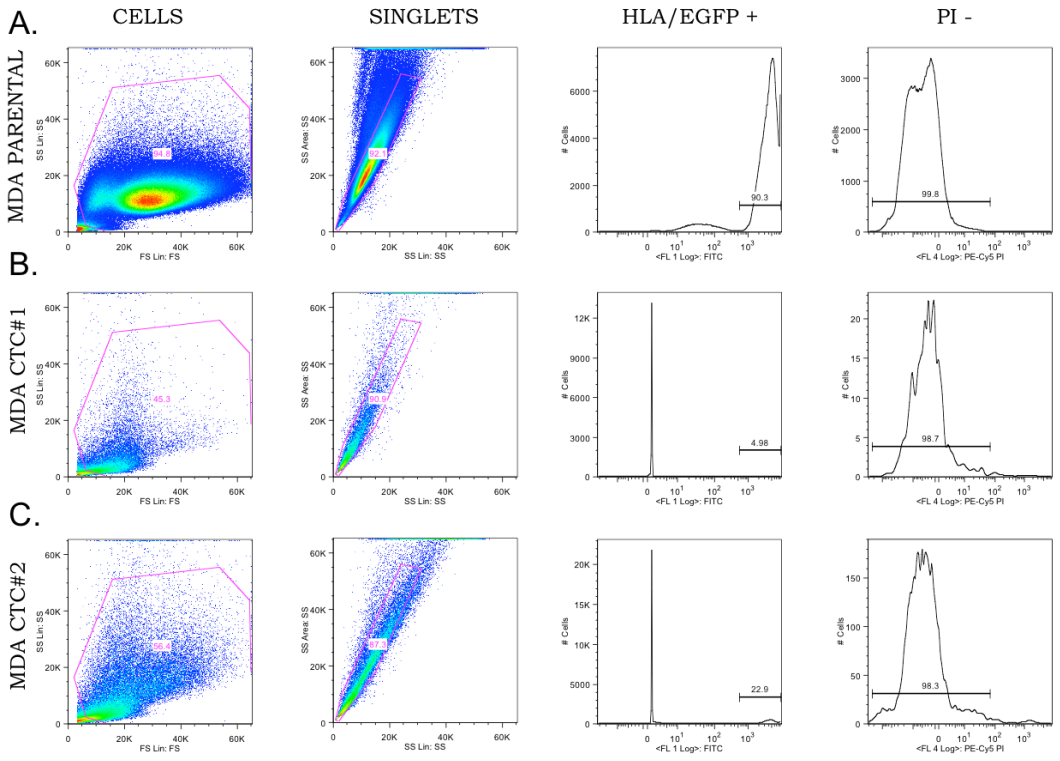

Figure 38. Gating strategy for the analysis of MDA-CTCs. Note that 98% of detected CTCs are generally viable. This is the case when looking at HLA positive cells in MDA-LUC injected mice as well as when looking at EGFP positive cells in MDA-EGFP+ injected mice. **A**. MDA-MB-231 cell line, **B**: MDA-CTC example #1, **C**. MDA-CTC example #2. HLA = Human Leukocyte Antigen, PI = Propidium Iodide; EGFP = Enhanced Green Fluorescent Protein.

First, all CTCs expressed EPCAM (Figure 39), a marker that is still controversial in the field.

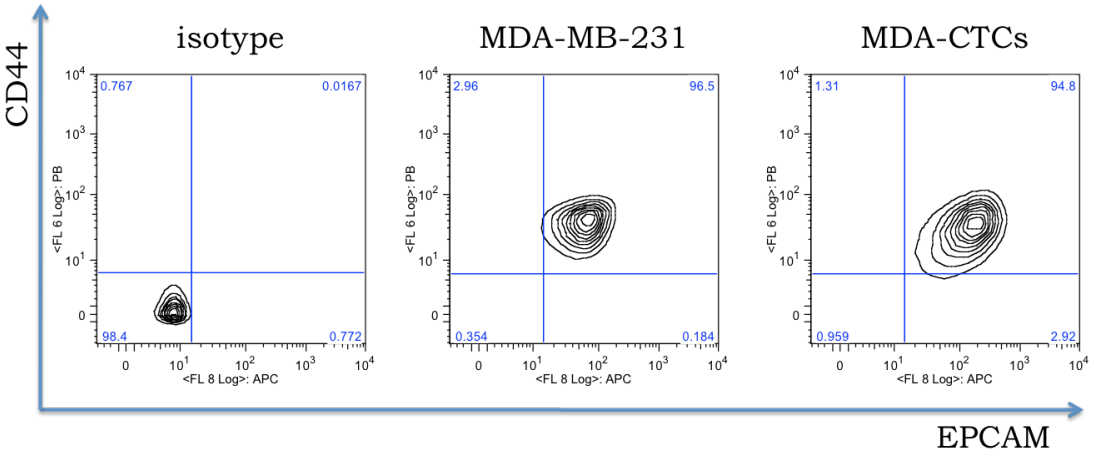

Figure 39. EPCAM status in MDA-CTCs. Most of MDA-CTCs were found to be EPCAM positive, as the MDA-MB-231 parental cells. The expression of CD44 seemed to vary a bit, more cells displaying a lower expression of CD44 in MDA-CTCs than in the parental cell line.

Overall, a strong variability in cell surface protein expression was detected. In looking at differentially expressed markers, CD26, a pleiotropic enzyme recently discovered as a marker for colon metastasizing cancer stem cells (Pang et al., 2010), was expressed in a low fraction of MDA-CTCs (4%), in metastases (5.4%), but not in parental cells (Figure 40).

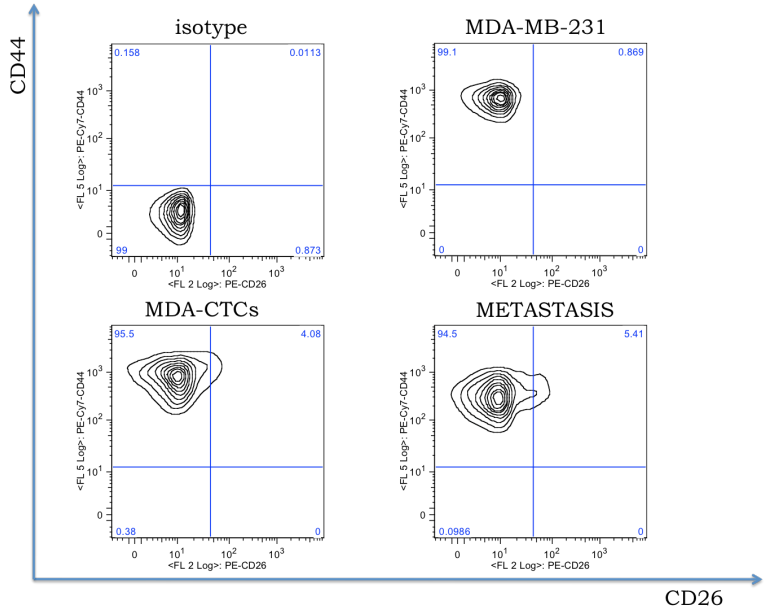

Figure 40. CD26 expression in MDA-CTCs. The cells were gated for doublet exclusion, negativity for Propidium Iodide (PI), negativity for H2KD (a pan mouse marker) and positivity for EGFP. An isotype control was compared to the parental cells, and to CTCs as well as to lymph node metastatic cells for CD26 positivity: while the isotype control and the parental cells show less than 1% of positive cells, CTCs show 4% and metastatic cells 5.4% positivity for CD26.

C-MET, the tyrosine kinase receptor for HGF (HEPATOCYTE GROWTH FACTOR), which is known to induce invasion and tumor growth in carcinomas (Pennacchietti et al., 2003), (Gentile et al., 2008), (Boccaccio and Comoglio, 2006) and (Trusolino et al., 2010), was also found to be differentially expressed in MDA-CTCs. Not all MDA-CTCs expressed C-MET (Figure 41), while parental cells were all positive. The proportion of C-MET negative CTCs varied from mouse to mouse between 3% and 75% (Figure 42).

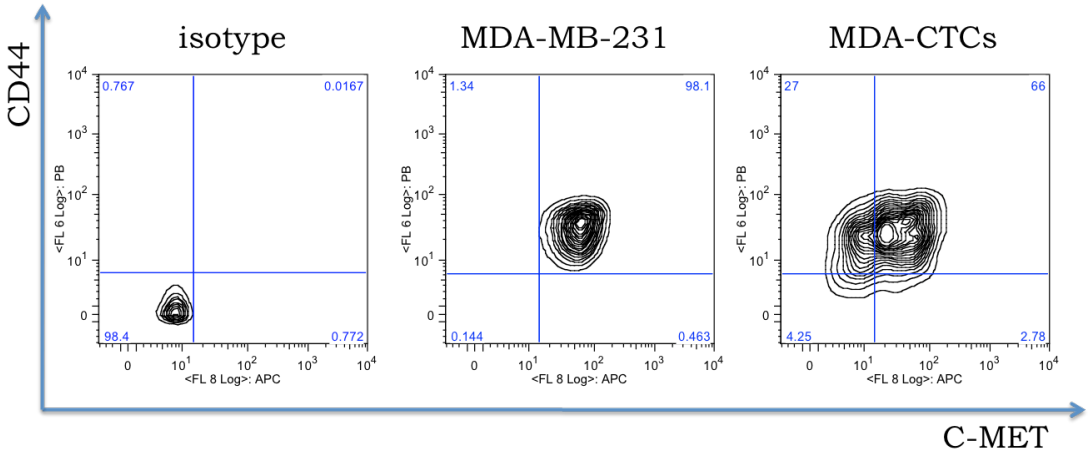

Figure 41. C-MET expression in MDA-CTCs. FACS plot of C-MET expression in an isotype control, in parental MDA-MB-231 cells and in MDA-CTCs. CTCs could be divided in 2 populations: C-MET negative and C-MET positive, while C-MET expression in parental cells was homogeneously positive.

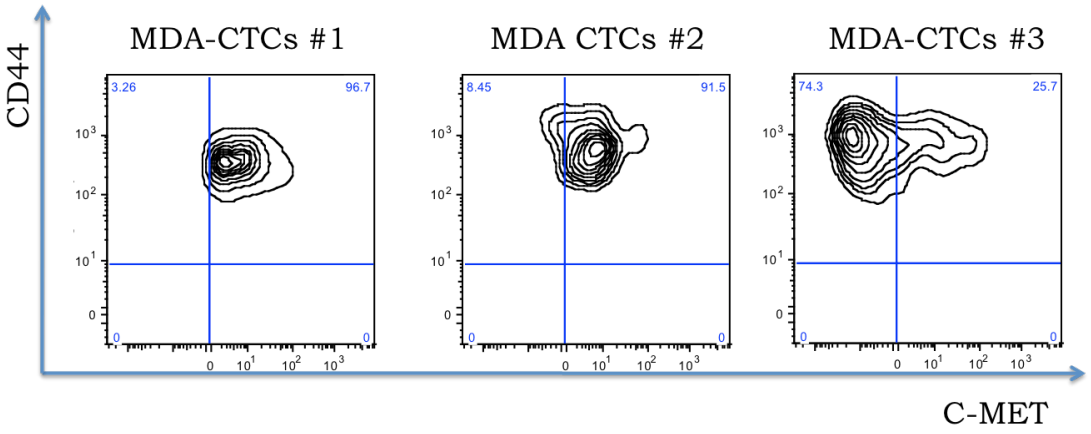

Figure 42. Variability of C-MET expression in MDA-CTCs. Examples of C-MET expression in MDA-CTCs. The proportion of C-MET negative CTC subpopulation varied from 3% to 75%.

Moreover, CD47, which was recently discovered as a major player in tumor cell shielding from macrophage scavenging during dissemination (Chan et al., 2009), (Chan et al., 2010), was also found to have a variable expression level in MDA-CTCs. While parental cells all expressed CD47, 18% to 96% of CTCs expressed the molecule, depending on the mouse (Figure 43).

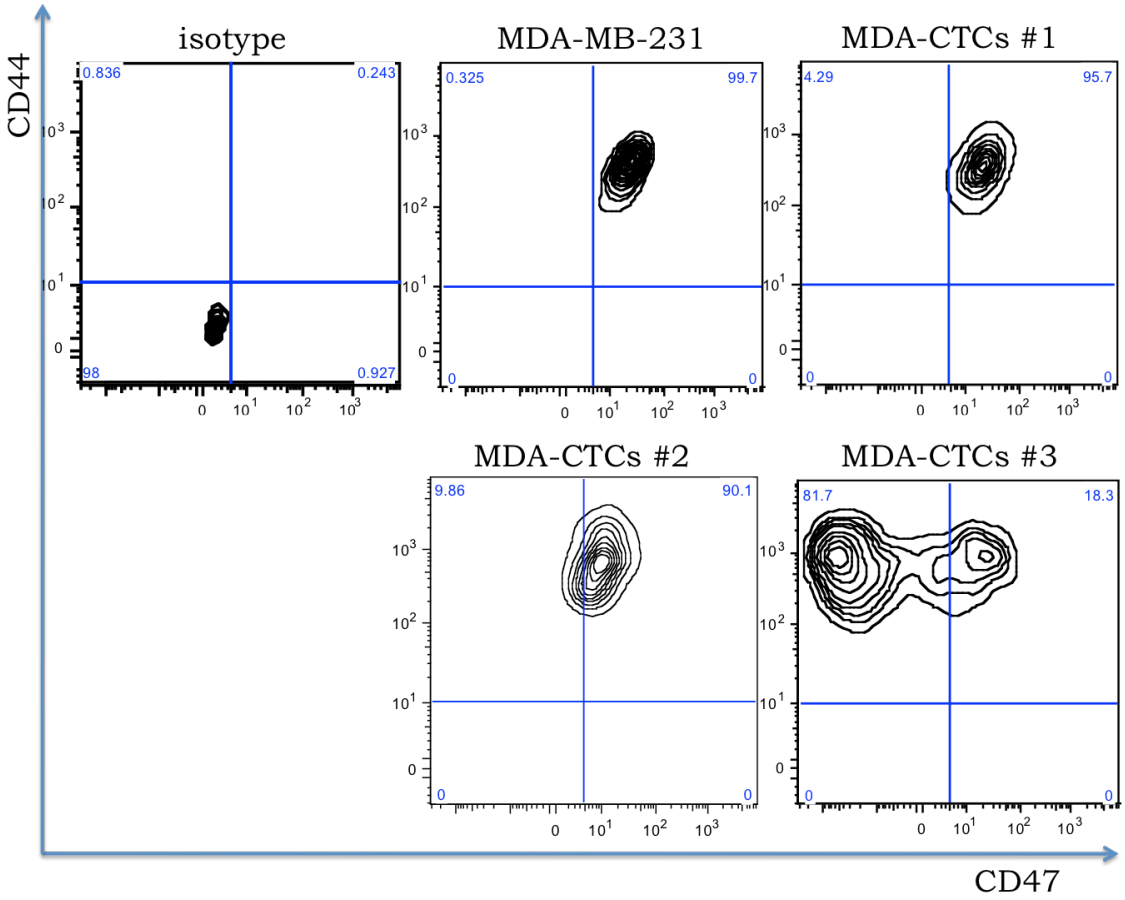

Figure 43. CD47 expression in MDA-CTCs. FACS plot of CD47 expression in an isotype control, in parental MDA-MB-231 cells and in 3 examples of MDA-CTCs. CTCs could be divided in 2 populations: CD47 negative and CD47 positive, while CD47 expression in parental cells was homogeneously positive. The proportion of CD47 negative CTC subpopulation varied from 4% to 82%.

Overall, CD44 expression varied in MDA-CTCs from very high (as in the parental cell line) to lower, but still positive levels (Figures 39 to 43).

Last but not least, C-MET and Ki67 expressions were found to be positively associated, while CD26 expression was associated with quiescence (absence of Ki67 expression), as shown in Figure 44.

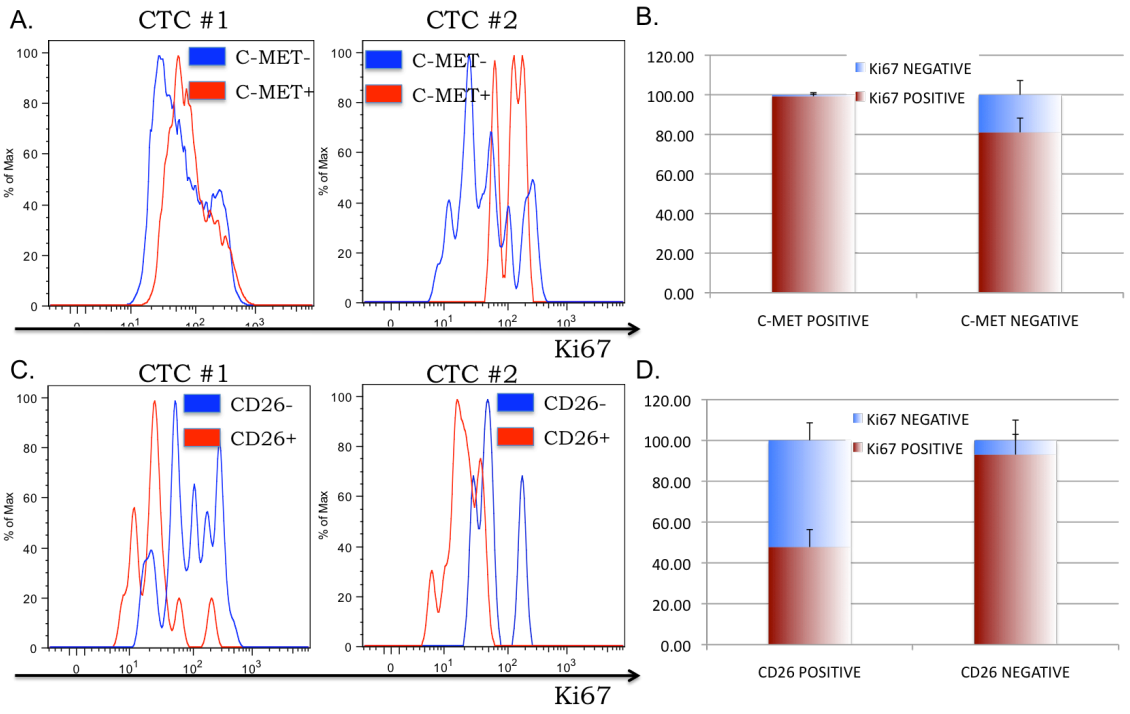

Figure 44. C-MET expression, CD26 expression and cell cycle status of MDA-CTCs. **A.** and **B.** C-MET positivity was found to be associated with Ki67 positivity while **C.** and **D.** CD26 positivity was found to be associated with Ki67 negativity.

As a conclusion for this chapter, MDA-CTCs were found to be mostly non-apoptotic cells and were more quiescent than parental and metastatic cells. As a consequence, they were less clonogenic and less tumorigenic. Also, MDA-CTCs seemed to be heterogeneous since subpopulations of CTCs expressing different levels of CD26, C-MET and CD47 were observed. CD44 expression varied as well from very high levels (as in the parental cell line) to lower but still positive expression levels. Interestingly, associations between quiescence and CD26 expression, as well as between Ki67 expression and C-MET expression were observed in MDA-CTCs.

Thus, even in a relatively standardized assay using a cell line, CTCs were found to be greatly heterogeneous. Indeed, CTCs might gather very different types of tumor cells: for instance, cells that just intravasated into the circulation, or cells that have traveled for some time in big vessels, or also cells that are about to extravasate from a small capillary into a distant organ… The detection of differentially expressed markers will enable the sub-categorization of CTCs according to their cellular state. However, an extensive functional analysis of all CTC subpopulations is required to unravel which markers are useful for the detection of functional MetICs.

4.5 Functional characterization of carcinoma patient Disseminating Tumor Cells

In order to have access to carcinoma patient DgTCs, a series of clinical studies was set up.

4.5.1 Clinical studies for the functional analysis of Disseminating Tumor Cells

* CLINICAL STUDY #1 (BREAST CANCER):

This study was built in collaboration with Prof. Dr. Klaus Pantel and Dr. Sabine Riethdorf from the Institute of Tumor Biology in Hamburg. Blood samples of breast cancer patients were collected between August 2007 and June 2009. One duplicate of each sample was tested in Hamburg for the presence of tumor cells using the FDA-approved CellSearch™ technology, (Pantel and Brakenhoff, 2004), (see chapter 2.3), while the other 7.5 mL of blood was sent to our laboratory for functional analysis of the CTCs (Figure 45). The samples spent at least 24 hours at room temperature in the mail (shipment from Hamburg (Germany) to Lausanne (Switzerland), location of Prof. Dr. Trumpp's laboratory before moving to the DKFZ).

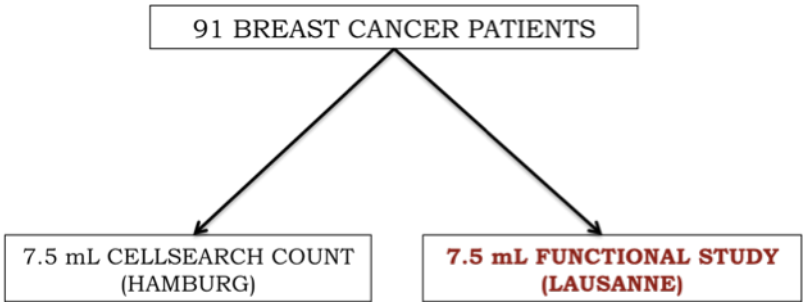

Figure 45. Scheme of clinical study #1 in collaboration with Prof. Dr. Klaus Pantel and Dr. Riethdorf from the Institute for Tumor Biology in Hamburg.

7.5 mL blood samples from 91 breast cancer patients were received (see table number 2, chapter 7.1). 9 of the patients were diagnosed with M0 stage carcinoma, while the 82 remaining patients were metastatic. For technical reasons, the Cellsearch™ device could not measure 6 samples. Out of the 84 remaining patients, 83.33% (70 patients) were found to bear between 0 and 4 CTCs, 10.71% (9 patients) between 5 and 50 CTCs, 1.19% (1 patient) between 51 and a 100 CTCs, 3.57% (3 patients) between a 101 and 500 CTCs and, finally, 1 patient had more than 500 CTCs (Figure 46).

CTC counts were not yet available at the time of the samples' arrival to the laboratory. Therefore, all samples were "blindly" transplanted in mice using the newly established intra-bone xenograft model (see chapter 4.1 and 4.3), in order to detect potential MetICs.

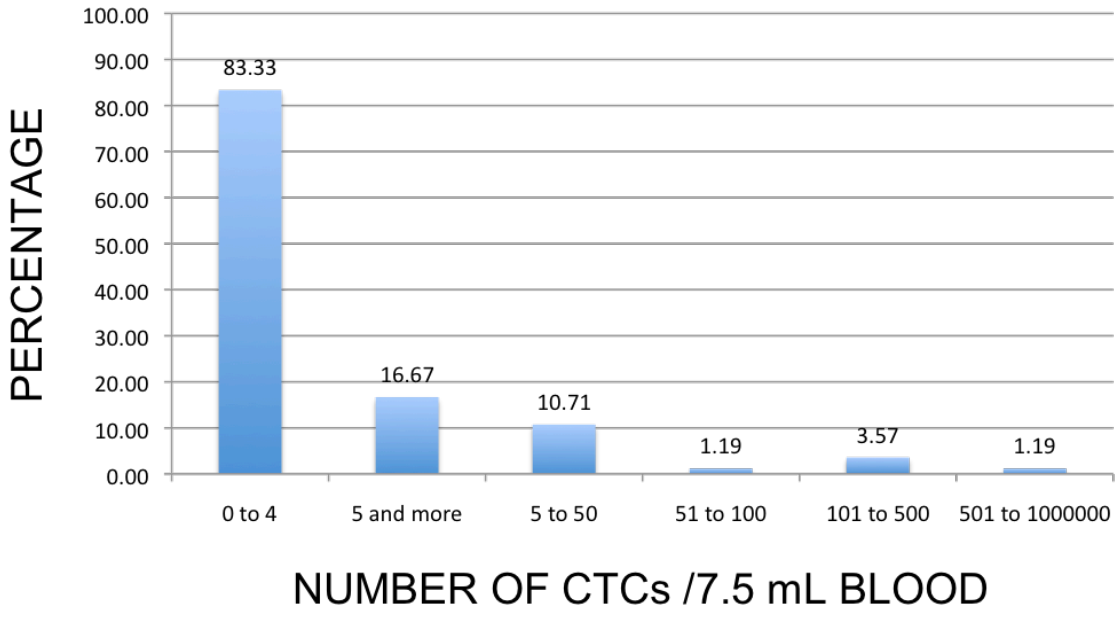

Figure 46. Percentage of patients and CTC counts, Clinical Study #1. CTC numbers were evaluated by the CellSearch™ system in Hamburg (work of Dr. Sabine Riethdorf).

* CLINICAL STUDY #2 (PROSTATE CANCER):

The second study took place between January 2009 and January 2010, with the collaboration of Prof. Dr. Hohenfellner and Dr. Thomas Höfner from the urology department of the Surgery Clinic in Heidelberg. Freshly drawn 30 mL blood samples were collected from prostate carcinoma patients and directly brought to the laboratory. In total, 37 patients were processed. 26 patients had a metastatic disease, and 11 patients had a local cancer (see Table 3, chapter 7.1).

Unfortunately, these samples could not be analyzed for CTC counts. Therefore, the results obtained from this study are difficult to interpret (see chapter 4.5.3). Nevertheless, all samples were injected in mice, using the novel intra-bone xenograft assay.

* CLINICAL STUDY #3 (BREAST CANCER):

The third study started in January 2010, in collaboration with Prof. Dr. Schneeweiss and Dr. Wallwiener from the Heidelberg Frauenklinik and is still on going. Fresh phlebotomies are directly brought to the laboratory and sent to Hamburg to Prof. Dr. Pantel and Dr. Riethdorf for Cellsearch™ analysis. Only patients showing more than 50 CTCs per 7.5 mL of blood are called again shortly after the first screen: 40 mL of blood (containing CTCs) as well as 30 mL of BM (potentially containing DTCs) are then collected for the DgTC functional analysis (Figure 47).

So far, blood samples from 155 breast cancer patients were received, all of metastatic stage (see Table 4, chapter 7.1). 70.27% of the patient cohort (104 patients) had between 0 and 4 CTCs, 20.95% (31 patients) between 5 and 50 CTCs, 4.05% (6 patients) had between 51 and a 100 CTCs, 3.38% (5 patients) displayed between a 101 and 500 CTCs and only 2 patients (1.35%) had more than 500 CTCs per 7.5 mL of blood (Figure 48). 8.78% (13 patients) had more than 50 CTCs per 7.5 mL of blood and were subsequently analyzed with the functional intra-bone xenograft assay.

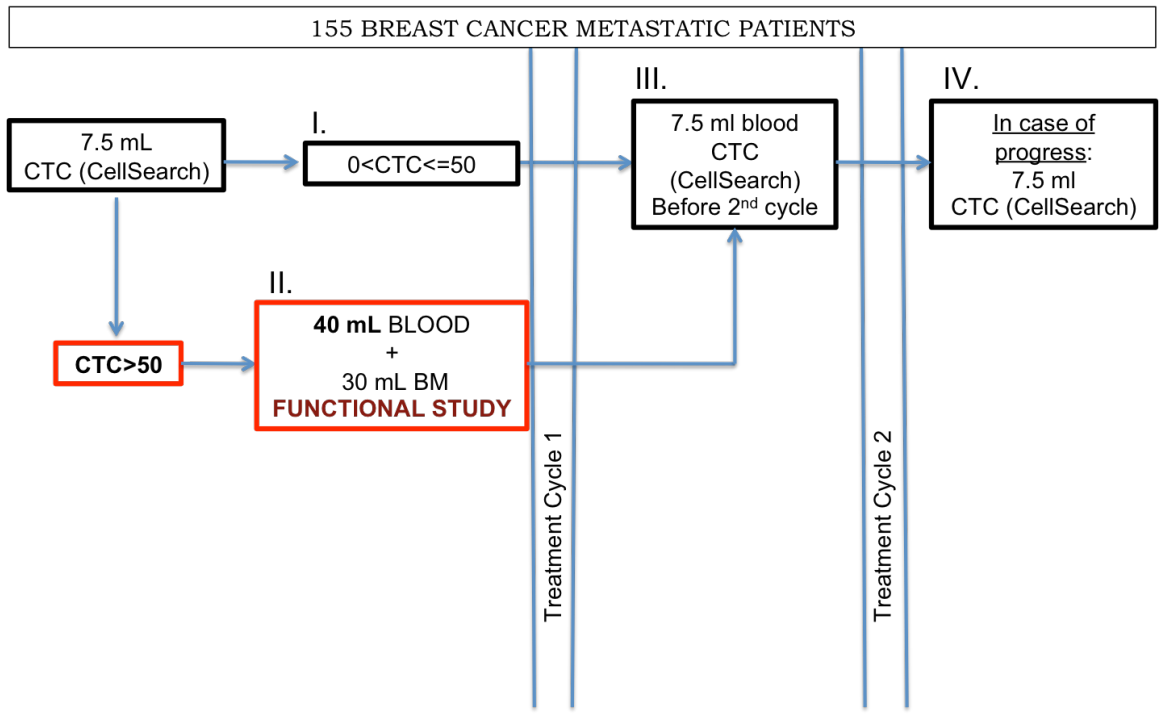

Figure 47. Scheme of Clinical Study #3, in collaboration with Prof. Dr. Schneeweiss and Dr. Wallwiener from the Frauenklink in Heidelberg.The blood samples are labeled I, II, III and IV according to the different time points at which they are collected, as shown in the scheme.

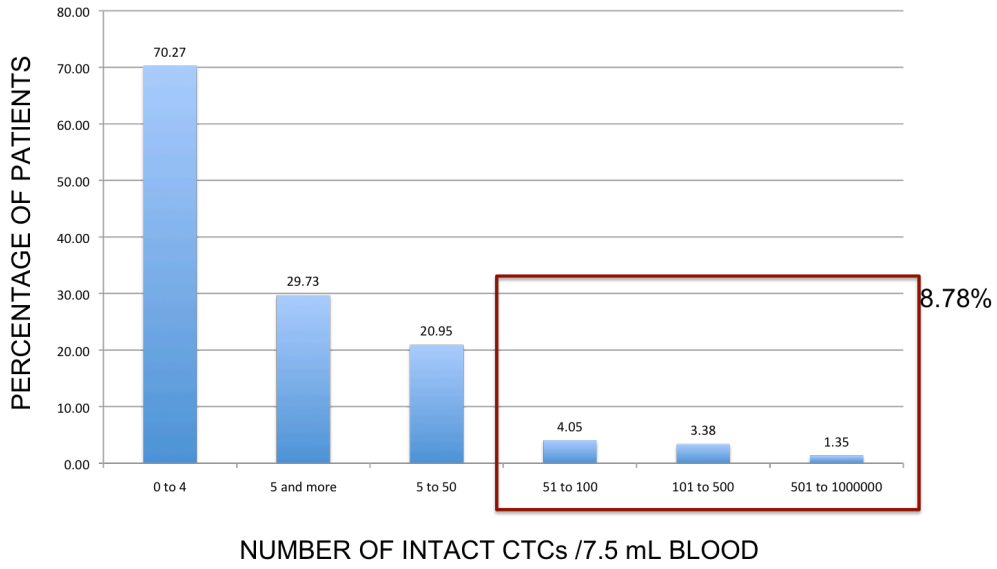

Figure 48. Percentage of patients and intact CTC numbers, Clinical Study #3. CTCs were detected using the CellSearch™ system (Dr. Sabine Riethdorf). Almost 9% of the patients were included in the functional assay (patients with more than 50 CTCs per 7.5 mL of blood).

Cellsearch™ counts were performed by Dr. Sabine Riethdorf in Hamburg. A recent study revealed the presence of many different types of $EPCAM^{+}/CK^{+}/CD45^{-}$ elements (Coumans et al., 2010). It was therefore decided to distinguish full intact CTCs from enucleated-looking CTCs and from apoptotic CTCs when analyzing the Cellsearch™ results (Figure 49).

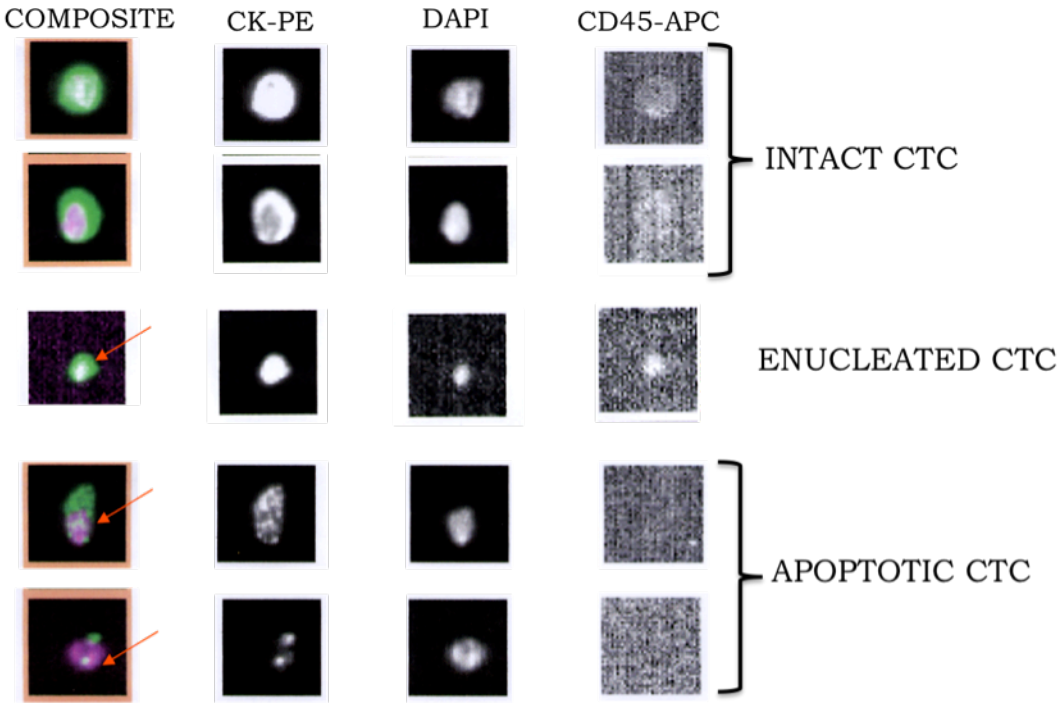

Figure 49. Examples of CTC Cellsearch™ counts for Clinical Study #3. Intact looking CTCs were counted separately from enucleated and apoptotic looking EPCAM positive CD45 negative cells. Cellsearch™ counts were done in Hamburg by Dr. Riethdorf.

The reproducibility of such measurements was tested by analysis of blood sample duplicates. The results shown in Figure 50 suggest that the measurements are highly stable.

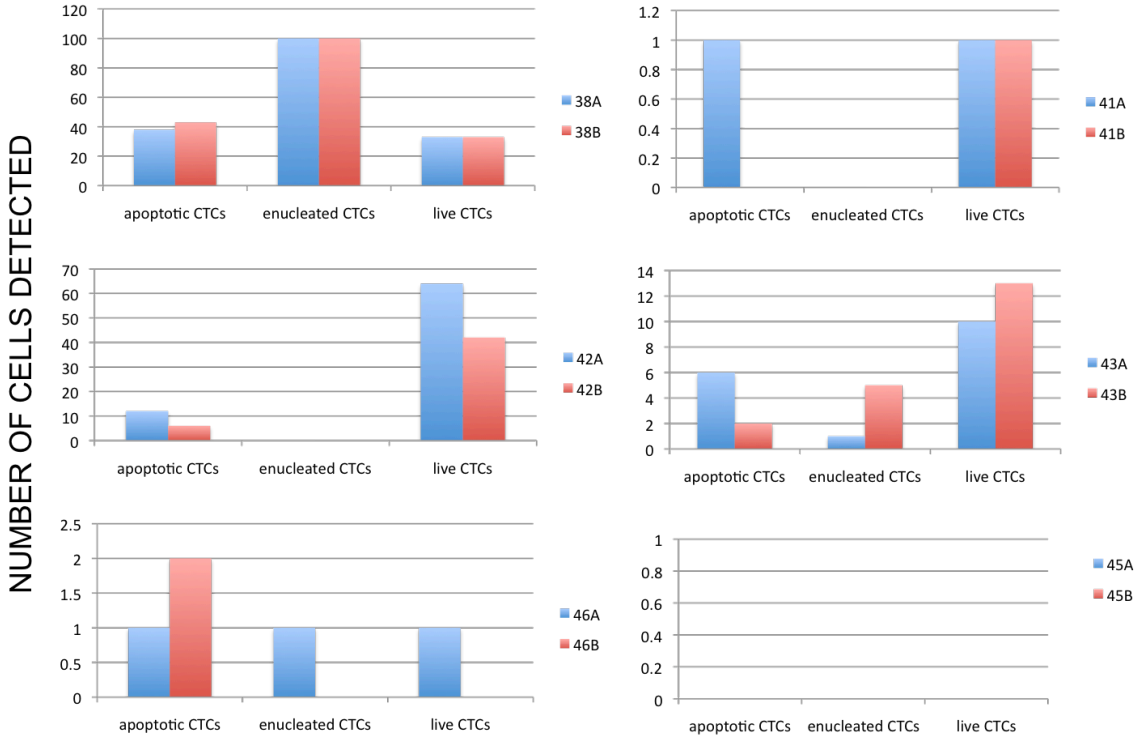

Figure 50. Examples of CTC sample duplicates in Clinical Study #3 to test the reproducibility of CTC counts. Overall, the number of intact CTCs ("live-CTCs"), enucleated CTCs and apoptotic CTCs were highly stable from one duplicate to the other.

The patient cohort repartition of CLINICAL STUDY #3 (Figure 48) does not resemble the one published by Cristofanilli a few years ago (Cristofanilli et al., 2007): the authors found for instance that 44% of their breast cancer metastatic patients had more than 5 CTCs per 7.5 mL of blood. Indeed, the CTC counts included in Figure 47 only gather intact-looking CTCs (since the interest of the study is a functional characterization of live DgTCs). When adding up enucleated-looking and apoptotic-looking CTCs, a similar patient cohort repartition can be obtained (see Figure 56 Chapter 7.1).

CTC counts varied widely during treatment (see chapter 7.2, Figure 57). For instance, in patient #22, after 5 days of irradiation before blood take II, the number of intact CTCs dropped very quickly, while the number of apoptotic and enucleated CTCs increased, suggesting a rapid effect of the treatment on CTCs. In general, all CTC numbers decreased, even though patients underwent disease progression (blood take # III and IV).

Disseminated Tumor Cells (DTCs) were also detected on BM cytospins as CK+ (CYTOKERATIN) / CD45- cells (Figure 51). As in the case of CTCs, DTCs were found to be quite heretogeneous: some cells appeared as clusters (patient 4, Figure 51), or, in other cases, DTCs appeared as isolated single cells (patient 12, Figure 51). Sometimes, DTCs appeared as degraded cells (patient 9, Figure 51).

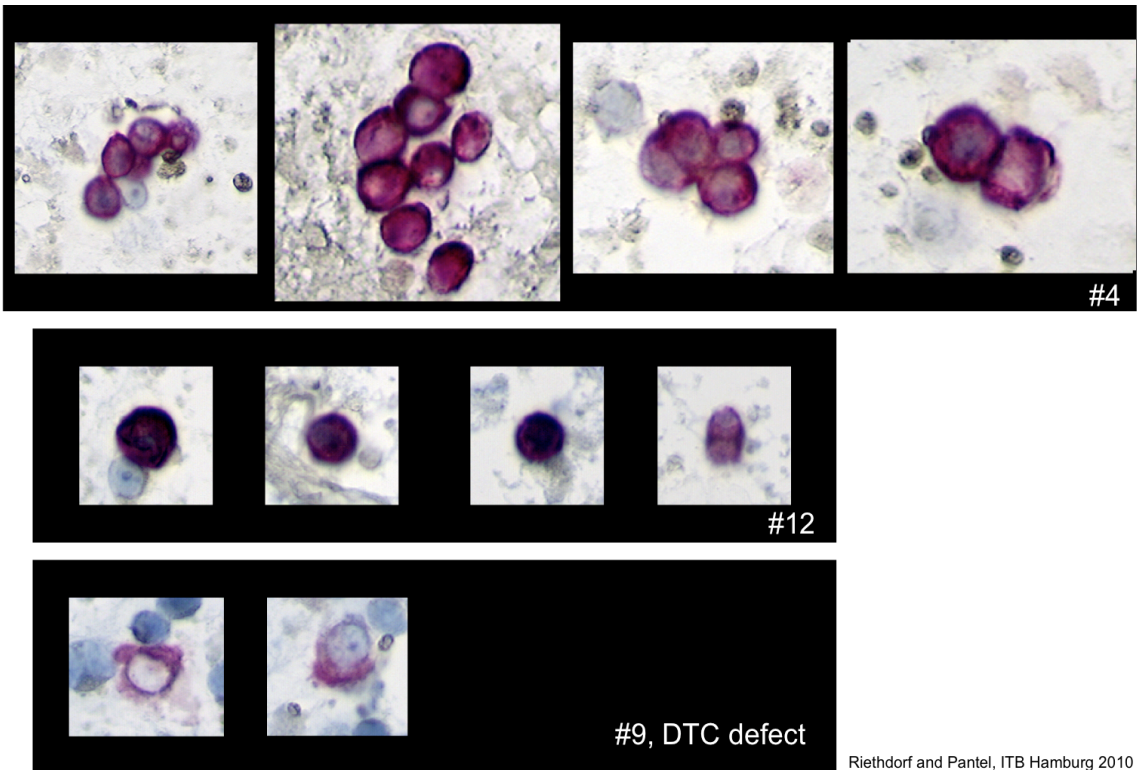

Figure 51. Examples of DTC counts for Clinical Study #3 made on cytospins using an anti-CK (CYTOKERATIN) antibody. The stainings were done in Hamburg by Dr. Riethdorf. DTCs from patient #4, #12 and #9 (Clinical Study #3) are shown.

The presence of DTCs counted in the BM of Clinical Study #3 patients was not associated with the presence of CTCs in the blood. As shown in Table 5 (Chapter 7.3), some patients (for instance patients #42, #51 and #88) had CTCs in their blood but no DTC was detected in their BM. The concordance between CTC positivity and DTC positivity has been studied only in non-metastatic breast cancer (Fehm et al., 2009) where a very weak correlation between CTCs and DTCs was observed. The number of patients analyzed so far for DTCs in Clinical Study #3 is very low, and more data should be gathered to further address this question.

4.5.2 *In vitro* culture optimization for Disseminating Tumor Cell amplification

In order to amplify rare CTCs and DTCs, *in vitro* cultures were carried out. Blood and BM RosetteSep®-depleted samples (see list Table 5, Chapter 7.3) were seeded in culture dishes, using different growth conditions (see chapter 6, Materials § Methods).

Out of BM, some cells expanded (Figure 52 A. and B.). These cells were detected as EPCAM$^-$/CD47$^-$/CD44$^+$/CD26$^+$ cells by flow cytometry analyses (Figure 52 C. and D.). Because of their lack of EPCAM expression, these cultures were probably not consisting of cancer cells but rather of mesenchymal cells initially present in the BM of patients. In any case, these cultured cells were also injected in mice in order to assess their tumorigenic capacity. The mice are currently being monitored.

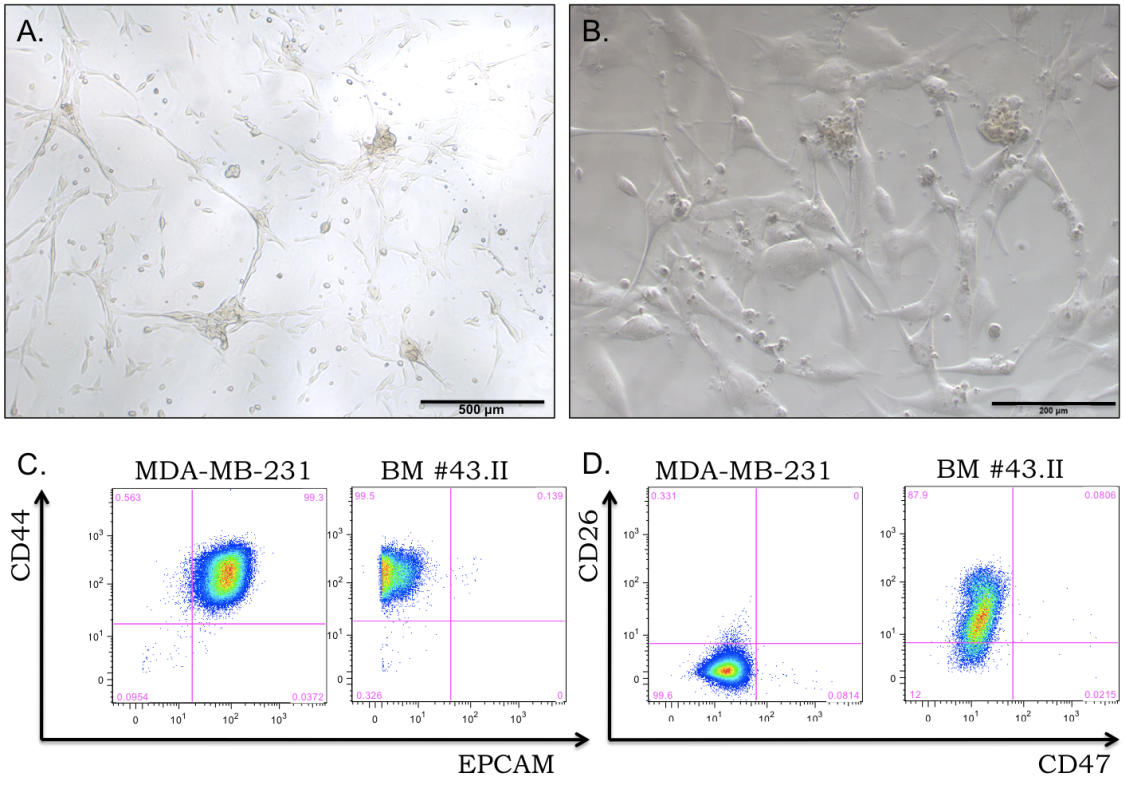

Figure 52. Culture trials for DTCs from BM of **A**. patient #38 (initially containing 4 DTCs per 2 million BM cells, see chapter 7.3) and **B**. patient #43 (number of DTCs not determined, see chapter 7.3) after RosetteSep® depletion. **C.** These cells were however EPCAM negative, therefore I doubt that these cells are tumor cells, but rather mesenchymal cells. **D**. The cultured cells were also found to be CD44 and CD26 positive but CD47 negative.

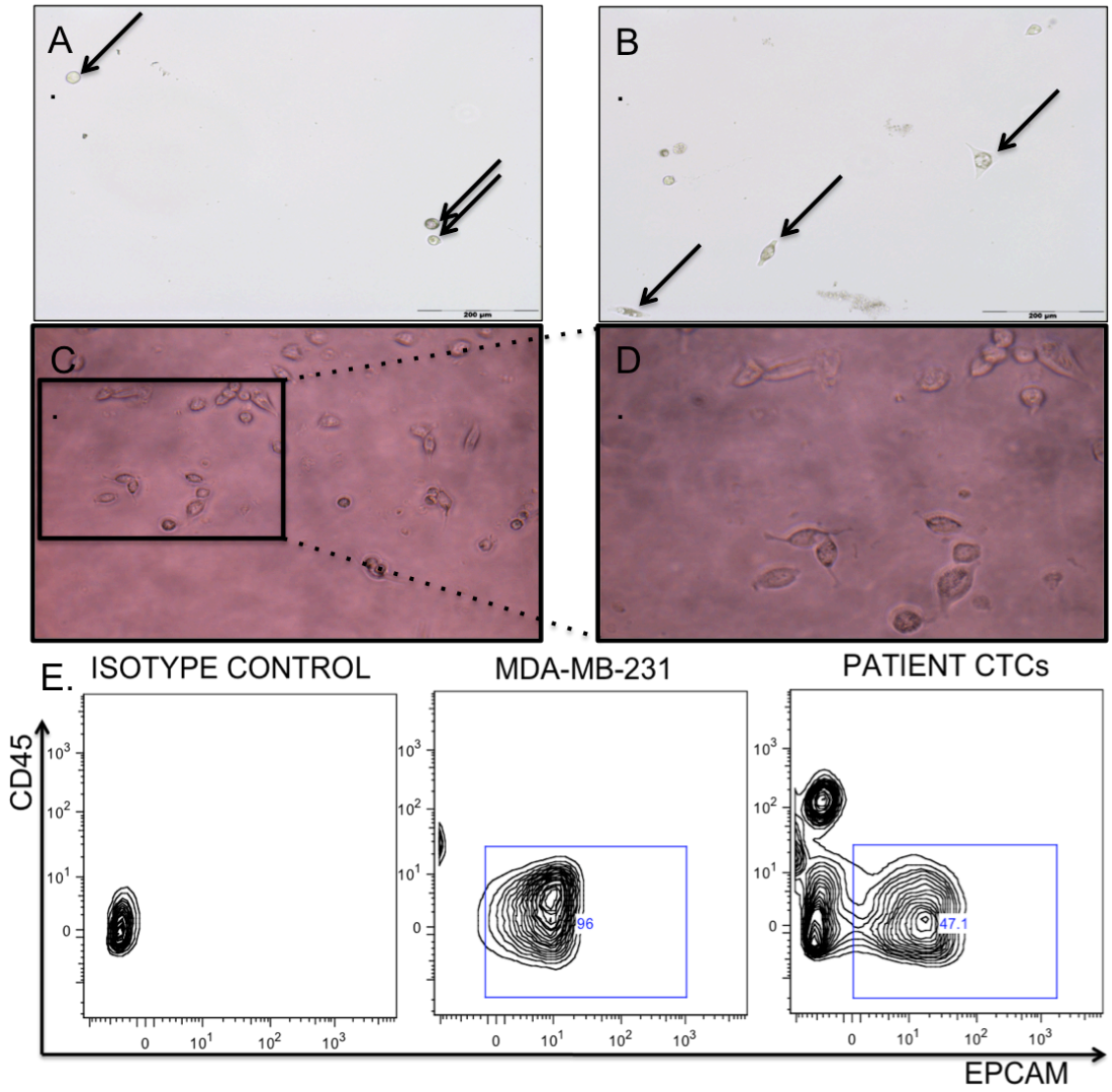

Figure 53. Culture trials of sorted CTCs (defined as PI-/CD45-/EPCAM+ cells) from patient #86 (Clinical Study #3) as shown in **E.** Cells were first seeded first at low density, 7000 cells in a 25-cm3 dish (**A.** and **B.**). In as second trial, CTCs were seeded at high density, 7000 cells in the round-bottom well of a 96-well plate (**C.** and **D.**). However, in both trials, even if CTCs attached to the plastic (**B.** and **D.**), they hardly divided and eventually senesced within a month.

Twice, FACS sort purified CTCs from an exceptionally high-CTC patient (Patient #86, Clinical Study #3, Figure 53 E.) were seeded in culture: first at low density, 7000 cells in a 25 cm^3 dish (Figure 53 A. and B.) and the second time at high density, 7000 cells in the round-bottom well of a 96-well plate (Figure 53 C. and D.). In both cases, cells first successfully attached to the dish but then hardly divided and eventually senesced within a month, indicating that the culture conditions used were not yet optimal.

4.5.3 Optimization of Metastasis Initiating Cell detection *in vivo*

All samples from CLINICAL STUDY #1 and CLINICAL STUDY #2 were injected in mice, following the established metastatic xenograft assay (see chapter 4.1 and 4.3).

CLINICAL STUDY #1:

Half of the samples were used to optimize the technique (see chapter 4.3). Out of 50 sample-injected female mice, 25 were injected with CTC-negative samples and 25 with CTC-positive samples. All mice were analyzed at around 1 year of age. One-year-old non-injected control NOD/SCID/$\gamma_c^{-/-}$ mice developed tumors at a base-line frequency of 10%. A similar frequency of tumors was observed in mice injected with CTC-null samples (12% *i.e.* 3 out of 25). However, the frequency of tumors observed in CTC positive sample-injected mice (44% *i.e.* 11/25) and the frequency of tumors in CTC>=5 /7.5 mL of blood-injected mice (70% *i.e.* 9 out of 13) was significantly increased (p= 0,03 in a Pearson's Chi-square test), (Figure 54). Tumors were mostly found in the lungs, a frequent site of metastasis in human breast cancer (Paget, 1889) and also a frequent site of observed metastasis in my xenograft model (see chapter 4.1).

A collaboration with a pathologist was set up in order to analyze the obtained tumors. Antibodies directed against human cytokeratins, human mitochondrial proteins, against human or mouse Ki67, and against luciferase were used to analyze the paraffin sections (see Chapters 7.4 and 7.5). After 1 and a half-year of misleading immunohistochemical analyses, DNA-based methods such as human specific qPCR (see chapter 6, Materials § Methods) finally revealed that all the tumors found in the recipient mice were of murine origin and consequently that most antibodies used for immunohistochemical analyses were cross-reacting with murine tissues. Indeed, even if positive (human MDA-MB-231 induced tumors in mouse tissues) and negative controls (mouse tissues) were used to set up the immunostainings, tumors developed by the mice were more prone to unspecific binding than healthy murine tissues.

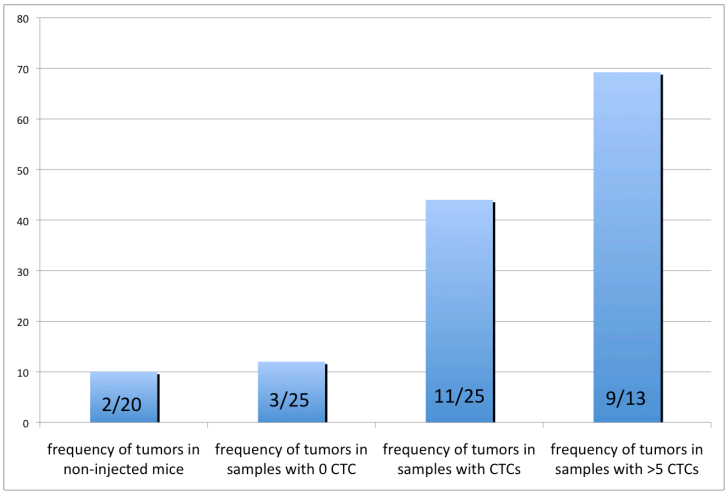

Figure 54. Repartition of murine tumors, Clinical Study #1. Number of murine tumors detected in the host mice according to the CTC numbers of the samples injected. There seems to be a correlation between the presence of CTCs in the samples and the development of murine tumors.

CLINICAL STUDY #2:

All samples were injected in one or several recipient male mice. The mice were analyzed at around 1 year of age. Out of a control group of 20 non-injected male mice, 2 mice (10%) developed tumors. In the cohort of 54 mice injected with cells retrieved from the blood of prostate cancer patients, 23 mice (43%) developed tumors. Unfortunately, the frequency of tumors could not be related to the number of CTCs in the samples because the samples were not analyzed for their CTC content.

The tumors developed mostly in the liver; a few developed in the lungs. These organs are frequent sites of metastasis in prostate cancer (Paget, 1889). However, like in STUDY #1, qPCR analyses revealed that all tumors were of murine origin.

The increased growth of murine tumors in both studies is puzzling. Current experiments aim to investigate whether these murine tumors might be induced by viral means. Indeed, several publications describe the existence of breast and prostate tumor specific viruses, which might be involved in tumor progression (Bindra et al., 2007), (Silverman et al., 2010). This point will be further discussed in Chapter 5.

Due to the results obtained in the first two clinical studies, major optimizations were set up for the organization of CLINICAL STUDY #3.

CLINICAL STUDY #3:

Thanks to a pre-screening of patients (see Figure 47) only samples containing more than 50 CTCs per 7.5 mL of blood were processed. 23 mice were injected with selected CTC-containing samples (see Table 5, Chapter 7.3). The cut-off of at least 50 CTCs/7.5 mL and the sample volume of 40 mL ensured that at least 266 CTCs were available before starting sample processing. The total recovery rate of the assay has been estimated at 35% (see chapter 4.3), so at least 93 cells should have been injected in each recipient mouse. In practice, due to CTC number variation between blood take I. and blood take II., from 0 to 10^5 cells, with a median of only 33 cells were potentially injected per recipient mouse.

80% of breast cancers are hormone-sensitive. CTCs and DTCs are often found to display different hormonal status than their corresponding primary tumors (Fehm et al., 2009). It is therefore impossible *a priori* to predict whether blood samples contain ER+ or ER- CTCs. The endogenous level of estrogen in female NOD/SCID/$\gamma_c^{-/-}$ mice is much lower than in women. In order to enhance the level of estrogen present in the mice, many laboratories use estrogen releasing pellets, as described in a recent publication (Pece et al., 2010). 15 DgTC-receiving mice were therefore subjected to estrogen treatment *via* the implantation of sub-cutaneous estrogen pellets ((high (0.72 mg/pellet) or low (0.18 mg/pellet) concentrations). However, even at low doses of estrogen treatment, the recipient mice developed massive uteri, causing urethral compression and urinary outlet obstruction, leading to uremia and finally to host death within 6 to 8 months after the xenograft.
In these mice, as well as in the remaining 8 other mice, no human tumor was detected so far.

4.5.4 Patient Circulating Tumor Cell characterization: a case report

A 52-year-old patient (patient #86, CLINICAL STUDY #3) was diagnosed with a luminal-A, HER2 negative, ER and PR (PROGESTERONE RECEPTOR) positive invasive lobular carcinoma of the right breast, staging pT1c, pN1bii (5/27), M0, G1. The tumor of the patient was excised as well as the axilliary lymph nodes. The patient was then treated with success by poly-chemotherapy following an ETC regimen (epirubicin (E), paclitaxel (T), and cyclophosphamide (C)), by radiotherapy of the right breast and of the ipsilateral internal lymph nodes, and by a 5-year Tamoxifen anti-hormonal treatment. She unfortunately relapsed 7 years later, with signs of bone metastasis in the backbone and cardiac metastasis in the right ventricular wall. The patient was then treated with percutaneous radiotherapy as well as with bisphosphonate therapy (zoledronic acid). However, the disease further progressed, with pleural effusion occurrence and the patient died 18 months later.

Live CTCs, defined as $PI^-/CD45^-/EPCAM^+$, were sorted from the blood of this patient (Figure 55 A. and Figure 53 E.), and further characterized by flow cytometry analysis. Around 53% of the CTCs were found to be C-MET positive while 47% were C-MET negative (Figure 55 B.). In both fractions, $CD44^{medium}/CD24^+$ and $CD44^{medium}/CD24^-$ subpopulations were present (Figure 55 C.). However, the C-MET positive population only was found to withhold phenotypic breast cancer stem cells, defined as $CD44^{high}/CD24^-$ (Al-Hajj et al., 2003). 2.25% of C-MET positive CTCs and 1.2% of total CTCs thus displayed a cancer stem cell phenotype (Figure 55 C.). Some of these circulating phenotypic cancer stem cells expressed a higher level of C-MET than $C\text{-}MET^+/CD44^{medium}/CD24^+$ and $C\text{-}MET^+/CD44^{medium}/CD24^-$ populations (Figure 55 D.). In addition, all CTCs were found to express CD47, but the circulating phenotypic cancer stem cell subpopulation showed a higher expression of this molecule (Figure 55 F.) However, some of the circulating phenotypic CSCs expressed EPCAM at a lower level than the rest of the CTCs (Figure 55 E.), as described in the EMT process (see Chapter 2.1.2). Also, 1.3% of the CTCs and 1.22% of circulating phenotypic CSCs were found to express CD26 (Figure 55 G.). Most CTCs (96%) and most circulating phenotypic cancer stem cells (98%) were found to express Ki67, indicating that they were activated when isolated from the patient. On the other hand, a 10% higher proportion of quiescent cells ($Ki67^-$) was observed in the CD26 fraction compared to the rest of the CTCs (Figure 55 H.).

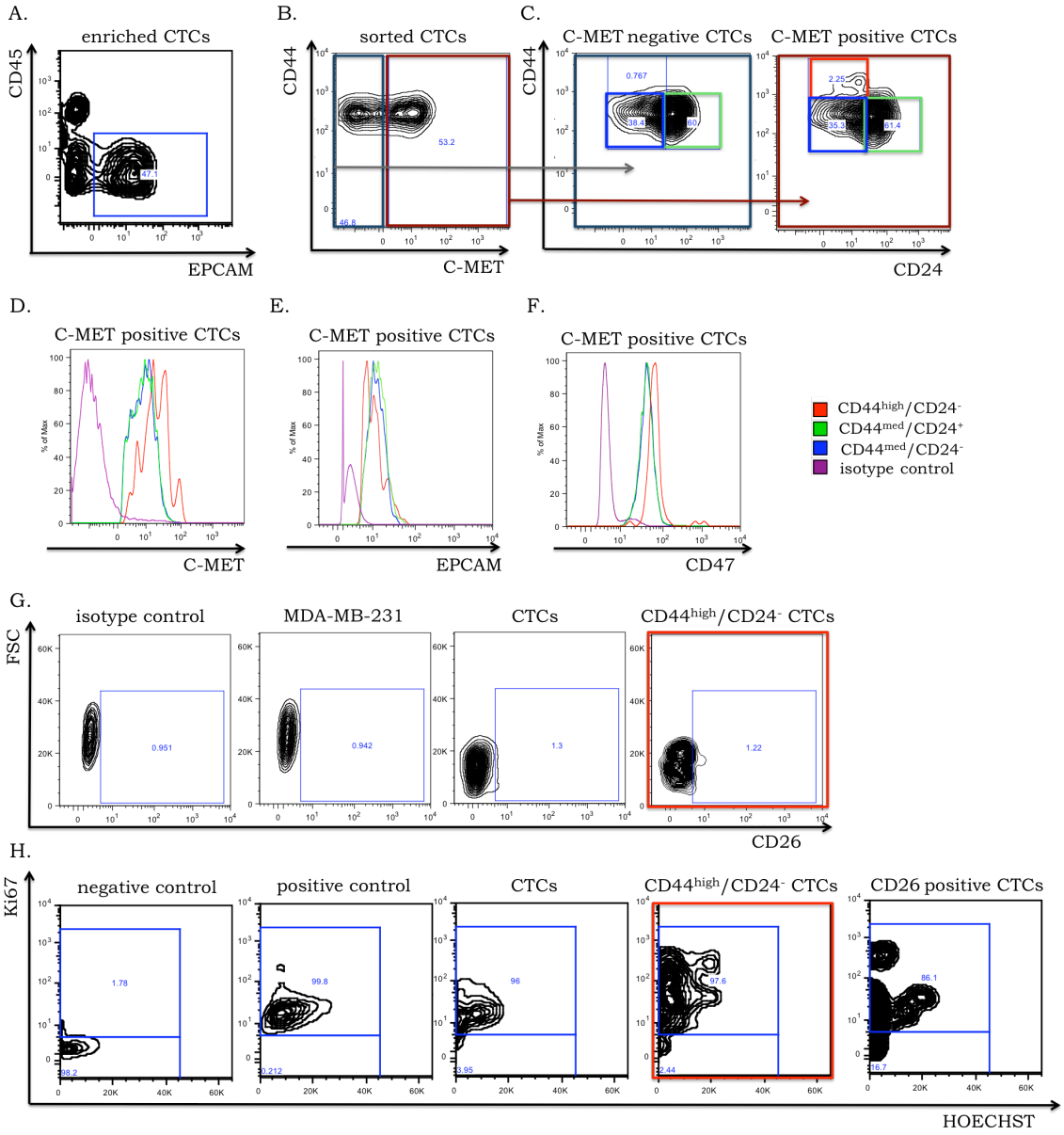

Figure 55. Detection of CTC subpopulations in a patient sample. **A.** Gating of CTCs for flow cytometry sorting defined as PI$^-$/CD45$^-$/EPCAM$^+$ cells, as shown also in Figure 53 E. **B.** and **C.** The CD44^{high}/CD24^{low} (phenotypic circulating CSC) subpopulation was found exclusively in the C-MET positive CTC fraction. **D.** and **F.** C-MET positive phenotypic circulating CSCs expressed higher levels of C-MET and CD47 than the rest of the C-MET positive CTCs, but **E.** lower levels of EPCAM. **F.** CTCs and phenotypic circulating CSCs displayed a 1.2 to 1.3% CD26 positive subpopulation. **G.** CTCs and phenotypic circulating CSCs were mostly Ki67 positive, while CD26 positive CTCs displayed a 10% increase of quiescent cells.

As a conclusion for this last chapter, 3 different clinical studies were carried out in order to try to functionally characterize carcinoma patient DgTCs. So far, DgTCs could neither be grown *in vitro* nor *in vivo*. The possible explanations for this failure will be discussed in chapter 5.

Nevertheless, a case study of patient CTCs lead to the verification of some findings observed in cell line-CTCs, presented in chapter 4.4: patient CTCs were also found to be highly heterogeneous, with different expression levels of CD44, CD24, EPCAM, CD26, CD47 and C-MET. In addition, a small subpopulation of circulating phenotypic CSCs ($CD44^{high}/CD24^{-}$) was found to be exclusively sheltered within C-MET^{+} CTCs. These circulating CSCs had an increased expression level of C-MET and CD47 and were highly activated ($Ki67^{+}$) while their level of EPCAM expression was decreased. On the other hand, the 1% subpopulation of $CD26^{+}$ CTCs was 10% more quiescent than the rest of the CTC population.

5. DISCUSSION § OUTLOOK

5.1 Can patient Metastasis Initiating Cells be detected by a xenograft assay?

Despite a thorough histological analysis (serial sectioning) of all organs susceptible to show metastatic infiltrates (lungs, liver, bones), no human tumor cells were detectable in the DgTC recipient mice. Surprisingly, murine granulomas were often observed, either in the lungs or in the liver (Figure 58, Chapter 7.5). These chronic inflammation sites might be the result of the former presence of human cells in these organs, detected as foreign by the host. However, no trace of human tumor cells was found in these lesions. Therefore, it is difficult to decipher whether human tumor cells (or remaining haematopoietic cells from the patients) ever engrafted in the xenograft model.

Several reasons might explain the failure to detect human tumor cells in our xenograft model. First, from the moment blood samples are drawn from patients until the recipient mice are injected, 75% of the tumor cells might be lost on the way, even when choosing the depletion method with the best recovery rate (see chapter 4.3). Furthermore, DgTCs are very rare cells: even when selecting only patients having more than 50 CTCs/7.5 mL of blood (Clinical Study #3), from 0 to 10^5 cells, with a median of only 33 cells were potentially injected per recipient mouse.

Second, the proportion of MetICs within the pool of these rare DgTCs might be very low. For instance, assuming that CTCs are released at a constant rate, if, in 7.5 mL of blood, at a time-point T, 1 CTC would have the capacity to initiate metastasis, it means that in the patient (5L of blood) there were at this time-point at least 666 CTCs with metastatic initiation capacity in the patient circulation. If a CTC can remain in the circulation for less than a day (as proposed by (Meng et al., 2004)), it then means that, per day, a patient would disseminate at least 666 functional metastatic cells in his body. Which means that during days, months or even years, this patient would be able to start to grow at least 666 metastases per day… Fortunately enough, patients rarely develop 666 metastases, which means that the frequency of MetICs release within CTCs is much lower than 1 per 7.5 mL of blood per day. As discussed in chapter 2.2, MetICs might be deriving from CSCs. In breast cancer, it was

shown by immunocytochemistry, that between 33 and 100% of the M0 stage DTCs display a putative CSC (CD44+/CD24-) cell surface phenotype (Balic et al., 2006). Also, in metastatic breast cancer, between 1 and 40% of M-1 CTCs were observed to display a CSC phenotype (Theodoropoulos et al., 2010). If the exact proportion of disseminating putative CSCs might vary depending on the cancer, on the type of DgTC, on the staging of the disease and on the patient, one can still speculate that not each disseminating CSC has a metastasis initiation capacity. Indeed, following the same reasoning as before, if each disseminating CSC were able to initiate metastasis, patients would have far too many metastases compared to what is observed in the clinic.

A third possible alternative is that MetICs are disseminating within the pool of DgTCs only at specific time-points during disease progression: most of the time, DgTCs would only represent passively shed cells, without any metastasis initiation function but, at some rare moments, functional MetICs would be migrating out of the primary tumor, at a high frequency and start to seed metastasis in distant organs. The correlation between CTC numbers in metastatic patients and decreased relapse free survival and decreased overall survival (Cristofanilli et al., 2007), (de Bono et al., 2008) and (Cohen et al., 2009) might be due to the increased probability for patients bearing CTCs to undergo a MetIC spread, compared to patients who do not tend to disseminate tumor cells in their blood. As exposed in chapter 2.2.1, the scientific community is still debating whether metastatic clones are migrating out of the primary tumor early or late during tumor progression. Some recent data tend to show that metastatic clones are disseminating rather late (Yachida et al., 2010). This is why we chose to collect samples mostly from metastatic patients and not from primary breast cancer patients. However, one may speculate that a kinetic study involving sample collection at different time points of disease progression, might be more adequate to uncover the wave of MetIC dissemination, which in the context of our study set up, has already occurred at least once before, since the patients are already metastatic.

A fourth explanation would be that the frequency of MetICs is high but that their propagation *in vivo* requires a specific microenvironment that could be providing permissive/instructive signals for the MetIC clone to expand, or even more distal control emanating from the primary tumor. If this is the case, the xenograft model, as established during my PhD work might not be fulfilling these requirements: indeed, if MetICs are

dormant longer than 1 year, this exceeds the lifetime of an immuno-compromised mouse. In particular for breast and prostate cancers, metastatic relapse can occur decades after the primary tumor growth. Also, if MetICs are activated by the establishment of a pre-metastatic niche under the control of the primary tumor, the established xenograft model does not provide these conditions either. Therefore, experiments are underway to establish a new xenograft model using patients' primary tumors, with the idea of re-creating a complete metastatic model: from primary tumor growth to metastasis formation.

In conclusion, improving the established xenotrasnplant model, such as inclusion of the primary tumor, will hopefully allow detecting the speculated presence of MetICs. This task might be very challenging since the frequency of these cells might be extremely low within the DgTCs. In addition, if these patient MetICs are dormant, one may consider improving their xenotransplantation, by identifying means that could activate them.

5.2 Induction of murine tumors by Circulating Tumor Cell positive samples

During the thorough histological analysis (serial sectioning) of the organs of the host mice, murine tumors were discovered in Clinical Study #1 and #2 (see chapter 4.5.3). These carcinomas were found in the lungs, the liver or the peritoneal cavity (see chapter 7.5). The frequency of murine tumors observed in CTC positive sample-injected mice (44%) and the frequency of murine tumors in CTC>=5 /7.5 mL of blood-injected mice (70%) was significantly increased (p= 0,03 in a Pearson's Chi-square test), compared to non-injected control and CTC-nul injected mice (10% and 12%) (Figure 54).

As shown in the case of cervical cancer, some carcinomas are mediated by viral infection (zur Hausen, 2009). Also in breast and prostate cancers, some publications reveal the presence of tumor specific viruses, which could have a link with disease initiation and progression (Bindra et al., 2007), (Silverman et al., 2010). Therefore, experiments aiming to investigate whether these murine tumors might have been induced by viral means are underway. This possibility is indeed realistic, if one infected tumor cell is sufficient to transmit the virus to a host mouse: according to the recovery rate of the assay (35%), mice that received samples containing more than 3 CTCS might have in reality received 1 potentially infected CTC and be primed for carcinoma development. In support with this

hypothesis, a high increase of tumor occurrence was detected in mice that received samples containing initially 5 and more CTCs per sample (Clinical Study #1, Figure 54).

An alternative explanation would be that tumorigenesis of the host mice is induced by pre-metastatic cells residing specifically in CTC-positive samples. BM derived precursor cells might have been injected along with the enriched CTCs and these cells might have started to build pre-metastatic niches in the peripheral organs of the host mice, thus promoting tumor development in the host mice. Indeed, some studies describe increased pre-metastatic niche cell dissemination through blood, depending on the tumor stage and on the metastatic burden (Naik et al., 2008), (Diaz-Montero et al., 2009). However, this hypothesis is difficult to prove since no human cell was found in/in the vicinity of the murine tumors by histology or by qPCR.

Eventually, a third explanation would be that CTC-positive samples were more immunogenic and therefore introduced a strong inflammatory state in the recipient mice compared to the other mice. It is indeed known that inflammatory states induce carcinogenesis (Scrivo et al., 2011). Moreover, granulomas were detected in the recipient mice (see chapter 7.5, Figure 58), sign of active immune reactions present in the lungs and livers of the host animals. However, the mechanism by which the immunogenicity of the samples would be increased in CTC-containing blood samples still remains to be investigated.

5.3 Heterogeneous DgTCs shelter quiescent and activated circulating CSCs

CTCs were studied both in a cell line-based model as well as in carcinoma patients (see chapter 4.4 and 4.5). In both cases, a tremendous variability in CTC numbers was observed, even though all mice and most of the patients were highly metastatic. CTC numbers did not correlate with total tumor burden, as measured by total bioluminescence in the cell line-based model (Figure 19 A.). This is in agreement with what was observed in patients, as reported in the literature (Muller et al., 2005). Since CTCs are cells entering the blood circulation, it is tempting to speculate that CTC numbers may rather be linked to the extent of vascularization in the primary and secondary tumors of the patients as opposed to simply correlating with the tumor size itself. In order to test this hypothesis, future experiments

will evaluate the level of tumor vascularization by MRI and test whether it correlates with the number of CTCs detected in the recipient mice.

In the cell line-based model, CTCs were found to be on average more quiescent than the parental cell line and than the metastases isolated from the host mice (see chapter 4.4.3). However, there was a strong heterogeneity among the recipient mice. In the case of patient #86, Clinical Study #3, I detected mostly Ki67 positive CTCs. This cell cycle heterogeneity is in agreement with recent publications, which show that 1% to 80% of M-1 CTCs can be Ki67 positive, depending on the type of cancer and on the progression of the disease (Muller et al., 2005), (Stott et al., 2010). The distinction between quiescent and activated CTC dissemination stages might better describe disease progression. For instance, the presence of 96% activated CTCs in the blood of patient #86 corresponded to a rapid and fatal outcome.

In addition to their cycling behavior, the cell surface phenotype of these cells was also analyzed, and some qualitative and quantitative differences in cell surface markers were observed, which could have important implications for their function *in vivo*.

CD26 or dipeptidyl peptidase IV (DPPIV) is a pleoitropic enzyme, which is expressed on several cell types, notably on activated T cells. It can bind to several proteins, among which FIBROBLAST ACTIVATING PROTEIN ALPHA (FAP-ALPHA), PLASMINOGEN, ADENOSINE DEAMINASE (ADA), the tyrosine phosphatase CD45, and the chemokine receptor CXCR4. It can also bind to the extracellular matrix (ECM) and depending on the presence of other ligands, this process can either lead to increased or decreased invasive activity of the cells on which it is expressed. Therefore, it can act as a tumor suppressor or activator depending on the tumor type. It was for instance recently described as a marker for metastasizing CSCs in colon cancer (Pang et al., 2010). However in prostate cancer, a metastasis suppressor role was suggested for CD26, *via* the degradation of SDF1 (Sun et al., 2008). In breast cancer, CD26 was proposed to inhibit metastasis and the level of CD26 expression was reported to be low (Havre et al., 2008). CD26 expression was indeed found to be rare in breast cancer CTCs (between 1 and 5% of CTCs, see chapter 4.4.4 and 4.5.4) and CD26 expression associated with increased quiescent fractions of CTCs, both in the cell line-based model and in the CTCs of patient #86. In breast cancer, CD26 might be expressed by quiescent CTCs and quiescent circulating CSCs. Because quiescence can lead to chemo-resistance and radio-

resistance capacities, future experiments will aim to test the resistance of $CD26^{+}$ cells during chemotherapy or radiotherapy.

CD47 is a cell surface protein, responsible for the increase in intracellular calcium concentration that occurs upon cell adhesion to ECM. Many different cell types express CD47. This protein was recently incriminated in bladder cancer as a tool for tumor cells to evade macrophage scavenging (Chan et al., 2009), (Chan et al., 2010). CD47 might be crucial for MetICs, as they have to be able to migrate out of the tumor, to survive in the circulation and to seed in a distant organ, without being detected as abnormal by the surrounding immune system. The increased CD47 expression by the circulating CSC pool (see chapter 4.5.4) might represent an increased MetIC ability for such cells. Future functional experiments will investigate the metastatic potential of $CD47^{high}$ cells compared to $CD47^{low}$ cells.

C-MET is a tyrosine kinase receptor for HGF (HEPATOCYTE GROWTH FACTOR) (Bottaro et al., 1991). C-MET transcripts were detected in CTCs, in 44% of breast cancer patients (Chen et al., 2006). Abnormal C-MET activation in cancer correlates with poor prognosis, triggering tumor growth, invasion and EMT (Pennacchietti et al., 2003), (Gentile et al., 2008) and (Boccaccio and Comoglio, 2006). This could be verified using the cell line-based model, where C-MET expression level in CTCs was associated with increased Ki67 expression (see chapter 4.4.4). Most importantly, in the case of breast cancer metastatic patient #86 (see chapter 4.5.4), circulating phenotypic CSCs ($CD44^{high}/CD24^{-}$) were only found in the C-MET positive CTC fraction and showed a higher expression of C-MET than the other CTCs and also a high proliferative capacity, with 97 % of the circulating phenotypic CSCs being Ki67 positive (see chapter 4.5.4). Most relevant, CD44 isoforms have been shown to form a ternary complex with HGF and C-MET that mediates activation of the receptor and its link to ACTIN microfilaments, which subsequently activates RAS signaling (Orian-Rousseau et al., 2002).

C-MET has been proposed as a CSC marker (Boccaccio and Comoglio, 2006), (Trusolino et al., 2010). In line with this proposition, phenotypic circulating CSCs were detected only within the pool of C-MET positive CTCs in the blood of patient #86. Moreover, in steady-state conditions, C-MET is not expressed by the differentiated haematopoietic cells present in the peripheral blood (Beilmann et al., 1997). Therefore, high expression of C-MET can be

considered as a good candidate marker for putative circulating breast CSCs, in combination with EPCAM, CD44 (positive markers), CD24 and CD45 (negative markers). This raises the possibility to use new anti-C-MET therapy to target putative circulating CSCs. The results would of course need to be confirmed by future analyses of other patient CTC populations. Very interestingly, some of the patient phenotypic circulating CSC population also showed a decreased expression of EPCAM, further supporting the idea that these cells underwent EMT, as also suggested by the increased expression of C-MET (see Chapter 2.1.2).

Based on immunofluorescence microscopy experiments, it was reported that between 1 and 40% of M-1 CTCs display a $CD44^{high}/CD24^{-}$ phenotype (Theodoropoulos et al., 2010). In our study, the blood of patient #86 showed that phenotypic CSCs were present at a frequency of 1.2% of the total CTC population (see chapter 4.5.4). Of note, this patient displayed extraordinarily high CTC numbers, and therefore carried around 40 circulating CSCs per 7.5 mL of blood as determined by FACS, while by immunofluorescence, only 1 to 20 $CD44^{high}/CD24^{-}$ CTCs /7.5 mL of blood were observed (Theodoropoulos et al., 2010). Moreover, these circulating phenotypic CSCs were activated (Ki67 positive). The elevated number of activated (Ki67 poistive) circulating putative CSCs identified in this patient might reflect an aggressive phenotype more characteristic of terminal stages.

In conclusion, a very high heterogeneity of CTCs was observed both in the cell line-based model and in patients. This is in agreement with the wide phenotypic CTC heterogeneity also observed by careful cytomorphologic analyses in the case of colon cancer (Marrinucci et al., 2010). Moreover, differentially activated CTC cell cycle states were observed. The distinction between quiescent CTCs and activated CTCs might allow a better distinction between slow and rapid disease evolution phases. Markers indicative of such cell cycle states might lead to the development of targeted therapy against activated circulating CTCs, probably representing an immediate threat for the patients. In addition, a putative circulating breast CSC population was detected in a patient sample. Since these $CD44^{high}/CD24^{-}$ CTCs not only expressed the highest level of C-MET and CD44 but also the "don't eat me" signal CD47 and lower levels of EPCAM (sign of EMT), it seems likely that this sub-population harbors the most malignant character and might contain MetICs.

On the whole, only a small fraction of these highly heterogeneous CTCs might be able to initiate metastasis: functional characterizations of each separate CTC subpopulation remain mandatory for the detection of MetICs within quiescent or activated CTCs/within quiescent or activated circulating CSCs.

5.4 Metastatic cells: intruders of the physiological bone marrow niche

In agreement with the work of others (Phadke et al., 2006), our data showed that breast tumor cells engraft preferentially at the endosteum, in the trabecular zone of the long bones (see chapter 4.2.1). Using a competitive BM reconstitution assay, metastatic tumor cells were found to inhibit exogenous HSC BM repopulating activity, suggesting a competition between tumor cells and HSCs for the occupation of the BM niche (see chapter 4.2.2). Surprisingly, the number of resident HSCs also decreased in bones injected with breast tumor cells, suggesting that tumor cells can also dislodge resident HSCs from their niche. This effect was local, as the non-tumor-cell-injected bones did not show such decrease in foreign and resident HSC numbers.

The mechanisms by which tumor cells compete with HSCs for the occupancy of the BM niche remains to be identified. Also, the fate of the outcompeted HSCs needs to be investigated. In the future, examining the number of HSCs in the spleen and in the blood circulation will determine whether HSCs have been mobilized. Also, a cell cycle and cell death analysis of the remaining HSCs might provide useful information.

Estrogen treatments have been shown to increase the risk for breast cancer development and breast cancer invasiveness, as shown by studies on hormonal replacement therapy in menopausal women (Chlebowski et al., 2010), (Liang et al., 2010). In addition, using BM reconstitution assays, our data showed that high dose estrogen affected the BM niche occupancy by HSCs: it negatively affected foreign and resident HSCs in the BM, leading to total BM failure (see chapter 4.2.3). Therefore, estrogen treatments might further enhance the capacity for breast metastatic cells to colonize the BM stem cell niches.

It is overall very surprising to detect such a strong effect of estrogen on HSC engraftment. Indeed, no such observation has been reported previously in the literature. On the contrary, estrogen is known to down-regulate parathyroid hormone (PTH), which has a negative effect on HSCs and their niche (Lemieux et al., 2008). Estrogen also induces the production

of PROSTAGLANDIN E2, which improves HSC homing (Hoggatt et al., 2009). Last but not least, female NOD/SCID/γc-/- mice have shown much better engraftment rates of human HSCs than male NOD/SCID/γc-/- mice (Notta et al., 2010). However, in our experiment, much higher doses of estrogen were applied than in physiological conditions. The effect of estrogen on HSCs might be dose-dependent. Indeed, the survival of chimera mice treated with lower concentration estrogen pellets was increased when compared to mice treated with higher concentration estrogen pellets. The reasons of such differences will be further investigated in future experiments.

Estrogen has 2 receptors: ER-α and ER-β. Neither is reported to be expressed by HSCs and by haematopoietic progenitors. However, ER-β is expressed by endothelial and bone cells. Estrogen is indeed known to inhibit bone resorption (*via* the inhibition of follicle stimulating hormone, FSH) and to induce osteoblast differentiation (Nicks et al., 2010). In the endothelial compartment, estrogen induces vasodilatation and vessel permeabilisation (Guo et al., 2005). The observed effect of estrogen on HSCs might therefore be indirect, mediated by BM niche cells. Indeed, the bone marrow environment seemed to be invaded by fat droplets, which might be a sign of niche deregulation (Omatsu et al., 2010). Future experiments will aim to investigate which cells are responsible for estrogen-induced effect on HSCs in the BM.

In addition, high-dose estrogen treatment induced a massive CD34 up-regulation. CD34 is a transmembrane protein that is highly expressed on murine ST-HSCs and progenitors; despite its importance as a marker for HSCs, its function is still poorly understood, although a role in cell adhesion has been demonstrated by *in vitro* experiments (Majdic et al., 1994), (Healy et al., 1995). The up-regulation of CD34 could be a consequence of the BM failure, as an attempt to retain HSCs in the BM, by up-regulating their cyto-adhesiveness. Alternatively, this increase in CD34 expression might be the sign of an activation of LT-HSCs into ST-HSCs (expressing CD34), which in turn differentiate into progenitors and differentiated cells. This shift from LT-HSCs to activated ST-HSCs might cause a quick exhaustion of the stem cell pool and lead to the observed BM failure.

Moreover, we could show that exogenous and resident HSCs after estrogen treatment are not mobilized to peripheral organs (see Figure 25). Cell cycle and cell death analyses will be carried out to further investigate the fate of HSCs during high-dose estrogen treatment.

The CXCR4-SDF1 axis, which is pivotal for HSC engraftment into the BM niche is also very important for breast cancer cell engraftment in the BM: a long-term treatment might leave HSCs unaffected (Broxmeyer et al., 2005) but might prevent breast tumor cells from engrafting into the BM (see chapter 4.2.4). Furthermore, no increase of tumor growth was observed in other organs, suggesting that bone-attracted cancer cells do not engraft at all in the host mice. Such types of preventive treatments might therefore be proposed to prevent breast cancer DTC engraftment in the BM of non-metastatic patients.

As a conclusion for this chapter, breast cancer metastatic cells were observed to be able to usurp the BM stem cell niche, and this process might be further enhanced by estrogen treatments (for instance in the case of post-menopausal hormone replacement therapy). In addition, preventive treatments such as AMD3100, able to target specifically metastatic cells but not HSCs, might help to prevent the development of bone metastases as well as the establishment of a DgTC reservoir in the BM. Such strategies should be further investigated as they might strongly reduce the development of fully metastatic cells and therefore reduce metastasis occurrence in breast cancer patients.

5.5 Conclusions

Even though DgTCs were not able to form tumors in the newly established xenograft model, interesting information was gained about CTC heterogeneity and about circulating phenotypic CSCs in breast cancer. Also, the acquired data indicate that DgTCs can be further divided into quiescent and activated populations. Some markers associated with these two different states were uncovered. Last, but not least, new mechanisms of DgTC engraftment in the BM were discovered, showing that metastatic cells are able to usurp the physiological BM stem cell niche. Some mouse experiments suggest that AMD3100 pre-treatment of non-metastatic patients could prevent the engraftment of DgTCs in the BM. Such preventive treatments might strongly reduce the development of fully metastatic DgTCs and therefore reduce metastasis occurrence in breast cancer patients.

6. MATERIALS § METHODS

MICE:

Mice used were NOD/SCID or NOD/SCID/$\gamma_c^{-/-}$. Authorization numbers 1728 and 1967 in Switzerland as well as G-114/08 in Germany were obtained from the respective national authorities for research experiments on animals. Mice were maintained in the ISREC/EPFL (Lausanne) and DKFZ (Heidelberg) animal facilities under specific pathogen free (SPF) conditions and housed in individually ventilated cages (IVC).

INTRA-FEMORAL INJECTIONS:

Briefly, cells were mixed in 20 µL of 4:1 PBS/Matrigel (BD Biosciences) or pure PBS per femur and kept on ice. The mice were anesthetized with a mixture of xylazin (2%) /ketamin (100 mg/mL), 10 µL per gram of body weight. The anesthetized mice were kept on a heating pad in order to maintain their body temperature until they woke up. A whole was drilled into the femur of the mice with the help of a 26G needle, just underneath the patella, the leg being hold at 90°C angle. Once the whole was drilled, the cells were injected in the same whole, using a 29G plastic syringe. The detailed protocol is given in chapter 7.8.1.

CELL PURIFICATION AND CELL ENRICHMENT:

-MURINE CELLS:

For HSCs, BM was isolated from femurs. Single cell-suspensions were made from crushing bones after removal of muscle and connective tissue and were filtered through a 70-micrometer mesh. All mouse cell surface stainings were performed in a solution of 50% PBS + 2% Fetal Calf Serum (FCS); 50% cultured supernatant from the 24G2 hybridoma (rat monoclonal antibody directed against the CD16/32 FcR antigen). An example of FACS gating strategy for HSC analysis is shown in chapter 7.9.

-HUMAN CELLS FROM MICE:

For blood collection, mice were bled using a 1 ml syringe containing PBS and heparin, *via* a cardiac puncture. For tumor cell isolation, tumors were first resected from the mice, kept as short as possible on ice in DMEM F-12 (GIBCO), 10% FCS. The tumors were then sterily minced and filtered using a 100-micrometer mesh. All human surface stainings were performed in a solution of PBS + 2% FCS and 1:10 Intratect (Biotest, Germany), a human immunoglobulin solution to prevent unspecific binding of antibodies.

-HUMAN TUMOR CELLS FROM PATIENT BLOOD OR BONE MARROW:

For spike-in experiments, a controlled amount of MDA-MB-231 $EGFP^+$ expressing cells was added to the samples *prio*r to the processing (entire protocol or particular step of the process). The numbers of MDA-MB-231 $EGFP^+$ cells prior and after processing were evaluated by FACS analysis.

Blood and BM samples were incubated during 20 minutes at room temperature with the RosetteSep® antibody cocktail (according to the manufacturer's recommendations, Stemcell Technologies). The samples were then diluted 1:1 with PBS + 2% FCS, laid over 1 volume of Ficoll-Paque™ and centrifuged for 20 minutes at 1200g, without brake, at room temperature. The interphase was then collected and washed with cold PBS. Eventually, the remaining cells were kept on ice, before being used for *in vivo* processing, *in vitro* processing or FACS analysis.

LIST OF FACS ANTIBODIES:

- ANTI-MOUSE ANTIBODIES:

CD34 (RAM 34)-Alexa 647; CD150-PE-Cy5; CD117 (ckit 2B8)-APC-Cy7; Sca1 (D7)-PE-Cy7, lineage (B220, Ter119, CD4, CD8, CD11b and Gr1)-biotin, CD45.1-PE and CD45.2-Pacific blue were used. All monoclonal antibody conjugates were purchased from eBiosciences or purified and conjugated in our laboratory according to standard protocols.

- ANTI-HUMAN ANTIBODIES:

See list in chapter 7.11.

CELL CYCLE ANALYSIS ON EPITHELIAL CELLS:

Cell cycle analyses were performed by using a cell surface stain, in combination with Ki67/Hoechst antibodies. Cells were fixed and permeabilized according to the

manufacturer's instructions (BD Biosciences) in ice-cold 70% EtOH during 2 hours at -20°C. The cells were then incubated with an anti human Ki67 (BD Biosciences) antibody overnight. Hoechst (Molecular Probes) at 20µg/ml was added for 10 minutes prior to analysis.

FLOW-CYTOMETRY:

Cell sorting was performed on a FACS Aria™ Flow Cytometer (Becton Dickinson, San Jose, CA) for cell lines and on a high performance biosafety level 3 BD Influx™ sorter (BD Biosciences) for primary human samples. 7 to 9 colours and cell cycle analyses were carried out on a CyAn ADP™ (DAKO, Glostrup, Denmark). Data were analysed with the FlowJo software (Tree Star, Ashland, OR).

BM RECONSTITUTIONS:

CD45.2$^+$ C57BL/6 female mice were purchased respectively from Harlan. BM reconstitutions were performed as follows. Recipient NOD/SCID/$\gamma_c^{-/-}$ mice (CD45.1$^+$) were sub-lethally irradiated (200 rads), 24 hours before reconstitution. Donor CD45.2$^+$ C57BL/6 mice were sacrificed, their BM was isolated as described above, stained with an antibody against Thy1.1 (CD90, AT83 clone, 1:20), treated with rabbit complement (1:20, 30 mn at 37°C), washed and counted. A total of 1x10^6 cells/mouse was injected intravenously in recipient mice.

In competition experiments, 50 000 tumor cells were injected intra-femorally in the left leg of the recipient mice 6 hours after irradiation and 18 hours before reconstitution.

IMMUNO-HISTOCHEMISTRY:

All histological samples were collected and fixed for 4h at 4°C in 10% neutral buffered formalin solution (SIGMA) on a rotor. For bones, an additional decalcification step was performed in 0.4M EDTA, pH 7.2 for 10 days at 4°C, on a rotor.

Fixed tissues were paraffin embedded, sectioned (4µm) and stained with hematoxilin and eosin (H&E) for morphological analysis or following the immunohistochemical protocols listed in Chapter 7.8.

Light-microscopic analysis was performed using an Axioscope equipped with a Progress C10plus Camera (Zeiss).

CELL LINES AND CELL CULTURE METHODS:

MDA-MB-231 and MCF7 cells were maintained in DMEM GLUTAMAX (GIBCO) supplemented with 10% FCS, 2mM L-Glutamin and Penicilin/Streptomycin (PS) 200U/mL (GIBCO). In addition, 10ng/mL insulin (Sigma) were added for the culture of MCF7.

MCF10a cells were maintained in DMEM F-12 medium (GIBCO) supplemented with 5% horse serum (SIGMA), EGF 20ng/mL (Invitrogen), hydrocortisone 50ng/mL (Sigma), choleratoxin 100ng/mL (Sigma), insulin 8µg/mL (Sigma) and Penicilin/Streptomycin (PS) 200 U/mL (GIBCO).

Mammosphere or spheroid assays were performed in Ultra Low Attachment (ULA) plates (Corning), using a "mammosphere medium": DMEM F-12 medium, with EGF 20ng/mL (Invitrogen), bFGF 20ng/mL (Invitrogen), B27 1X (GIBCO), Insulin 4µg/mL (Sigma) and PS 200 U/mL (GIBCO).

The *in vitro* culture optimizations with patient samples were carried out using the breast cancer specific culture medium WIT-T (StemGent) or CnT27 (CELLnTEC) in Primaria plates (BD Biosciences), in standard cell culture plates or in ULA plates (Corining).

IN VIVO IMAGING:

- XENOGEN (IVIS-200 CALIPER) *IN VIVO* BIOLUMINESCENCE DETECTION:

Mice were injected intra-peritoneal with 10 µL per gram of body weight D-Luciferine Firefly Potassium salt (15 mg/mL in PBS, Biosynth), 10 minutes before imaging. The animals were anesthetized using 4.5% isoflurane in oxygen, maintained at 1.5% isoflurane in oxygen and analyzed in the heated camera chamber using the Living Image software, according to the manufacturer's instructions (IVIS 200, CALIPER). Minimum BINNING (high resolution) and maximum F-STOP (deeper imaging) were chosen for all data acquisitions.

- CT-SCAN IMAGING:

Mice were anesthetized, using xylazin (2%) /ketamin (100 mg/mL), 10 µL per gram of body weight and placed into a Skyscan 1072 instrument (Skyscan). Image acquisition was performed at 65 kV and 154 µA, with a 0.45° rotation between frames to obtain two-dimensional images and a resolution of 9-18 um. Three-dimensional reconstruction and quantitative analyses were performed on a computer (Dell) using the NRecon, ANT, and CTAn software supplied with the Skyscan instrument.

IN VIVO TREATMENTS:

- OSMOTIC PUMPS:

Alzet® pumps #1004 (4 weeks duration) were filled with 100 µL AMD3100 (2.5 mg/kg of body weight per day, SIGMA). The pumps were implanted sub-cutaneous to enable systemic delivery of 0.11 µL per hour of the compound.

- ESTROGEN PELLETS:

90-days release estrogen pellets with high (0.72 g/pellet) and low (0.18 g/pellet) concentrations were purchased at Innovative Research of America. They were implanted sub-cutaneaous at the same time as intra-bone injections were being performed.

LENTIVIRUSES:

High titer lentiviruses were produced following the Tronolab protocol (http://tcf.epfl.ch/site/tcf/page-6764.html) for second generation virus production, using psPAX2 and pMD2.G as packaging plasmids. psPAX2 contains a robust CAG promoter for efficient expression of packaging proteins. pMD2.G is the plasmid coding for the envelope for producing viral particles. The MA-186 plasmid containing the LUC insert (see map in chapter 7.6) was a kind gift from Prof. Dr. Aguet and Dr. Eyckerman. The EGFP expressing lentivirus was a kind gift from Dr. Shakhbazov. In order to obtain cells expressing both LUC and EGFP, two consecutive transductions were carried out several months apart, and the cells were eventually sorted by flow cytometry for EGFP positivity.

QUANTITATIVE PCR:

Real-time PCR using SYBR Green was performed on a LightCycler (Roche), according to the manufacturer's instructions. The primer sequences used to detect human cells according to ALU sequences detection were ALU-Sb-II-SENSE: AACAAGGTGAAACCCCGTCT and ALU-Sb-II-ANTISENSE: CCATTCTCCTGCCTCAGC, concentration 10 µM. An annealing temperature of 65°C and 50 cycles of amplifications were used. Amplification plots were analysed using the second derivative method with LC data analysis 3.5 software (Roche).

STATISTICAL ANALYSES:

All analyses were performed using two tailed t-tests.

Statistical significance is indicated by * ($p < 0.05$), ** ($p < 0.001$) and *** ($p < 0.0005$).

7. APPENDIX

7.1 List of samples (CLINICAL STUDIES #1, 2 and 3)

The three following tables represent the list of patient samples received for the functional study of DgTCs (see chapter 4.5). Blue fonts correspond to primary cancers (M0 stage) while black fonts correspond to metastatic cancers (M1 stage). Abbreviation: BL = blood, ND = not determined.

TABLE 2: CLINICAL STUDY NUMBER 1		
SAMPLE ID	**CANCER**	**# CTCs /7.5 mL**
BL 1	BREAST	34
BL 2	BREAST	0
BL 3	BREAST	0
BL 4	BREAST	16
BL 5	BREAST	0
BL 6	BREAST	0
BL 7	BREAST	0
BL 8	BREAST	4
BL 9	BREAST	0
BL 10	BREAST	0
BL 11	BREAST	1
BL 12	BREAST	4
BL 13	PROSTATE	0
BL 14	BREAST	2
BL 15	BREAST	0
BL 16	BREAST	0
BL 17	BREAST	0
BL 18	BREAST	0
BL 19	BREAST	0
BL 20	BREAST	1
BL 21	BREAST	3
BL 22	BREAST	171
BL 23	BREAST	0
BL 24	BREAST	1
BL 25	BREAST	1
BL 26	BREAST	0
BL 27	BREAST	330
BL 28	BREAST	0
BL 29	BREAST	0
BL 30	BREAST	3

BL 31	BREAST	18
BL 32	BREAST	ND
BL 33	BREAST	0
BL 34	BREAST	0
BL 35	BREAST	41
BL 36	BREAST	ND
BL 37	BREAST	3
BL 38	BREAST	0
BL 39	BREAST	1
BL 40	BREAST	0
BL 41	BREAST	0
BL 42	BREAST	35
BL 43	BREAST	0
BL 44	BREAST	0
BL 45	BREAST	20
BL 46	BREAST	0
BL 47	BREAST	0
BL 48	BREAST	ND
BL 49	BREAST	0
BL 50	BREAST	1
BL 51	BREAST	1
BL 52	BREAST	0
BL 53	BREAST	0
BL 54	BREAST	ND
BL 55	BREAST	2
BL 56	BREAST	9
Bl 57	BREAST	0
BL 58	BREAST	0
BL 59	BREAST	1
BL 60	BREAST	1
BL 61	BREAST	1
BL 62	BREAST	0
BL 63	BREAST	37
BL 64	BREAST	600
BL 65	BREAST	0
BL 66	BREAST	2
BL 67	BREAST	1
BL 68	BREAST	0
BL 69	BREAST	0
BL 70	BREAST	ND
BL 71	BREAST	0
BL 72	BREAST	0
BL 73	BREAST	40
BL 74	BREAST	0
BL 75	BREAST	3
BL 76	BREAST	0
BL 77	BREAST	73

BL 78	BREAST	1
BL 79	BREAST	0
BL 80	BREAST	0
BL 81	BREAST	0
BL 82	BREAST	0
BL 83	BREAST	0
BL 84	BREAST	ND
BL 85	BREAST	0
BL 86	BREAST	0
BL 87	BREAST	0
BL 88	BREAST	175
BL 89	BREAST	0
BL 90	BREAST	0
BL 91	BREAST	0

TABLE 3: CLINICAL STUDY NUMBER 2		
SAMPLE ID	**DATE RECEIVED**	**CANCER**
Pr BL Hd 1	29/05/08	PROSTATE
Pr BL Hd 2	29/05/08	PROSTATE
Pr BL Hd 3	26/06/08	PROSTATE
Pr BL Hd 4	1.9.09	PROSTATE
Pr BL Hd 5	1.9.09	PROSTATE
Pr BL Hd 6	13/1/09	PROSTATE
Pr BL Hd 7	13/1/09	PROSTATE
Pr BL Hd 8	15/01/09	PROSTATE
Pr BL Hd 9	19/01/09	PROSTATE
Pr BL Hd 10	27/01/09	PROSTATE
Pr BL Hd 11	28/01/09	PROSTATE
Pr BL Hd 12	03/02/09	PROSTATE
Pr BL Hd 13	03/02/09	PROSTATE
Pr BL Hd 14	04/02/09	PROSTATE
Pr BL Hd 15	05/02/09	PROSTATE
Pr BL Hd 16	06/02/09	PROSTATE
Pr BL Hd 17	10/02/09	PROSTATE
Pr BL Hd 18	12/02/09	PROSTATE
Pr BL Hd 19	12/02/09	PROSTATE
Pr BL Hd 20	24/03/09	PROSTATE
Pr BL Hd 21	24/03/09	PROSTATE
Pr BL Hd 22	25/03/09	PROSTATE
Pr BL Hd 23	31/03/09	PROSTATE
Pr BL Hd 24	31/03/09	PROSTATE
Pr BL Hd 25	01/04/09	PROSTATE
Pr BL Hd 26	02/04/09	PROSTATE
Pr BL Hd 27	07/04/09	PROSTATE
Pr BL Hd 28	08/04/09	PROSTATE

Pr BL Hd 29	15/04/09	PROSTATE
Pr BL Hd 30	21/04/09	PROSTATE
Pr BL Hd 31	21/04/09	PROSTATE
Pr BL Hd 32	28/04/09	PROSTATE
Pr BL Hd 33	08/05/09	PROSTATE
Pr BL Hd 34	19/05/09	PROSTATE
Pr BL Hd 35	26/05/09	PROSTATE
Pr BL Hd 36	11.1.10	PROSTATE
Pr BL Hd 37	15.1.10	PROSTATE

TABLE 4: CLINICAL STUDY # 3

PATIENT		NUMBER OF CTCS			
CANCER	**#**	**APOPTOTIC**	**ENUCLEATED**	**INTACT**	**TOTAL**
BREAST	1	0	0	0	**0**
BREAST	2	0	0	ND	**ND**
BREAST	3	0	0	ND	**ND**
BREAST	4	0	0	500	**500**
BREAST	5	6	0	12	**18**
BREAST	6	0	0	0	**0**
BREAST	7	36	0	52	**88**
BREAST	8	214	0	440	**654**
BREAST	9	10	0	10	**20**
BREAST	10	1	0	2	**3**
BREAST	11	5	0	1	**6**
BREAST	12	2	0	120	**122**
BREAST	13	0	0	0	**0**
BREAST	14	0	0	7	**7**
BREAST	15	0	0	0	**0**
BREAST	16	0	0	10	**10**
BREAST	17	14	24	54	**92**
BREAST	18	0	0	0	**0**
BREAST	19	13	24	12	**49**
BREAST	20	0	0	0	**0**
BREAST	21	0	240	40	**280**
BREAST	22	17	0	47	**64**
BREAST	23	0	0	2	**2**
BREAST	24	0	0	1	**1**
BREAST	26	0	0	0	**0**
BREAST	27	0	0	0	**0**
BREAST	28	3	100	0	**103**
BREAST	29	0	0	0	**0**
BREAST	30	0	0	0	**0**
BREAST	31	5	100	9	**114**
BREAST	32	1	5	2	**8**

BREAST	33	1	5	2	**8**
BREAST	34	13	600	20	**633**
BREAST	35	4	10	1	**15**
BREAST	36	3	35	6	**44**
BREAST	37	0	0	0	**0**
BREAST	38A	38	100	33	**171**
BREAST	39	1	15	4	**20**
BREAST	40A	0	0	0	**0**
BREAST	41A	1	0	1	**2**
BREAST	42A	12	0	64	**76**
BREAST	43A	6	1	10	**17**
BREAST	44	0	0	0	**0**
BREAST	45A	0	0	0	**0**
BREAST	46A	1	1	1	**3**
BREAST	48	0	0	0	**0**
BREAST	49	2	0	0	**2**
BREAST	50	23	40	29	**92**
BREAST	51	5	500	29	**534**
BREAST	52	0	0	0	**0**
BREAST	53	2	0	0	**2**
BREAST	54	23	100	0	**123**
BREAST	55	2	0	0	**2**
BREAST	56	1	0	0	**1**
BREAST	57	0	0	0	**0**
BREAST	58	31	10	9	**50**
BREAST	59	0	0	0	**0**
BREAST	60	10	55	7	**72**
BREAST	61	1	0	2	**3**
BREAST	62	31	100	28	**159**
BREAST	63	0	0	0	**0**
BREAST	64	0	0	0	**0**
BREAST	65	18	50	18	**86**
BREAST	66	3	6	0	**9**
BREAST	67	1	0	0	**1**
BREAST	68	1	0	0	**1**
BREAST	69	0	0	0	**0**
BREAST	70	2	0	0	**2**
BREAST	71	0	0	1	**1**
BREAST	72	0	0	0	**0**
BREAST	73	17	50	40	**107**
BREAST	74	0	0	0	**0**
BREAST	75	0	0	0	**0**
BREAST	76	8	5	68	**81**
BREAST	77	4	20	1	**25**
BREAST	78	0	10	0	**10**
BREAST	79	1	0	0	**1**
BREAST	80	34	50	21	**105**

BREAST	81	20	300	52	**372**
BREAST	82	0	0	0	**0**
BREAST	83	8	20	0	**28**
BREAST	84	95	1000	120	**1215**
BREAST	85	0	0	0	**0**
BREAST	86	0	0	200000	**200000**
BREAST	88	450	0	400	**850**
BREAST	89	0	0	0	**0**
BREAST	90	5	44	18	**67**
BREAST	91	0	0	0	**0**
BREAST	92	0	0	0	**0**
BREAST	93	0	0	0	**0**
BREAST	94	0	0	0	**0**
BREAST	95	10	50	4	**64**
BREAST	96	42	80	11	**133**
BREAST	97	0	0	0	**0**
BREAST	98	0	0	1	**1**
BREAST	99	0	0	0	**0**
BREAST	100	0	0	1	**1**
BREAST	101	0	0	7	**7**
BREAST	102	1	0	0	**1**
BREAST	103	0	0	0	**0**
BREAST	104	0	0	0	**0**
BREAST	105	0	20	0	**20**
BREAST	106	1	0	0	**1**
BREAST	107	1	0	0	**1**
BREAST	108	0	0	0	**0**
BREAST	109	2	20	2	**24**
BREAST	110	0	0	0	**0**
BREAST	111	1	15	0	**16**
BREAST	112	0	0	0	**0**
BREAST	114	1	0	0	**1**
BREAST	115	0	20	4	**24**
BREAST	116	0	0	0	**0**
BREAST	117	0	10	1	**11**
BREAST	118	2	0	0	**2**
BREAST	119	0	0	0	**0**
BREAST	120	0	0	0	**0**
BREAST	121	5	60	28	**93**
BREAST	122	1	0	1	**2**
BREAST	123	1	40	4	**45**
BREAST	124	0	0	0	**0**
BREAST	125	0	0	0	**0**
BREAST	126	0	1	1	**2**
BREAST	127	0	18	1	**19**
BREAST	128	200	500	80	**780**
BREAST	129	0	0	0	**0**

BREAST	130	0	0	0	**0**
BREAST	131	0	0	0	**0**
BREAST	132	0	0	0	**0**
BREAST	133	0	5	6	**11**
BREAST	134	5	4	2	**11**
BREAST	135	30	60	15	**105**
BREAST	136	1	0	0	**1**
BREAST	137	0	1	2	**3**
BREAST	138	1	0	2	**3**
BREAST	139	0	0	0	**0**
BREAST	140	0	0	0	**0**
BREAST	141	2	0	1	**3**
BREAST	142	9	38	7	**54**
BREAST	143	0	0	0	**0**
BREAST	144	0	5	0	**5**
BREAST	145	0	0	0	**0**
BREAST	146	0	0	0	**0**
BREAST	147	1500	900	2760	**5160**
BREAST	148	0	0	0	**0**
BREAST	149	0	20	5	**25**
BREAST	150	6	25	5	**36**
BREAST	151	29	40	21	**90**
BREAST	152	0	6	3	**9**
BREAST	153	0	0	0	**0**
BREAST	154	0	5	9	**14**
BREAST	155	2	28	0	**30**

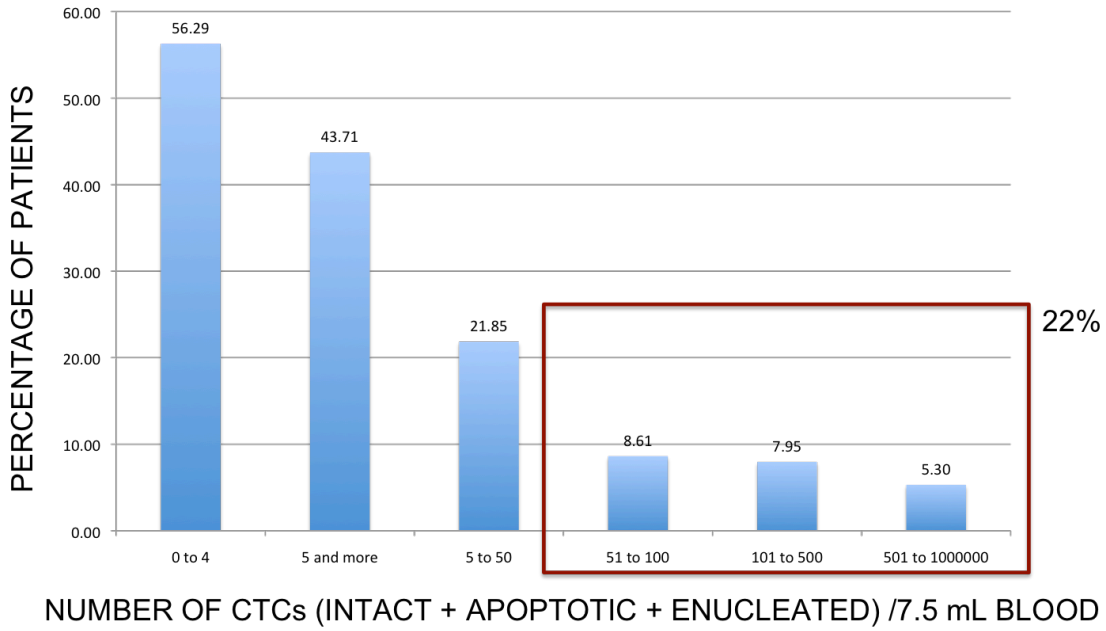

Figure 56. Percentage of patients and CTC counts, CLINICAL STUDY #3. CTC counts (including intact, apoptotic and enucleated-looking CTCs) were measured by Dr. Sabine Riethdorf on the Cellsearch™ device.

7.2 Evolution of CTC counts (CLINICAL STUDY #3)

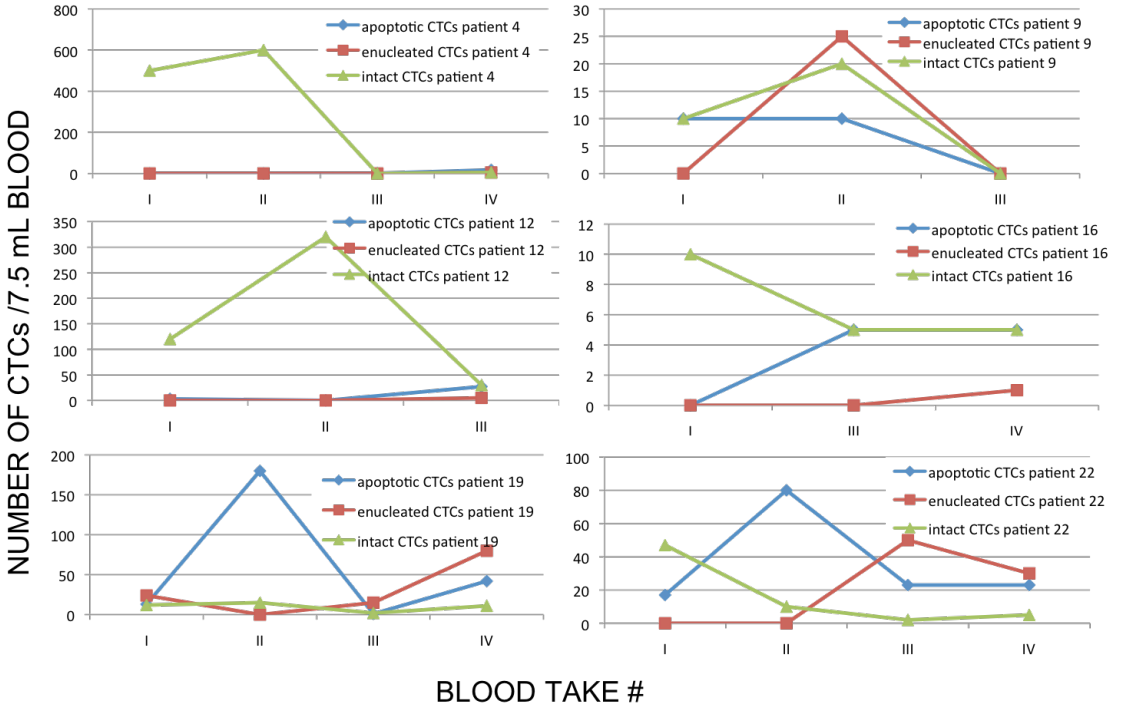

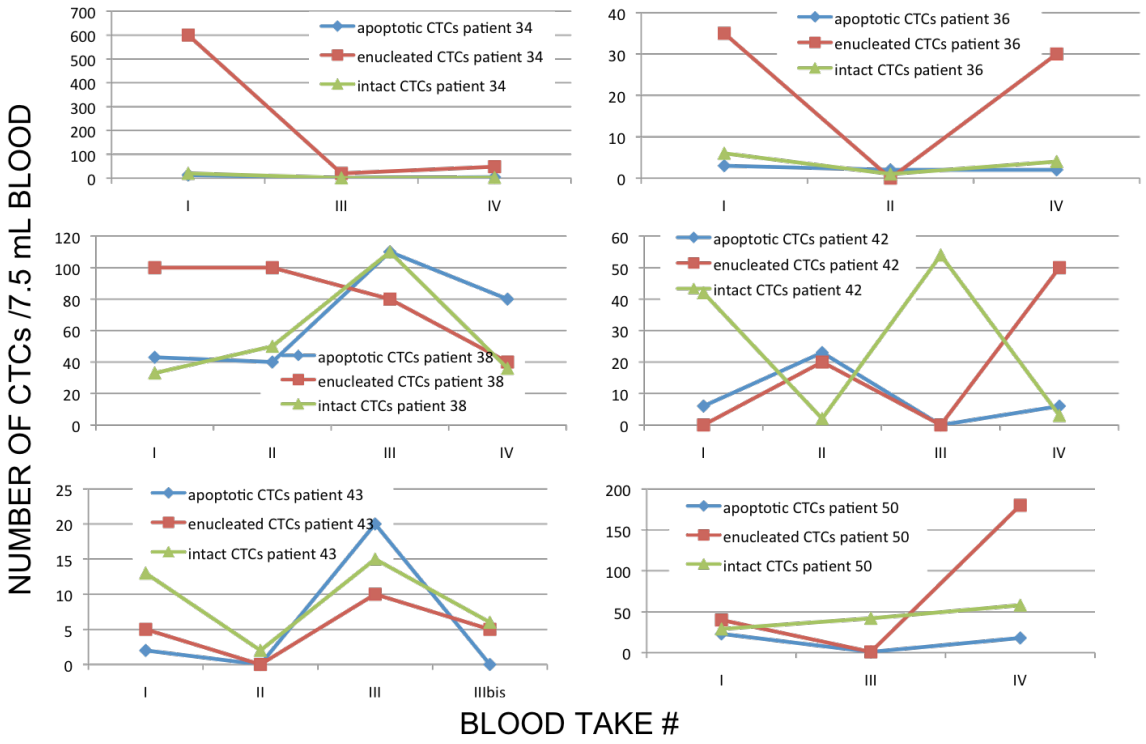

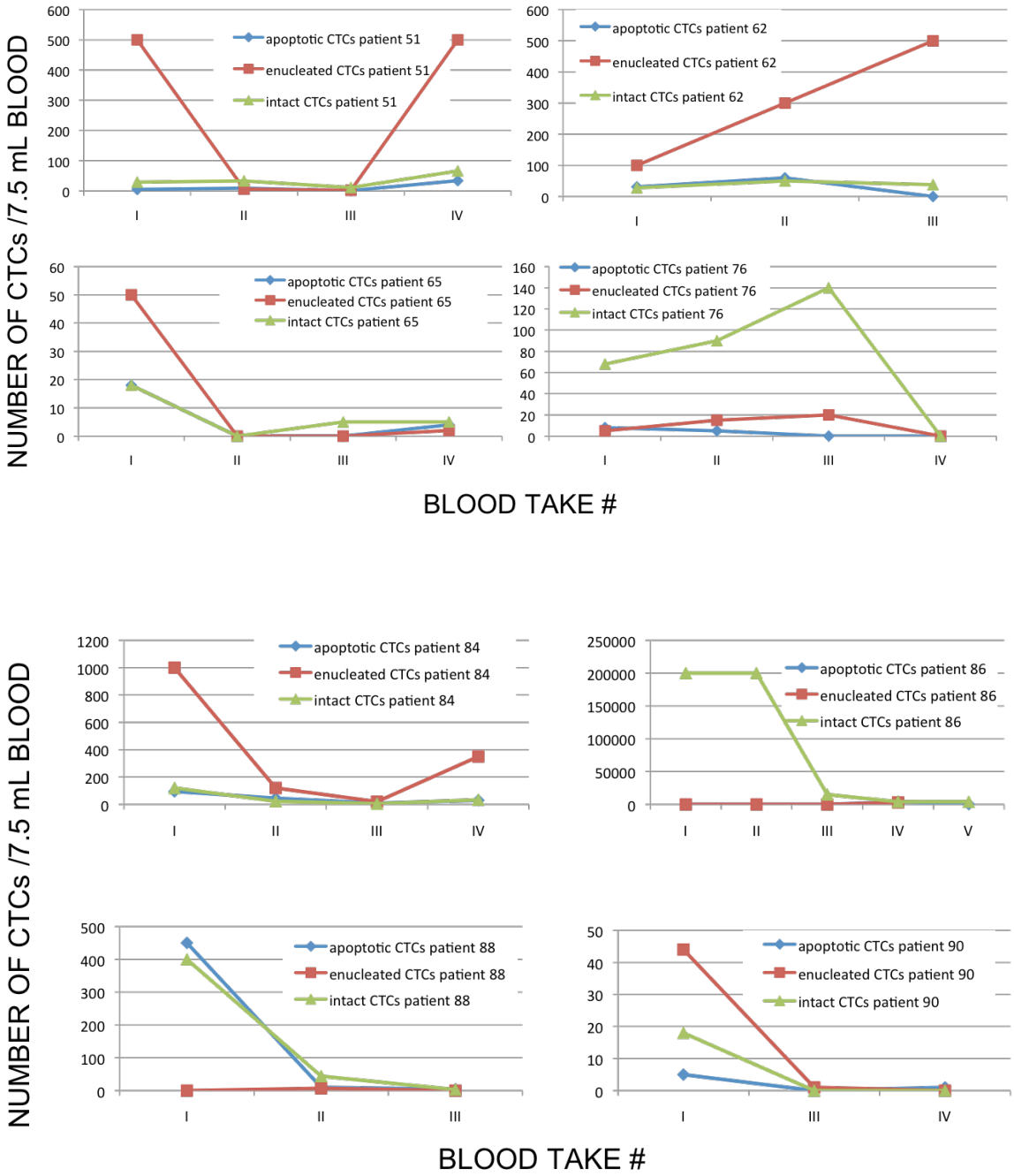

Figure 57. CTC count evolution during disease progression CLINICAL STUDY #3. See code for blood take # I, II, III and IV in Figure 47.

7.3 List of processed samples (CLINICAL STUDY #3)

TABLE 5: PROCESSED SAMPLES IN CLINICAL STUDY # 3			
		INTACT CTCS /7.5 mL	
SAMPLE	PATIENT #	DTCS/2 million MNC)	PROCESSING
BL	4.II	600	*IN VIVO*
BM	4.II	70	*IN VIVO*
BL	5.II	20	*IN VIVO*
BM	5.II	ND	*IN VIVO*
BL	9.II	20	*IN VIVO*
BM	9.II	2	*IN VIVO*
BL	9.III	0	*IN VIVO*
BL	12.II	320	*IN VIVO*
BM	12.II	20	*IN VIVO*
BL	19.II	15	*IN VIVO*
BM	19.II	ND	*IN VIVO*
BL	21.II	40	*IN VIVO*
BL	22.II	10	*IN VIVO*
BM	22.II	ND	*IN VIVO*
BL	22.III	2	*IN VIVO*
BL	36.II	1	*IN VITRO*
BL	38.II	50	*IN VITRO*
BM	38.II	4	*IN VITRO*
BL	42.II	2	*IN VIVO*
BM	42.II	0	*IN VIVO*
BL	43.II	2	*IN VITRO*
BM	43.II	ND	*IN VITRO*
BL	51.II	33	*IN VITRO*
BM	51.II	0	*IN VITRO*
BL	84.II	23	FACS
BM	84.II	17	FACS
BL	86.II	200000	*IN VIVO*
BL	86.III	15 000	FACS
BL	86.IV	4000	FACS, SORT, *IN VITRO, IN VIVO*
BL	86.V	4000	FACS, *IN VITRO, IN VIVO*
BL	88.II	44	FACS
BM	88.II	0	FACS
BL	128.II	ND	*IN VITRO*
BM	128.II	ND	*IN VITRO*
BL	147.II	76	FACS, *IN VITRO, IN VIVO*
BM	147.II	ND	FACS, *IN VITRO, IN VIVO*

7.4 Immunohistochemistry set up

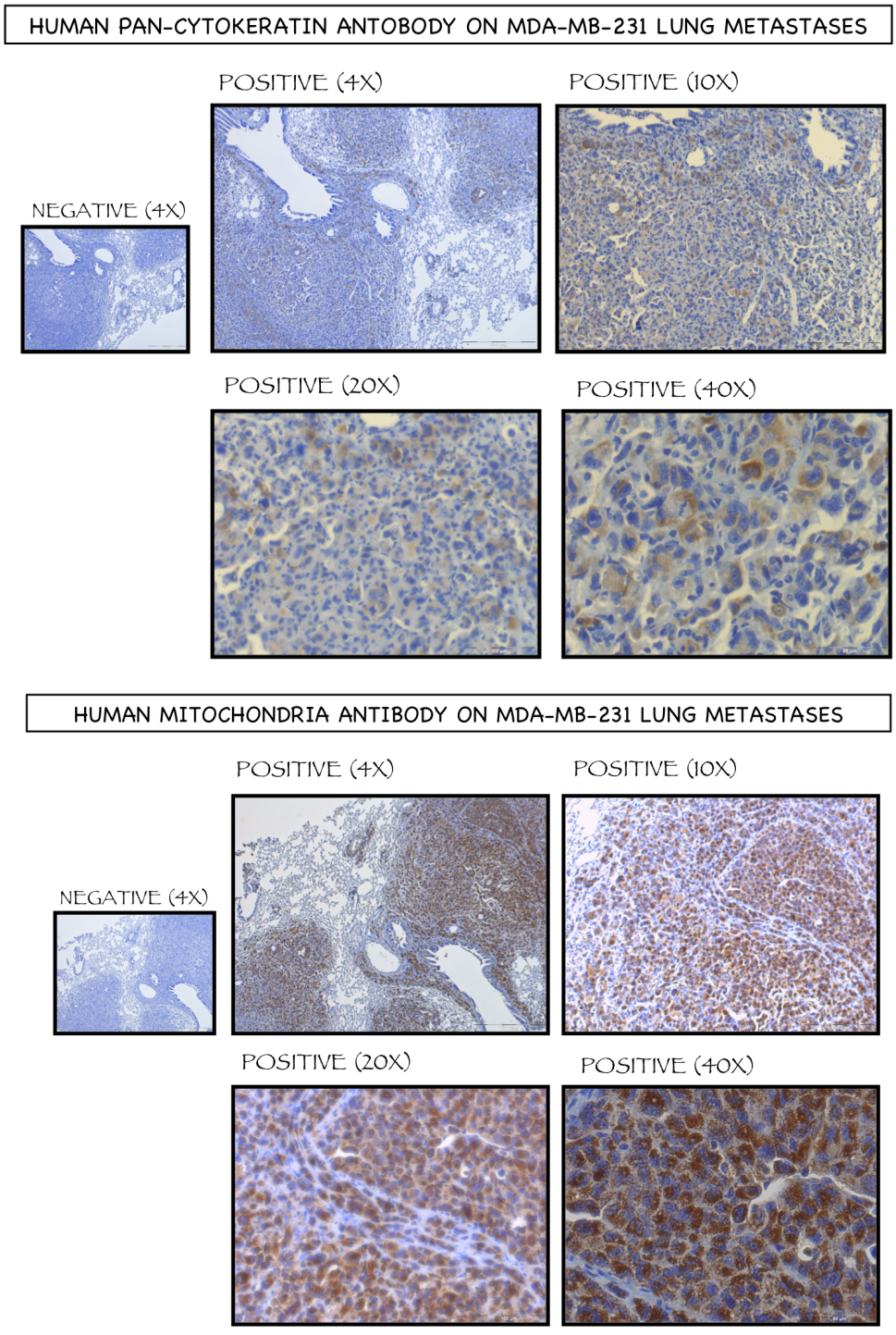

Reubinoff, B.E. *et al.* Nature Biotechnology, (2001)

FIREFLY LUCIFERASE ANTIBODY ON MDA-MB-231 LUC METASTASES

POSITIVE (4X)

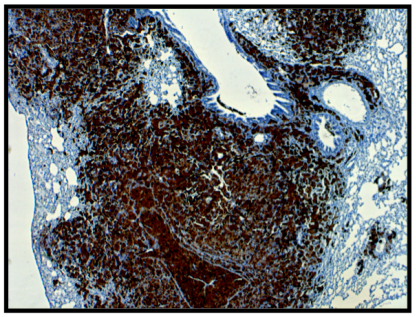

NEGATIVE (4X)

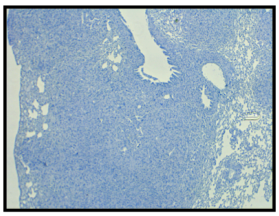

POSITIVE (20X)

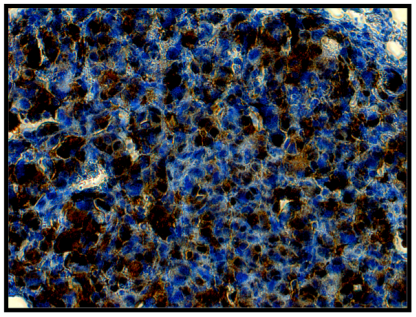

7.5 Examples of murine tumors and of murine granumloma

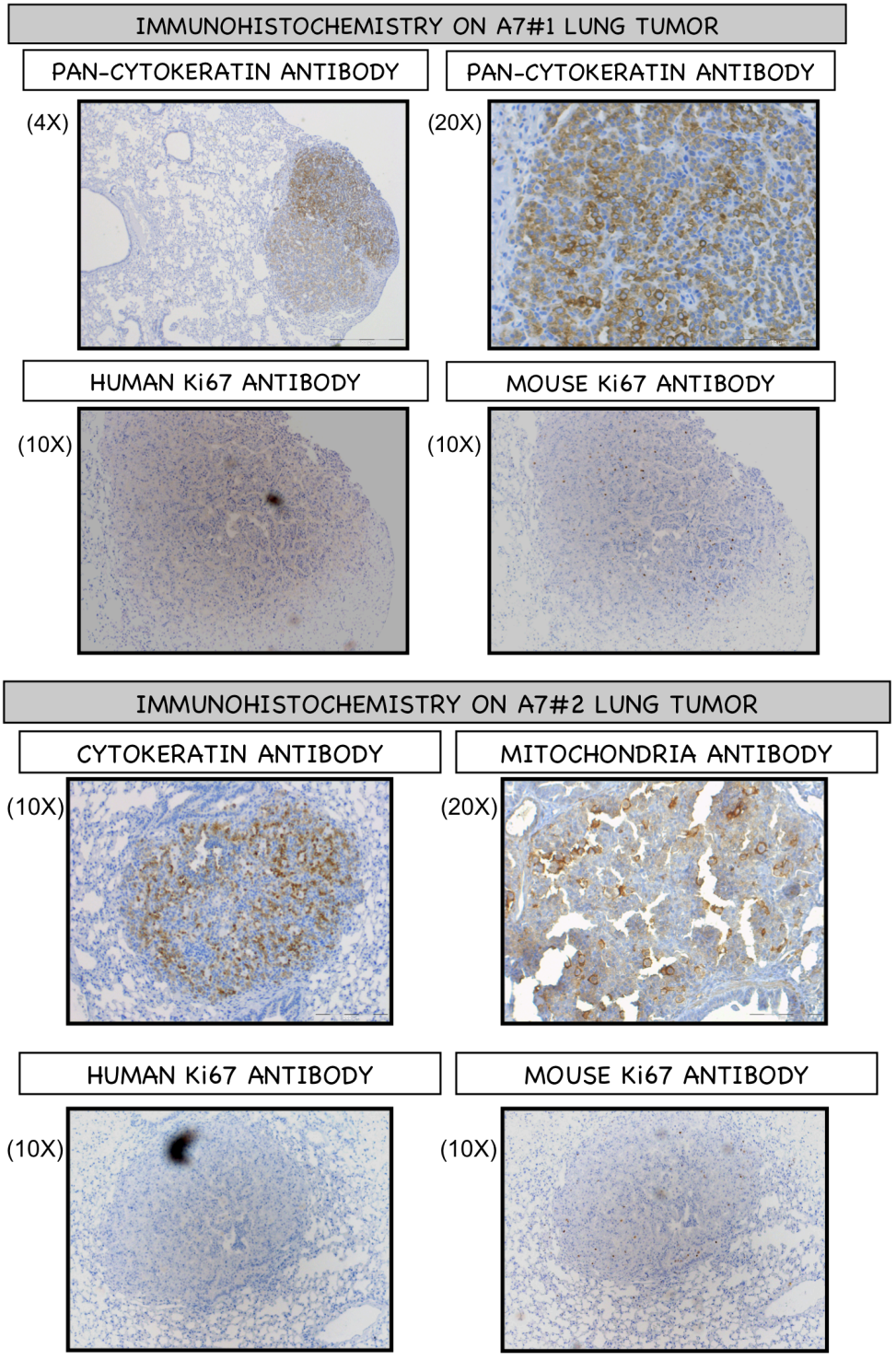

B7#5 ABDOMINAL TUMOR

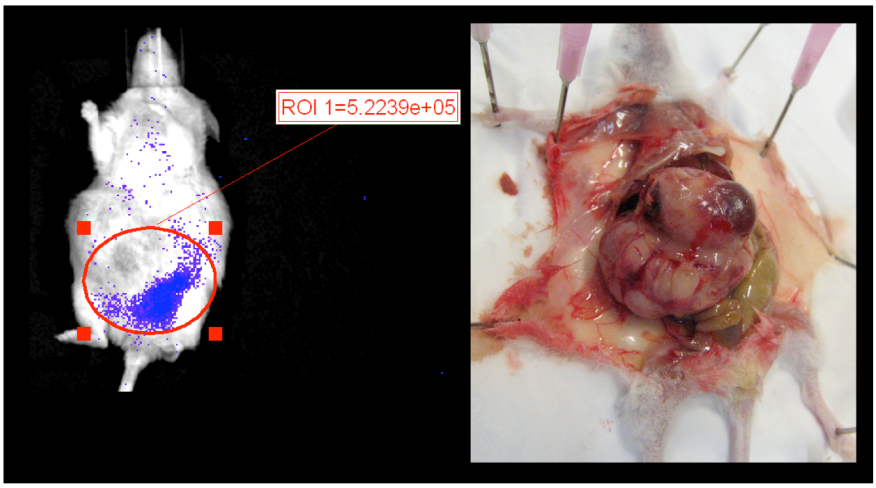

IMMUNOHISTOCHEMISTRY ON B7#5 ABDOMINAL TUMOR

CYTOKERATIN ANTIBODY

(20X)

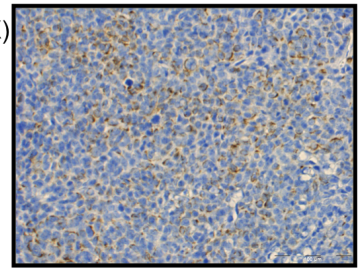

MITOCHONDRIA ANTIBODY

(20X)

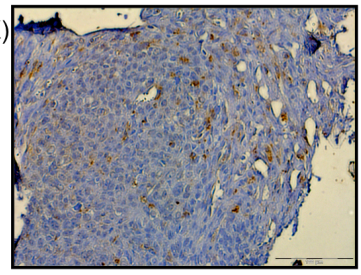

FIREFLY LUCIFERASE ANTIBODY

(20X)

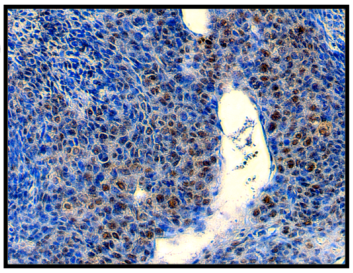

(20X)

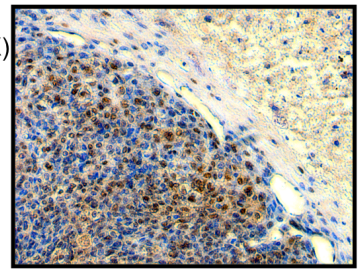

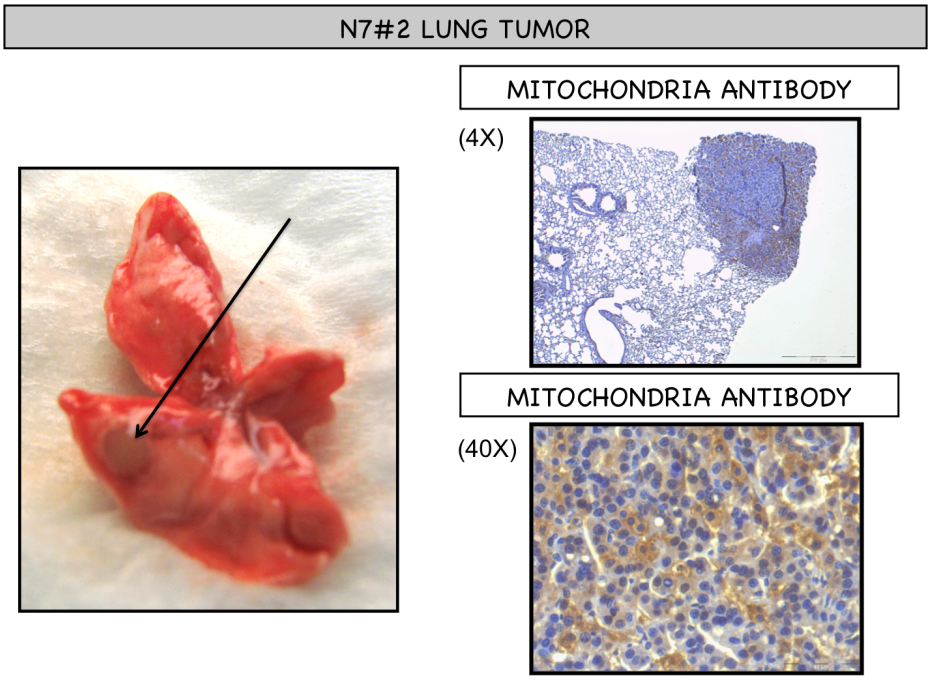

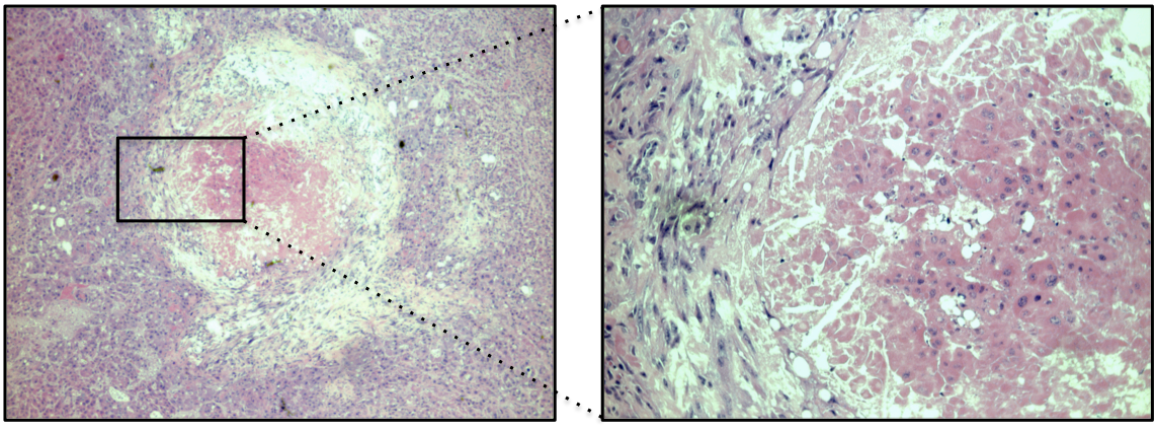

Figure 58. Murine granulomas in recipient mice, CLINICAL STUDY #1 Example of granuloma detected in the liver of a mouse receiving cells isolated from the blood of a metastatic prostate cancer patient. Fibrosis surrounds a half necrotic, half nucleated granulocytosis, as visible on the close up (on the right).

7.6 Luciferase lentiviral vector map

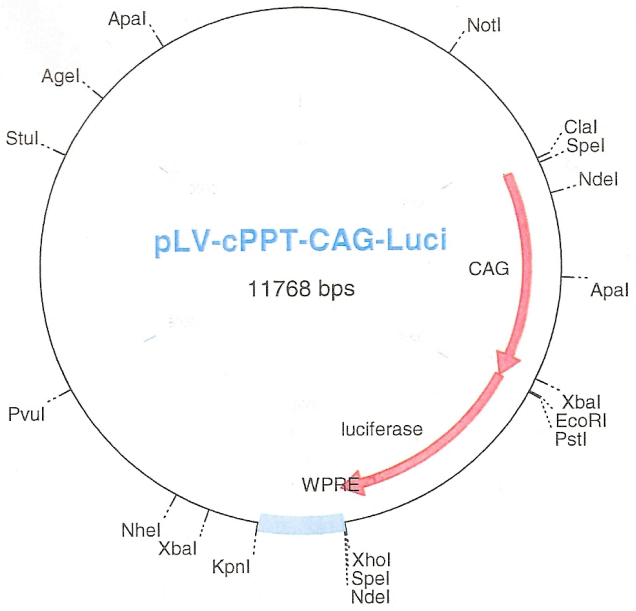

Molecule: pLV-cPPT-CAG-Luci, 11768 bps DNA Circular
File Name: MA-186.cm5, dated 08 Aug 2006

Description: Ligation of *'LTRtake2 into pLVcut

Notes:

Molecule Features:

Type	Start	End	Name	Description
GENE	2168	3889	CAG	
GENE	3891	5564	luciferase	
REGION	5585	6192	WPRE	

Enzymes (18 sites)

NotI	1144,	ClaI	2147,	SpeI	2182,	NdeI	2416
ApaI	3028,	XbaI	3793,	EcoRI	3889,	PstI	3899
XhoI	5578,	SpeI	5584,	NdeI	5590,	KpnI	6204
XbaI	6567,	NheI	6826,	PvuI	7914,	StuI	9675
AgeI	10168,	ApaI	10743,				

7.7 Hematologic profiling of estrogen-treated mice

EXAMPLE OF CONTROL CHIMERA MOUSE:

MASCOT™ HEMATOLOGY PROFILE: **HEMAVET**

Parameter(Units)		Results	Normal Range
Leukocytes:			
WBC	(K/µL)	1.90	1.8 - 10.7
NE	(K/µL)	0.09 L	0.1 - 2.4
LY	(K/µL)	1.77	0.9 - 9.3
MO	(K/µL)	0.02	0.0 - 0.4
EO	(K/µL)	0.02	0.0 - 0.2
BA	(K/µL)	0.00	0.0 - 0.2
NRBC	(K/µL)		RARE
NE	(%)	4.62 L	6.6 - 38.9
LY	(%)	92.96 H	55.8 - 91.6
MO	(%)	1.20	0.0 - 7.5
EO	(%)	0.97	0.0 - 3.9
BA	(%)	0.25	0.0 - 2.0
NRBC	(%)		RARE
Erythrocytes:			
RBC	(M/µL)	6.34 L	6.36 - 9.42
Hb	(g/dL)	10.3 L	11.0 - 15.1
HCT	(%)	29.3 L	35.1 - 45.4
MCV	(fL)	46.2	45.4 - 60.3
MCH	(pg)	16.2	14.1 - 19.3
MCHC	(g/dL)	35.2 H	30.2 - 34.2
RDW	(%)	21.3	12.4 - 27.0
RSD	(fL)		
Retics	(M/µL)		0.09 - 0.97
Retics	(%)		5.58 - 9.91
Thrombocytes:			
PLT	(K/µL)	1305.	592. - 2972.
PCT	(%)		
MPV	(fL)	4.7 L	5.0 - 20.0
PDW	(%)		

EXAMPLE OF ESTROGEN-TREATED CHIMERA MOUSE:

MASCOT™ HEMATOLOGY PROFILE: **HEMAVET**

Parameter(Units)		Results	Normal Range
Leukocytes:			
WBC	(K/µL)	0.22 *P1	1.8 - 10.7
NE	(K/µL)	0.05 L	0.1 - 2.4
LY	(K/µL)	0.12 L	0.9 - 9.3
MO	(K/µL)	0.03	0.0 - 0.4
EO	(K/µL)	0.02	0.0 - 0.2
BA	(K/µL)	0.00	0.0 - 0.2
NRBC	(K/µL)		RARE
NE	(%)	21.22	6.6 - 38.9
LY	(%)	54.52 L	55.8 - 91.6
MO	(%)	13.29 H	0.0 - 7.5
EO	(%)	9.41 HW5	0.0 - 3.9
BA	(%)	1.57	0.0 - 2.0
NRBC	(%)		RARE
Erythrocytes:			
RBC	(M/µL)	3.83 L	6.36 - 9.42
Hb	(g/dL)	7.4 L	11.0 - 15.1
HCT	(%)	19.5 L	35.1 - 45.4
MCV	(fL)	50.9	45.4 - 60.3
MCH	(pg)	19.3	14.1 - 19.3
MCHC	(g/dL)	37.9 H	30.2 - 34.2
RDW	(%)	29.5 H	12.4 - 27.0
RSD	(fL)		
Retics	(M/µL)		0.09 - 0.97
Retics	(%)		5.58 - 9.91
Thrombocytes:			
PLT	(K/µL)	687.	592. - 2972.
PCT	(%)		
MPV	(fL)	3.8 L	5.0 - 20.0
PDW	(%)		

7.8 Protocols

7.8.1 Intra-femoral injections

- inject COLD anesthetic mix
  - intra-peritoneal, 10 µL/g mouse, wait until the mouse is fast asleep
  - put some artificial tears on the eyes
- prepare a syringe with 20 µL of the solution to inject
- with a 26G needle, drill slowly a hole in the femur => hold the leg with one hand, place the needle in the same angle than the femur and drill the hole underneath the patella. Make sure that the needle is really in the bone and not in the surrounding muscles by moving gently the needle in all directions.
- remove the needle, put the injection syringe in the same hole and slowly inject the solution while withdrawing the syringe
- disinfect the knee with Betadine
- put some Cicatrex cream on the wound
- put the mouse in a heated recovery cage, on a clean tissue; add some paracetamol to the drinking water (500 mg per 500 mL bottle) and put some wet food on a corner of the cage

Anesthetic mix (for 11 mL):

- always keep it cold, otherwise the anesthetic effect will be lost !
- 1 mL Ketasol (ketamin > anesthetic)
- 0.8 mL Rompun (xylazine > analgesia and muscle relaxation)
- 9.2 mL H_2O

Material needed :

- heating pad
- balance
- 26G (brown) needles, 1mL 29G syringes
- artificial tears, Cicatrex cream, Betadine, Paracetamol

7.8.2 Immuno-histochemistry: mouse anti-human pan-cytokeratin antibody

(1) **Dewax § Rehydrate:**

- Pre-heat the slides at 60 °C
- Xylol or Roticlear 2x 3min
- Xylol: Ethanol 100% 1:1, then Ethanol 100% to 50% 3 min each
- Cold running tap water **10 min**

(2) **Quenching**

- Incubate in **PBS 3 % H2o2** for **at 10 min** (10X DAKO)
- Wash in PBS **1x** quickly, then **2 x 5 min** in PBS

(3) **Antigen Retrieval**: 10mM TriSodiumCitrate Buffer pH6 (10X DAKO)

- Wash the slide **5 min** in TrisSodiumCitrate Buffer
- Fill a glass coplin jar with 1X solution and place it inside a microwave
- Add the slides and once it is boiling, count **20 min**
- Let the slides cool down in a new bath of Antigen retrieval Buffer
- Cold running tap water **5 min**

(4) **Block**

- **PBS 1 % BSA** (filtered) for **at least 45 min RT**
- Remove excess solution (do not let the section dry!!!)
- Apply PAP'pen to isolate the areas of interest, on dried regions and let the pen dry for 1 min

(5) **Primary Antibody**

- Dilute 1° Ab 1:50 in **Blocking solution**
- Incubate the slides (in a humidified chamber**) 1 HOUR at RT/ON (4°C)**
- Wash **1x** quickly and **3x 5min** in **PBS**

(6) **Secondary Antibody**

- Wash briefly in **Blocking solution**
- Remove excess solution (do not rinse)
- Incubate the slides (in a humidified chamber) with Mouse Envision, RTU **40min at RT**
- Wash **1x** quickly and **2x 5min** in **PBS**
- Wash **1x** quickly and **1x 5min** in **0,05MTris-HCl pH7.6**

(7) **Enzyme substrate**

- **DAB** (DAKO, #k3466) 1 mL buffer + 1 drop of reagent, check under the microscope**.** Incubate between **3 to 10 min**
- Wash **1x** quickly and **1x 5min** in **0,05MTris-HCl pH7.6**
- Wash **1x 5min** with tap water

(8) **CounterStain**

- Mayer's Hematoxyline
- Wash **1x 5min** with cold running tap water
- Dehydrate 50% EtOH to 100% EtOH, xylol/Roticlear
- Embedding with organic mounting medium

* Primary Antibody

> Mouse anti- C11 (Novocastra, #NCL-C11)

> **NEGATIVE CONTROL** = blocking buffer

* Secondary Antibody

> Mouse Envision, (DAKO #K4004)

NOTE: cross-reactivity was observed with some (but not all!) mouse cytokeratins.

7.8.3 Immunohistochemistry: mouse anti-human mitochondria antibody

(1) **Dewax § Rehydrate:**

- Pre-heat the slides at 60 °C
- Xylol or Roticlear 2x 3min
- Xylol: Ethanol 100% 1:1, then Ethanol 100% to 50% 3 min each
- Cold running tap water **10 min**

(2) **Quenching**

- Incubate in **PBS 3 % H2o2** for **at 10 min** (10X DAKO)
- Wash in PBS **1x** quickly, then **2 x 5 min** in PBS

(3) **Antigen Retrieval**: 10mM TriSodiumCitrate Buffer pH6 (10X DAKO)

- Wash the slides **5 min** in TrisSodiumCitrate Buffer
- Fill a glass coplin jar with 1X solution and place it inside a microwave
- Add the slides and once it is boiling, count **20 min**
- Let the slides cool down in a new bath of RT TrisSodiumCitrate Buffer
- Cold running tap water **5 min**

(4) **Block**

- **PBS 0,5 % BSA** (filtered) for **at least 45 min RT**
- Remove excess solution (do not dry the section!!!!)
- Apply PAP'Pen on dried areas to isolate the regions of interest and let the pen dry for 1 min

(5) **Primary Antibody**

- Dilute 1° Ab 1:50 in **Blocking solution**
- Incubate the slides (in a humidified chamber**) ON at 4°C** (or 1h @ RT)
- Wash **1x** quickly and **3x 5min** in **PBS**

(6) **Secondary Antibody**

- Wash briefly in **Blocking solution**
- Remove excess solution (do not rinse)
- Incubate the slides (in a humidified chamber) with MouseEnvision, RTU during **40min at RT**
- Wash **1x** quickly and **2x 5min** in **PBS**
- Wash **1x** quickly and **1x 5min** in **0,05MTris-HCl pH7.6**

(7) **Enzyme substrate**

- **DAB** (DAKO, #k3466) 1 mL buffer + 1 drop of reagent, check under the microscope**.** Incubate between **3 to 10 min**
- Wash **1x** quickly and **1x 5min** in **0,05MTris-HCl pH7.6**
- Wash **1x 5min** with tap water

(8) **CounterStain**

- Mayer's Hematoxyline
- Wash **1x 5min** with cold running tap water
- Dehydrate 50% EtOH to 100% EtOH, xylol/Roticlear
- Embedding with organic mounting medium

* Primary Antibody

> Mouse anti-human mitochondria (Chemicon, #MAB1273)

> **NEGATIVE CONTROL** = blocking buffer

* Secondary Antibody

> Mouse Envision, (DAKO #K4004)

NOTE: this mouse anti-human mitochondria antibody is supposed to be anti-human specific (Reubinoff et al., 2001), but a cross-reaction with mouse tissues was observed.

7.8.4 Immunohistochemistry: mouse anti-human Ki67 antibody

(1) **Dewax § Rehydrate:**

- Pre-heat the slides at 60 °C
- Xylol or Roticlear 2x 3min
- Xylol: Ethanol 100% 1:1, then Ethanol 100% to 50% 3 min each
- Cold running tap water **10 min**

(2) **Quenching**

- Incubate in **PBS 3 % H2o2** for **at 10 min** (10X DAKO)
- Wash in PBS **1x** quickly, then **2 x 5 min** in PBS

(3) **Antigen Retrieval**: 10mM TriSodiumCitrate Buffer pH9 (10X DAKO)

- Wash the slides **5 min** in TrisSodiumCitrate Buffer
- Fill a glass coplin jar with 1X solution and place it inside a microwave
- Add the slides and once it is boiling, count **20 min**
- Let the slides cool down in a new bath of Anitigen retrieval Buffer
- Cold running tap water **5 min**

(4) **Block**

- **PBS 1 % BSA** (filtered) for **at least 45 min RT**
- Remove excess solution (do not let the sections dry!!!)
- Apply PAP'Pen to isolate the areas of interest, on dried regions and let the pen dry for 1 min

(5) **Primary Antibody**

- Dilute 1° Ab 1:100 in **Blocking solution**
- Incubate slide (in humidified chamber**) 40 min at RT/ON (4°C)**
- Wash **1x** quickly and **3x 5min** in **PBS**

(6) **Secondary Antibody**

- Wash briefly in **Blocking solution**
- Remove excess solution (do not rinse)
- Incubate the slides (in a humidified chamber) with mouse Envision**,** 40min **at RT**
- Wash **1x** quickly and **2x 5min** in **PBS**
- Wash **1x** quickly and **1x 5min** in **0,05MTris-HCl pH7.6**

(7) **Enzyme substrate**

- **DAB** (DAKO, #k3466) 1 mL buffer + 1 drop of reagent, check under the microscope**.** Incubate between **3 to 10 min**
- Wash **1x** quickly and **1x 5min** in **0,05MTris-HCl pH7.6**
- Wash **1x 5min** with tap water

(8) **CounterStain**

- Mayer's Hematoxyline
- Wash **1x 5min** with cold running tap water
- Dehydrate 50% EtOH to 100% EtOH, xylol/Roticlear
- Embedding with organic mounting medium

* Primary Antibody

> mouse anti-human Ki67 (DAKO, #M7240)

> **NEGATIVE CONTROL** = blocking buffer

* Secondary Antibody

> Mouse Envision (DAKO, #K4004)

NOTE: no cross-reactivity with mouse tissue was observed.

7.8.5 Immunohistochemistry: rat anti-mouse Ki67 antibody

(1) **Dewax § Rehydrate:**

- Pre-heat the slides at 60 °C
- Xylol or Roticlear 2x 3min
- Xylol: Ethanol 100% 1:1, then Ethanol 100% to 50% 3 min each
- Cold running tap water **10 min**

(2) **Quenching**

- Incubate in **PBS 3 % H2o2** for **at 10 min** (10X DAKO)
- Wash in PBS **1x** quickly, then **2 x 5 min** in PBS

(3) **Antigen Retrieval**: 10mM TriSodiumCitrate Buffer pH9 (10X DAKO)

- Wash the slides **5 min** in TrisSodiumCitrate Buffer
- Fill a glass coplin jar with 1X solution and place it inside a microwave
- Add the slides and once it is boiling, count **20 min**
- Let the slides cool down in a new bath of Ag retrieval Buffer
- Cold running tap water **5 min**

(4) **Block**

- **PBS 1 % BSA** (filtered) for **at least 45 min RT**
- Remove excess solution (do not let the sections dry!!!)
- Apply PAP'Pen on dries areas in order to isolate the regions of interest and let the pen dry for 1 min

(5) **Primary Antibody**

- Dilute 1° Ab 1:50 in **Blocking solution**
- Incubate slide (in humidified chamber**) 1 HOUR at RT/ON (4°C)**
- Wash **1x** quickly and **3x 5min** in **PBS**

(6) **Secondary Antibody**

- Wash briefly in **Blocking solution**
- Remove excess solution (do not rinse)
- Incubate the slides (in a humidified chamber) with biotinylated rabbit Anti-Rat, **1/200,** 40min **at RT**
- Wash **1x** quickly and **2x 5min** in **PBS**
- Wash **1x** quickly and **1x 5min** in **0,05MTris-HCl pH7.6**

(7) **Enzyme substrate**

- **DAB** (DAKO, #k3466) 1 mL buffer + 1 drop of reagent, check under the microscope**.** Incubate between **3 to 10 min**
- Wash **1x** quickly and **1x 5min** in **0,05MTris-HCl pH7.6**
- Wash **1x 5min** with tap water

(8) **CounterStain**

- Mayer's Hematoxyline
- Wash **1x 5min** with cold running tap water
- Dehydrate 50% EtOH to 100% EtOH, xylol/Roticlear
- Embedding with organic mounting medium

* Primary Antibody

> rat anti-mouse Ki67 (DAKO, #M7249)

> **NEGATIVE CONTROL** = blocking buffer

* Secondary Antibody

> Biotinylated Rabbit Anti-Rat, **1/200** (DAKO, #E0468)

NOTE: no cross-reactivity with human tissue was observed.

7.8.6 Immunohistochemistry: anti Firefly Luciferase (LUC) antibody

(1) **Dewax § Rehydrate:**

- Pre-heat the slides at 60 °C
- Xylol or Roticlear 2x 3min
- Xylol: Ethanol 100% 1:1, then Ethanol 100% to 50% 3 min each
- Cold running tap water **10 min**

(2) **Quenching**

- Incubate in **PBS 3 % H2o2** for **at 10 min** (10X DAKO)
- Wash in PBS **1x** quickly, then **2 x 5 min** in PBS

(3) **Antigen Retrieval**: 10mM TriSodiumCitrate Buffer pH6 (10X DAKO)

- Wash the slides **5 min** in TrisSodiumCitrate Buffer
- Fill a glass coplin jar with 1X solution and place it inside a microwave
- Add the slides and once it is boiling, count **20 min**
- Let the slides cool down in a new bath of Antigen retrieval Buffer
- Cold running tap water **5 min**

(4) **Block**

- **PBS 1 % BSA** (filtered) for **at least 45 min RT**
- Remove excess solution (do not let the sections dry!!!)
- Apply PAP'Pen on dried areas to isolate the regions of interest and let the pen dry for 1 min

(5) **Primary Antibody**

- Dilute 1° Ab 1:100 in **Blocking solution**
- Incubate slide (in humidified chamber**) 1 HOUR at RT/ON (4°C)**
- Wash **1x** quickly and **3x 5min** in **PBS**

(6) **Secondary Antibody**

- Wash briefly in **Blocking solution**
- Remove excess solution (do not rinse)
- Incubate the slides (in a humidified chamber) with Rabbit Envision, RTU **40min at RT**
- Wash **1x** quickly and **2x 5min** in **PBS**
- Wash **1x** quickly and **1x 5min** in **0,05MTris-HCl pH7.6**

(7) **Enzyme substrate**

- **DAB** (DAKO, #k3466) 1 mL buffer + 1 drop of reagent, check under the microscope**.** Incubate between **3 to 10 min**
- Wash **1x** quickly and **1x 5min** in **0,05MTris-HCl pH7.6**
- Wash **1x 5min** with tap water

(8) **CounterStain**

- Mayer's Hematoxyline
- Wash **1x 5min** with cold running tap water
- Dehydrate 50% EtOH to 100% EtOH, xylol/Roticlear
- Embedding with organic mounting medium

* Primary Antibody

> rabbit anti- LUC (PROMEGA, #G7451)

> **NEGATIVE CONTROL** = blocking buffer

* Secondary Antibody

> Rabbit Envision (DAKO #K4008)

7.9 HSC gating strategy

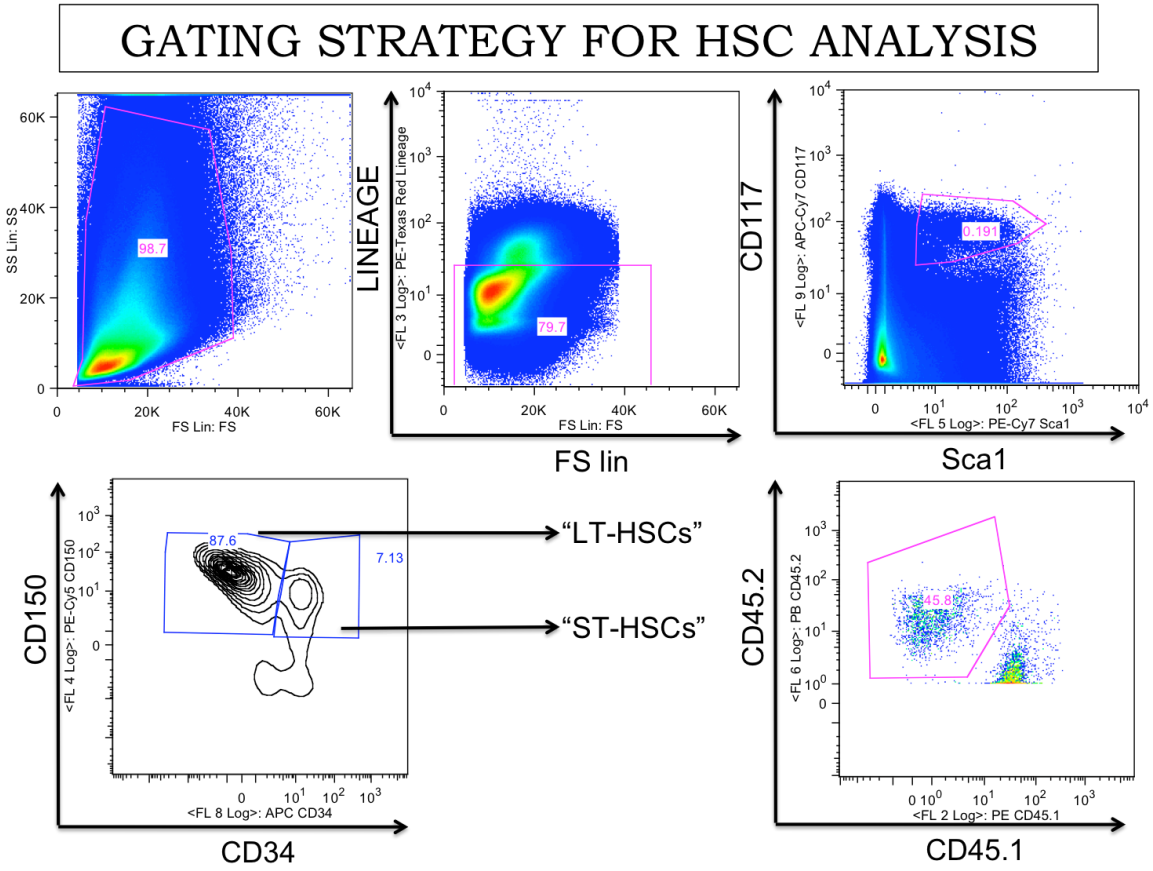

7.10 CXCR4 expression on MDA-MB-231 cells

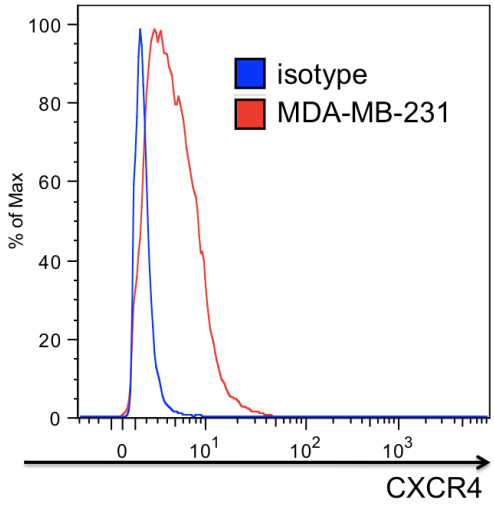

7.11 List of FACS antibodies used for the characterization of human cells

ANTIGEN	COMPANY	CATALOGUE#	CLONE	ISOTYPE	CONJUGATE
CD24	BioLegend	311120	ML5	Mouse IgG2a k	**PE-Cy7**
CD26	BD	555437	M-A261	Mouse IgG1 k	**PE**
	BD	555436	M-A261	Mouse IgG1 k	**FITC**
CD44	eBioscience	25-0441-81	IM7	Mouse IgG1 k	**PE-Cy7**
	eBioscience	15-0441-82	IM7	Rat IgG2b k	**PE-Cy5**
	BioLegend	103028	IM7	Rat IgG2b k	**APC-Cy7**
	BioLegend	103020	IM7	Rat IgG2b k	**Pacific Blue**
	BD	555477	G44-26	Mouse IgG2b, k	**Biotin**
	BD	559942	G44-26	Mouse IgG2b k	**APC**
	BD	555478	G44-26	Mouse IgG2b k	**FITC**
	BD	555479	G44-26	Mouse IgG2b k	**PE**
CD45	BioLegend	304022	HI30	Mouse IgG1 k	**Pacific Blue**
	eBioscience	25 0459 42	HI30	Mouse IgG1	**PE-Cy7**
CD47	BD	556046	B6H12	Mouse IgG1 k	**PE**
	BioLegend	322404	HCD47	Mouse IgG1 k	**Biotin**
CD326 (EPCAM)	Miltenyi	130-080-301	HEA-125	Mouse IgG1	**FITC**
	BD	347200	EBA-1	Mouse IgG1 L	**APC**
C-MET	eBioscience	13-8858	eBioclone 97	Mouse IgG1 k	**Biotin**
	R&D	FAB3582A	95106	Mouse IgG1	**APC**
CXCR4 (CD184)	eBioscience	12-9999-71	12G5	Mouse IgG2a k	**PE**
HLA-ABC	BD	555552	G46-2.6	Mouse IgG1 k	**FITC**
	ebioscience	12-9983	W6/32	Mouse IgG2a k	**PE**
	ebioscience	13-9983	W6/32	Mouse IgG2a k	**Biotin**
Ki67	BD	558615	B56	Mouse IgG1 k	**AlexaFluor 647**
	BD	556026	B56	Mouse IgG1 k	**FITC**
anti-mouse H2Kd	BioLegend	116612	SF1-1.1	Mouse IgG2a k	**AlexaFluor 647**
	BioLegend	116604	SF1-1.1	Mouse IgG2ak	**Biotin**
	BioLegend	116616	SF1-1.1	Mouse IgG2a k	**Pacific Blue**

8. ABBREVIATIONS

ADA: ADENOSINE DEAMINASE

ANGPTL4: ANGIOPOIETIN LIKE 4

APC: Allophycocyanin

bFGF: basic Fibroblast Growth Factor

BL: blood

BM: Bone Marrow

BMDCs. Bone Marrow Derived Cells

BMP: BONE MORPHOGENETIC PROTEIN

BRMS1: BREAST METASTASIS SUPPRESSOR 1

BSA: Bovine Serum Albumin

CAM: Collagen Adhesion Matrix

CAR: CXCL-12 ABUNDANT RETICULAR

CK: Cytokeratin

CMV: cytomegalovirus

CSCs: Cancer Stem Cells

CSF1: COLONY STIMULATING FACTOR 1

CSF1-R: COLONY STIMULATING FACTOR 1 RECEPTOR

CTCs: Circulating Tumor Cells

CT-SCAN: Computed Tomography Scan

CXCR4: CXC RECEPTOR 4

CXCL-12: CXC CHEMOCHINE LIGAND 12

Cy: Cyanin

DAPI: 4',6-Diamidin-2'-phenylindol-dihydrochlorid

DARC: DUFFY ANTIGEN CHEMOCHINE RECEPTOR

DNA: Desoxy Ribonucleic Acid

DTCs: Disseminated Tumor Cells

DgTCs: Disseminating Tumor Cells

ECM: Extra-Cellular Matrix

EGF: EPIDERMAL GROWTH FACTOR

EGFP: ENHANCED GREEN FLUORESCENT PROTEIN

EMMPRIN: EXTRACELLULAR MATRIX METALLOPROTEINASE INDUCER

EMT: Epithelial to Mesenchymal Transition

EPCAM: EPITHELIAL CELL ADHESION MOLECULE

EPCs: Endothelial Progenitor Cells

ER: ESTROGEN RECEPTOR

ESTR: estrogen

ETC: Epirubicin, Paclitaxel, Cyclophosphamide

FACS: Fluorescence Activated Cell Sorting

FAP-ALPHA: FIBROBLAST ACTIVATING PROTEIN ALPHA

FCS: Fetal Calf Serum

FDA: Food and Drug Administration

FITC: Fluorescein isothiocyanate

FSH: follicle stimulating hormone

GvHD: Graft versus Host Disease

H§E: HEMATOXYLIN AND EOSIN

HGF: HEPATOCYTE GROWTH FACTOR

HIV: Human Immunodeficiency Virus

HLA: HUMAN LEUKOCYTE ANTIGEN

HPCs: Haematopoietic Progenitor Cells

HSCs: Haematopoietic Stem Cells

ID1: INHIBITOR OF DIFFERENTIATION 1

IF: Intra-Femoral

IFNα: INTERFERON ALPHA

IGF1R: INSULIN GROWTH FACTOR 1 RECEPTOR

IL: INTERLEUKIN

IL-R: INTERLEUKIN RECEPTOR

IRAK1: INTERLEUKIN 1 RECEPTOR-ASSOCIATED KINASE 1

ITCs: Isolated Tumor Cells

IV: Intra-Venous

IVC: Individually Ventilated Cage

LN: Lymph node

LNTCs: Lymph Node Tumor Cells

LOX: LYSYL OXIDASE

LPAR1: LYSOPHOSPHATIC ACID RECPETOR

LRC: Label Retaining Cell

LT-HSCs: Long-Term Haematopoietic Stem Cells

LUC: Luciferase

MDSCs: Myeloid Derived Suppressor Cells

MET: Mesenchymal to Epithelial Transition

MetICs: Metastasis Initiating Cells

MHC: MAJOR HISTOCOMPATIBILITY COMPLEX

MiRNA: Micro Ribonucleic Acid

MMP: MATRIX METALLOPROTEINASE

MNC: Mono Nucleated Cells

MRI: Magnetic Resonance Imaging

MSCs: Mesenchymal Stem Cells

mRNA: Messenger RNA

ND: Not Determined

NFκB: NUCLEAR FACTOR KAPPA B

NOD/SCID: Nonobese Diabetic/Severe Combined Immunodeficiency Disease

NSG: NOD/SCID/$\gamma_c^{-/-}$.

OPN: OSTEPOPONTIN

PB: PACIFIC BLUE

PBS: Phophate Buffer Saline

PCR: Polymerase Chain Reaction

PE: Phycoerythrin

PI: Propidium Iodide

PlGF: PLACENTAL GROWTH FACTOR

PR: PROGESTERONE RECEPTOR

PS: Penicillin Streptomycin

PTGD2: PROSTAGLANDIN G/H SYNTHASE 2

PTH: parathyroid hormone

PTHRP: PARATHYROID HORMONE-RELATED PROTEIN

qPCR: quantitative Polymerase Chain Reaction

RNA: Ribonucleic Acid

RTKs: RECEPTOR TYROSINE KINASES

SCF: STEM CELL FACTOR

SDF1: STROMAL CELL-DERIVED FACTOR 1

SHH: SONIC HEDGEHOG

SLN: Sentinel Lymph Node

SPF: Specific Pathogen Free

ST-HSCs: Short-Term Haematopoietic Stem Cells

TAC: Tetrameric Antibody Complex

TAMs: Tumor Associated Macrophages

TF: TISSUE FACTOR

TGFβ: TRANSFORMING GROWTH FACTOR BETA

TNFα: TUMOR NECROSIS FACOR ALPHA

TNM: Tumor, Node, Metastasis

TRAF6: TNF RECEPTOR-ASSOCIATED FACTOR 6

UPAR: UROKINASE PLASMINOGEN ACTIVATOR RECEPTOR

VEGFA: VASCULAR ENDOTHELIAL GROWTH FACTOR A

VEGFR1: VASCULAR ENDOTHELIAL GROWTH FACTOR RECEPTOR 1

VLA4: VERY LATE ANTIGEN 4

WPRE: Woodchck post-transcriptional response element

9. LIST OF FIGURES

10. BIBLIOGRAPHY

Aguirre-Ghiso, J.A. (2007). Models, mechanisms and clinical evidence for cancer dormancy. Nat Rev Cancer *7*, 834-846.

Aktas, B., Tewes, M., Fehm, T., Hauch, S., Kimmig, R., and Kasimir-Bauer, S. (2009). Stem cell and epithelial-mesenchymal transition markers are frequently overexpressed in circulating tumor cells of metastatic breast cancer patients. Breast Cancer Res *11*, R46.

Al-Hajj, M., Wicha, M.S., Benito-Hernandez, A., Morrison, S.J., and Clarke, M.F. (2003). Prospective identification of tumorigenic breast cancer cells. Proc Natl Acad Sci U S A *100*, 3983-3988.

Alexopoulou, A.N., Couchman, J.R., and Whiteford, J.R. (2008). The CMV early enhancer/chicken beta actin (CAG) promoter can be used to drive transgene expression during the differentiation of murine embryonic stem cells into vascular progenitors. BMC Cell Biol *9*, 2.

Alix-Panabieres, C., Muller, V., and Pantel, K. (2007). Current status in human breast cancer micrometastasis. Curr Opin Oncol *19*, 558-563.

Alix-Panabieres, C., Vendrell, J.P., Slijper, M., Pelle, O., Barbotte, E., Mercier, G., Jacot, W., Fabbro, M., and Pantel, K. (2009). Full-length cytokeratin-19 is released by human tumor cells: a potential role in metastatic progression of breast cancer. Breast Cancer Res *11*, R39.

Allard, W.J., Matera, J., Miller, M.C., Repollet, M., Connelly, M.C., Rao, C., Tibbe, A.G., Uhr, J.W., and Terstappen, L.W. (2004). Tumor cells circulate in the peripheral blood of all major carcinomas but not in healthy subjects or patients with nonmalignant diseases. Clin Cancer Res *10*, 6897-6904.

Ameri, K., Luong, R., Zhang, H., Powell, A.A., Montgomery, K.D., Espinosa, I., Bouley, D.M., Harris, A.L., and Jeffrey, S.S. (2010). Circulating tumour cells demonstrate an altered response to hypoxia and an aggressive phenotype. Br J Cancer *102*, 561-569.

Bailey, J.M., Singh, P.K., and Hollingsworth, M.A. (2007). Cancer metastasis facilitated by developmental pathways: Sonic hedgehog, Notch, and bone morphogenic proteins. J Cell Biochem *102*, 829-839.

Balic, M., Lin, H., Young, L., Hawes, D., Giuliano, A., McNamara, G., Datar, R.H., and Cote, R.J. (2006). Most early disseminated cancer cells detected in bone marrow of breast cancer patients have a putative breast cancer stem cell phenotype. Clin Cancer Res *12*, 5615-5621.

Bandyopadhyay, S., Zhan, R., Chaudhuri, A., Watabe, M., Pai, S.K., Hirota, S., Hosobe, S., Tsukada, T., Miura, K., Takano, Y.*, et al.* (2006). Interaction of KAI1 on tumor cells with DARC on vascular endothelium leads to metastasis suppression. Nat Med *12*, 933-938.

Barker, N., Ridgway, R.A., van Es, J.H., van de Wetering, M., Begthel, H., van den Born, M., Danenberg, E., Clarke, A.R., Sansom, O.J., and Clevers, H. (2009). Crypt stem cells as the cells-of-origin of intestinal cancer. Nature *457*, 608-611.

Beilmann, M., Odenthal, M., Jung, W., Vande Woude, G.F., Dienes, H.P., and Schirmacher, P. (1997). Neoexpression of the c-met/hepatocyte growth factor-scatter factor receptor gene in activated monocytes. Blood *90*, 4450-4458.

Benoy, I.H., Elst, H., Philips, M., Wuyts, H., Van Dam, P., Scharpe, S., Van Marck, E., Vermeulen, P.B., and Dirix, L.Y. (2006). Real-time RT-PCR detection of disseminated tumour cells in bone marrow has superior prognostic significance in comparison with circulating tumour cells in patients with breast cancer. Br J Cancer *94*, 672-680.

Bez, A., Corsini, E., Curti, D., Biggiogera, M., Colombo, A., Nicosia, R.F., Pagano, S.F., and Parati, E.A. (2003). Neurosphere and neurosphere-forming cells: morphological and ultrastructural characterization. Brain Res *993*, 18-29.

Bhaumik, D., Scott, G.K., Schokrpur, S., Patil, C.K., Campisi, J., and Benz, C.C. (2008). Expression of microRNA-146 suppresses NF-kappaB activity with reduction of metastatic potential in breast cancer cells. Oncogene *27*, 5643-5647.

Biancone, L., Araki, M., Araki, K., Vassalli, P., and Stamenkovic, I. (1996). Redirection of tumor metastasis by expression of E-selectin in vivo. J Exp Med *183*, 581-587.

Bidard, F.C., Mathiot, C., Degeorges, A., Etienne-Grimaldi, M.C., Delva, R., Pivot, X., Veyret, C., Bergougnoux, L., de Cremoux, P., Milano, G.*, et al.* (2010). Clinical value of circulating endothelial cells and circulating tumor cells in metastatic breast cancer patients treated first line with bevacizumab and chemotherapy. Ann Oncol *21*, 1765-1771.

Bindra, A., Muradrasoli, S., Kisekka, R., Nordgren, H., Warnberg, F., and Blomberg, J. (2007). Search for DNA of exogenous mouse mammary tumor virus-related virus in human breast cancer samples. J Gen Virol *88*, 1806-1809.

Boccaccio, C., and Comoglio, P.M. (2006). Invasive growth: a MET-driven genetic programme for cancer and stem cells. Nat Rev Cancer *6*, 637-645.

Bonnet, D., and Dick, J.E. (1997). Human acute myeloid leukemia is organized as a hierarchy that originates from a primitive hematopoietic cell. Nat Med *3*, 730-737.

Bottaro, D.P., Rubin, J.S., Faletto, D.L., Chan, A.M., Kmiecik, T.E., Vande Woude, G.F., and Aaronson, S.A. (1991). Identification of the hepatocyte growth factor receptor as the c-met proto-oncogene product. Science *251*, 802-804.

Boucharaba, A., Serre, C.M., Guglielmi, J., Bordet, J.C., Clezardin, P., and Peyruchaud, O. (2006). The type 1 lysophosphatidic acid receptor is a target for therapy in bone metastases. Proc Natl Acad Sci U S A *103*, 9643-9648.

Braun, S., and Pantel, K. (1999). Biological characteristics of micrometastatic cancer cells in bone marrow. Cancer Metastasis Rev *18*, 75-90.

Braun, S., Vogl, F.D., Naume, B., Janni, W., Osborne, M.P., Coombes, R.C., Schlimok, G., Diel, I.J., Gerber, B., Gebauer, G.*, et al.* (2005). A pooled analysis of bone marrow micrometastasis in breast cancer. N Engl J Med *353*, 793-802.

Brown, D.M., and Ruoslahti, E. (2004). Metadherin, a cell surface protein in breast tumors that mediates lung metastasis. Cancer Cell *5*, 365-374.

Broxmeyer, H.E., Orschell, C.M., Clapp, D.W., Hangoc, G., Cooper, S., Plett, P.A., Liles, W.C., Li, X., Graham-Evans, B., Campbell, T.B.*, et al.* (2005). Rapid mobilization of murine and human

hematopoietic stem and progenitor cells with AMD3100, a CXCR4 antagonist. J Exp Med *201*, 1307-1318.

Budd, G.T., Cristofanilli, M., Ellis, M.J., Stopeck, A., Borden, E., Miller, M.C., Matera, J., Repollet, M., Doyle, G.V., Terstappen, L.W.*, et al.* (2006). Circulating tumor cells versus imaging--predicting overall survival in metastatic breast cancer. Clin Cancer Res *12*, 6403-6409.

Cailleau, R., Young, R., Olive, M., and Reeves, W.J., Jr. (1974). Breast tumor cell lines from pleural effusions. J Natl Cancer Inst *53*, 661-674.

Calvi, L.M., Adams, G.B., Weibrecht, K.W., Weber, J.M., Olson, D.P., Knight, M.C., Martin, R.P., Schipani, E., Divieti, P., Bringhurst, F.R.*, et al.* (2003). Osteoblastic cells regulate the haematopoietic stem cell niche. Nature *425*, 841-846.

Campbell, P.J., Yachida, S., Mudie, L.J., Stephens, P.J., Pleasance, E.D., Stebbings, L.A., Morsberger, L.A., Latimer, C., McLaren, S., Lin, M.L.*, et al.* (2010). The patterns and dynamics of genomic instability in metastatic pancreatic cancer. Nature *467*, 1109-1113.

Chaffer, C.L., Thompson, E.W., and Williams, E.D. (2007). Mesenchymal to epithelial transition in development and disease. Cells Tissues Organs *185*, 7-19.

Chambers, A.F., Groom, A.C., and MacDonald, I.C. (2002). Dissemination and growth of cancer cells in metastatic sites. Nat Rev Cancer *2*, 563-572.

Chan, K.S., Espinosa, I., Chao, M., Wong, D., Ailles, L., Diehn, M., Gill, H., Presti, J., Jr., Chang, H.Y., van de Rijn, M.*, et al.* (2009). Identification, molecular characterization, clinical prognosis, and therapeutic targeting of human bladder tumor-initiating cells. Proc Natl Acad Sci U S A *106*, 14016-14021.

Chan, K.S., Volkmer, J.P., and Weissman, I. (2010). Cancer stem cells in bladder cancer: a revisited and evolving concept. Curr Opin Urol *20*, 393-397.

Chang, Y.S., di Tomaso, E., McDonald, D.M., Jones, R., Jain, R.K., and Munn, L.L. (2000). Mosaic blood vessels in tumors: frequency of cancer cells in contact with flowing blood. Proc Natl Acad Sci U S A *97*, 14608-14613.

Charafe-Jauffret, E., Ginestier, C., Iovino, F., Tarpin, C., Diebel, M., Esterni, B., Houvenaeghel, G., Extra, J.M., Bertucci, F., Jacquemier, J.*, et al.* (2010). Aldehyde dehydrogenase 1-positive cancer stem cells mediate metastasis and poor clinical outcome in inflammatory breast cancer. Clin Cancer Res *16*, 45-55.

Chen, C.C., Hou, M.F., Wang, J.Y., Chang, T.W., Lai, D.Y., Chen, Y.F., Hung, S.Y., and Lin, S.R. (2006). Simultaneous detection of multiple mRNA markers CK19, CEA, c-Met, Her2/neu and hMAM with membrane array, an innovative technique with a great potential for breast cancer diagnosis. Cancer Lett *240*, 279-288.

Chen, Y.C., Hsu, H.S., Chen, Y.W., Tsai, T.H., How, C.K., Wang, C.Y., Hung, S.C., Chang, Y.L., Tsai, M.L., Lee, Y.Y.*, et al.* (2008). Oct-4 expression maintained cancer stem-like properties in lung cancer-derived CD133-positive cells. PLoS One *3*, e2637.

Cheng, P., Corzo, C.A., Luetteke, N., Yu, B., Nagaraj, S., Bui, M.M., Ortiz, M., Nacken, W., Sorg, C., Vogl, T.*, et al.* (2008). Inhibition of dendritic cell differentiation and accumulation of myeloid-derived suppressor cells in cancer is regulated by S100A9 protein. J Exp Med *205*, 2235-2249.

Chlebowski, R.T., Anderson, G.L., Gass, M., Lane, D.S., Aragaki, A.K., Kuller, L.H., Manson, J.E., Stefanick, M.L., Ockene, J., Sarto, G.E.*, et al.* (2010). Estrogen plus progestin and breast cancer incidence and mortality in postmenopausal women. JAMA *304*, 1684-1692.

Cohen, S.J., Punt, C.J., Iannotti, N., Saidman, B.H., Sabbath, K.D., Gabrail, N.Y., Picus, J., Morse, M.A., Mitchell, E., Miller, M.C.*, et al.* (2009). Prognostic significance of circulating tumor cells in patients with metastatic colorectal cancer. Ann Oncol *20*, 1223-1229.

Collins, A.T., Berry, P.A., Hyde, C., Stower, M.J., and Maitland, N.J. (2005). Prospective identification of tumorigenic prostate cancer stem cells. Cancer Res *65*, 10946-10951.

Colmone, A., Amorim, M., Pontier, A.L., Wang, S., Jablonski, E., and Sipkins, D.A. (2008). Leukemic cells create bone marrow niches that disrupt the behavior of normal hematopoietic progenitor cells. Science *322*, 1861-1865.

Condeelis, J., and Segall, J.E. (2003). Intravital imaging of cell movement in tumours. Nat Rev Cancer *3*, 921-930.

Coumans, F.A., Doggen, C.J., Attard, G., de Bono, J.S., and Terstappen, L.W. (2010). All circulating EpCAM+CK+CD45- objects predict overall survival in castration-resistant prostate cancer. Ann Oncol *21*, 1851-1857.

Cristofanilli, M., Broglio, K.R., Guarneri, V., Jackson, S., Fritsche, H.A., Islam, R., Dawood, S., Reuben, J.M., Kau, S.W., Lara, J.M.*, et al.* (2007). Circulating tumor cells in metastatic breast cancer: biologic staging beyond tumor burden. Clin Breast Cancer *7*, 471-479.

Cserni, G. (2008). Minimal disease in sentinel nodes. Pathol Oncol Res *14*, 117-121.

de Bono, J.S., Scher, H.I., Montgomery, R.B., Parker, C., Miller, M.C., Tissing, H., Doyle, G.V., Terstappen, L.W., Pienta, K.J., and Raghavan, D. (2008). Circulating tumor cells predict survival benefit from treatment in metastatic castration-resistant prostate cancer. Clin Cancer Res *14*, 6302-6309.

Diaz-Montero, C.M., Salem, M.L., Nishimura, M.I., Garrett-Mayer, E., Cole, D.J., and Montero, A.J. (2009). Increased circulating myeloid-derived suppressor cells correlate with clinical cancer stage, metastatic tumor burden, and doxorubicin-cyclophosphamide chemotherapy. Cancer Immunol Immunother *58*, 49-59.

Dontu, G., Abdallah, W.M., Foley, J.M., Jackson, K.W., Clarke, M.F., Kawamura, M.J., and Wicha, M.S. (2003). In vitro propagation and transcriptional profiling of human mammary stem/progenitor cells. Genes Dev *17*, 1253-1270.

Eccles, S.A., and Welch, D.R. (2007). Metastasis: recent discoveries and novel treatment strategies. Lancet *369*, 1742-1757.

Epstein, R.J. (2004). The CXCL12-CXCR4 chemotactic pathway as a target of adjuvant breast cancer therapies. Nat Rev Cancer *4*, 901-909.

Erler, J.T., Bennewith, K.L., Cox, T.R., Lang, G., Bird, D., Koong, A., Le, Q.T., and Giaccia, A.J. (2009). Hypoxia-induced lysyl oxidase is a critical mediator of bone marrow cell recruitment to form the premetastatic niche. Cancer Cell *15*, 35-44.

Essers, M.A., Offner, S., Blanco-Bose, W.E., Waibler, Z., Kalinke, U., Duchosal, M.A., and Trumpp, A. (2009). IFNalpha activates dormant haematopoietic stem cells in vivo. Nature *458*, 904-908.

Fang, D.D., Kim, Y.J., Lee, C.N., Aggarwal, S., McKinnon, K., Mesmer, D., Norton, J., Birse, C.E., He, T., Ruben, S.M.*, et al.* (2010). Expansion of CD133(+) colon cancer cultures retaining stem cell properties to enable cancer stem cell target discovery. Br J Cancer *102*, 1265-1275.

Fehm, T., Braun, S., Muller, V., Janni, W., Gebauer, G., Marth, C., Schindlbeck, C., Wallwiener, D., Borgen, E., Naume, B.*, et al.* (2006). A concept for the standardized detection of disseminated tumor cells in bone marrow from patients with primary breast cancer and its clinical implementation. Cancer *107*, 885-892.

Fehm, T., Hoffmann, O., Aktas, B., Becker, S., Solomayer, E.F., Wallwiener, D., Kimmig, R., and Kasimir-Bauer, S. (2009). Detection and characterization of circulating tumor cells in blood of primary breast cancer patients by RT-PCR and comparison to status of bone marrow disseminated cells. Breast Cancer Res *11*, R59.

Fidler, I.J. (1970). Metastasis: guantitative analysis of distribution and fate of tumor embolilabeled with 125 I-5-iodo-2'-deoxyuridine. J Natl Cancer Inst *45*, 773-782.

Fuchs, E. (2007). Scratching the surface of skin development. Nature *445*, 834-842.

Fukagawa, T., Sasako, M., Shimoda, T., Sano, T., Katai, H., Saka, M., Mann, G.B., Karpeh, M., Coit, D.G., and Brennan, M.F. (2009). The prognostic impact of isolated tumor cells in lymph nodes of T2N0 gastric cancer: comparison of American and Japanese gastric cancer patients. Ann Surg Oncol *16*, 609-613.

Galanzha, E.I., Shashkov, E.V., Kelly, T., Kim, J.W., Yang, L., and Zharov, V.P. (2009). In vivo magnetic enrichment and multiplex photoacoustic detection of circulating tumour cells. Nat Nanotechnol *4*, 855-860.

Gao, D., Nolan, D., McDonnell, K., Vahdat, L., Benezra, R., Altorki, N., and Mittal, V. (2009). Bone marrow-derived endothelial progenitor cells contribute to the angiogenic switch in tumor growth and metastatic progression. Biochim Biophys Acta *1796*, 33-40.

Gao, D., Nolan, D.J., Mellick, A.S., Bambino, K., McDonnell, K., and Mittal, V. (2008). Endothelial progenitor cells control the angiogenic switch in mouse lung metastasis. Science *319*, 195-198.

Gentile, A., Trusolino, L., and Comoglio, P.M. (2008). The Met tyrosine kinase receptor in development and cancer. Cancer Metastasis Rev *27*, 85-94.

Ginestier, C., Hur, M.H., Charafe-Jauffret, E., Monville, F., Dutcher, J., Brown, M., Jacquemier, J., Viens, P., Kleer, C.G., Liu, S.*, et al.* (2007). ALDH1 is a marker of normal and malignant human mammary stem cells and a predictor of poor clinical outcome. Cell Stem Cell *1*, 555-567.

Gort, E.H., Groot, A.J., van der Wall, E., van Diest, P.J., and Vooijs, M.A. (2008). Hypoxic regulation of metastasis via hypoxia-inducible factors. Curr Mol Med *8*, 60-67.

Gradilone, A., Naso, G., Raimondi, C., Cortesi, E., Gandini, O., Vincenzi, B., Saltarelli, R., Chiapparino, E., Spremberg, F., Cristofanilli, M.*, et al.* (2011). Circulating tumor cells (CTCs) in metastatic breast cancer (MBC): prognosis, drug resistance and phenotypic characterization. Ann Oncol.

Gregory, P.A., Bracken, C.P., Bert, A.G., and Goodall, G.J. (2008). MicroRNAs as regulators of epithelial-mesenchymal transition. Cell Cycle *7*, 3112-3118.

Guise, T.A., and Mundy, G.R. (1998). Cancer and bone. Endocr Rev *19*, 18-54.

Guo, X., Razandi, M., Pedram, A., Kassab, G., and Levin, E.R. (2005). Estrogen induces vascular wall dilation: mediation through kinase signaling to nitric oxide and estrogen receptors alpha and beta. J Biol Chem *280*, 19704-19710.

Gupta, G.P., Nguyen, D.X., Chiang, A.C., Bos, P.D., Kim, J.Y., Nadal, C., Gomis, R.R., Manova-Todorova, K., and Massague, J. (2007a). Mediators of vascular remodelling co-opted for sequential steps in lung metastasis. Nature *446*, 765-770.

Gupta, G.P., Perk, J., Acharyya, S., de Candia, P., Mittal, V., Todorova-Manova, K., Gerald, W.L., Brogi, E., Benezra, R., and Massague, J. (2007b). ID genes mediate tumor reinitiation during breast cancer lung metastasis. Proc Natl Acad Sci U S A *104*, 19506-19511.

Havre, P.A., Abe, M., Urasaki, Y., Ohnuma, K., Morimoto, C., and Dang, N.H. (2008). The role of CD26/dipeptidyl peptidase IV in cancer. Front Biosci *13*, 1634-1645.

He, W., Kularatne, S.A., Kalli, K.R., Prendergast, F.G., Amato, R.J., Klee, G.G., Hartmann, L.C., and Low, P.S. (2008). Quantitation of circulating tumor cells in blood samples from ovarian and prostate cancer patients using tumor-specific fluorescent ligands. Int J Cancer *123*, 1968-1973.

Healy, L., May, G., Gale, K., Grosveld, F., Greaves, M., and Enver, T. (1995). The stem cell antigen CD34 functions as a regulator of hemopoietic cell adhesion. Proc Natl Acad Sci U S A *92*, 12240-12244.

Hedley, B.D., and Chambers, A.F. (2009). Tumor dormancy and metastasis. Adv Cancer Res *102*, 67-101.

Hemsen, A., Riethdorf, L., Brunner, N., Berger, J., Ebel, S., Thomssen, C., Janicke, F., and Pantel, K. (2003). Comparative evaluation of urokinase-type plasminogen activator receptor expression in primary breast carcinomas and on metastatic tumor cells. Int J Cancer *107*, 903-909.

Hermann, P.C., Huber, S.L., Herrler, T., Aicher, A., Ellwart, J.W., Guba, M., Bruns, C.J., and Heeschen, C. (2007). Distinct populations of cancer stem cells determine tumor growth and metastatic activity in human pancreatic cancer. Cell Stem Cell *1*, 313-323.

Hess, K.R., Varadhachary, G.R., Taylor, S.H., Wei, W., Raber, M.N., Lenzi, R., and Abbruzzese, J.L. (2006). Metastatic patterns in adenocarcinoma. Cancer *106*, 1624-1633.

Hirakawa, S., Brown, L.F., Kodama, S., Paavonen, K., Alitalo, K., and Detmar, M. (2007). VEGF-C-induced lymphangiogenesis in sentinel lymph nodes promotes tumor metastasis to distant sites. Blood *109*, 1010-1017.

Hiratsuka, S., Watanabe, A., Aburatani, H., and Maru, Y. (2006). Tumour-mediated upregulation of chemoattractants and recruitment of myeloid cells predetermines lung metastasis. Nat Cell Biol *8*, 1369-1375.

Hiratsuka, S., Watanabe, A., Sakurai, Y., Akashi-Takamura, S., Ishibashi, S., Miyake, K., Shibuya, M., Akira, S., Aburatani, H., and Maru, Y. (2008). The S100A8-serum amyloid A3-TLR4 paracrine cascade establishes a pre-metastatic phase. Nat Cell Biol *10*, 1349-1355.

Hoggatt, J., Singh, P., Sampath, J., and Pelus, L.M. (2009). Prostaglandin E2 enhances hematopoietic stem cell homing, survival, and proliferation. Blood *113*, 5444-5455.

Husemann, Y., Geigl, J.B., Schubert, F., Musiani, P., Meyer, M., Burghart, E., Forni, G., Eils, R., Fehm, T., Riethmuller, G.*, et al.* (2008). Systemic spread is an early step in breast cancer. Cancer Cell *13*, 58-68.

Janni, W., Rack, B., Schindlbeck, C., Strobl, B., Rjosk, D., Braun, S., Sommer, H., Pantel, K., Gerber, B., and Friese, K. (2005). The persistence of isolated tumor cells in bone marrow from patients with breast carcinoma predicts an increased risk for recurrence. Cancer *103*, 884-891.

Jemal, A., Siegel, R., Xu, J., and Ward, E. (2010). Cancer Statistics, 2010. CA Cancer J Clin.

Jin, D.K., Shido, K., Kopp, H.G., Petit, I., Shmelkov, S.V., Young, L.M., Hooper, A.T., Amano, H., Avecilla, S.T., Heissig, B.*, et al.* (2006). Cytokine-mediated deployment of SDF-1 induces revascularization through recruitment of CXCR4+ hemangiocytes. Nat Med *12*, 557-567.

Johansson, J.E., Andren, O., Andersson, S.O., Dickman, P.W., Holmberg, L., Magnuson, A., and Adami, H.O. (2004). Natural history of early, localized prostate cancer. JAMA *291*, 2713-2719.

Jones, S., Chen, W.D., Parmigiani, G., Diehl, F., Beerenwinkel, N., Antal, T., Traulsen, A., Nowak, M.A., Siegel, C., Velculescu, V.E.*, et al.* (2008). Comparative lesion sequencing provides insights into tumor evolution. Proc Natl Acad Sci U S A *105*, 4283-4288.

Joyce, J.A., and Pollard, J.W. (2009). Microenvironmental regulation of metastasis. Nat Rev Cancer *9*, 239-252.

Kang, Y., and Massague, J. (2004). Epithelial-mesenchymal transitions: twist in development and metastasis. Cell *118*, 277-279.

Kang, Y., Siegel, P.M., Shu, W., Drobnjak, M., Kakonen, S.M., Cordon-Cardo, C., Guise, T.A., and Massague, J. (2003). A multigenic program mediating breast cancer metastasis to bone. Cancer Cell *3*, 537-549.

Kaplan, R.N., Riba, R.D., Zacharoulis, S., Bramley, A.H., Vincent, L., Costa, C., MacDonald, D.D., Jin, D.K., Shido, K., Kerns, S.A., *et al.* (2005). VEGFR1-positive haematopoietic bone marrow progenitors initiate the pre-metastatic niche. Nature *438*, 820-827.

Karnoub, A.E., Dash, A.B., Vo, A.P., Sullivan, A., Brooks, M.W., Bell, G.W., Richardson, A.L., Polyak, K., Tubo, R., and Weinberg, R.A. (2007). Mesenchymal stem cells within tumour stroma promote breast cancer metastasis. Nature *449*, 557-563.

Keysar, S.B., and Jimeno, A. (2010). More Than Markers: Biological Significance of Cancer Stem Cell-Defining Molecules. Mol Cancer Ther.

Kim, I., He, S., Yilmaz, O.H., Kiel, M.J., and Morrison, S.J. (2006). Enhanced purification of fetal liver hematopoietic stem cells using SLAM family receptors. Blood *108*, 737-744.

Kim, M.Y., Oskarsson, T., Acharyya, S., Nguyen, D.X., Zhang, X.H., Norton, L., and Massague, J. (2009). Tumor self-seeding by circulating cancer cells. Cell *139*, 1315-1326.

Klein, C.A., Blankenstein, T.J., Schmidt-Kittler, O., Petronio, M., Polzer, B., Stoecklein, N.H., and Riethmuller, G. (2002). Genetic heterogeneity of single disseminated tumour cells in minimal residual cancer. Lancet *360*, 683-689.

Kyle, R.A., and Rajkumar, S.V. (2008). Multiple myeloma. Blood *111*, 2962-2972.

Lapidot, T., and Kollet, O. (2002). The essential roles of the chemokine SDF-1 and its receptor CXCR4 in human stem cell homing and repopulation of transplanted immune-deficient NOD/SCID and NOD/SCID/B2m(null) mice. Leukemia *16*, 1992-2003.

Lapidot, T., Sirard, C., Vormoor, J., Murdoch, B., Hoang, T., Caceres-Cortes, J., Minden, M., Paterson, B., Caligiuri, M.A., and Dick, J.E. (1994). A cell initiating human acute myeloid leukaemia after transplantation into SCID mice. Nature *367*, 645-648.

Lataillade, J.J., Pierre-Louis, O., Hasselbalch, H.C., Uzan, G., Jasmin, C., Martyre, M.C., and Le Bousse-Kerdiles, M.C. (2008). Does primary myelofibrosis involve a defective stem cell niche? From concept to evidence. Blood *112*, 3026-3035.

Laurenti, E., Varnum-Finney, B., Wilson, A., Ferrero, I., Blanco-Bose, W.E., Ehninger, A., Knoepfler, P.S., Cheng, P.F., MacDonald, H.R., Eisenman, R.N.*, et al.* (2008). Hematopoietic stem cell function and survival depend on c-Myc and N-Myc activity. Cell Stem Cell *3*, 611-624.

Lee, Y.T. (1985). Patterns of metastasis and natural courses of breast carcinoma. Cancer Metastasis Rev *4*, 153-172.

Leinung, S., Wurl, P., Weiss, C.L., Roder, I., and Schonfelder, M. (2000). Cytokeratin-positive cells in bone marrow in comparison with other prognostic factors in colon carcinoma. Langenbecks Arch Surg *385*, 337-343.

Lemieux, C., Cloutier, I., and Tanguay, J.F. (2008). Estrogen-induced gene expression in bone marrow c-kit+ stem cells and stromal cells: identification of specific biological processes involved in the functional organization of the stem cell niche. Stem Cells Dev *17*, 1153-1163.

Levenson, A.S., and Jordan, V.C. (1997). MCF-7: the first hormone-responsive breast cancer cell line. Cancer Res *57*, 3071-3078.

Liang, Y., Benakanakere, I., Besch-Williford, C., Hyder, R.S., Ellersieck, M.R., and Hyder, S.M. (2010). Synthetic progestins induce growth and metastasis of BT-474 human breast cancer xenografts in nude mice. Menopause *17*, 1040-1047.

Liang, Z., Wu, T., Lou, H., Yu, X., Taichman, R.S., Lau, S.K., Nie, S., Umbreit, J., and Shim, H. (2004). Inhibition of breast cancer metastasis by selective synthetic polypeptide against CXCR4. Cancer Res *64*, 4302-4308.

Lim, E., Modi, K.D., and Kim, J. (2009). In vivo bioluminescent imaging of mammary tumors using IVIS spectrum. J Vis Exp.

Lu, J., Fan, T., Zhao, Q., Zeng, W., Zaslavsky, E., Chen, J.J., Frohman, M.A., Golightly, M.G., Madajewicz, S., and Chen, W.T. (2010). Isolation of circulating epithelial and tumor

progenitor cells with an invasive phenotype from breast cancer patients. Int J Cancer *126*, 669-683.

Luzzi, K.J., MacDonald, I.C., Schmidt, E.E., Kerkvliet, N., Morris, V.L., Chambers, A.F., and Groom, A.C. (1998). Multistep nature of metastatic inefficiency: dormancy of solitary cells after successful extravasation and limited survival of early micrometastases. Am J Pathol *153*, 865-873.

Ma, L., Teruya-Feldstein, J., and Weinberg, R.A. (2007). Tumour invasion and metastasis initiated by microRNA-10b in breast cancer. Nature *449*, 682-688.

MacDonald, I.C., Groom, A.C., and Chambers, A.F. (2002). Cancer spread and micrometastasis development: quantitative approaches for in vivo models. Bioessays *24*, 885-893.

Majdic, O., Stockl, J., Pickl, W.F., Bohuslav, J., Strobl, H., Scheinecker, C., Stockinger, H., and Knapp, W. (1994). Signaling and induction of enhanced cytoadhesiveness via the hematopoietic progenitor cell surface molecule CD34. Blood *83*, 1226-1234.

Mani, S.A., Guo, W., Liao, M.J., Eaton, E.N., Ayyanan, A., Zhou, A.Y., Brooks, M., Reinhard, F., Zhang, C.C., Shipitsin, M.*, et al.* (2008). The epithelial-mesenchymal transition generates cells with properties of stem cells. Cell *133*, 704-715.

Marrinucci, D., Bethel, K., Lazar, D., Fisher, J., Huynh, E., Clark, P., Bruce, R., Nieva, J., and Kuhn, P. (2010). Cytomorphology of circulating colorectal tumor cells:a small case series. J Oncol *2010*, 861341.

Massague, J. (2007). Sorting out breast-cancer gene signatures. N Engl J Med *356*, 294-297.

Matsuda, J., Kitagawa, Y., Fujii, H., Mukai, M., Dan, K., Kubota, T., Watanabe, M., Ozawa, S., Otani, Y., Hasegawa, H.*, et al.* (2004). Significance of metastasis detected by molecular techniques in sentinel nodes of patients with gastrointestinal cancer. Ann Surg Oncol *11*, 250S-254S.

Mazurier, F., Doedens, M., Gan, O.I., and Dick, J.E. (2003). Rapid myeloerythroid repopulation after intrafemoral transplantation of NOD-SCID mice reveals a new class of human stem cells. Nat Med *9*, 959-963.

Mendez-Ferrer, S., Michurina, T.V., Ferraro, F., Mazloom, A.R., Macarthur, B.D., Lira, S.A., Scadden, D.T., Ma'ayan, A., Enikolopov, G.N., and Frenette, P.S. (2010). Mesenchymal and haematopoietic stem cells form a unique bone marrow niche. Nature *466*, 829-834.

Meng, F., Henson, R., Wehbe-Janek, H., Ghoshal, K., Jacob, S.T., and Patel, T. (2007). MicroRNA-21 regulates expression of the PTEN tumor suppressor gene in human hepatocellular cancer. Gastroenterology *133*, 647-658.

Meng, S., Tripathy, D., Frenkel, E.P., Shete, S., Naftalis, E.Z., Huth, J.F., Beitsch, P.D., Leitch, M., Hoover, S., Euhus, D.*, et al.* (2004). Circulating tumor cells in patients with breast cancer dormancy. Clin Cancer Res *10*, 8152-8162.

Meng, S., Tripathy, D., Shete, S., Ashfaq, R., Saboorian, H., Haley, B., Frenkel, E., Euhus, D., Leitch, M., Osborne, C.*, et al.* (2006). uPAR and HER-2 gene status in individual breast cancer cells from blood and tissues. Proc Natl Acad Sci U S A *103*, 17361-17365.

Minn, A.J., Gupta, G.P., Siegel, P.M., Bos, P.D., Shu, W., Giri, D.D., Viale, A., Olshen, A.B., Gerald, W.L., and Massague, J. (2005). Genes that mediate breast cancer metastasis to lung. Nature *436*, 518-524.

Minna, J.D., Kurie, J.M., and Jacks, T. (2003). A big step in the study of small cell lung cancer. Cancer Cell *4*, 163-166.

Moreno-Bueno, G., Portillo, F., and Cano, A. (2008). Transcriptional regulation of cell polarity in EMT and cancer. Oncogene *27*, 6958-6969.

Morgan, T.M., Lange, P.H., Porter, M.P., Lin, D.W., Ellis, W.J., Gallaher, I.S., and Vessella, R.L. (2009). Disseminated tumor cells in prostate cancer patients after radical prostatectomy and without evidence of disease predicts biochemical recurrence. Clin Cancer Res *15*, 677-683.

Muller, A., Homey, B., Soto, H., Ge, N., Catron, D., Buchanan, M.E., McClanahan, T., Murphy, E., Yuan, W., Wagner, S.N.*, et al.* (2001). Involvement of chemokine receptors in breast cancer metastasis. Nature *410*, 50-56.

Muller, V., Alix-Panabieres, C., and Pantel, K. (2010). Insights into minimal residual disease in cancer patients: implications for anti-cancer therapies. Eur J Cancer *46*, 1189-1197.

Muller, V., Stahmann, N., Riethdorf, S., Rau, T., Zabel, T., Goetz, A., Janicke, F., and Pantel, K. (2005). Circulating tumor cells in breast cancer: correlation to bone marrow micrometastases, heterogeneous response to systemic therapy and low proliferative activity. Clin Cancer Res *11*, 3678-3685.

Myers, C., Charboneau, A., Cheung, I., Hanks, D., and Boudreau, N. (2002). Sustained expression of homeobox D10 inhibits angiogenesis. Am J Pathol *161*, 2099-2109.

Nagrath, S., Sequist, L.V., Maheswaran, S., Bell, D.W., Irimia, D., Ulkus, L., Smith, M.R., Kwak, E.L., Digumarthy, S., Muzikansky, A.*, et al.* (2007). Isolation of rare circulating tumour cells in cancer patients by microchip technology. Nature *450*, 1235-1239.

Naik, R.P., Jin, D., Chuang, E., Gold, E.G., Tousimis, E.A., Moore, A.L., Christos, P.J., de Dalmas, T., Donovan, D., Rafii, S.*, et al.* (2008). Circulating endothelial progenitor cells correlate to stage in patients with invasive breast cancer. Breast Cancer Res Treat *107*, 133-138.

Naumov, G.N., Townson, J.L., MacDonald, I.C., Wilson, S.M., Bramwell, V.H., Groom, A.C., and Chambers, A.F. (2003). Ineffectiveness of doxorubicin treatment on solitary dormant mammary carcinoma cells or late-developing metastases. Breast Cancer Res Treat *82*, 199-206.

Nguyen, D.X., Bos, P.D., and Massague, J. (2009). Metastasis: from dissemination to organ-specific colonization. Nat Rev Cancer *9*, 274-284.

Nguyen, D.X., and Massague, J. (2007). Genetic determinants of cancer metastasis. Nat Rev Genet *8*, 341-352.

Nicks, K.M., Fowler, T.W., and Gaddy, D. (2010). Reproductive hormones and bone. Curr Osteoporos Rep *8*, 60-67.

Notta, F., Doulatov, S., and Dick, J.E. (2010). Engraftment of human hematopoietic stem cells is more efficient in female NOD/SCID/IL-2Rgc-null recipients. Blood *115*, 3704-3707.

Ntouroupi, T.G., Ashraf, S.Q., McGregor, S.B., Turney, B.W., Seppo, A., Kim, Y., Wang, X., Kilpatrick, M.W., Tsipouras, P., Tafas, T.*, et al.* (2008). Detection of circulating tumour cells in peripheral blood with an automated scanning fluorescence microscope. Br J Cancer *99*, 789-795.

Ohtaki, T., Shintani, Y., Honda, S., Matsumoto, H., Hori, A., Kanehashi, K., Terao, Y., Kumano, S., Takatsu, Y., Masuda, Y.*, et al.* (2001). Metastasis suppressor gene KiSS-1 encodes peptide ligand of a G-protein-coupled receptor. Nature *411*, 613-617.

Omatsu, Y., Sugiyama, T., Kohara, H., Kondoh, G., Fujii, N., Kohno, K., and Nagasawa, T. (2010). The essential functions of adipo-osteogenic progenitors as the hematopoietic stem and progenitor cell niche. Immunity *33*, 387-399.

Orian-Rousseau, V., Chen, L., Sleeman, J.P., Herrlich, P., and Ponta, H. (2002). CD44 is required for two consecutive steps in HGF/c-Met signaling. Genes Dev *16*, 3074-3086.

Ostrand-Rosenberg, S. (2008). Immune surveillance: a balance between protumor and antitumor immunity. Curr Opin Genet Dev *18*, 11-18.

Ostrand-Rosenberg, S., and Sinha, P. (2009). Myeloid-derived suppressor cells: linking inflammation and cancer. J Immunol *182*, 4499-4506.

Pachmann, K., Camara, O., Kavallaris, A., Krauspe, S., Malarski, N., Gajda, M., Kroll, T., Jorke, C., Hammer, U., Altendorf-Hofmann, A.*, et al.* (2008). Monitoring the response of circulating epithelial tumor cells to adjuvant chemotherapy in breast cancer allows detection of patients at risk of early relapse. J Clin Oncol *26*, 1208-1215.

Padua, D., Zhang, X.H., Wang, Q., Nadal, C., Gerald, W.L., Gomis, R.R., and Massague, J. (2008). TGFbeta primes breast tumors for lung metastasis seeding through angiopoietin-like 4. Cell *133*, 66-77.

Paget, S. (1889). The distribution of secondary growths in cancer of the breast. 1889. Cancer Metastasis Rev *8*, 98-101.

Palmieri, D., Halverson, D.O., Ouatas, T., Horak, C.E., Salerno, M., Johnson, J., Figg, W.D., Hollingshead, M., Hursting, S., Berrigan, D.*, et al.* (2005). Medroxyprogesterone acetate

elevation of Nm23-H1 metastasis suppressor expression in hormone receptor-negative breast cancer. J Natl Cancer Inst *97*, 632-642.

Palumbo, J.S. (2008). Mechanisms linking tumor cell-associated procoagulant function to tumor dissemination. Semin Thromb Hemost *34*, 154-160.

Pang, R., Law, W.L., Chu, A.C., Poon, J.T., Lam, C.S., Chow, A.K., Ng, L., Cheung, L.W., Lan, X.R., Lan, H.Y.*, et al.* (2010). A subpopulation of CD26+ cancer stem cells with metastatic capacity in human colorectal cancer. Cell Stem Cell *6*, 603-615.

Pantel, K., and Alix-Panabieres, C. (2010). Circulating tumour cells in cancer patients: challenges and perspectives. Trends Mol Med.

Pantel, K., Alix-Panabieres, C., and Riethdorf, S. (2009). Cancer micrometastases. Nat Rev Clin Oncol *6*, 339-351.

Pantel, K., and Brakenhoff, R.H. (2004). Dissecting the metastatic cascade. Nat Rev Cancer *4*, 448-456.

Pantel, K., Schlimok, G., Braun, S., Kutter, D., Lindemann, F., Schaller, G., Funke, I., Izbicki, J.R., and Riethmuller, G. (1993). Differential expression of proliferation-associated molecules in individual micrometastatic carcinoma cells. J Natl Cancer Inst *85*, 1419-1424.

Pantel, K., and Woelfle, U. (2005). Detection and molecular characterisation of disseminated tumour cells: implications for anti-cancer therapy. Biochim Biophys Acta *1756*, 53-64.

Patterson, G.H., Knobel, S.M., Sharif, W.D., Kain, S.R., and Piston, D.W. (1997). Use of the green fluorescent protein and its mutants in quantitative fluorescence microscopy. Biophys J *73*, 2782-2790.

Pawelek, J.M., and Chakraborty, A.K. (2008). The cancer cell--leukocyte fusion theory of metastasis. Adv Cancer Res *101*, 397-444.

Pece, S., Tosoni, D., Confalonieri, S., Mazzarol, G., Vecchi, M., Ronzoni, S., Bernard, L., Viale, G., Pelicci, P.G., and Di Fiore, P.P. (2010). Biological and molecular heterogeneity of breast cancers correlates with their cancer stem cell content. Cell *140*, 62-73.

Pennacchietti, S., Michieli, P., Galluzzo, M., Mazzone, M., Giordano, S., and Comoglio, P.M. (2003). Hypoxia promotes invasive growth by transcriptional activation of the met protooncogene. Cancer Cell *3*, 347-361.

Phadke, P.A., Mercer, R.R., Harms, J.F., Jia, Y., Frost, A.R., Jewell, J.L., Bussard, K.M., Nelson, S., Moore, C., Kappes, J.C.*, et al.* (2006). Kinetics of metastatic breast cancer cell trafficking in bone. Clin Cancer Res *12*, 1431-1440.

Polyak, K., and Weinberg, R.A. (2009). Transitions between epithelial and mesenchymal states: acquisition of malignant and stem cell traits. Nat Rev Cancer *9*, 265-273.

Psaila, B., Kaplan, R.N., Port, E.R., and Lyden, D. (2006). Priming the 'soil' for breast cancer metastasis: the pre-metastatic niche. Breast Dis *26*, 65-74.

Psaila, B., and Lyden, D. (2009). The metastatic niche: adapting the foreign soil. Nat Rev Cancer *9*, 285-293.

Quintana, E., Shackleton, M., Sabel, M.S., Fullen, D.R., Johnson, T.M., and Morrison, S.J. (2008). Efficient tumour formation by single human melanoma cells. Nature *456*, 593-598.

Raaijmakers, M.H., and Scadden, D.T. (2008). Evolving concepts on the microenvironmental niche for hematopoietic stem cells. Curr Opin Hematol *15*, 301-306.

Ramaswamy, S., Ross, K.N., Lander, E.S., and Golub, T.R. (2003). A molecular signature of metastasis in primary solid tumors. Nat Genet *33*, 49-54.

Reimers, N., Zafrakas, K., Assmann, V., Egen, C., Riethdorf, L., Riethdorf, S., Berger, J., Ebel, S., Janicke, F., Sauter, G.*, et al.* (2004). Expression of extracellular matrix metalloproteases inducer on micrometastatic and primary mammary carcinoma cells. Clin Cancer Res *10*, 3422-3428.

Reubinoff, B.E., Itsykson, P., Turetsky, T., Pera, M.F., Reinhartz, E., Itzik, A., and Ben-Hur, T. (2001). Neural progenitors from human embryonic stem cells. Nat Biotechnol *19*, 1134-1140.

Reya, T., Morrison, S.J., Clarke, M.F., and Weissman, I.L. (2001). Stem cells, cancer, and cancer stem cells. Nature *414*, 105-111.

Ricci-Vitiani, L., Lombardi, D.G., Pilozzi, E., Biffoni, M., Todaro, M., Peschle, C., and De Maria, R. (2007). Identification and expansion of human colon-cancer-initiating cells. Nature *445*, 111-115.

Riethdorf, S., Fritsche, H., Muller, V., Rau, T., Schindlbeck, C., Rack, B., Janni, W., Coith, C., Beck, K., Janicke, F.*, et al.* (2007). Detection of circulating tumor cells in peripheral blood of patients with metastatic breast cancer: a validation study of the CellSearch system. Clin Cancer Res *13*, 920-928.

Riethdorf, S., Muller, V., Zhang, L., Rau, T., Loibl, S., Komor, M., Roller, M., Huober, J., Fehm, T., Schrader, I.*, et al.* (2010). Detection and HER2 expression of circulating tumor cells: prospective monitoring in breast cancer patients treated in the neoadjuvant GeparQuattro trial. Clin Cancer Res *16*, 2634-2645.

Rutgers, E.J. (2008). Sentinel node biopsy: interpretation and management of patients with immunohistochemistry-positive sentinel nodes and those with micrometastases. J Clin Oncol *26*, 698-702.

Sachdev, D., Zhang, X., Matise, I., Gaillard-Kelly, M., and Yee, D. (2009). The type I insulin-like growth factor receptor regulates cancer metastasis independently of primary tumor growth by promoting invasion and survival. Oncogene *29*, 251-262.

Salcido, C.D., Larochelle, A., Taylor, B.J., Dunbar, C.E., and Varticovski, L. (2010). Molecular characterisation of side population cells with cancer stem cell-like characteristics in small-cell lung cancer. Br J Cancer *102*, 1636-1644.

Sato, T., Vries, R.G., Snippert, H.J., van de Wetering, M., Barker, N., Stange, D.E., van Es, J.H., Abo, A., Kujala, P., Peters, P.J.*, et al.* (2009). Single Lgr5 stem cells build crypt-villus structures in vitro without a mesenchymal niche. Nature *459*, 262-265.

Schardt, J.A., Meyer, M., Hartmann, C.H., Schubert, F., Schmidt-Kittler, O., Fuhrmann, C., Polzer, B., Petronio, M., Eils, R., and Klein, C.A. (2005). Genomic analysis of single cytokeratin-positive cells from bone marrow reveals early mutational events in breast cancer. Cancer Cell *8*, 227-239.

Scrivo, R., Vasile, M., Bartosiewicz, I., and Valesini, G. (2011). Inflammation as "common soil" of the multifactorial diseases. Autoimmun Rev.

Sheehan, K.M., Gulmann, C., Eichler, G.S., Weinstein, J.N., Barrett, H.L., Kay, E.W., Conroy, R.M., Liotta, L.A., and Petricoin, E.F., 3rd (2008). Signal pathway profiling of epithelial and stromal compartments of colonic carcinoma reveals epithelial-mesenchymal transition. Oncogene *27*, 323-331.

Sheridan, C., Kishimoto, H., Fuchs, R.K., Mehrotra, S., Bhat-Nakshatri, P., Turner, C.H., Goulet, R., Jr., Badve, S., and Nakshatri, H. (2006). CD44+/CD24- breast cancer cells exhibit enhanced invasive properties: an early step necessary for metastasis. Breast Cancer Res *8*, R59.

Shields, J.D., Fleury, M.E., Yong, C., Tomei, A.A., Randolph, G.J., and Swartz, M.A. (2007). Autologous chemotaxis as a mechanism of tumor cell homing to lymphatics via interstitial flow and autocrine CCR7 signaling. Cancer Cell *11*, 526-538.

Silverman, R.H., Nguyen, C., Weight, C.J., and Klein, E.A. (2010). The human retrovirus XMRV in prostate cancer and chronic fatigue syndrome. Nat Rev Urol *7*, 392-402.

Singh, S.K., Hawkins, C., Clarke, I.D., Squire, J.A., Bayani, J., Hide, T., Henkelman, R.M., Cusimano, M.D., and Dirks, P.B. (2004). Identification of human brain tumour initiating cells. Nature *432*, 396-401.

Sipkins, D.A., Wei, X., Wu, J.W., Runnels, J.M., Cote, D., Means, T.K., Luster, A.D., Scadden, D.T., and Lin, C.P. (2005). In vivo imaging of specialized bone marrow endothelial microdomains for tumour engraftment. Nature *435*, 969-973.

Spangrude, G.J., Heimfeld, S., and Weissman, I.L. (1988). Purification and characterization of mouse hematopoietic stem cells. Science *241*, 58-62.

Steeg, P.S. (2006). Tumor metastasis: mechanistic insights and clinical challenges. Nat Med *12*, 895-904.

Steeg, P.S., Bevilacqua, G., Kopper, L., Thorgeirsson, U.P., Talmadge, J.E., Liotta, L.A., and Sobel, M.E. (1988). Evidence for a novel gene associated with low tumor metastatic potential. J Natl Cancer Inst *80*, 200-204.

Stoecklein, N.H., Hosch, S.B., Bezler, M., Stern, F., Hartmann, C.H., Vay, C., Siegmund, A., Scheunemann, P., Schurr, P., Knoefel, W.T.*, et al.* (2008). Direct genetic analysis of single disseminated cancer cells for prediction of outcome and therapy selection in esophageal cancer. Cancer Cell *13*, 441-453.

Stoecklein, N.H., and Klein, C.A. (2009). Genetic disparity between primary tumours, disseminated tumour cells, and manifest metastasis. Int J Cancer *126*, 589-598.

Stott, S.L., Lee, R.J., Nagrath, S., Yu, M., Miyamoto, D.T., Ulkus, L., Inserra, E.J., Ulman, M., Springer, S., Nakamura, Z.*, et al.* (2010). Isolation and characterization of circulating tumor cells from patients with localized and metastatic prostate cancer. Sci Transl Med *2*, 25ra23.

Sun, Y.X., Pedersen, E.A., Shiozawa, Y., Havens, A.M., Jung, Y., Wang, J., Pienta, K.J., and Taichman, R.S. (2008). CD26/dipeptidyl peptidase IV regulates prostate cancer metastasis by degrading SDF-1/CXCL12. Clin Exp Metastasis *25*, 765-776.

Sweeney, T.J., Mailander, V., Tucker, A.A., Olomu, A.B., Zhang, W., Cao, Y., Negrin, R.S., and Contag, C.H. (1999). Visualizing the kinetics of tumor-cell clearance in living animals. Proc Natl Acad Sci U S A *96*, 12044-12049.

Talasaz, A.H., Powell, A.A., Huber, D.E., Berbee, J.G., Roh, K.H., Yu, W., Xiao, W., Davis, M.M., Pease, R.F., Mindrinos, M.N.*, et al.* (2009). Isolating highly enriched populations of circulating epithelial cells and other rare cells from blood using a magnetic sweeper device. Proc Natl Acad Sci U S A *106*, 3970-3975.

Talmadge, J.E. (2007). Clonal selection of metastasis within the life history of a tumor. Cancer Res *67*, 11471-11475.

Tavazoie, S.F., Alarcon, C., Oskarsson, T., Padua, D., Wang, Q., Bos, P.D., Gerald, W.L., and Massague, J. (2008). Endogenous human microRNAs that suppress breast cancer metastasis. Nature *451*, 147-152.

Theodoropoulos, P.A., Polioudaki, H., Agelaki, S., Kallergi, G., Saridaki, Z., Mavroudis, D., and Georgoulias, V. (2010). Circulating tumor cells with a putative stem cell phenotype in peripheral blood of patients with breast cancer. Cancer Lett *288*, 99-106.

Trumpp, A., and Wiestler, O.D. (2008). Mechanisms of Disease: cancer stem cells--targeting the evil twin. Nat Clin Pract Oncol *5*, 337-347.

Trusolino, L., Bertotti, A., and Comoglio, P.M. (2010). MET signalling: principles and functions in development, organ regeneration and cancer. Nat Rev Mol Cell Biol *11*, 834-848.

Uribarrena-Amezaga, R., Ortego, J., Fuentes, J., Raventos, N., Parra, P., and Uribarrena-Echevarria, R. (2010). Prognostic value of lymph node micrometastasis in patients with colorectal cancer in Dukes stages A and B (T1-T4, N0, M0). Rev Esp Enferm Dig *102*, 176-186.

Vaidya, K.S., Harihar, S., Phadke, P.A., Stafford, L.J., Hurst, D.R., Hicks, D.G., Casey, G., DeWald, D.B., and Welch, D.R. (2008). Breast cancer metastasis suppressor-1 differentially modulates growth factor signaling. J Biol Chem *283*, 28354-28360.

van Rijk, M.C., Peterse, J.L., Nieweg, O.E., Oldenburg, H.S., Rutgers, E.J., and Kroon, B.B. (2006). Additional axillary metastases and stage migration in breast cancer patients with micrometastases or submicrometastases in sentinel lymph nodes. Cancer *107*, 467-471.

van Rijn, R.S., Simonetti, E.R., Hagenbeek, A., Hogenes, M.C., de Weger, R.A., Canninga-van Dijk, M.R., Weijer, K., Spits, H., Storm, G., van Bloois, L.*, et al.* (2003). A new xenograft model for graft-versus-host disease by intravenous transfer of human peripheral blood mononuclear cells in RAG2-/- gammac-/- double-mutant mice. Blood *102*, 2522-2531.

Vincan, E., and Barker, N. (2008). The upstream components of the Wnt signalling pathway in the dynamic EMT and MET associated with colorectal cancer progression. Clin Exp Metastasis *25*, 657-663.

Watson, M.A., Ylagan, L.R., Trinkaus, K.M., Gillanders, W.E., Naughton, M.J., Weilbaecher, K.N., Fleming, T.P., and Aft, R.L. (2007). Isolation and molecular profiling of bone marrow

micrometastases identifies TWIST1 as a marker of early tumor relapse in breast cancer patients. Clin Cancer Res *13*, 5001-5009.

Weckermann, D., Polzer, B., Ragg, T., Blana, A., Schlimok, G., Arnholdt, H., Bertz, S., Harzmann, R., and Klein, C.A. (2009). Perioperative activation of disseminated tumor cells in bone marrow of patients with prostate cancer. J Clin Oncol *27*, 1549-1556.

Wiedswang, G., Borgen, E., Karesen, R., Qvist, H., Janbu, J., Kvalheim, G., Nesland, J.M., and Naume, B. (2004). Isolated tumor cells in bone marrow three years after diagnosis in disease-free breast cancer patients predict unfavorable clinical outcome. Clin Cancer Res *10*, 5342-5348.

Wiedswang, G., Borgen, E., Schirmer, C., Karesen, R., Kvalheim, G., Nesland, J.M., and Naume, B. (2006). Comparison of the clinical significance of occult tumor cells in blood and bone marrow in breast cancer. Int J Cancer *118*, 2013-2019.

Wilson, A., Laurenti, E., Oser, G., van der Wath, R.C., Blanco-Bose, W., Jaworski, M., Offner, S., Dunant, C.F., Eshkind, L., Bockamp, E.*, et al.* (2008). Hematopoietic stem cells reversibly switch from dormancy to self-renewal during homeostasis and repair. Cell *135*, 1118-1129.

Wilson, A., Laurenti, E., and Trumpp, A. (2009). Balancing dormant and self-renewing hematopoietic stem cells. Curr Opin Genet Dev *19*, 461-468.

Wilson, A., Murphy, M.J., Oskarsson, T., Kaloulis, K., Bettess, M.D., Oser, G.M., Pasche, A.C., Knabenhans, C., Macdonald, H.R., and Trumpp, A. (2004). c-Myc controls the balance between hematopoietic stem cell self-renewal and differentiation. Genes Dev *18*, 2747-2763.

Wilson, A., Oser, G.M., Jaworski, M., Blanco-Bose, W.E., Laurenti, E., Adolphe, C., Essers, M.A., Macdonald, H.R., and Trumpp, A. (2007). Dormant and self-renewing hematopoietic stem cells and their niches. Ann N Y Acad Sci *1106*, 64-75.

Wilson, A., and Trumpp, A. (2006). Bone-marrow haematopoietic-stem-cell niches. Nat Rev Immunol *6*, 93-106.

Wimberger, P., Heubner, M., Otterbach, F., Fehm, T., Kimmig, R., and Kasimir-Bauer, S. (2007). Influence of platinum-based chemotherapy on disseminated tumor cells in blood and bone marrow of patients with ovarian cancer. Gynecol Oncol *107*, 331-338.

Wong, N.S., Kahn, H.J., Zhang, L., Oldfield, S., Yang, L.Y., Marks, A., and Trudeau, M.E. (2006). Prognostic significance of circulating tumour cells enumerated after filtration enrichment in early and metastatic breast cancer patients. Breast Cancer Res Treat *99*, 63-69.

Wulfing, P., Borchard, J., Buerger, H., Heidl, S., Zanker, K.S., Kiesel, L., and Brandt, B. (2006). HER2-positive circulating tumor cells indicate poor clinical outcome in stage I to III breast cancer patients. Clin Cancer Res *12*, 1715-1720.

Wyckoff, J.B., Wang, Y., Lin, E.Y., Li, J.F., Goswami, S., Stanley, E.R., Segall, J.E., Pollard, J.W., and Condeelis, J. (2007). Direct visualization of macrophage-assisted tumor cell intravasation in mammary tumors. Cancer Res *67*, 2649-2656.

Xu, J.H., Guo, X.Z., Ren, L.N., Shao, L.C., and Liu, M.P. (2008). KAI1 is a potential target for anti-metastasis in pancreatic cancer cells. World J Gastroenterol *14*, 1126-1132.

Yachida, S., Jones, S., Bozic, I., Antal, T., Leary, R., Fu, B., Kamiyama, M., Hruban, R.H., Eshleman, J.R., Nowak, M.A*., et al.* (2010). Distant metastasis occurs late during the genetic evolution of pancreatic cancer. Nature *467*, 1114-1117.

Yahata, T., Ando, K., Nakamura, Y., Ueyama, Y., Shimamura, K., Tamaoki, N., Kato, S., and Hotta, T. (2002). Functional human T lymphocyte development from cord blood CD34+ cells in nonobese diabetic/Shi-scid, IL-2 receptor gamma null mice. J Immunol *169*, 204-209.

Yang, J., and Weinberg, R.A. (2008). Epithelial-mesenchymal transition: at the crossroads of development and tumor metastasis. Dev Cell *14*, 818-829.

Yang, Z.F., Ho, D.W., Ng, M.N., Lau, C.K., Yu, W.C., Ngai, P., Chu, P.W., Lam, C.T., Poon, R.T., and Fan, S.T. (2008). Significance of CD90+ cancer stem cells in human liver cancer. Cancer Cell *13*, 153-166.

Yu, Q., Toole, B.P., and Stamenkovic, I. (1997). Induction of apoptosis of metastatic mammary carcinoma cells in vivo by disruption of tumor cell surface CD44 function. J Exp Med *186*, 1985-1996.

Zhang, J., Niu, C., Ye, L., Huang, H., He, X., Tong, W.G., Ross, J., Haug, J., Johnson, T., Feng, J.Q.*, et al.* (2003). Identification of the haematopoietic stem cell niche and control of the niche size. Nature *425*, 836-841.

Zhang, X.H., Wang, Q., Gerald, W., Hudis, C.A., Norton, L., Smid, M., Foekens, J.A., and Massague, J. (2009). Latent bone metastasis in breast cancer tied to Src-dependent survival signals. Cancer Cell *16*, 67-78.

Zlotnik, A. (2008). New insights on the role of CXCR4 in cancer metastasis. J Pathol *215*, 211-213.

zur Hausen, H. (2009). Papillomaviruses in the causation of human cancers - a brief historical account. Virology *384*, 260-265.

11. ACKNOWLEDGMENTS

First of all, I would like to thank you, **Andreas,** for offering me to join your laboratory in Lausanne. Little did I know about the wild ride that came along with the position: two lab moves, a temporary group leader position, a massive lab expansion and the opportunity to discover Switzerland and Germany. Well, I do not regret one bit of it, even if the path was not as even and straight as I originally thought. I learned and am still learning a lot thanks to the talented, open-minded and motivated people you keep hiring and thanks to the impressive technologies you keep adding up to the lab ☺. I wish to find such a live, entertaining and powerful atmosphere in my future labs! Thank you also for the trust and freedom you gave me all along my PhD work.

Thank you **Armin**, my PhD-twin and very good friend. Thanks for being who you are: a rock, a rocker and you know you rock! ☺ I don't know how I would have gone through these years without you.

I would like to thank all my former colleagues and friends from Lausanne, whom I miss very much. **Sandra**, merci pour ton aide pendant mes années lausannoises et pour la suite, encore plus! Tu m'as initiée au monde de l'expérimentation animale et depuis ces moments inoubliables passés en ta compagnie je n'ai pas décroché; tu me manques beaucoup, beaucoup! **Kostya**, thanks so much for your craziness, for your constant help and for your long-lasting friendship. I wish you to find your way back to climbing-land, and for sure I will meet you there (I mean, at the bottom, you know I can't climb!!!)! **Christelle,** merci pour ta bonne humeur et tes expressions suisses, je compte bien revenir te faire part de ma collection d'expressions allemandes et embrasser tes enfants. **Elisa,** merci beaucoup pour ces moments passés en ta compagnie et l'exemple que tu représentes pour moi. Je te souhaite de réussir, tu le mérites amplement! **Gaby,** merci beaucoup pour ta patience et ces moments passés à apprendre à tes côtés, je ne l'oublierai jamais. **Nicole,** thanks for helping me at the very beginning of my start in Lausanne, I really enjoyed your energy and joyfulness. **Will,** merci pour ton calme et tes conseils avisés, tu nous manque beaucoup à Heidelberg! ☺ **Maike,** thanks for sharing these years, I hope that you enjoy your PostDoc life. **Stelle,** thanks for your joyfulness and for your pink attitude, did I tell you that my

German office is called the “pink aquarium”? **Raghav,** merci beaucoup pour ta compagnie, très appréciée, à Lausanne et pour ton amitié; je te souhaite plein de bonheur pour la suite. **Yulia et Raphi,** merci pour votre fraicheur et bonne humeur, ce fut un plaisir de travailler à vos côtés.

Importantly, I would like to thank **Sabrina, Ute, Sven, Gisèle, Antonietta and all the animal caretakers** in Lausanne, without whom, I would not have been able to start my PhD work. Thank you very much also, **Jessica and the histology platform in Lausanne,** for organizing the histological screening of my endless sample collection. I would like to thank **Nicolo** and **Jean-Christophe** for their help in the characterization of the tumors growing in my mice. Too bad that the stainings were not specific for human cells and that it took such a long time for us to realize it! However, you both made a lot of work and patiently introduced me to the uncertain world of Immunohistochemistry, I will never forget it.

Marieke, thanks so much for your organizing skills and strength that enabled the lab moves and lab expansion to be successful. I learned a lot about how to organize a new lab thanks to you. Thanks also for your moral support along these years. I wish you a more sedentary lifestyle in the coming months (boy, how exhausting can shuttling be)!

I would also like to thank my “new” colleagues and friends in Heidelberg. **Meli,** thank you very much for your scientific discussions, manuscript corrections and for your pink spirit! I have much appreciated sharing philosophical discussions and building up a beautiful friendship with you. Pink we are and pink we shall remain! **Anja,** thanks a lot for bearing me as your supervisor for a year and still being a wonderful friend to me! Thanks for your pink spirit and also for making me discover and like Germany! ☺ **Corinna,** thanks for your humor, your strength and your intelligence. Your help is not measurable; I owe you a lot, and I will never thank you enough for it! **Christian,** thanks for having me, a woman (!), as a supervisor for a year: I hope that your strong Bavarian personality did not suffer too much from it! ;-) Seriously, it was real fun working with you and I wish you all the best for the future! **Tom,** thanks very much for coming along in our MetICs group and for having me as a supervisor for a few months, which were not the easiest ones. I really enjoyed learning from you and sharing views on science and on life in general. Thank you so much also for your incredibly efficient manuscript correction skills! **Hind,** un grand grand merci, Miss, pour ton aide pour mon manuscrit de thèse, tes conseils, ta franchise et ton amitié, ta venue au labo

m'a apporté un grand bol d'air frais et d'énergie! Je te souhaite de tout coeur de réussir dans ce monde testost-erronné. ☺ **Marina,** thanks so much for taking care of ALL the not-so-small, and so-important things, with such efficiency: I remain positive that you are the BEST SECRETARY OF THE WORLD! **Teresa,** thanks for joining the MetICS and for your humor, I am happy to share the pink aquarium with you everyday. All the best of luck for the future! **Andrea T.,** thanks for the tons of injections you did for me. Your efficiency and precision are admirable! **Martin,** thanks for coming along in the MetICs group and for bringing your joyfulness at a time the group greatly needed it. I wish you the best for leading the MetICs further. **Andrea K.,** thanks a lot for your help during the lab moves and lab set up, really from scratch! **Vanessa,** I am very happy that you joined the group. Many thanks for your humor and for your help in histology. **Jasmin,** thanks for your gentleness, I wish you all the best in your new studies! **Tobi,** thanks for your humor and attention (especially feeding me after 12 hours of non-stop FACS!) **Gelo,** thanks so much for you patience and humor while FACS sorting with me, chasing the too few cells again and again!! ☺ **Raphael,** thanks for your humor and kindness, it was a pleasure working next to you. **Katja,** thank you for bearing me as a supervisor when you started in our lab, for your help in histology and for genotyping my mice. **Ines,** thanks for your laughter and for your humor, it is a pleasure to "hear" you working. ☺ **Stephan,** thanks for staying calm in all occasions. **Larissa,** thanks a lot for correcting my thesis manuscript and for bringing sunshine in our lab. **Daniel,** thank you very much for your help on all security-linked issues in our lab and for allowing me to quickly start again my experiments according to the German laws. Thanks also for your craziness on the soccer field, pure happiness moments! **Pia,** thanks for your humor and endless philosophical discussions on how we could make the world a better place! I do hope that it will get better. ☺ **Mick,** thank you very much for your interest, your help and your advice. I really appreciate the time you take to discuss science, whatever the topic might be (even (!) solid tumors and metastases) ☺. **Roberta,** thank you for being patient with the MetICs, ever more numerous, like yeast… ☺ **Lisa,** I wish you all the best in your PhD work, you are in very good hands. ☺ **Nina,** I am very happy that you decided to come in our lab and I wish you all the best in Heidelberg! **Sandra,** thanks a lot for taking care of our HUGE antibody stocks, with a smile, above all! **Steve,** thanks for your joyfulness, I wish you all the best for the end of your PhD. **Dorit,** thank you very much for helping me get through the ethics vote and other tricks of the German law in order to be allowed to get samples from the clinic, it is much appreciated! **Amelie,** I wish you all the best for your PhD in our lab.

Azeem, I wish you all the best for the future. **Petra** and **Hanna** welcome to the lab! **Sinna,** thanks a lot for your helpfulness, for taking care of so many things without even mentioning it. **Steffi,** I wish you all the best for your PhD. **Laura, Amelie and Christoph,** I wish you all the best for your projects! Importantly, I would also like to thank **Klaus,** for FACS sorting on the Influx, the best machine in the world (☺), **Norma, Michaela, Stefan, Theresa, Anja and all the animal care takers in the DKFZ,** without whom, I would not have been able to finish my PhD work.

Without my long-standing collaborators, **Klaus and Sabine**, my work would not have been possible. Thank you very much for your help, support and trust during all these years. In particular, **Sabine**, thank you very much for the astounding amount of work and help you provided all along my PhD.

I cannot find the words to thank all the **cancer patients** who agreed to participate to the 3 Clinical Studies. Even if they appear as numbers in my thesis manuscript, I deeply appreciate their generosity and faith in scientific research, while facing death. Thank you as well to our medical collaborators: **Prof. Dr. Hohenfellner, Tom, Prof. Dr. Schneeweiss and Dr. Wallwiener,** who enthusiastically accepted to participate to the Clinical Studies. Thank you very much **Martina, Bettina, Sabine, Claudia and the DKFZ receptionists** for organizing the logistics of the numerous samples. Thank you very much also to **Prof. Dr. Sinn** and **Dr. Aulmann** for pathology counseling.

I would also like to thank dear friends, whom I met during my PhD and who supported me in many ways. **Irina**, **Charlotte, Daniel, Astrid, Stéphane, Sylvie, Aurélie, Ruth, Maasi and Matze** I will never thank you enough for your support and for the sunshine you all bring, in different ways, to my everyday life and work.

Last but not least, I would like to thank my **parents and family**, who stood by me during these years. Merci à toi, **Marie-Francoise** pour ton aide et tes conseils qui m'ont permis de me lancer dans cette aventure! Merci à vous **frérots § soeur**, pour votre soutien et aide au quotidien. On ne prend pas souvent le temps de se le dire, alors voilà: MERCI!!

Mille fois merci **Maman** et mille fois merci **Papa** pour vos encouragements, votre patience et vos conseils constants, qui m'ont permis de passer de durs moments, la tête haute.

I dedicate my thesis to **Thomas**. No word can describe the extent and the strength of your support.

In memory of my cousin, ***Pierre-Jean*** *and of my grandfather,* ***Antoine.***